T.C.

AKDENİZ ÜNİVERSİTESİ

VISUAL MODFLOW PROGRAMI KULLANILARAK KARSTİK AKİFERLERDEKİ YERALTISUYU KAYNAKLARININ YÖNETİMİ: ALTINOVA-TÜRKİYE ÖRNEK UYGULAMASI

Alex Modi Lomoro WANI

FEN BİLİMLERİ ENSTİTÜSÜ

ÇEVRE MÜHENDİSLİĞİ

ANABİLİM DALI

YÜKSEK LİSANS TEZİ

OCAK 2019

ANTALYA

T.C.

AKDENİZ ÜNİVERSİTESİ

VISUAL MODFLOW PROGRAMI KULLANILARAK KARSTİK AKİFERLERDEKİ YERALTISUYU KAYNAKLARININ YÖNETİMİ: ALTINOVA-TÜRKİYE ÖRNEK UYGULAMASI

Alex Modi Lomoro WANI

FEN BİLİMLERİ ENSTİTÜSÜ

ÇEVRE MÜHENDİSLİĞİ

ANABİLİM DALI

YÜKSEK LİSANS TEZİ

OCAK 2019

ANTALYA

T.C.

AKDENİZ ÜNİVERSİTESİ

FEN BİLİMLERİ ENSTİTÜSÜ

VISUAL MODFLOW PROGRAMI KULLANILARAK KARSTİK AKİFERLERDEKİ YERALTISUYU KAYNAKLARININ YÖNETİMİ: ALTINOVA-TÜRKİYE ÖRNEK UYGULAMASI

Alex Modi Lomoro WANI

ÇEVRE MÜHENDİSLİĞİ

ANABİLİM DALI

YÜKSEK LİSANS TEZİ

Bu tez 30/01/2019 tarihinde jüri tarafından Oybirliği / Oyçokluğu ile kabul edilmiştir.

Prof. Dr. Habib MUHAMMETOĞLU (Danışman)

Dr. Oğr. Firdes YENİLMEZ

Doç. Dr. Orhan GÜNDÜZ

ÖZET

VISUAL MODFLOW PROGRAMI KULLANILARAK KARSTİK AKİFERLERDEKİ YERALTISUYU KAYNAKLARININ YÖNETİMİ: ALTINOVA-TÜRKİYE ÖRNEK UYGULAMASI.

Alex Modi Lomoro WANI

Yüksek Lisans Tezi, Çevre Mühendisliği Anabilim Dalı

Danışman: Prof. Dr. Habib MUHAMMETOĞLU

Ocak 2019; 162 sayfa

Bu çalışma, Antalya'nın karstik özellikteki Altınova bölgesi için gerçekleştirilmiştir. Çalışmanın amacı, Visual MODFLOW Flex kullanarak Altınova'nın karst bölgesindeki yeraltısuyu (YAS) hareketinin simüle edilmesidir. Ek olarak, Altınova'daki YASın mevcut durumunun analiz edilmesi ve geleceğe yönelik yönetim senaryoları kapsamında bölgedeki YAS seviyesinin incelenmesi hedeflenmiştir. YAS seviye değişimi model tahminleri ile elde edilmiştir. Model uygulamasında, mekânsal çözünürlük 25600 m2'lik boyutta ve yaklaşık 75 km2'lik bir alan üzerinde tasarlanmıştır. Model uygulama alanı, jeolojik formasyona göre iki farklı beslenme ve hidrolik iletkenlik bölgesine bölünmüştür. Model, iki boyutlu, kararlı akım koşullarında çalıştırılmıştır. Yanal yöndeki hidrolik iletkenlik, tek kalibrasyon parametresi olarak ele alınmıştır. Modelden elde edilen YAS seviyesi tahminleri, Kasım 2015, Şubat 2016 ve Mayıs 2016'da sahada ölçülen YAS seviyeleri ile karşılaştırılarak model kalibrasyonu gerçekleştirilmiştir. Kurşunlu formasyonunda yer alan ve karstik olmayan alandaki kalibrasyon çalışması sonuçları, traverten karstik alanı için elde edilen sonuçlara göre daha düşük model hatası vermiştir. Genel olarak ölçülen ve tahmin edilen YAS seviyeleri arasındaki korelasyon katsayısı 0,99 olarak hesaplanmıştır. Hem karst hem de karst olmayan alanlar için hidrolik iletkenliğin kalibre edilmiş değerleri 0,01 ila 266 m/gün arasında değişmiştir. Simülasyon dönemi için oluşturulan su bütçesi, akifere giren su akışı ve akiferden çıkan su akışı arasında iyi bir denge olduğunu göstermektedir. Net beslenme, su bütçesindeki en yüksek akış değerini oluşturur ve model sonuçları üzerinde çok etkilidir. Model kalibrasyonu çalışması sonrasında, üç senaryo koşulu oluşturulmuştur. Üç farklı hidrolojik senaryo koşulu için YAS seviyesinde düşüşler görülmüştür. Model tahminleri kullanılarak, YAS akım yönü haritası oluşturulmuştur. Genel olarak, çalışma alanındaki karstik travertendeki YAS kuzeyden güneybatıya ve devamında güneye doğru hareket etmekte iken, karst olmayan akiflerde YAS hareketinin güneye doğru olduğu belirlenmiştir.

ANAHTAR KELİMELER: Altınova, Karstik akifer, Modelleme, Visual MODFLOW Flex, YAS seviyesi.

JÜRİ: Prof. Dr. Habib MUHAMMETOĞLU

Dr. Oğr. Üyesi Firdes YENİLMEZ

Doç. Dr. Orhan GÜNDÜZ

ABSTRACT

MANAGEMENT OF GROUNDWATER RESOURCES IN KARSTIC AQUIFER USING VISUAL MODFLOW: CASE STUDY OF ALTINOVA TURKEY

Alex Modi Lomoro WANI

MSc Thesis in Environmental Engineering

Supervisor: Dr. Habib MUHAMMETOĞLU

January 2019; 162 pages

This study was carried out over the karstic area of Altınova region in Antalya-Turkey. The aim of this study is to simulate groundwater in the karst region of Altınova using Visual MODFLOW Flex. The study also aims at assessing the current condition of groundwater in Altınova and formulate scenarios to foresee the future groundwater table elevation. The model girds were designed in such a way that the spatial resolution has a dimension of 25600 m2 over an area of approximately 75 km2. The model domain was divided into two recharge and hydraulic conductivity zones based on the geological formation. The model was run as two dimensional in steady-state. Hydraulic conductivity in the lateral direction was handled as the only calibration parameter. The computed groundwater table elevations were calibrated by comparing with average observed groundwater table elevations data collected in Nov 2015, Feb 2016 and May 2016. The calibration results in the Kurşunlu non- karstic area tend to be more satisfactory with lower residual values than in the travertine karstic area. Overall the correlation coefficient between measured and simulated groundwater table elevation was reasonable with the value of 0.99. The calibrated values of hydraulic conductivity in both karst and non-karst area ranged from 0.01 to 266 m/day. Overall, the calibrated values of hydraulic conductivity in both karst and non-karst areas of Altınova were within the literature ranges. The water budget in the period of the simulation shows a good balance between inflow and outflow. Recharge was the highest component of inflow in the water budget for the entire study area and was sensitive in the model. Following the model calibration, three management scenarios were developed. The groundwater table elevation imperiled to decline under different three hydrological scenarios. A groundwater flow direction map was produced based on modeling outputs. Overall, the groundwater flows from north to southwest then to south in the karstic travertine, while in the non-karst Kurşunlu formation the groundwater flows from north to the south.

KEYWORDS: Altınova, Groundwater table elevation, Karstic aquifer, Modeling, Visual MODFLOW Flex.

COMMITTEE: Prof. Dr. Habib MUHAMMETOĞLU

Dr. Oğr. Üyesi Firdes YENİLMEZ

Assoc. Prof. Dr. Orhan GÜNDÜZ

ÖNSÖZ

Antalya’nın Akdeniz bölgelerinde yer alan karstik akiferler genel olarak yoğun kullanım ve kirlenme baskısı altındadır ve bazı bölgelerde karstik alanlar sürekli olarak daralmaktadır. Bu nedenle de bu kırılgan karst kaynağının kalite ve miktar açısından korunması zorunludur. Bu değerli karstik yeraltısuyu kaynağını sürdürülebilir şekilde kullanmak ve yönetmek için, akifer koşullarının matematiksel modeller kullanılarak ve farklı senaryolar altında simüle edilmesi önem kazanmaktadır. Bu çalışma sonuçları, karar vericilerin yeraltısuyu kaynaklarını korumak için uygun önlemler almalarında destek sağlayacak öneriler sunmayı amaçlamaktadır. Bu tez çalışmasında kullanılan veri seti, Prof. Dr. Ayşe MUHAMMETOĞLU'nun yürütücüsü olduğu ve yakın süre önce tamamlanmış olan 114Y696 nolu TÜBİTAK projesi veri tabanından elde edilmiştir.

Danışmanım olan Prof. Dr. Habib MUHAMMETOĞLU'na, beni tez öğrencisi olarak kabul ettiği, ilk dersi olarak Yeraltısuyu Kirliliği ve Kontrolü’nü verdiği ve bu tez konusunu seçmemde beni cesaretlendirdiği için özel şükranlarımı sunarım. Bu çalışmayı, kendisinin yürekten katılımı, gözetimi, değerli eleştirileri, bilimsel tavsiyeleri, desteği ve sürekli cesareti olmadan gerçekleştirmem mümkün olmazdı. Bana sadece tez çalışmamda yardımcı olmakla kalmadı, bana birçok şey öğretti ve ayrıca hayatımda ilerlemem için beni motive etti. Kendisine gösterdiği yakın ilgi ve destek için çok teşekkür ederim.

Tez çalışmasında bana destek olan Prof. Dr. Ayşe MUHAMMETOĞLU'na gerekli veri ve araştırma araçlarını sağladığı, yüksek lisans derslerinde eleştirel düşünceyi öğrettiği ve pratik veri analizi yapmamızı sağladığı için içten teşekkürlerimi sunarım. Model uygulamasında destek olan Dr. Ziyad ABUNADA'ya da değerli yorumları için teşekkür ederim.

Sonuncusu ama en önemlisi, bana yüksek lisans tez çalışmasını yapabilmem için burs desteği veren Yurtdışı Türkler ve Akraba Topluluklar Başkanlığı’na takdirlerimi ifade etmek isterim. Onların desteği olmadan, bu çalışmanın gerçekleşmesi mümkün olmayacaktı. Mentorluk ve çok değerli yardımlarından dolayı Diana THOMAS'a teşekkür ederim. Son olarak, aileme sonsuz ve sürekli destekleri ve hayatım boyunca ve akademik yolculuğum boyunca cesaret verdikleri için teşekkür etmek istiyorum. Hedeflerime ulaşmaya yönelik fedakârlıklarını asla unutmayacağım.

İÇİNDEKİLER

ÖZET i
ABSTRACT ii
ÖNSÖZ iii
AKADEMİK BEYAN vi
SİMGELER VE KISALTMALAR vii
ŞEKİLLER DİZİNİ viii
ÇİZELGELER DİZİNİ ix
1. GİRİŞ 1
2. KAYNAK TARAMASI 2
2.1. Yeraltısuyuna Genel Bakış 2
2.1.1. İklim değişikliğinin karstik yeraltısularındaki potansiyel etkisi 2
2.2. Türkiye'nin Akdeniz İllerinde Karstik Akiferlerin Dağılımı 2
2.3. Yeraltısuyu Modelleme Teknikleri ve Kategorileri 3
2.3.1. Yeraltısuyu modelleme çalışması için gerekli veriler. 3
2.4. Model Kalibrasyonu 4
2.5. Karst Sistemlerinde Yeraltısuyu Akımını Tanımlamak için Yaklaşımlar 4
3. MATERYAL VE METOT 6
3.1. Çalışma Alanının Genel Tanımı ve Özellikleri 6
3.2. Model Uygulaması 8
3.2.1. Saha çalışması 8
3.3. Model Tasarımı ve Ayrıştırma Teknikleri 9
3.4. Model Kalibrasyonu ve Değerlendirme 10
3.5. Yönetim Senaryolarının Analizi 11
4. BULGULAR VE TARTIŞMA 12
4.1. Hidrolik İletkenlik Parametresinin Kalibrasyonu 12
4.2. Kalibre edilmiş yeraltısuyu akış modeli sonuçları 14
4.3. Karst ve Karst olmayan Alanlar için Yeraltısuyu Seviyesi Tahminlerinin Karşılaştırılması 15
4.4. Yeraltısuyu Akım Modeli ile Hazırlanan Su Bütçesi Sonuçları 18
4.5. Çalışma Alanındaki Yeraltısuyu Akış Yönü 18
4.6. Farklı Yönetim Senaryolarının Etkileri 19

4.6.1. Senaryo (A) için yeraltısuyu seviyeleri 20
4.6.2. Senaryo (B) için yeraltısuyu seviyeleri 21
4.6.3. Senaryo (C) için yeraltısuyu seviyeleri 22
4.7. Yeraltısuyu Akış Modeli Uygulamasına İlişkin Sınırlandırmalar 24
5. SONUÇLAR 25
5.1. Gelecek Araştırmalar için Öneriler 26
6. KAYNAKLAR 27
7. EKLER 30
7.1. EK-1 Tezin İngilizce versiyonu 30
ÖZGEÇMİŞ

AKADEMİK BEYAN

Yüksek Lisans Tezi olarak sunduğum "Visual MODFLOW Programı Kullanılarak Karstik Akiferlerdeki Yeraltısuyu Kaynaklarının Yönetimi: Altınova-Türkiye Örnek Uygulaması" adlı bu çalışmanın, akademik kurallar ve etik değerlere uygun olarak yazıldığını belirtir, bu tez çalışmasında bana ait olmayan tüm bilgilerin kaynağını gösterdiğimi beyan ederim.

30/01/2019
Alex Modi Lomoro WANI

SİMGELER VE KISALTMALAR

Simgeler

C : İletkenlik

°C : Santigrat derece

M : Metre

Mm : Milimetre

m^3 : Metreküp

% : Yüzde

Km^2 : Kilometre kare

K : Hidrolik iletkenlik

S_y : Spesifik verim

S_s : Gözenekli medya depolayabilme

Mg : Miligram

L : Litre

W^* : Birim hacim bölü hacim akışı

Kısaltmalar

DEM : Dijital Yükseklik Modeli

GCM : Küresel Sirkülasyon Modelleri

CBS : Coğrafi Bilgi Sistemi

MAE : Ortalama Mutlak Hata

NRMSE : Normalize Kök Ortalama Kare Hatası

PCG : Precondition Conjugated Gradient

PEST : Parametre Tahmin Aracı

RMSE : Ortalama Karekök Hatası

YAS : Yeraltısuyu

ŞEKİLLER DİZİNİ

Şekil 2.1.. Türkiye'deki karst alanlarının mekansal gösterimi. 3

Şekil 3.1.Türkiye'de Antalya-Altınova'da seçilen pilot çalışma sahasının lokasyonu 7

Şekil 3.2 Altınova'nın karstik ve karstik olmayan bölgesinde ortalama YAS seviyeleri 8

Şekil 3.3.. Kararlı durum modeli için uygulanan koşul sınırları..... 10

Şekil 4.1. Kalibrasyondan önceki hidrolik iletkenlik tanımları a); ve kalibrasyondan sonraki hidrolik iletkenlik değerleri b)..... 13

Şekil 4.2.. Kalibrasyon sonucu modelden tahmin edilen ve ölçülen YAS seviyeleri..... 14

Şekil 4.3. Ölçülen (a) ve kalibrasyon çalışması sonucunda tahmin edilen (b) YAS seviyelerinin mekansal dağılımı..... 15

Şekil 4.4.. Kalibrasyon sonucunda karstik olmayan bölge için tahmin edilen ve ölçülen YAS seviyeleri 16

Şekil 4.5. Kalibrasyon sonucunda karstik bölge için tahmin edilen ve ölçülen YAS seviyeleri 16

Şekil 4.6. Karstik bölge için model tahminleri ile ölçülen YAS seviyeleri arasındaki farklar (Tahmin - Ölçüm)..... 17

Şekil 4.7. Karstik olmayan bölge için model tahminleri ile ölçülen YAS seviyeleri arasındaki farklar (Tahmin - Ölçüm) 17

Şekil 4.8. Akifer için model ile hesaplanan genel su bütçesi..... 18

Şekil 4.9. YAS akış yönü ve YAS seviyesinin mekansal dağılımı..... 19

Şekil 4.10. a) Senaryo (A) koşulu için hesaplanan YAS seviyesindeki düşüş miktarı; ve buna karşılık gelen yüzdelik değişim **b)**..... 21

Şekil 4.11. a) Senaryo (B) koşulu için hesaplanan YAS seviyesindeki düşüş miktarı; ve buna karşılık gelen yüzdelik değişim **b)**..... 22

Şekil 4.12. a) Senaryo (C) koşulu için hesaplanan YAS seviyesindeki düşüş miktarı ve buna karşılık gelen yüzdelik değişim **b)**..... 23

ÇİZELGELER DİZİNİ

Çizelge 2.1. YAS modellemesi için fiziksel ve hidrolojik çerçeve verilerinin özeti.....4

Çizelge 3.1..Model yönetimi senaryolar.....11

Çizelge 4.1. Altınova çalışma bölgesi için geliştirilen yönetim senaryoları.....20

Çizelge 4.2. Farklı senaryolar için elde edilen YAS seviyesindeki düşüş miktarlarının karşılaştırılması (YAS seviyesi farkı = Baz Simülasyon – Senaryo tahmini).....23

1. GİRİŞ

Karst akiferi temel olarak çözünmeyen kayaç (örneğin alçıtaşı, tuz kayası, kuvarsit) olarak geliştirilmiş bir peyzaj ortamı olarak tanımlanır. Karst bölgeleri mağaralar, batan akarsu ve su kaynakları gibi kendine özgü hidroloji ve yer şekilleri sergilerler (Ford ve Williams, 2007). Türkiye'nin güneyindeki Akdeniz bölgesinde yaygındırlar ve genelinde önemli içme ve sulama suyu kaynaklarını oluştururlar (Güner vd. 2015). Karst akifer, Akdeniz bölgeleri boyunca hem tarım, hem de içme suyu talebinin ana unsuru olarak görülmektedir (Elhatı, 1997; Günay, 2010; Sargın vd. 2000).

Akdeniz bölgelesinde yer alan Antalya'da yeraltısuyu (YAS) genel olarak baskı altında bulunmaktadır ve bazı bölgelerde karstik alanlar sürekli olarak daralmaktadır. Bu nedenle, bu kırılgan karst traverteninde miktar ve nitelik bakımından su tasarrufu esastır. Traverten karst bölgelerindeki temel problemler tarım alanlarının, sanayileşmenin ve kentleşmenin hızla genişlemesidir. Traverten bölgesinde tarım arazilerinde gübre ve tarım ilaçlarının yaygın kullanımı YAS kirliliğine yol açmaktadır.

Antalya'nın bazı traverten karstik bölgesinde YAS kalitesinde düşüş bildirilmiştir (Günay, 2001; Muhammetoglu ve Yalçın, 2003). Çalışma alanında aktif YAS yönetimi planı bulunmamaktadır ve çalışma alanında YASın korunması konusunda yerel karar vericileri yönlendirecek ileri düzeyde bir model uygulaması bulunmamaktadır. Tez çalışmasında, kısa süre önce tamamlanan bir TÜBİTAK projesi kapsamında, bölgedeki YAS kirlilik risklerinin değerlendirilmesi amacı ile elde edilen izleme verilerinin, Visual MODFLOW Flex programı uygulamasında kullanılması ve Altınova bölgesindeki karstik akiferlerin korunması için önerilerin ortaya konulması amaçlanmıştır. Çalışmada hem mevcut durumun analiz edilmesi hem de mevcut verilere dayanılarak geliştirilen senaryolar için gelecekte oluşabilecek YAS seviyesi durumunun tahmin edilmesi hedeflenmektedir. Ek olarak Altınova'da yer alan karstik akifer sisteminin uygun şekilde korunması için yönetim stratejilerinin önerilmesi amaçlanmaktadır. Bu çalışmada kullanılan veriler, Ekim 2017'de tamamlanan 114Y696 nolu TÜBİTAK projesi kapsamında Altınova bölgesi için elde edilmiştir (Muhammetoğlu vd. 2017).

Bu tez çalışması, Altınova bölgesindeki YAS akışı ve modellemesi konusunda özgün sonuçlara ulaşılması açısından önemlidir. Visual MODFLOW, standart profesyonel iki boyutlu ve üç boyutlu YAS akışı ve kirletici taşınımı simülasyonu için kanıtlanmış olan kapasitesi nedeniyle seçilmiştir.

Bu çalışmada elde edilen bulgular ve sonuçların, yerel karar vericilere Altınova'daki YAS seviyesinin değişimi ve mevcut durumunun anlaşılması açısından yardımcı olması beklenmektedir. Bu çalışma aynı zamanda, çalışma alanında ve genel olarak Antalya'da karstik sistemin daha iyi anlaşılması için Conduit Boru Akış Süreci Modeli (Flow Process Model MODFLOW-2005 CFP) kullanılarak gelecekteki çok katmanlı bir YAS akış modelinin geliştirilmesi için iyi bir başlangıç noktası sağlamaktadır. Çalışmanın bölgedeki YAS kaynaklarının tutarlı ve uyumlu yönetimine yardımcı olması beklenmektedir.

2. KAYNAK TARAMASI

2.1. Yeraltısuyuna Genel Bakış

YAS, yeryüzündeki tatlı suyun yaklaşık üçte birini oluşturur. YAS, enerji ve gıda güvenliği, insan sağlığı ve ekosistem için önemli bir doğal kaynaktır. Dünyanın birçok bölgesinde tatlı sular bir kıtlıkla karşı karşıyadır. İklimsel koşullardaki değişimler ve ekonomik kalkınma ile ilişkili su kullanımlarındaki artış ile nüfus artışı nedeniyle, su sıkıntısının gelecekte artması beklenmektedir (Lelieveld vd. 2012). Bu durum, Türkiye için de geçerlidir ve yaşanan sorunların çözülebilmesi açısından sürdürülebilir su yönetimi zorunlu hale gelmiştir. YAS, dünyada en çok kullanılan doğal kaynaktır. YAS, Avrupa Birliği ülkelerinde su temininde önemli bir rol oynamakta ve dünyanın birçok bölgesinde tarım ve sanayi sektörlerine önemli ölçüde katkıda bulunmaktadır (Vrba vd. 2006). YAS, dünya genelinde birçok akiferde aşırı pompalama veya diğer antropojenik faaliyetlerle kirlenmiş ve azalmıştır (Maliva 2016).. Bu çalışmanın içeriği, Türkiye'nin özellikle Akdeniz Bölgesi'nde bulunan karst akifer sistemine odaklanmaktadır.

Akdeniz karst bölgelerindeki YAS kaynakları, tarih boyunca hem eski şehirlerin hem de krallıkların gelişimi için gerekli olmuştur. Bakalowicz (2005), Piccini ve Mecchia (2009) tarafından karst kaynaklarının tüketim için doğrudan çıkarılmış en temiz su kaynaklarından biri olduğu belirtilmiştir. Akdeniz ülkelerindeki karst akiferlerine genel bir bakış Ek-1(sayfa 5 – 8)'de sunulmuştur.

2.1.1. İklim değişikliğinin karstik yeraltısularındaki potansiyel etkisi

İklim değişikliği, bir dizi karst hidrojeolojisi, su ve çevre sorunlarına neden olan kritik faktörlerden biridir. Küresel Sirkülasyon Modellerinden (GCMs) alınan iklim değişikliği projeksiyonları, birçok karst bölgesindeki yağış ve sıcaklık rejimlerinde önemli değişiklikler olduğunu göstermektedir (Chen 2017). Hartmann vd. (2014), iklim değişikliğinden dolayı karst suyunda hem nitelik, hem de miktar açısından dramatik bir değişim beklendiğini belirtmiştir. Benzer şekilde, Hartmann vd. (2015) tarafından potansiyel iklim değişikliğinin YAS beslenim üzerindeki önemli etkisi, Avrupa karstik bölgesi için rapor edilmiştir. Türkiye'nin Akdeniz bölgesi, iklim değişikliğine hassastır (Tayanç vd. 2009; Lelieveld vd. 2012). Bu nedenle, iklim değişikliği, Akdeniz karst bölgesindeki YAS kaynakları üzerindeki baskıyı daha da artıracaktır.

2.2. Türkiye'nin Akdeniz İllerinde Karstik Akiferlerin Dağılımı

Karstik akiferlerden elde edilen YAS kaynakları, dünya genelinde içme-kullanma ve sulama suyu talebinin karşılanmasında çok önemli bir yere sahiptir. Türkiye'deki karstik akiferler, toplam alanının yaklaşık üçte birini kapsamaktadır. Bu karst bölgeleri önemli miktarda suya sahiptir ve özellikle Akdeniz havzasında su ihtiyaçlarının önemli bir kısmını karşılamaktadır. Sulanabilir arazi yüzeyinin yaklaşık %20'si karst YAS ile sulanmaktadır. Türkiye'nin güneyindeki tüm bölgelerde yoğun karstlaşma mevcuttur (Elhatı 1997; Günay 2010; Güner vd. 2015). Karstik akiferlerden kaynaklanan YAS, Türkiye'nin Akdeniz bölgesi boyunca sulama, sanayi ve içme suyu ihtiyacının karşılanmasında önemli bir rol oynamaktadır (Elhatı 1997; Günay 2010; Güner vd. 2015).

Türkiye'deki karstik akiferler dört farklı bölgede gruplandırılmaktadır. Bunlar, Anadolu'nun kuzeybatısında yer alan Trakya karst bölgesi, Orta Anadolu'da ve Konya havzasında yer alan akiferler, Toros karst bölgesi ve Güneydoğu Anadolu karst bölgesi olarak adlandırılmaktadır (Güner vd. 2015). Dört farklı karst bölgesi Şekil 2.1'de sunulmuştur ve detaylar Ek-1 (sayfa 8)'de verilmiştir.

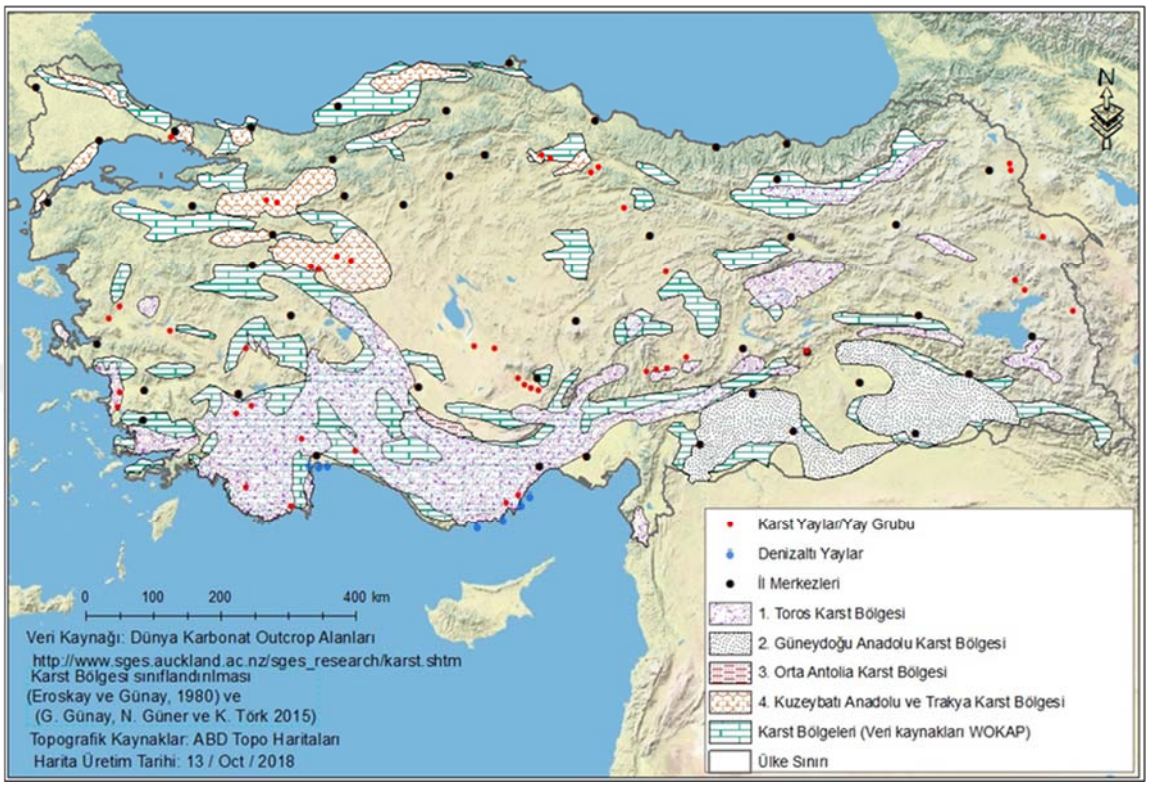

Şekil 2.1.. Türkiye'deki karst alanlarının mekansal gösterimi.

2.3. Yeraltısuyu Modelleme Teknikleri ve Kategorileri

YAS modellemesi, karmaşık, doğal, gerçek dünyanın basitleştirilmiş bir temsilidir ve bu nedenle, fiziksel sistemin kesin bir tanımı değildir (Anderson vd. 1990). YAS modellemesi çalışmalarında, bir veya iki boyutlu basit veya daha sofistike olarak üç boyutlu modeller kullanılabilir. Hill (2006) tarafından modelleme çalışmasının hedefleri karşılandığı sürece, YAS modellemesinde basit modellerden başlamanın, modelleme konsepti açısından değerli olduğu belirtilmiştir. YAS modellemesi ile ilgili farklı kategorilere ait bilgiler Ek-1 (sayfa 9-15)'te açıklanmıştır.

2.3.1. Yeraltısuyu modelleme çalışması için gerekli veriler.

Veri toplama, model uygulama sürecindeki önemli bileşenlerden biridir. Sayısal bir modelin geliştirilmesi ve test edilmesi için gerekli olan kantitatif hidrolojik veriler iki kısma ayrılabilir: (A) fiziksel ve (B) hidrolojik çerçeveler. YAS modellemesi için fiziksel ve hidrolojik çerçeve verilerinin özeti Çizelge 2.1'de özetlenmiştir. Verilerin detay açıklaması ve modele göre kullanımı Ek-1 (sayfa 15)'te sunulmuştur.

Çizelge 2.1. YAS modellemesi için fiziksel ve hidrolojik çerçeve verilerinin özeti

Fiziksel çerçeve altındaki veriler	**Bu çalışmada kullanılan veri tipleri**	**Hidrolojik çerçeve altındaki veriler**	**Bu çalışmada kullanılan veri tipleri**
Topografya	✓	YAS yükselme seviyesi	✓
Jeoloji	✓	Yağıştan (net) beslenme	✓
Akifer türleri	✓	Deşarj oranı (pompalama)	✓
Akifer kalınlığı	✓	YAS beslenim alanlarının türü ve kapsamı	✓
Akifer sınırları	✓	Deşarj alanlarının türü ve kapsamı	
Litolojik veriler		Terleme ve buharlaşma	
Akifer özellikleri		Hidrolik iletkenlik değerleri	✓
		Geçirgenlik	

2.4. Model Kalibrasyonu

Bu tez çalışmasında uygulanan model kalibrasyonu aşaması, önceden belirlenmiş bir hata aralığı içinde kalmak üzere alan ölçüm değerleriyle eşleşen hidrolik iletkenlik, net beslenim ve hidrolojik sınır koşulları gibi bir dizi parametre değerinin bulunmasını içerir. Kalibrasyon aşaması, öngörü simülasyonunu sağlayan modelleme sürecinin zorunlu bir parçasıdır. YAS modelinde kullanılabilecek kalibrasyon seçenekleri: (A) deneme-ve-yanılma yoluyla manuel kalibrasyon, (B) bir bilgisayar algoritması yardımıyla otomatik kalibrasyon (parametre tahmini) ya da (PEST) olarak sınıflandırılabilir. Anderson vd. (1990), YAS modellemesinin ilk adımında manuel kalibrasyonu önermiştir ve sonrasında otomatik kalibrasyon (parametre tahmini) gerçekleştirilebilir. Bu çalışmada, her iki kalibrasyon yaklaşımı kullanılmış ise de, parametre tahmin aracı (PEST) kullanılarak otomatik kalibrasyon yapılması seçeneğine daha fazla önem verilmeye çalışılmıştır. Model kalibrasyonu ile ilgili ayrıntılar Ek-1 (sayfa 17 – 19)'da açıklanmıştır.

2.5. Karst Sistemlerinde Yeraltısuyu Akımını Tanımlamak için Yaklaşımlar

Karst akiferleri yüksek heterojenlik ve süreksizlik, beslenim ikiliği/çiftlik (duality), infiltrasyon gözenekliliği, depolama ve akış ile karakterize edilir (Ford ve Williams 2007; Goldscheider ve Drew 2007). Bu nedenle, karstik sistemlerinin modellenmesi için özel araştırma tekniklerine ihtiyaç duyulur. Karst akiferleri poroz ortamdan (porous media) önemli ölçüde farklı olduğundan, karakterizasyon yöntemleri de farklıdır (Groves 2007). Goldscheider (2015) tarafından karst akiferlerinde kullanılan yöntemlerin çoğunun poroz ortam hidrojeolojisinde kullanılan yöntemlere benzediğini ileri sürmektedir. Ayrıca Goldscheider (2015), bu yöntemleri bir karst alanında kullanırken spesifik modifikasyonların gerekli olduğunu belirtmiştir. Karst akiferindeki YAS akışının modellenmesi için farklı yaklaşımların detayları Ek-1 (sayfa 20 – 22)'de

yer almaktadır. Günümüzde karst akiferlerinde YAS akışını karakterize etmek için kullanılan çeşitli teknikler vardır ve her birinin avantaj ve dezavantajları da mevcuttur. Karst akiferleri için iki genel modelleme metodu tanımlanmıştır: (a) mekansal olarak toplu modeller (spatially lumped models) ve (b) mekansal olarak dağıtılan modeller (spatially distributed models). Karst akiferlerinde modelleme yöntemleri ve önceki çalışmaların özeti Ek-1 (sayfa 23-26)'da sunulmuştur.

Altinova bölgesinde grafiksel Visual MOFLOW Flex tabanlı eşdeğer gözenekli medya yaklaşımı kullanılarak gerçekleştirilmiştir. Visual MODFLOW gibi sayısal model birçok araştırmacı tarafından YAS kaynaklarının modellenmesinde ve yönetiminde kullanılmıştır (Wang, S vd. 2007; Elc vd. 2010; Xu, vd. 2011; Varouchakis vd. 2015; Qadir vd. 2016). Panagopoulos (2012), Visual MODFLOW'un akifer parametrelerini geliştirmek, tahmin etmek ve iklim değişikliği ya da akifer sistemindeki YAS çekimin değişikliğinin etkisini tahmin etmek için yararlı bir araç olduğunu belirtilmiştir. Bu tez çalışması, Altınova bölgesindeki YAS akışı ve modellemesi konusunda özgün sonuçlara ulaşılması açısından önemlidir ve bu çalımasın Altınova bölgesindeki ilk kez Visual MODFLOW flex kullanarak YAS akış sistemini simüle gerçekleştirilmiştir. Bu ilk deneme Altınova bölgesinde YAS akış bilgisini önemli yönde sağlanmıştır ve aynı yaklaşım benzer bir karst bölgesinde uygulanabilir.

3. MATERYAL VE METOT

3.1. Çalışma Alanının Genel Tanımı ve Özellikleri

Çalışma alanı olan Altınova bölgesi yaklaşık 75 km2'lik bir alanı kapsamakta olup, dağların bir traverten platosunun düzlüklerini oluşturan güney yönünde dağıldığı bir ovada yer almaktadır. Bölge, Antalya uluslararası havalimanının kuzeybatı sınırında, 36° 54'0' ve 37°2'0' kuzey enlemleri ile 30° 43'0' ve 30° 50'0' doğu boylamları arasında yer almaktadır. Çalışma bölgesinin batı sınırı boyunca Düden Nehri ve doğu sınırı boyunca Isparta yolu uzanır. Çalışma alanı platonun kuzey sınırında olup, deniz seviyesinden ortalama 80 m yükseklikte bulunmaktadır. Bölgenin topografyası, güney sınırında 50 m'den daha az ve kuzey sınırında 300 m'den daha fazla değişmektedir. Çalışma alanı ve topoğrafyası Şekil 3.1'de gösterilmektedir. Traverten kalınlığı üst platoda 160-240 m, alt platoda 60-120 m arasında değişmektedir (Efe ve Soykan, 2008). Antalya'nın kuzeydoğu kesiminde toplam kalınlık 20-30 m'ye düşmektedir. Altınova bölgesindeki Kurşunlu ve Traverten formasyonlarının kalınlığı 30-180 m arasında değişmektedir ve bu konuya ilişkin detaylar Ek-1(sayfa 44)'te sunulmaktadır.

Çalışma bölgesi ağırlıklı olarak çiftçiler için bir yerleşim yeridir. Son on yılda, bölgede yoğun tarımsal gelişme gerçekleşmiş olup alanın çoğu tarımsal araziler ve seralar ile kaplanmıştır (Çil vd. 2016). Çalışma alanındaki seraların toplam alanı 13,7 km2'dir. Seralarda yaygın olarak yetiştirilen meyze/sebzeler; domates, salatalık, maydanoz, kavun, karpuz, çilek olup bölgede çiçek yetiştiriciliği de yoğun olarak görülmektedir. Pilot çalışma bölgesindeki açık alanlarda bazı meyve ağaçları, tarım alanları ve hayvancılık faaliyetleri de bulunmaktadır. Yağmurlu dönemde sadece üç ila dört ay boyunca net beslenim olan YAS, ana sulama kaynağıdır. Çiftçilerin çoğunun sulama için özel kuyuları vardır. Altınova bölgesinde sanayi ve yerleşim alanları da mevcut olup, ağırlıklı olarak sanayi faaliyetleri için YASa bağımlıdırlar. Pilot çalışma alanı içinde ruhsatlı olmayan (kaçak) kuyular da bulunmaktadır. Pilot çalışma alanındaki temel yaygın kirleticiler; evsel atıklar, endüstriyel atıklar, gübreler ve pestisitler gibi tarım amaçlı kullanılan kimyasalları içeren antropojenik kaynaklardır. Ayrıca, Altınova bölgesinde kentsel atıksuların uzaklaştırılması için kanalizasyon sistemi mevcut değildir; sadece bölgenin batı kısmında küçük bir şebeke bulunmaktadır (Çil vd. 2016). Buna bağlı olarak, bölge sakinlerinin atıksuları foseptik tankları aracılığıyla yeraltına boşalmaktadır.

Altınova bölgesinin kirlenmeye karşı hassas olan akiferindeki mevcut/çeşitli arazi kullanımları nedeniyle YASın kalitesi ve miktarı olumsuz etkilenmektedir. Altınova akiferinde ölçülen nitrat konsantrasyonları, 2 mg/L'den 100 mg/L'ye kadar olan yüksek mekansal değişimler göstermiştir, zamansal olarak önemli bir değişim yoktur (Çil vd. 2016). Çalışma alanının arazi kullanımına bağlı olarak, Altınova bölgesindeki akifer kaynaklarını tehdit eden en önemli kirleticiler, tarım ve evsel olmak üzere antropojenik kaynaklardan gelmektedir. Alanın temel arazi kullanım haritası Ek-1 (sayfa 28)'de sunulmuştur.

Antalya yöresinin jeolojik formasyonları kumtaşı, kireçtaşı, konglomera, killi kireçtaşı, taşlanmış kireçtaşı (brecciated limestone) ve kiltaşıdır (Dipova ve Doyuran 2006). Çalışma alanının jeolojik oluşumu başlıca traverten, konglomera ve alüvyondur. Çalışma alanının yaklaşık 63 km2'lik kısmı, karst traverten formasyonu ile kaplıdır.

Karst traverteni, Türkiye'nin Akdeniz bölgesinin güneybatısında hakim olan jeolojik oluşumlardan biridir. Karst traverteni, toplam çalışma alanının yaklaşık %85'ini oluşturmaktadır. Kumtaşı çoğunlukla çalışma alanının doğu kısmını kaplar ve yaklaşık %14'lük bir kısmı oluşturur. Üçüncü jeolojik oluşum ise, çalışma alanının sadece %1'ini kaplayan alüvyondur. Çalışma alanına ait jeoloji ve hidrojeoloji haritaları Ek-1 (sayfa 30 - 31)'de gösterilmiştir. Çalışma alanında Akdeniz iklimi hakimdir. 1994 - 2017 yılları arasındaki dönem için çalışma alanına en yakın meteoroloji istasyonundan (Antalya Havalimanı) elde edilen meteorolojik verilere göre, Altınova bölgesinin yıllık ortalama yağış miktarı 1191,5 mm/yıl olarak hesaplanmıştır. En yüksek toplam yağış miktarı 2001 yılında gözlemlenmiş, en düşük yağış ise 2015, 2016 ve 2017 yıllarında olmuştur. Çalışma alanının klimatolojik durumu Ek-1 (sayfa 31 – 33)'de sunulmuştur.

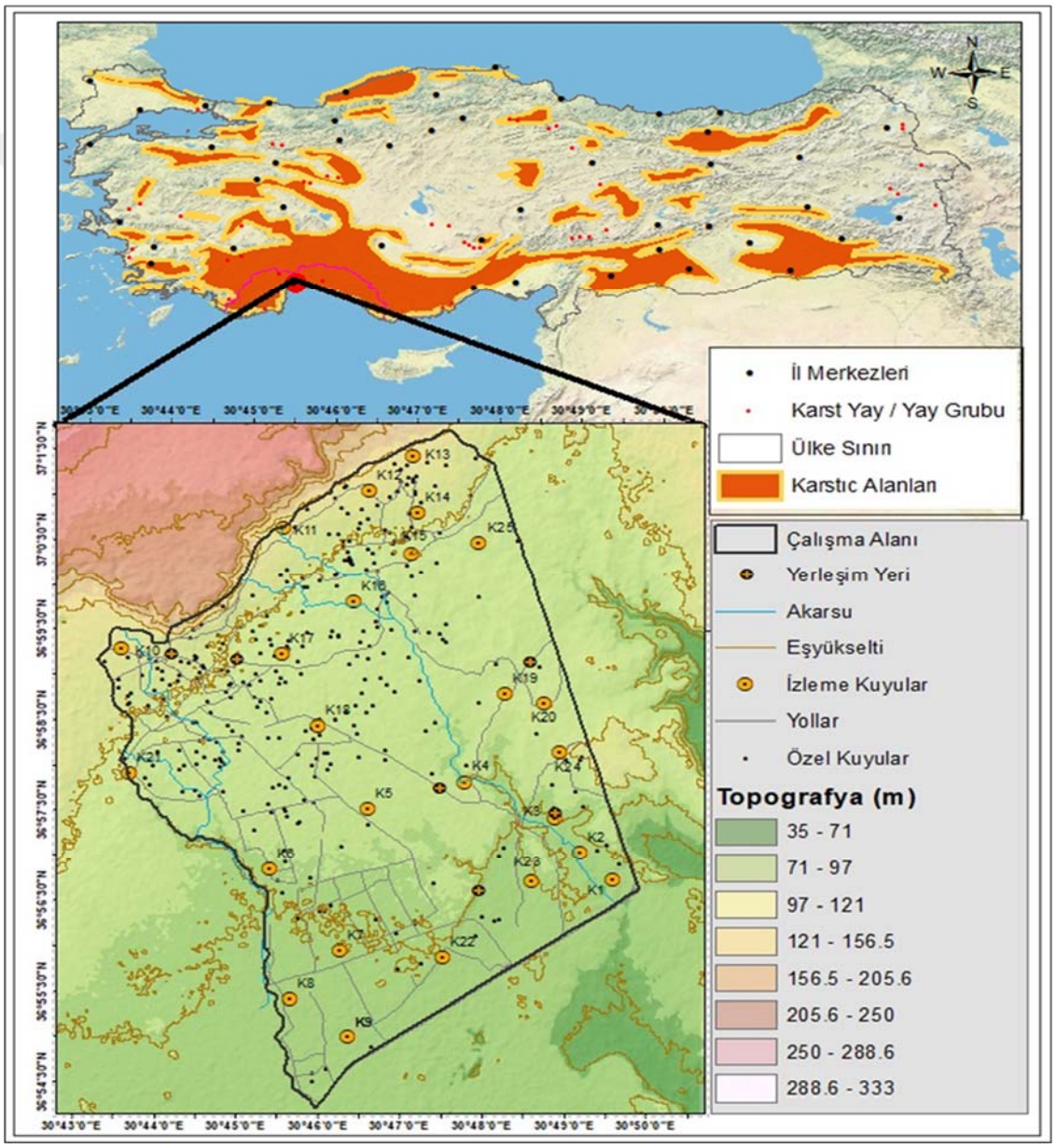

Şekil 3.1.Türkiye'de Antalya-Altınova'da seçilen pilot çalışma sahasının lokasyonu

3.2. Model Uygulaması

3.2.1. Saha çalışması

Verilerin toplanması ve organize edilmesi, başarılı bir YAS modeli uygulanmasının önemli bir kısmıdır. Yağış, sıcaklık gibi iklimsel veri kümeleri Antalya Meteoroloji Genel Müdürlüğü 4. Bölge Müdürlüğü'nden temin edilmiştir. YAS seviyesi verileri, daha önce tamamlanmış olan 114Y696 nolu TÜBİTAK projesi veri tabanından alınmıştır. TÜBİTAK proje ekibinin YAS seviyesini belirlemek için kullandığı yöntem ve saha teknikleri, Ek-1 (sayfa 33-34)'de açıklanmıştır. İlk izleme çalışmasında bölgeyi temsil eden 25 adet izleme/örnekleme kuyusu seçilmiştir. Proje ekibi, YAS derinliği ölçümlerini üç farklı dönemde gerçekleştirmiştir; Kasım 2015, Şubat 2016 ve Mayıs 2016. YAS seviyesi, ölçülen YAS derinliğinin yüzey kotundan çıkarılması ile hesaplanmıştır. Hesaplanan ortalama YAS seviyeleri Şekil 3.2'de sunulmuştur. Ortalama derinlikteki YAS haritaları Ek-1 (sayfa 35-36)'da sunulmuştur. Hidrolojik veriler, analiz edilmiş ve veri tabanı Coğrafi Bilgi Sistemi (CBS) yardımıyla sentezlenmiştir. Kasım 2015, Şubat 2016 ve Mayıs 2016 aylarına ait mevsimsel YAS seviyeleri Ek-1 (sayfa 37-39)'da sunulmuştur.

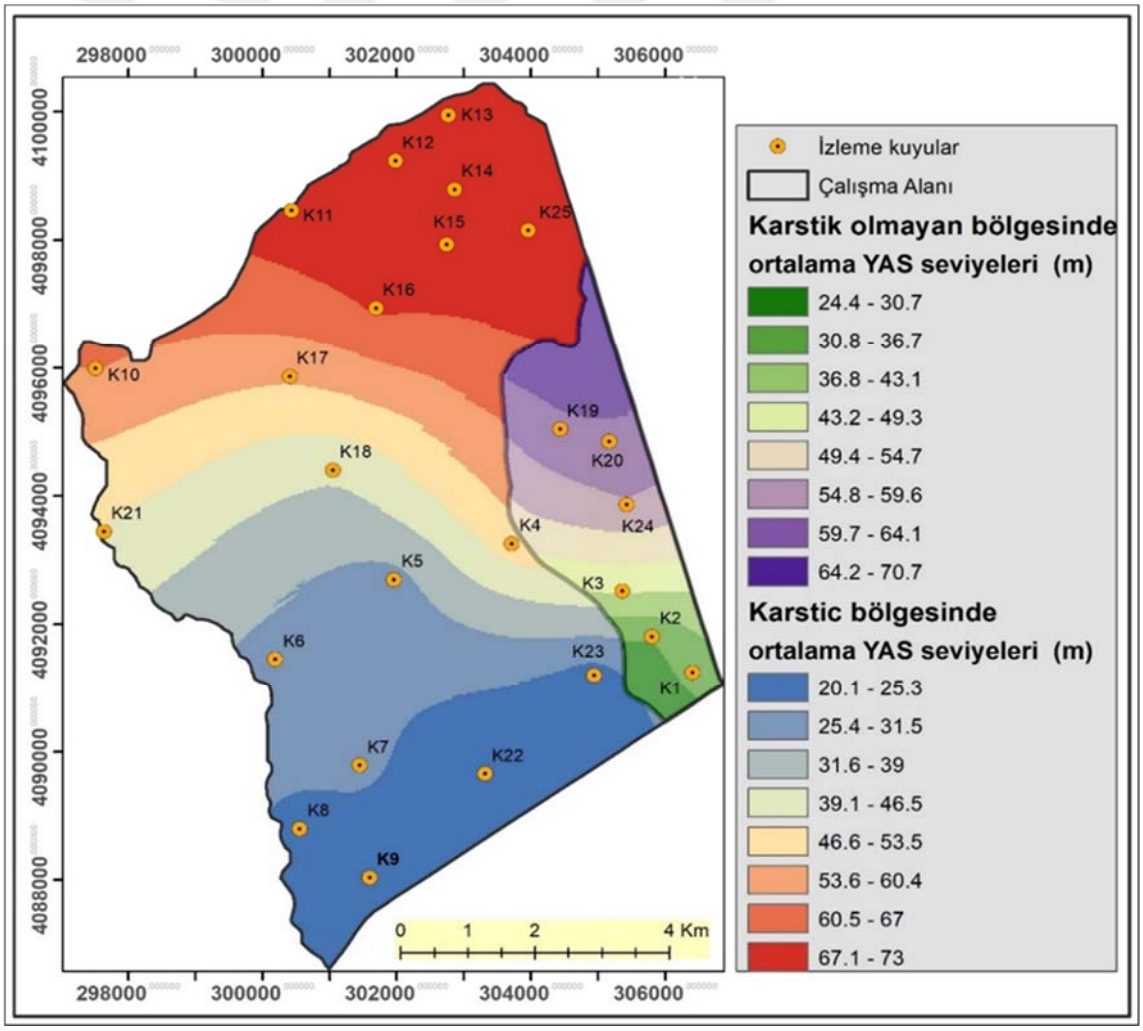

Şekil 3.2 Altınova'nın karstik ve karstik olmayan bölgesinde ortalama YAS seviyeleri

3.3. Model Tasarımı ve Ayrıştırma Teknikleri

Akış modeli, kararlı hal doymuş sabit yoğunluğa ayarlanmıştır. Simülasyon başlama tarihi 18.Kasım.2015 olarak belirlenmiş olup tam olarak YAS seviyesinin ilk alan ölçümü ile çakışan başlangıç tarihidir. Model, dikey/z-yönündeki (kz) hidrolik iletkenlik eksikliğinden dolayı tek katmanlı olarak belirlenmiştir. Öncelikle, kavramsal model alanı, tekdüze boyutlu sonlu farklar şebekesi veya hücre (finite-difference grids) yapısı kullanılarak ayrılmış ve mekânsal çözünürlük 25600 m2'lik bir boyutta tasarlanmıştır. Modellenen alan, 87 sütun ve 62 satır olmak üzere 10792 adet grid ağına bölünmüştür. Model uygulama alanı 5800 aktif ve 4992 inaktif hücreye bölünmüştür. Aktif olmayan hücreler, kavramsal modelin sayısal modele dönüştürülmesi sırasında otomatik olarak tanımlanmıştır. Model uygulama alanı dışındaki hücreler inaktif olarak, model uygulama alanı içindeki hücreler ise aktif olarak işaretlenmiştir. Model uygulamasında ikinci adım, kavramsal modelin sayısal modele dönüştürülmesidir. Modelin üst yüzeyi, doğrudan 30 m çözünürlükteki sayısal veya dijital yükseklik modelinden (DEM) elde edilmiştir. Modelin alt yüzeyi, dijital yükseklik modelinden, akifer kalınlığının çıkarılması yöntemi ve CBS yardımıyla hesaplanmıştır. Modelin üst ve alt yüzeylerinin iki boyutlu ve üç boyutlu görünümleri Ek-1 (sayfa 46 ve 47)'de sunulmuştur.

Hidrolik iletkenlik ve YASın yağıştan net beslenimi, modelin ana parametreleridir. Model alanı iki farklı beslenim ve hidrolik iletkenlik bölgesine ayrılmıştır. Yanal/yatay hidrolik iletkenlik (kyx) değerleri için ilk kabul değerleri TÜBİTAK projesi raporundan alınmıştır (Muhammetoğlu vd. 2017). Buna göre karstik alana ait hidrolik iletkenlik için ilk atanmış değer 86,4 m/gün, karstik olmayan formasyon içinse 0,864 m/gün değeri belirlenmiştir Ek-1 (sayfa 48).

Bu çalışmada, YASın yağışlardan net beslenim oranı, yağış miktarının yüzdesi olarak kabul edilmektedir. Yağışlardan net beslenim oranı, 2015-2016 yılları arasında kaydedilen yıllık yağış yüzdesi dikkate alınarak tahmin edilmiştir. Belirtilen yıllar, simülasyon dönemi ile çakıştığı için seçilmiştir. Çalışma alanında karst bölgesindeki yağış miktarının yaklaşık %44'ü ve karst olmayan bölgedeki yağışların yaklaşık %15'i akiferi beslemektedir (AMPR 2016). Bu nedenle, net YAS beslenimi meteorolojik veriler kullanılarak, karstik bölge için 279,2 mm/yıl ve karstik olmayan bölge için 95,2 mm/yıl olarak hesaplanmıştır. Modelde üç tür sınır koşulu tanımlanması gerekmektedir. Genel hidrolik yük sınırı veya genel seviye sınırı (General Head Boundary), beslenme sınırı, akış olmayan sınır (No flow boundary) **(**Şekil 3.3). Sayısal modelin sınır koşulları ile ilgili detaylar Ek-1 (sayfa 50 – 53)'te sunulmuştur. Bir diğer model giriş parametresi ise pompaj hızıdır (pumping rate).

Çalışma alanında pompaj hızı verisi eksikliği nedeniyle YAS çekilme oranı tahmin edilmiştir. YASın tarımsal su kaynaklarından çekilmesine ait tahmin protokolü, Ek-1 (sayfa 55-56)'da açıklanmıştır. Bu aşamada MODFLOW-2005 modelini çalıştırmak için Önşartlı Çekme Gradyanı veya (Preconditioned Conjugate Gradient Solver) (PCG) uygulanmıştır. Model kurulumu, PCG çözücü özellikleri, hidrolojik model yüzeylerin/katmanların geliştirilmesi ve model parametrelerinin açıklaması Ek-1 (sayfa 57 – 58)'de açıklanmıştır.

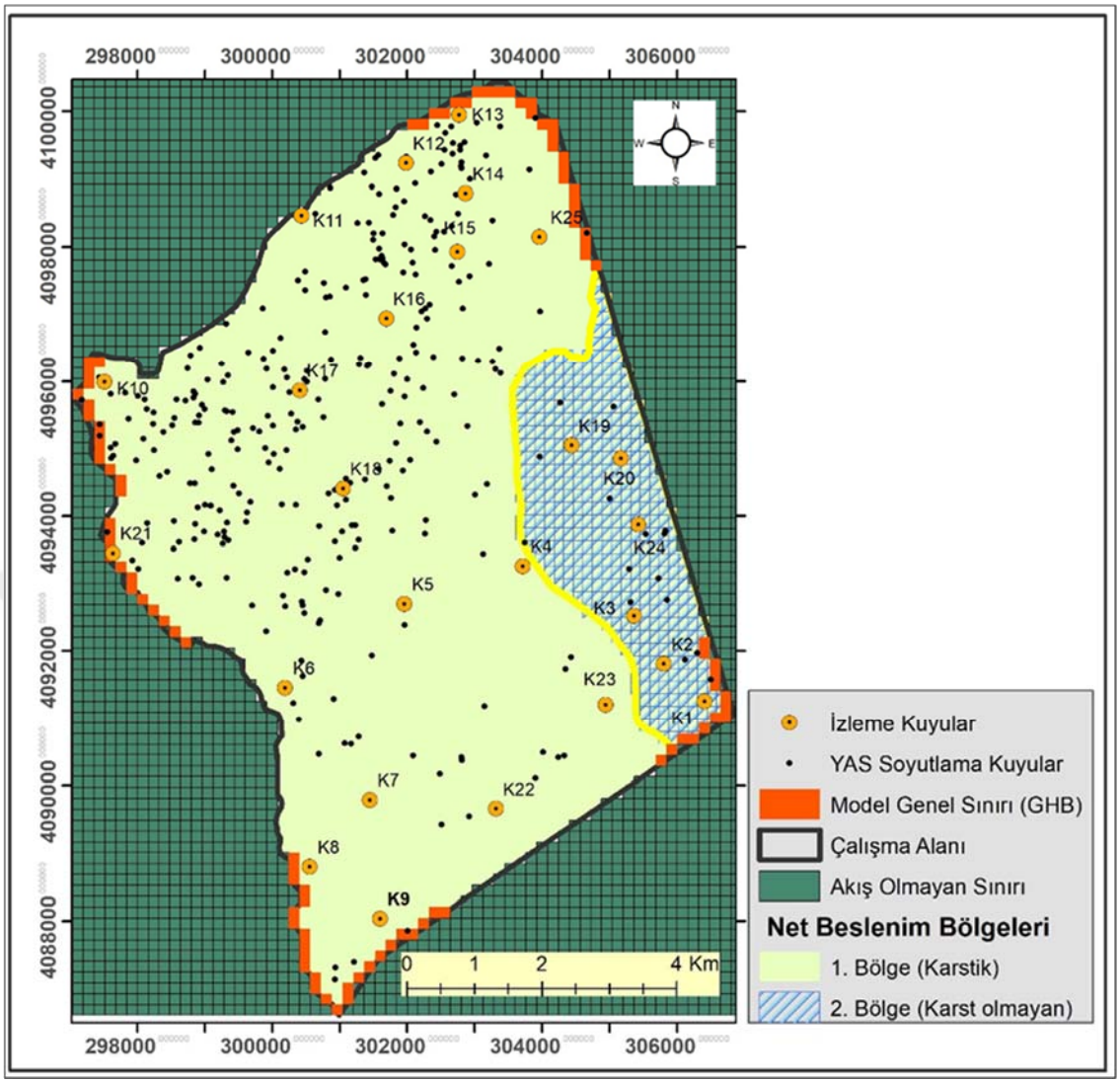

Şekil 3.3.. Kararlı durum modeli için uygulanan koşul sınırları

3.4. Model Kalibrasyonu ve Değerlendirme

YAS modellemesinde çok sayıda parametrenin varlığı nedeniyle YAS modelinin kalibrasyonu tüm modelleme sürecinde en zorlu görevdir (Doherty ve Hunt 2010). Bu nedenle, çalışmada model kalibrasyonu, parametre tahmin aracı (PEST) kullanılarak otomatik olarak gerçekleştirilmiştir (Doherty ve Hunt 2010; Waterloo 2018). Kalibrasyon işleminin amacı, model parametrelerini sistemli bir şekilde belirlemek ve böylece YAS seviyesi tahminleri ile ölçülen YAS seviyesi arasındaki uyumu sağlamaktır. Model Kasım 2015, Şubat 2016 ve Mayıs 2016'da 25 kuyuda ölçülen ortalama YAS verilerine göre kalibre edilmiştir. Kalibrasyon prosedürü, Ek-1 (sayfa 58 – 60)'da sunulmuştur. YAS modelinin performansını kantitatif olarak değerlendirmek için ortalama karekök hatası (RMSE), ortalama mutlak hata (MAE), korelasyon katsayısı (R2) ve normalize ortalama karekök hatasını (NRMSE) içeren bazı istatistiksel indeksler kullanılmıştır (Anderson vd. 1990). Model tahmin değerlendirmesi ve hata ölçümleri ile ilgili detaylar Ek-1 (sayfa 60 – 62)'de sunulmuştur.

3.5. Yönetim Senaryolarının Analizi

Türkiye'nin Akdeniz bölgeleri, iklim değişikliğine hassastır. Akdeniz bölgesindeki iklim değişikliği sonuçlarının sıcaklıkta artış ve yağışlarda azalmayı içerdiği bilinmektedir (Tayanç vd. 2009; Lelieveld vd. 2012; Unal vd. 2012; Kum ve Çelik 2014). Benzer şekilde, Antalya'daki tarımsal faaliyetlerdeki artış nedeniyle YAStan çekilen su miktarı da giderek artmakta, bu durum YAS kaynaklarının azalmasına neden olabilmektedir. Yağışların azalması ile YAStaki net beslenmenin azalması beklenmekte ve dolayısıyla sulama için YAS çekiminde ve pompaj hızında bir artışa neden olacağı düşünülmektedir. Bu bağlamda, tez çalışmasının da temel amacı, Altınova bölgesindeki yağış miktarındaki azalmanın ve YAS çekimindeki artışın etkilerinin sayısal bir model kullanılarak farklı yönetim senaryoları ile incelenmesidir. Araştırma amaçlarına ulaşmak için üç senaryo geliştirilmiştir. Senaryo (A) yağışlarda beklenen azalmayı, Senaryo (B) YAS çekimindeki artışı, Senaryo (C) ise yağışlarda beklenen azalmayı ve YAS çekimindeki artışı incelemek üzere tanımlanmıştır.

Model senaryolarının geliştirilmesinin temel amacı, Altınova'nın karstik ve karstik olmayan bölgesindeki YAS seviyesi değişimini değerlendirmektir. Oluşturulan senaryo koşulları; Senaryo (A): mevcut YAS çekimi ile yağışta %50 oranında bir azalma olduğunu varsaymıştır, Senaryo (B): mevcut yağış miktarında YAS çekiminde %50 oranında artış olduğunu varsaymıştır. Senaryo (C): yağış miktarında %50 oranında azalma ve YAS çekiminde %50 artış olduğunu varsaymıştır. Model yönetim senaryoları Çizelge 3.1'de özetlenmiştir. Altınova'nın karstik ve karstik olmayan akiferleri için farklı yönetim senaryoları sonucunda oluşan YAS seviyesi değişimleri mevcut durum ile karşılaştırılarak değerlendirilmiştir. Ayrıca, hidrolik iletkenlik için kalibre edilmiş değerler ±%50 oranında değiştirilerek model için duyarlılık analizi yapılmıştır. Duyarlılık analizi uygulanırken, hidrolik iletkenlik parametresinin etkisi test edildiğinden, diğer tüm model parametreleri kararlı hal durumunda tutulmuştur. Duyarlılık analizinde, parametre değeri tüm model alanı üzerinde eşit olarak değiştirilmiştir. Hidrolik iletkenliğin ± %50 oranında değiştirilmesi amacı ile toplam iki model çalışması yapılmıştır.

Çizelge 3.1..Model yönetimi senaryolar

Artış / Azalış Oranı	**Senaryolar**
Yağış miktarında %50 oranında azalma	Senaryo (A)
YAS çekiminde %50 oranında artış	Senaryo (B)
Yağış miktarında %50 oranında azalma + YAS çekiminde %50 oranında artış	Senaryo (C)

4. BULGULAR VE TARTIŞMA

4.1. Hidrolik İletkenlik Parametresinin Kalibrasyonu

Kararlı durumda, kalibrasyonda yer alan tek parametre yanal yöndeki hidrolik iletkenlik parametresidir. Kalibre edilmiş hidrolik iletkenlik değerleri Şekil 4.1'de mekânsal olarak sunulmuştur. Çalışma alanı için tanımlanan hidrolik iletkenlik değerleri 0,01 m/gün ile 266,5 m/gün arasında değişmektedir. Çalışma alanının karstik traverten bölgesinde 0,60 ile 239 m/gün arasında değişen hidrolik iletkenlik değerleri bulunmuştur. Ancak, karstik olmayan bölgedeki hidrolik iletkenlik değerleri 0,01 ila 1,13 m/gün arasında değişmektedir. Hidrolik iletkenlik değerlerinin karstik olmayan alanda düşük, karstik alanda daha yüksek olması tutarlıdır. Ayrıca, karst traverteninin güney kısımlarında daha düşük YAS yükselmesine bağlı olarak hidrolik iletkenlik değerleri de daha yüksektir. Bu durumun tersi, karst traverteninin kuzey kesiminde gerçekleşmiştir. Karst traverteninin güney kesiminde 266,5 m/gün'e kadar yükselen hidrolik iletkenlik değerleri gözlenmiştir (Şekil 4.1).

Bu modelleme çalışması, Altınova'nın traverten karst bölgesindeki hidrolik iletkenlik değerlerini tahmin etmek için yapılan ilk denemedir. Genel olarak, modelleme çalışmasında tanımlanan hidrolik iletkenlik değerlerinin mekânsal dağılımı, literatür değerleri ile uyumludur (Allan ve Cherry 1979). Çalışmamızda kalibre edilen yatay iletkenlik değerlerinin dağılımı, Altınova'nın karst traverten çalışılmasında kritik bir başlangıç noktası oluşturmaktadır. Ancak, model uygulamasında karst akiferlerin heterojenliği temsil edilmemektedir. Ayrıca, çalışma alanının karst sistemindeki uygun jeolojik verilerin bulunmaması nedeniyle mağaraların ve bataklıkların doğru konumları belirlenememiştir. Bu koşullar, çalışma alanının bazı kısımlarında kısmen hatalı hidrolik iletkenlik değerlerinin tanımlanmasına neden olabilmektedir.

İzleme kuyuları için kalibre edilen hidrolik iletkenlik değerleri traverten karst akiferde 0,6 ila 239 m/gün arasında değişmekte iken kurşunlu formasyonunda bulunan karstik olmayan alan için 0,01 ila 1,2 m/gün arasında değişmektedir. Karstik ve karstik olmayan alanlarda sırasıyla 0,01 ve 0,6 m/gün olarak kalibre edilen minimum hidrolik iletkenliği değerleri Denizli Kaklık'daki benzer bir akiferde yapılan çalışma ile uyumludur (Murat 2015). Altınova bölgesi için elde edilen maksimum hidrolik iletkenlik değerleri, Murat (2015) tarafından tahmin edilen değerlerin iki katıdır. Maksimum hidrolik iletkenlik değerlerindeki farklılığın, Murat (2015) tarafından kullanılan pompalama testi tahmin yaklaşımı ile bağlantılı olduğu düşünülmektedir. Karst akiferdeki kuyular için pompalama testi ile hesaplanan hidrolik iletkenlik değerleri, çoğu zaman gerçek değerlerden önemli ölçüde daha düşüktür (Scanlon vd. 2003).

Transmissivite değerleri 1,5 ile 42303 m2/gün arasında değişmekte olup aynı şekilde maksimum transmissivite değerleri Kaklık Akiferinde tahmin edilen değerlerden iki kat daha yüksektir (Murat 2015). Transmissivite değişimi, akifer kalınlığındaki değişime bağlıdır. Genel olarak, Altınova bölgesinin hem karstik, hem de karstik olmayan bölgesi için kalibre edilmiş hidrolik iletkenlik değerleri, literatür sınırları içerisindedir. Kuyuların izlenmesi için iletkenlik değerleri ve istatistiksel analizler, Ek-1 (sayfa 66 ve 67)'de sunulmuştur.

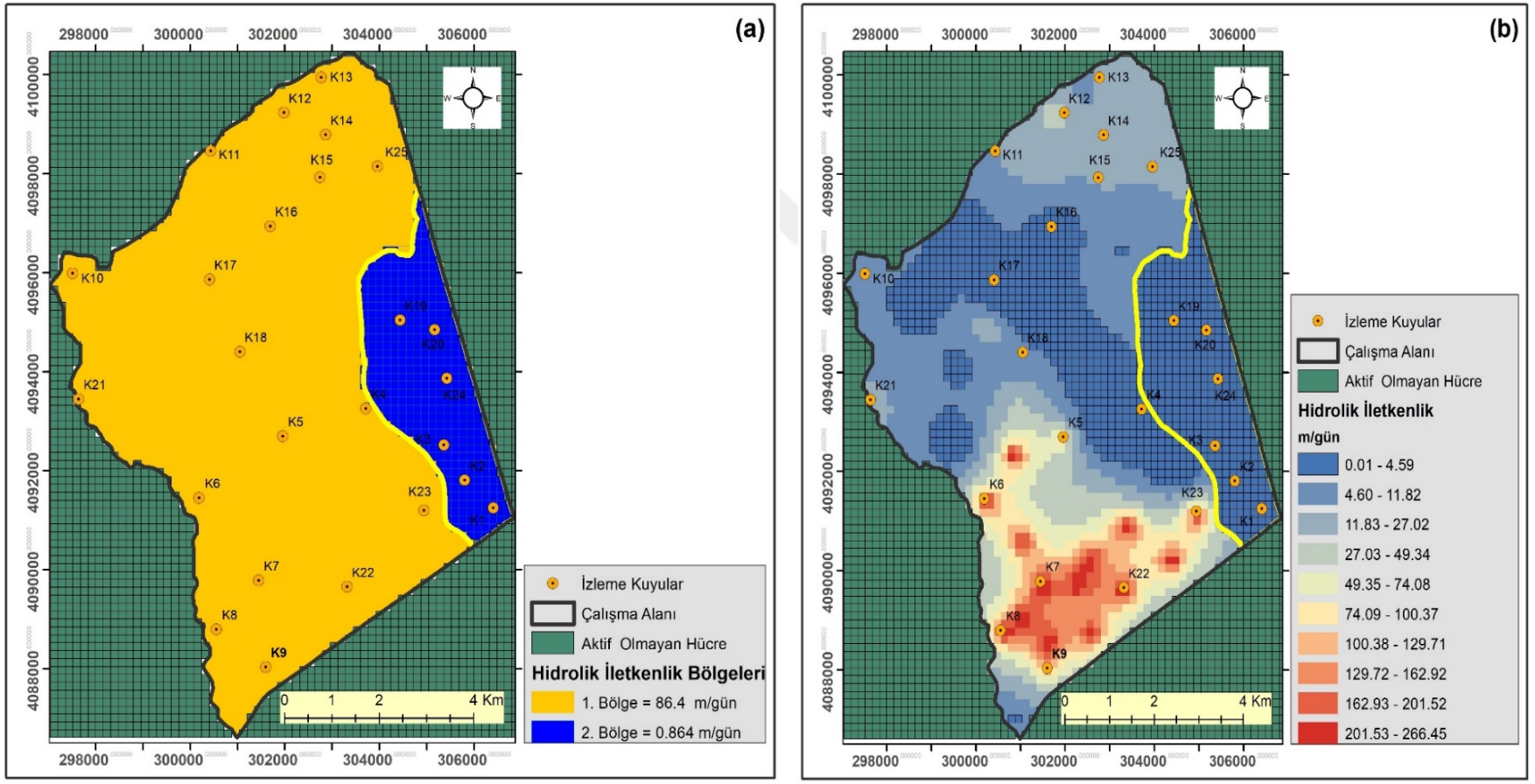

Şekil 4.1. Kalibrasyondan önceki hidrolik iletkenlik tanımları a); ve kalibrasyondan sonraki hidrolik iletkenlik değerleri b)

4.2. Kalibre edilmiş yeraltısuyu akış modeli sonuçları

Bu çalışmada modelin kalibrasyonu, parametre tahmin aracı (PEST) kullanılarak otomatik olarak gerçekleştirilmiştir. Kalibrasyon çalışmalarında modelin uyumluluğunu kontrol etmek için arazide ölçülen 25 adet kuyuda ölçülen YAS seviyesi verilerinden yararlanılmıştır. Seçilen 25 adet kuyuda ölçülen YAS seviyeleri, modelden elde edilen YAS seviyesi ile karşılaştırılmıştır. Genel olarak, çalışma alanı için kararlı durumda kalibrasyon sonucu elde edilen YAS seviyesi tahminleri, sahada ölçülen YAS sevileri arasında iyi bir uyum sağlanmıştır. Tahminler ve ölçümler arasındaki fark değerleri sıfır etrafında rastgele dağıtılmıştır. Fark değerleri için ortalama kalıntı (RM), ortalama mutlak hata (AME), ortalama karekök hatası (RMSE) ve normalize ortalama karekök hatası (NRMSE) sırasıyla 0,6 m, 1,5 m, 1,7 m ve %4,8'dir. Genel olarak, çalışma alanındaki kalibrasyon sonuçları, tahmin edilen ve ölçülen YAS seviyeleri arasında iyi uyum göstermiştir. Korelasyon katsayısı R2 değeri Şekil 4.2'de gösterildiği gibi 0,99 olarak hesaplanmıştır ve yüksek uyumu göstermektedir. Bu değer, model doğruluğunun kabul edilebilir olduğunu göstermiştir. Model tahminleri, çalışma alanının güney kısmında yer alan izleme kuyularında daha az başarılıdır (Şekil 4.3). Kasım 2015, Şubat 2016 ve Mayıs 2016'da ölçülen YAS seviyelerinin, kalibre edilmiş model ile tahmin edilen YAS seviyeleri ile karşılaştırılması Ek-1 (sayfa 86 – 89)'da sunulmuştur.

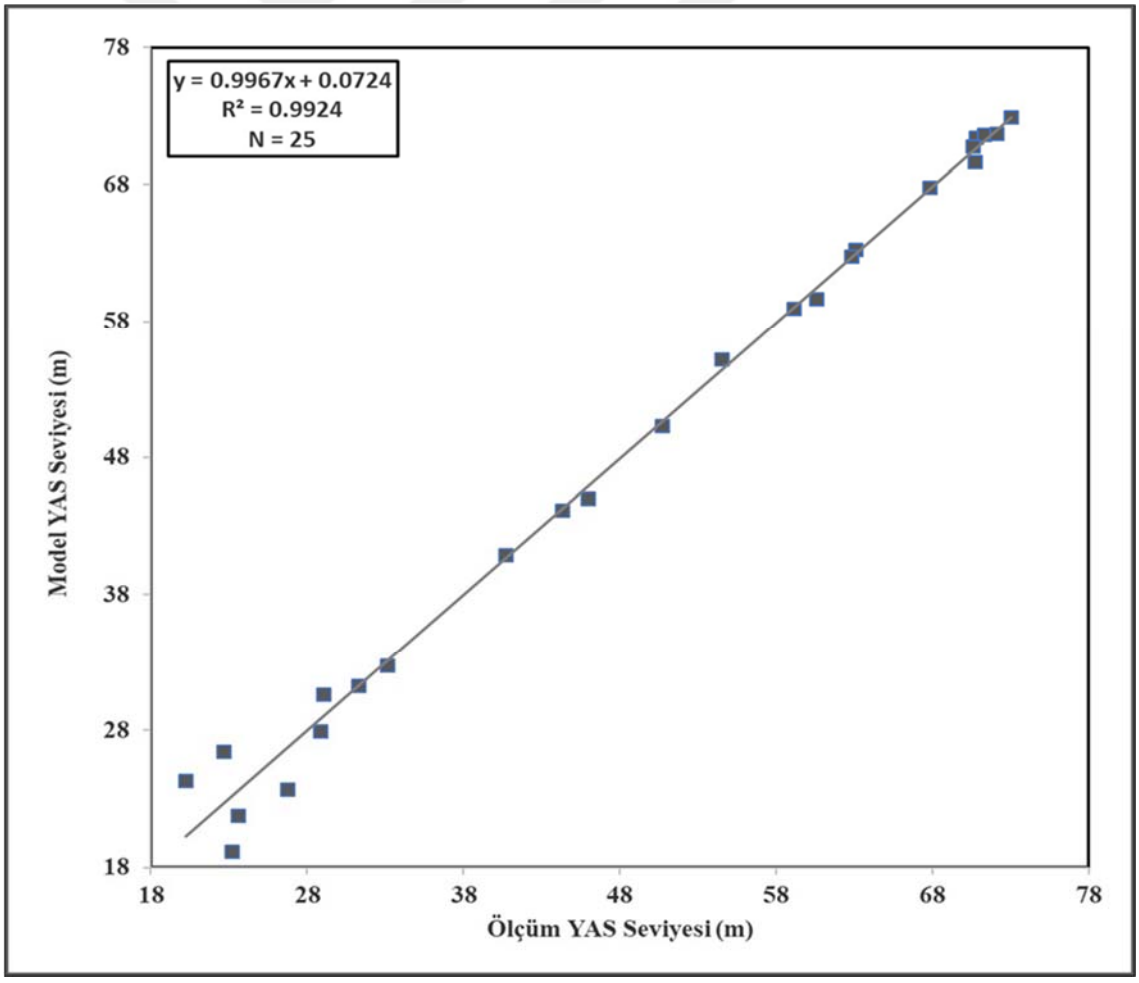

Şekil 4.2.. Kalibrasyon sonucu modelden tahmin edilen ve ölçülen YAS seviyeleri

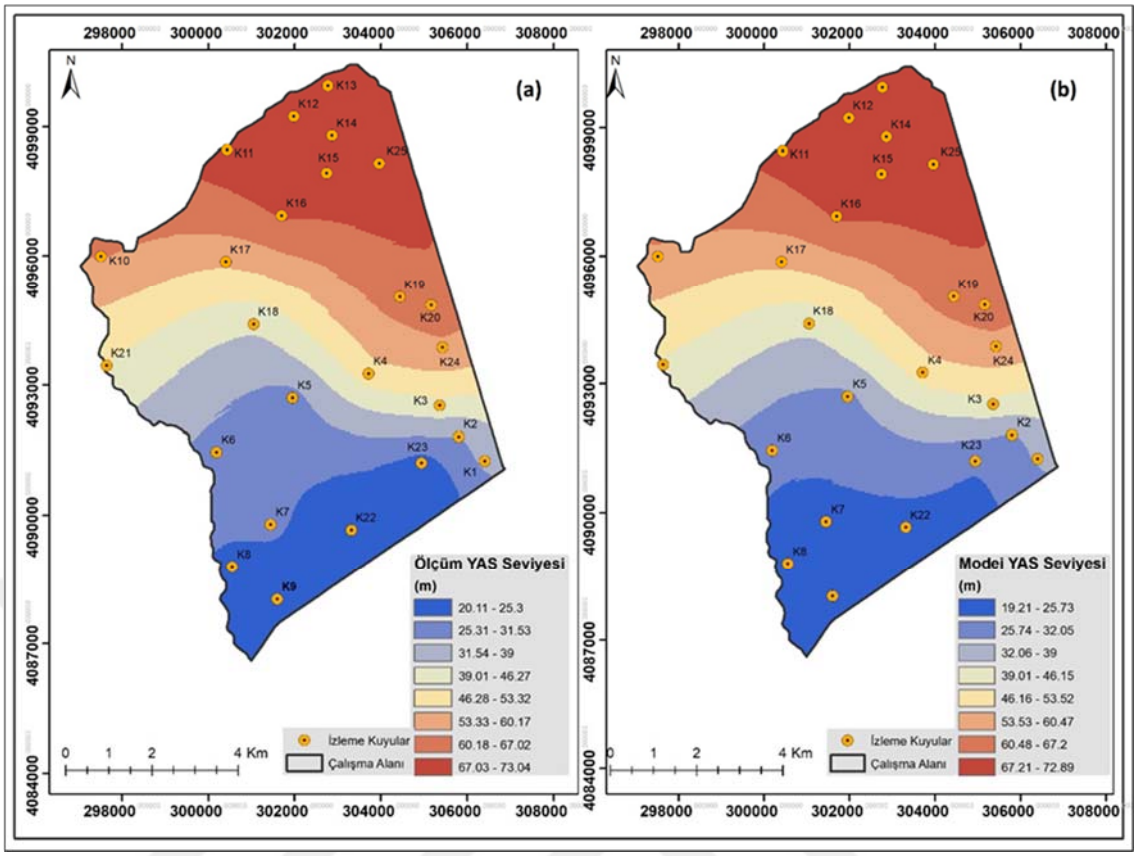

Şekil 4.3. Ölçülen (a) ve kalibrasyon çalışması sonucunda tahmin edilen (b) YAS seviyelerinin mekansal dağılımı

4.3. Karst ve Karst olmayan Alanlar için Yeraltısuyu Seviyesi Tahminlerinin Karşılaştırılması

Şekil 4.4 ve Şekil 4.5'te, karstik ve karstik olmayan bölgelerdeki YAS seviyelerinin karşılaştırılması gösterilmektedir. Karstik olmayan bölgedeki YAS seviyesi tahminleri 29-69 m arasında değişmektedir (Şekil 4.4). Karstik alandaki YAS seviyesi tahminleri ise Şekil 4.5'ten görüldüğü gibi 19 ila 72 m arasında değişmektedir. YAS modelinin karstik olmayan bölgedeki YAS seviyelerini, karstik olan bölgeye göre daha başarılı şekilde simüle ettiği görülmüştür. Şekil 4.6'dan görülebileceği gibi, karstik bölgede yer alan kuyularda ölçülen ve bu alan için tahmin edilen YAS seviyeleri arasındaki fark 5 m sınırı içinde kalmıştır. Karstik olmayan bölgede yer alan kuyularda ölçülen ve bu alan için tahmin edilen YAS seviyeleri arasındaki fark ise oldukça azdır ve sıfıra yakın olarak dağılmıştır. Altınova bölgesine ilişkin YAS modeli uygulamasında, karstik olmayan bölge için daha yüksek benzerlik oranı elde edilmiştir. Model sonuçları, karstik bölge için kabul edilebilir olmasına rağmen, çalışma alanının güney kesiminde daha az başarılıdır. Bu durum, Visual MODFLOW modelinin, karstik olmayan bölgede, traverten karst alanına göre daha öngörülebilir olduğunu göstermiştir. Bu çalışmada uygulanan yaklaşımın, karst sisteminin güçlü heterojenliğini dikkate almadığı unutulmamalıdır. Ayrıca akifer parametrelerine ilişkin detaylı veri setleri de bulunmamaktadır. Akifer parametrelerinin çoğu literatür kaynaklarına ve profesyonel yargıya dayanmaktadır. Bu faktörler simülasyon sonucunda tahmin hatalarına neden olabilmektedir.

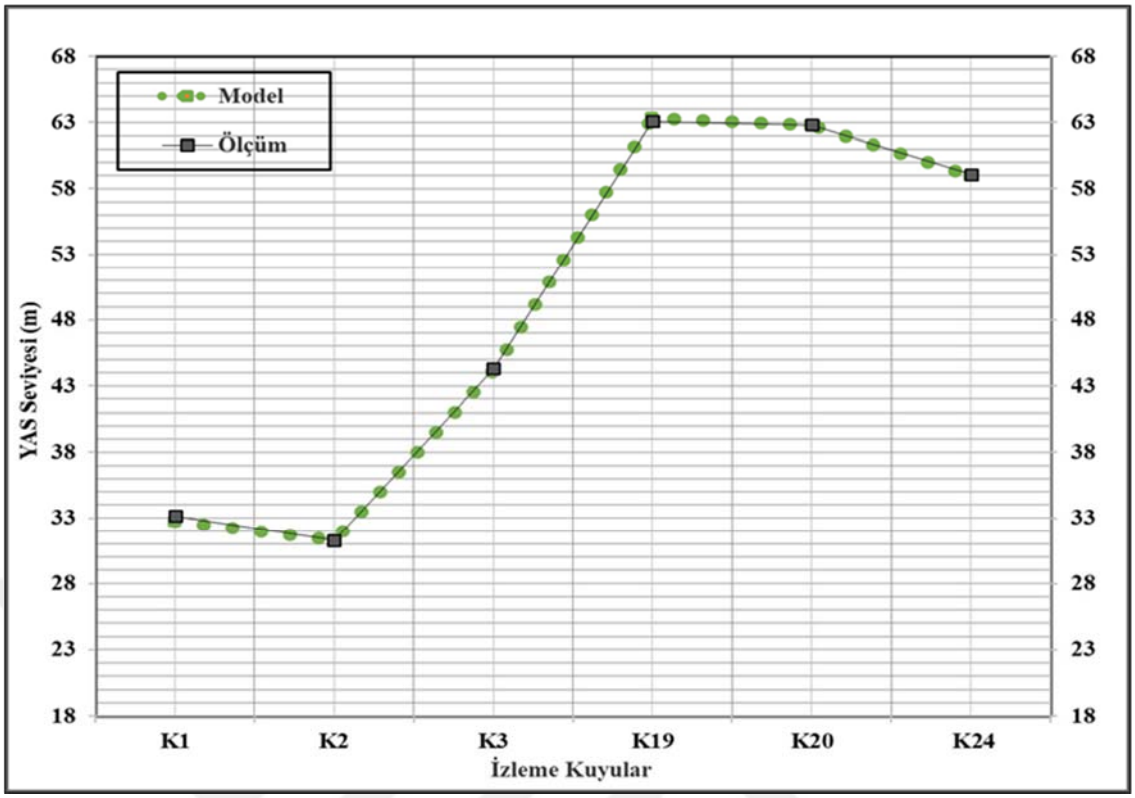

Şekil 4.4.. Kalibrasyon sonucunda karstik olmayan bölge için tahmin edilen ve ölçülen YAS seviyeleri

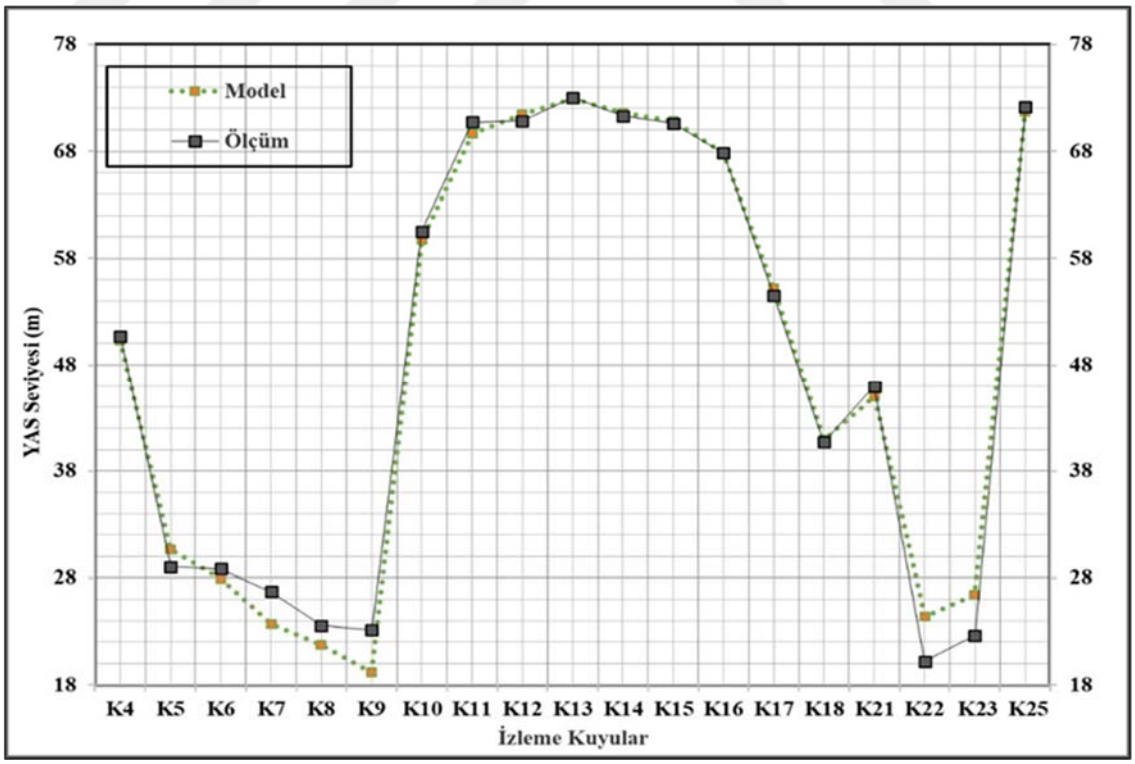

Şekil 4.5. Kalibrasyon sonucunda karstik bölge için tahmin edilen ve ölçülen YAS seviyeleri

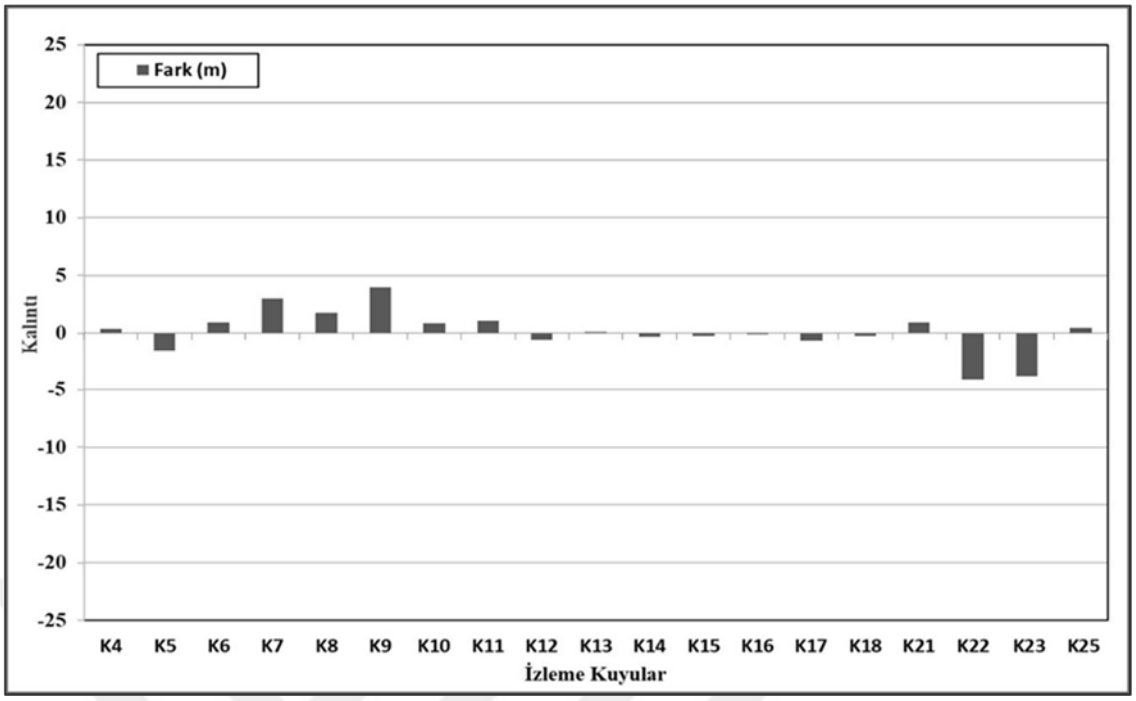

Şekil 4.6. Karstik bölge için model tahminleri ile ölçülen YAS seviyeleri arasındaki farklar (Tahmin - Ölçüm)

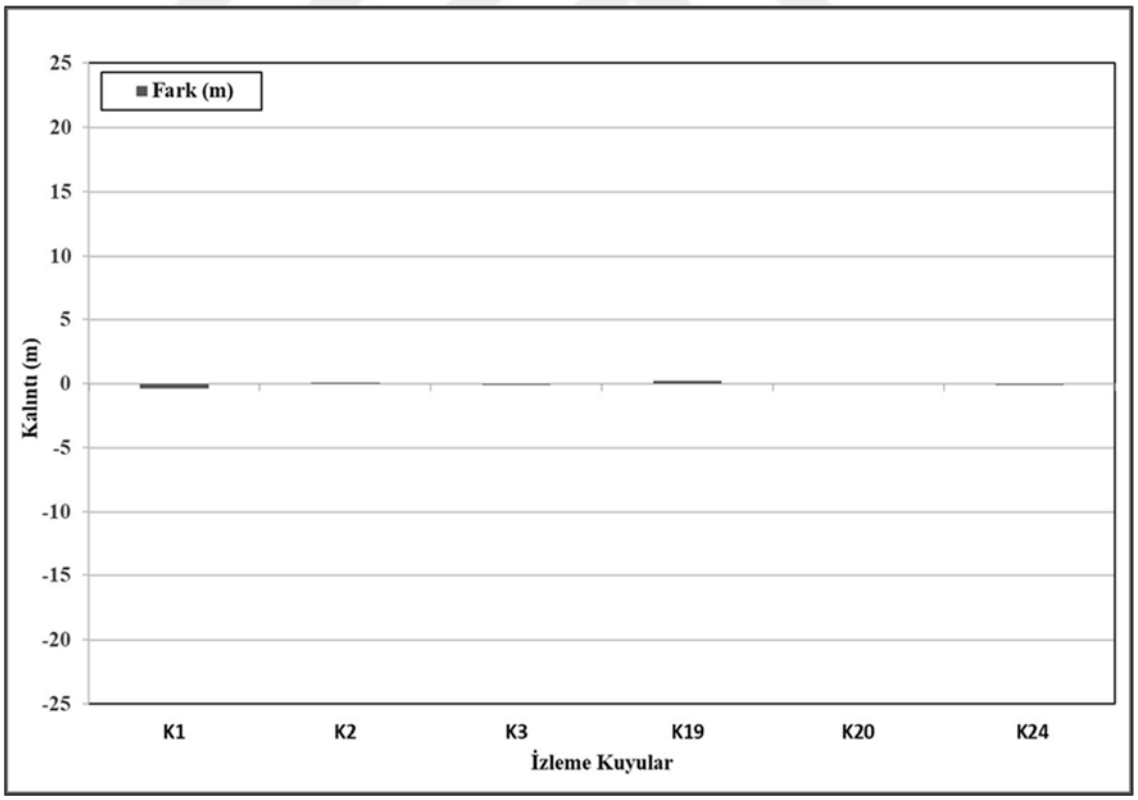

Şekil 4.7. Karstik olmayan bölge için model tahminleri ile ölçülen YAS seviyeleri arasındaki farklar (Tahmin - Ölçüm)

4.4. Yeraltısuyu Akım Modeli ile Hazırlanan Su Bütçesi Sonuçları

Yağıştan net beslenim ve kuyu çekimlerinin tahminindeki belirsizlikler mevcut olsa da, Altınova bölgesindeki karstik ve karstik olmayan alanlar için YAS sistemi analizinde toplam su dengesinin hesaplanması makul bir yaklaşım olarak dikkate alınabilir. Bu çalışmada, YAS bütçesindeki giriş akımları, yağıştan gelen net beslenme ve hidrolik yük sınırından oluşmaktadır. Çıkan su akışı ise, kuyulardan yapılan su çekimlerini ve hidrolik yük sınırlarını içermektedir. Şekil 4.8'de gösterilen YAS modeli su bütçesinde, yağıştan oluşan net beslenim, tüm çalışma alanı için toplam akış miktarının %73,4'ünü oluşturmaktadır ve bunun akifer girdilerinin ana kaynağı olduğu ortaya çıkmıştır. Genel hidrolik yük sınırı (General Head Boundary) akifer girdisinin %26,6'lık kısmını oluşturmaktadır. Ayrıca, antropojenik faaliyetlerden kaynaklanan (kuyulardan su çekimleri) çıkış suyu toplam bütçenin %33'ünü oluştururken, hidrolik yük sınırlarının %67'lik kısmı oluşturduğu gözlenmektedir. Şekil 4.8'de sunulan su bütçesi incelendiğinde, simülasyon dönemindeki su çekimlerinin yağıştan net beslenim miktarına oranı %46 olmuştur. Mevcut durumdaki YAS çekimlerinin, net beslenim miktarından az olduğunu göstermektedir. Bu durumda, yağış miktarını azaltabilecek iklim değişikliği ve YAS çekimlerinin Altınova akiferi üzerinde etkilerinin olması beklenebilir. Simülasyon döenmindeki su bütçesi, giren ve çıkan su akımları arasında iyi bir denge olduğunu göstermektedir.

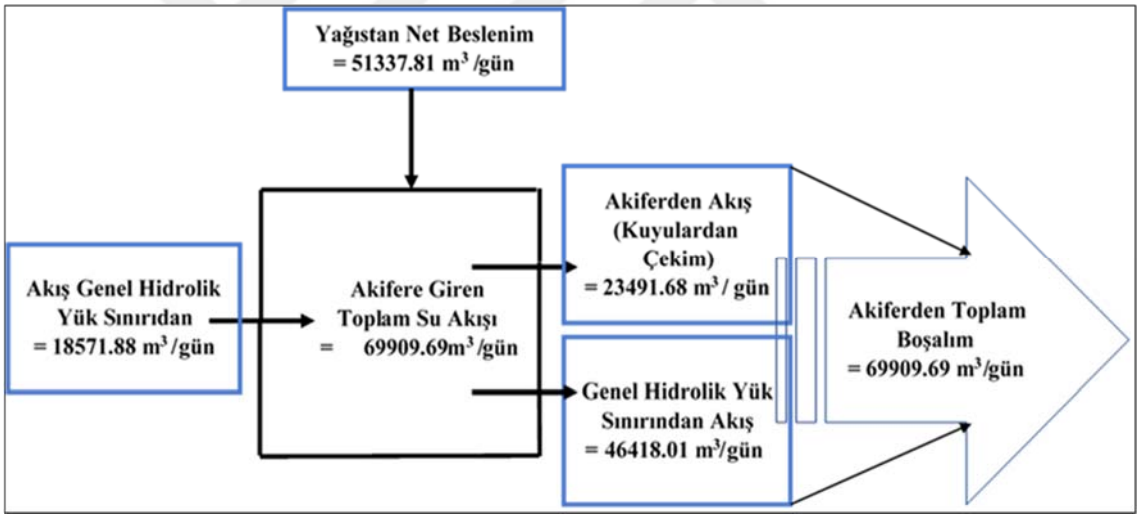

Şekil 4.8. Akifer için model ile hesaplanan genel su bütçesi

4.5. Çalışma Alanındaki Yeraltısuyu Akış Yönü

Traverten karst bölgesindeki ve Kurşunlu Formasyonunda bulunan karstik olmayan bölgedeki YAS akış yönüŞekil 4.9'da sunulmuştur. Genel YAS akış yönünün, YAS tablası yüksekliğine dik olduğu açıkça görülebilir. YAS, kuzeydeki yüksek YAS tablasından, güney yönüne doğru ilerlemektedir. Çalışma alanındaki YAS hareketinin belirtilen şekilde olması beklenilen bir durumdur. Bu akış davranışı, Barackman ve Brusseau (2002) tarafından YASın daha yüksek hidrolik seviye bölgelerinden, düşük hidrolik seviye bölgesine aktığı şeklinde ifade edilmiştir.

Şekil 4.9'da verilen YAS akış yönü haritasına göre, karstik olmayan alandaki YAS akış yönü kuzeyden güneye doğrudur. Aynı şekilde, traverten karst akiferindeki YAS, kuzeyden güneybatıya doğru akmakta ve çalışma alanının güney kısmına doğru yön değiştirmektedir. Altınova bölgesindeki karst traverten alandaki YAS akışının güneybatıya doğru yönelmesi, kuyulardan yapılan yüksek miktardaki su çekimlerinden dolayıdır. Elde edilen sonuçlardan, çalışma alanının batı kısmındaki YAS çekiminin daha yüksek olduğu belirlenmiştir. Çalışma alanının batı kesiminde çok sayıda kuyuların bulunması, sera ve diğer arazi kullanımına bağlı yüksek su çekimleri, bu bulguyu teyit etmektedir. Elde edilen YAS akış yönü, gerçek saha koşullarını temsil etmektedir.

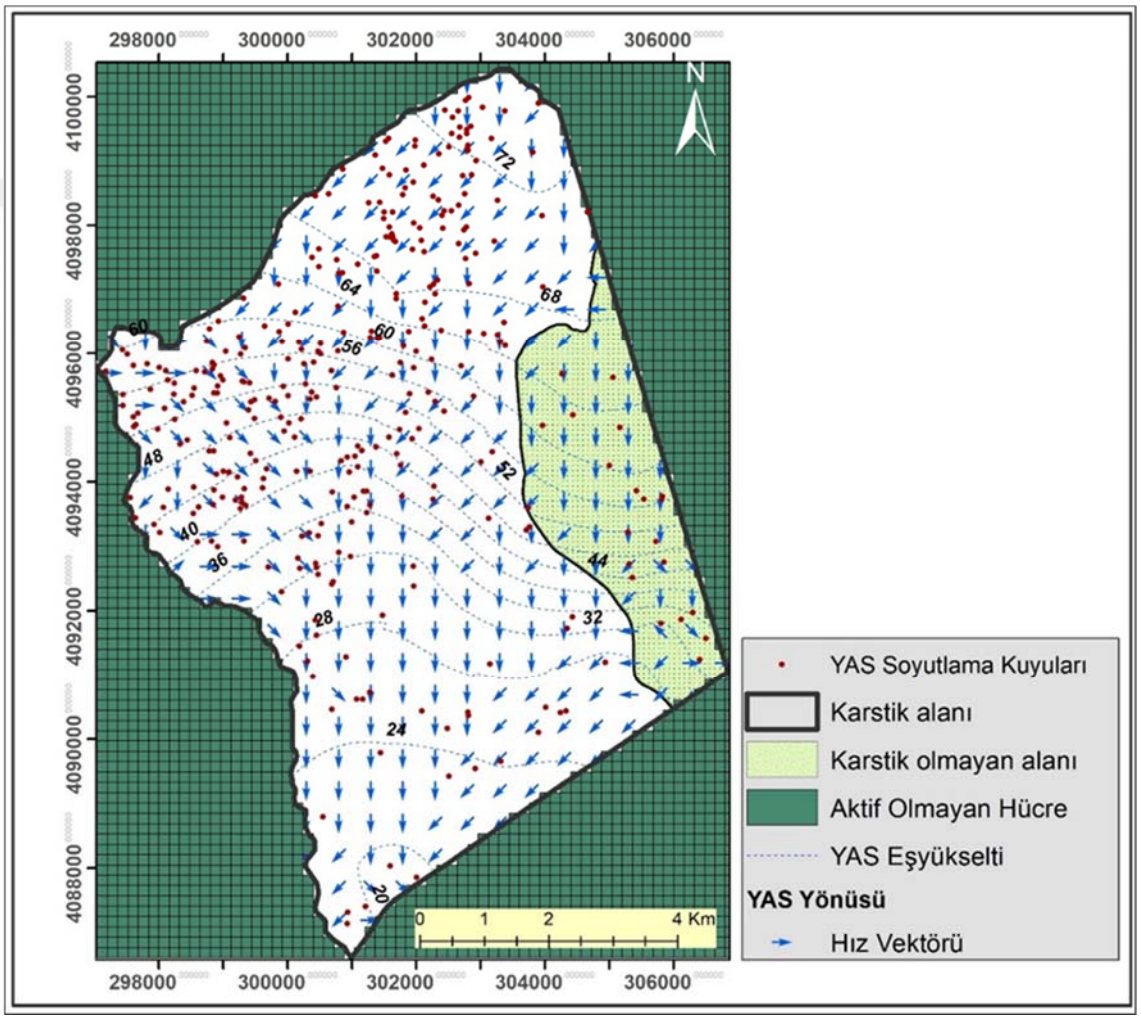

Şekil 4.9. YAS akış yönü ve YAS seviyesinin mekansal dağılımı

4.6. Farklı Yönetim Senaryolarının Etkileri

Bu çalışmada ele alınan üç farklı yönetim senaryosu, yağıştan net beslenim ve YAS çekimi gibi önemli model parametrelerindeki değişimleri içeren analizlerden elde edilmiştir. YAS seviyesindeki değişimlerin benzetimi için 2015-2016 dönemindeki yağış miktarı verilerinden ve tahmini YAS çekimi miktarları dikkate alınmıştır. Tez çalışmasında

Çizelge 4.1 ve Çizelge 4.1'de sunulan yönetim senaryoları incelenmiştir. Senaryo (A): mevcut YAS çekimi ile yağışta %50 oranında bir azalma olduğunu varsaymıştır, Senaryo (B): mevcut yağış miktarında YAS çekiminde %50 oranında artış olduğunu varsaymıştır. Senaryo (C): yağış miktarında %50 oranında azalma ve YAS çekiminde %50 artış olduğunu varsaymıştır. Tüm senaryolarda, spesifik depolama (Ss) ve Spesifik verim (Sy) akifer parametreleri sırasıyla 0,2 ve 1,00-05 1/m olarak kabul edilmiştir.

Çizelge 4.1. Altınova çalışma bölgesi için geliştirilen yönetim senaryoları

Artış / Azalış Oranı	**Bölgeler**		**Toplam Çekimler (m^3/yıl)**	**Senaryolar**
	(Karstik Bölgede) Yağıştan beslenme mm/yıl	**(Karstik olmayan bölgede) Yağıştan beslenme mm/yıl**		
Başlangıç değerleri	279.158	95.1675	-8574464	(Baz simülasyon kalibrasyon edilmiş)
Yağış miktarında %50 oranında azalma	139.58	47.58	-8574464	Senaryo (A)
YAS çekiminde %50 oranında artış	279.158	95.1675	-12861696	Senaryo (B)
Yağış miktarında %50 oranında azalma + YAS çekiminde %50 oranında artış	139.58	47.58	-12861696	Senaryo (C)

Baz simülasyon modelini geliştirmek için kalibre edilmiş hidrolik iletkenlik değerleri kullanılmıştır. Baz simülasyonda, çalışma alanının güney kısmındaki YAS seviyesi 18 m ve çalışma alanının kuzey kesiminde ise 72 m'dir. Senaryo (A), (B) ve (C) koşulları için tahmin edilen YAS seviyeleri, baz simülasyon sonuçları ile karşılaştırılmıştır. YAS seviyesindeki düşüşler, baz senaryo ile farklı senaryolar için elde edilen YAS seviyeleri arasındaki fark değerlerinden hesaplanmıştır.

4.6.1. Senaryo (A) için yeraltısuyu seviyeleri

Senaryo (A) için, tüm çalışma alanındaki YAS seviyeleri minimum 0,1 m ve maksimum 14 m azalmaktadır (Şekil 4.10). Senaryo (A) koşulu için karstik olmayan alandaki YAS seviyesinde 15 m'ye kadar önemli düşüşler gözlenmiştir. Tüm çalışma alanında, Senaryo (A)'da YAS seviyesi ortalama 4,6 m azalmıştır. İklim değişikliği etkisi ile hava sıcaklığının artması, buharlaşma miktarının artması ile topraktaki nem tutma kapasitesinin azalması beklenmektedir. Bu durumda YASın net beslenim miktarı azalacak ve YAS tablası düşecektir. Senaryo (A) koşulu için YAS seviyesindeki 0,2 m'lik minimum düşüş oranı, traverten karst bölgesinde yer alan K10 numaralı kuyuda meydana gelirken, aynı karstik bölgedeki K4 numaralı kuyu için maksimum 8 m'lik

düşüş gözlemlenmiştir. Senaryo (A) koşulu için karstik olmayan alandaki YAS seviyesindeki 15 m'lik maksimum düşüş oranı K24 numaralı kuyu için gözlemlenmiştir ve 1,1 m'lik minimum düşüş K1 numaralı kuyu için elde edilmiştir. Genel olarak, karstik alan için elde edilen YAS seviyesi düşüşü, karstik olmayan alandan daha fazladır. Bu sonuç, temel olarak çalışma alanının jeolojik yapısına bağlı olan hidrolik iletkenlik çeşitliliğinden kaynaklanmaktadır. Karstik alandaki infiltrasyon oranı, karstik olmayan alana göre daha yüksektir.

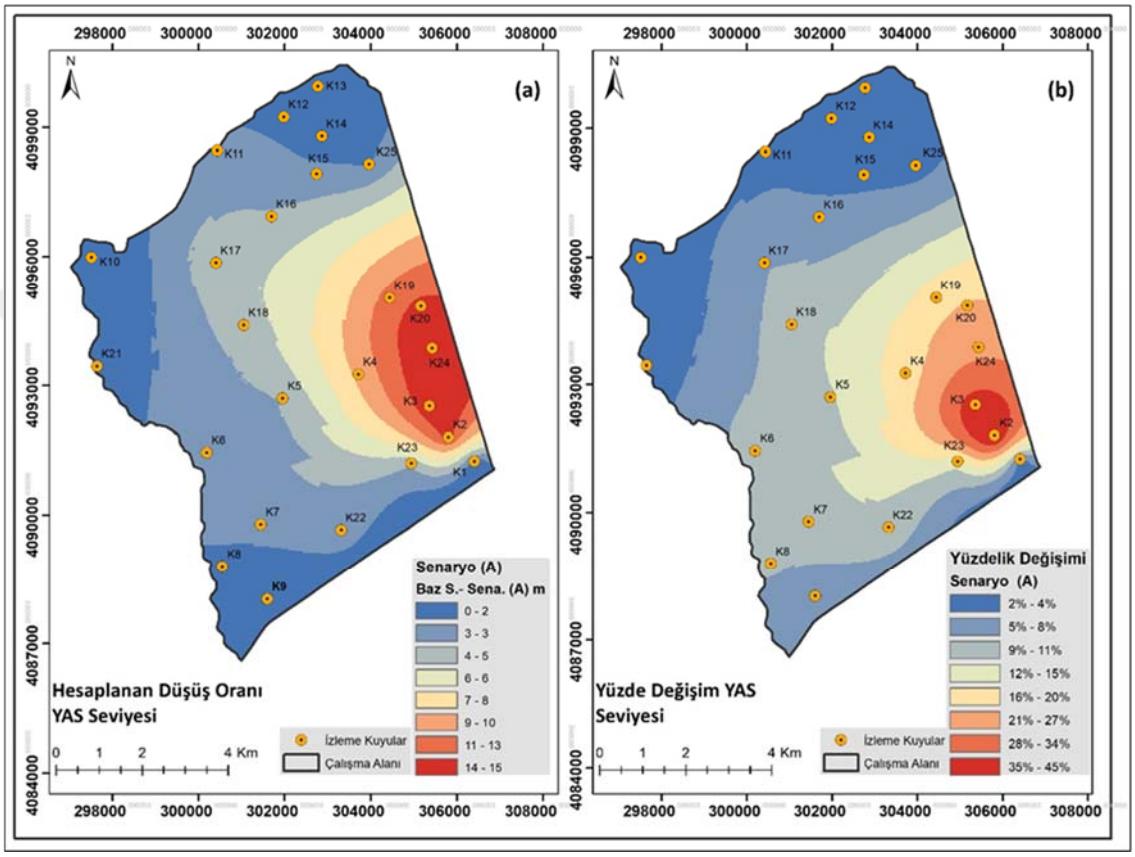

Şekil 4.10. a) Senaryo (A) koşulu için hesaplanan YAS seviyesindeki düşüş miktarı; ve buna karşılık gelen yüzdelik değişim **b)**

4.6.2. Senaryo (B) için yeraltısuyu seviyeleri

Senaryo (B) için mevcut yağış oranı ile YAS çekilmesinde (kuyulardan pompaj miktarı) %50 artış olması koşulu tanımlanmıştır. Senaryo (B) için, Şekil 4.11'de gösterildiği gibi, tüm çalışma alanındaki YAS seviyeleri minimum 0,3 m; ortalama 2,8 m ve maksimum 14 m azalmaktadır. Senaryo (B) koşulu için karstik olmayan alandaki YAS seviyesinde 14 m'ye kadar önemli düşüşler gözlenmiştir. YAS seviyesi için maksimum azalma değerleri karstik olmayan bölgelerde meydana gelmiştir. Senaryo (B) ile mevcut yağış oranında, YAS çekilmesindeki %50 oranındaki artışın, Altınova bölgesinde hem karstik hem de karstik olmayan akiferdeki bazı kuyularda YAS seviyesinde farklı düşüşlere sebep olduğunu göstermiştir. Senaryo (B) koşulu için YAS seviyesindeki 1,3 m'lik minimum düşüş oranı, traverten karst bölgesinde yer alan K1 numaralı kuyuda meydana gelirken, aynı karstik bölgedeki K3 numaralı kuyu için maksimum 14 m'lik düşüş gözlemlenmiştir. Senaryo (B) koşulu için karstik olmayan

alandaki YAS seviyesindeki 14 m'lik maksimum düşüş oranı K4 numaralı kuyu için gözlemlenmiştir ve 0,1 m'lik minimum düşüş K10 numaralı kuyu için elde edilmiştir.

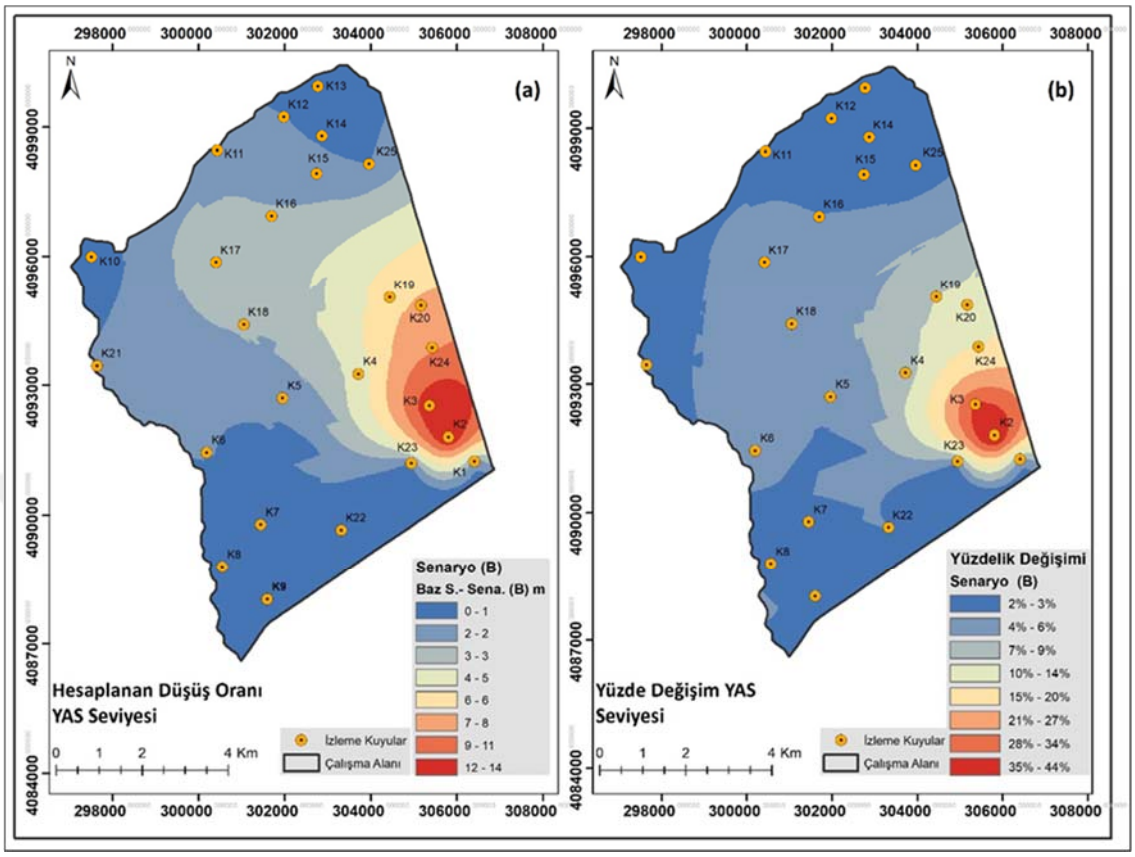

Şekil 4.11. a) Senaryo (B) koşulu için hesaplanan YAS seviyesindeki düşüş miktarı; ve buna karşılık gelen yüzdelik değişim **b)**

4.6.3. Senaryo (C) için yeraltısuyu seviyeleri

Senaryo (C) için mevcut yağış oranı %50 azaltılmış ve YAS çekilmesinde (kuyulardan pompaj miktarı) %50 artış olması koşulu tanımlanmıştır. Senaryo (C) için, Şekil 4.11'de gösterildiği gibi, tüm çalışma alanındaki YAS seviyeleri minimum 1,4 m ve maksimum 29 m azalmaktadır. Senaryo (C) koşulu için karstik alandaki YAS seviyesinde sırasıyla K4 ve K9 numaralı kuyularda maksimum 12 m ve minimum 1,4 m düşüşler gözlenmiştir. Karstik olmayan alanda bulunan K1 ve K2 kuyularında sırasıyla 2 m ve 29 m'lik düşüşler meydana gelmiştir. Tüm senaryolara ait istatistiksel analiz Çizelge 4.2.'de sunulmuştur. Senaryo (C) sonuçlarına göre, yağış oranındaki azalma ve YAS çekimlerindeki artış uzun süre devam ederse, çalışma alanının karstik olan kısmındaki birçok kuyunun kuruyacağı görülmektedir. YAS seviyesindeki düşüş miktarı Senaryo (C)'de diğer senaryolardan daha fazladır, çünkü Senaryo (C) en kötü durum senaryosudur.

Senaryo analizinde de görüldüğü gibi, Altınova bölgesindeki hassas akiferde YAS kaynaklarının azalmasını önlemek için bölgede kontrollü ve sürdürülebilir su kullanımı gereklidir. Her üç senaryo koşulu için, karstik olmayan bölgedeki hemen hemen tüm kuyularda YAS tablası yüksek oranda azalmakta iken bu durum karstik

bölgede farklıdır. İki farklı jeolojik formasyonda yer alan bölgeler için tahmin edilen YAS seviyesindeki düşüş miktarları, hidrolik iletkenlikteki değişikliklerle doğrudan bağlantılıdır.

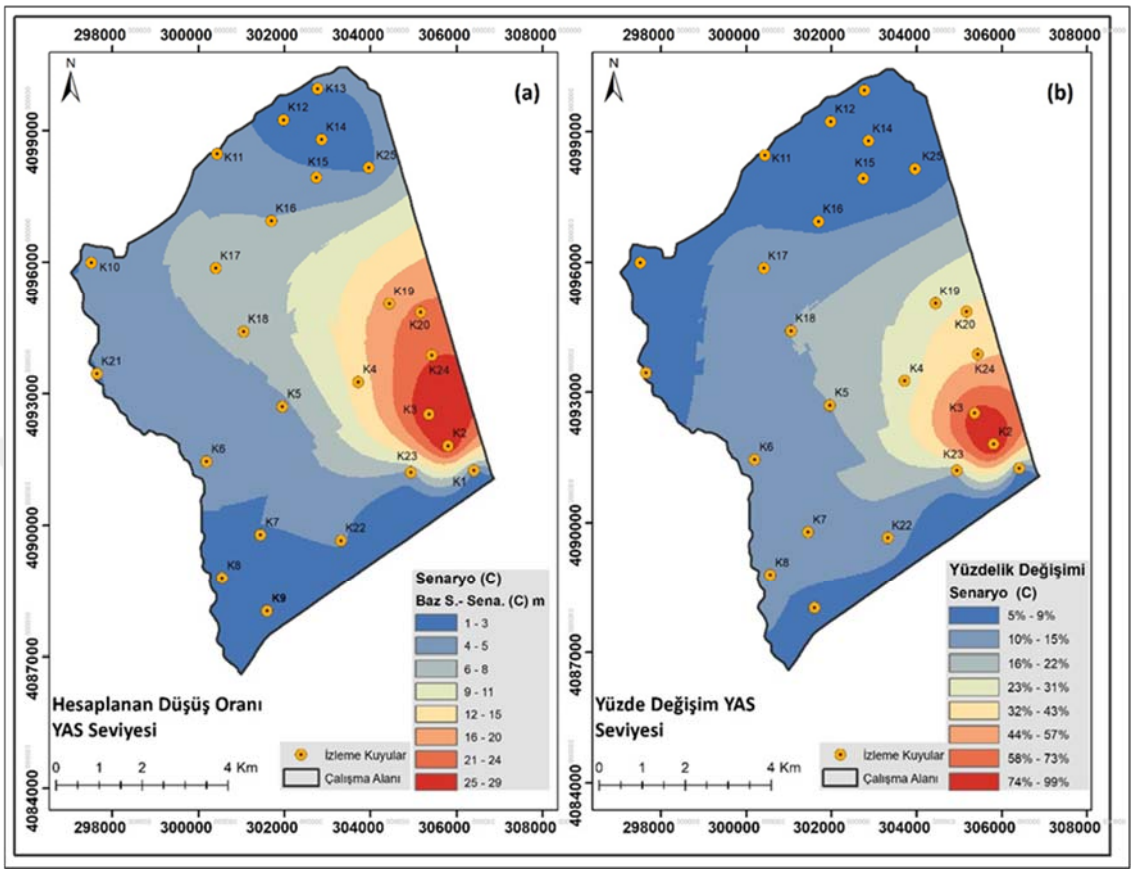

Şekil 4.12. a) Senaryo (C) koşulu için hesaplanan YAS seviyesindeki düşüş miktarı ve buna karşılık gelen yüzdelik değişim **b)**

Karstik olmayan bölgedeki hidrolik iletkenlik değerleri, karstik alana göre daha düşüktür. Bu durum, daha az YAS net beslenimi olduğunda, YAS su tablasındaki yükselmenin de az olduğunu göstermektedir. Benzer şekilde, karstik alanda hidrolik iletkenliğin daha yüksek olmasına bağlı olarak çalışma alanının karstik bölgesi için tahmin edilen YAS seviyelerindeki azalma ise daha düşüktür.

Yönetim senaryolarına ek olarak, hidrolik iletkenlik parametresinin kalibre edilmiş değerlerinin ±%50 oranında azaltılıp, arttırılması ile model duyarlılık analizi yapılmıştır. Bu çalışma, model duyarlılığını test etmek için yapılmıştır. Duyarlılık analizinin istatistiksel sonuçları, Ek-1 (sayfa 82)'de sunulmuştur.

Çizelge 4.2. Farklı senaryolar için elde edilen YAS seviyesindeki düşüş miktarlarının karşılaştırılması (YAS seviyesi farkı = Baz Simülasyon – Senaryo tahmini)

İstatistiksel Kriterler	**Senaryo (A)**	**Senaryo (B)**	**Senaryo (C)**
Minimum fark (m)	0,1	0,3	1,4

Çizelge 4.2'in devamı

İstatistiksel Kriterler	Senaryo (A)	Senaryo (B)	Senaryo (C)
Maksimum fark (m)	14,5	13,8	29,2
Medyan (m)	2,6	1,2	3,8
Ortalama (m)	4,6	2,8	8
Standart hata (m)	0,9	0,7	1,7
Standart sapma (m)	4,7	3,7	8,8
Aralık (m)	14,4	13,6	27,8

4.7. Yeraltısuyu Akış Modeli Uygulamasına İlişkin Sınırlandırmalar

Genel olarak, bu çalışmada kullanılan YAS akış modeli ile tahmin edilen YAS seviyeleri, sahada ölçülen YAS seviyeleri ile büyük benzerlik göstermiştir. Model uygulaması ile çalışma bölgesinin traverten karst alanı ve Kurşunlu Formasyonuda bulunan karstik olmayan bölgesi için değerli hidrolojeolojik bilgiler sağlanmıştır. Bu model uygulaması, Altınova bölgesi ve Antalya kompleks traverten karst sisteminin daha iyi anlaşılması ve gelecekte gerçekleştirilebilecek çok katmanlı bir model uygulaması için temel oluşturmuştur. Ancak, kararlı durum modeli, akifer parametrelerine ilişkin veriler üzerindeki sınırlandırmalar nedeniyle yönetim amaçlı YAS karakterizasyonu açısından sınırlı bir yaklaşım sunmaktadır. Her modelleme çalışmasında ve kullanılan modellerde çeşitli uygulama sınırları ve bir belirsizlik seviyesi vardır. Bu nedenle, model sonuçları kullanılırken dikkate alınması gereken bazı sınırlamalar ve varsayımlar vardır. Bu sınırlandırmalar Ek-1 (sayfa 89 – 90)'da sunulmuştur.

5. SONUÇLAR

Altınova bölgesinde karstik ve karstik olmayan akiferin 2 boyutlu sonlu farklar (finite-difference) yöntemi ve kararlı durum koşullarındaki YAS akış modellemesi için başarılı bir kalibrasyon çalışması gerçekleştirilmiştir. Kasım 2015, Şubat 2016 ve Mayıs 2016 dönemleri için tahmin edilen ve ölçülen ortalama YAS seviyeleri oldukça benzerdir.

Tahmin ve ölçüm değerleri için hesaplanan korelasyon katsayısı 0,99 olup iyi bir uyum gösterirmiştir. Jeolojik formasyon farklılığı dikkate alındığında, karstik olmayan alandaki YAS seviyesi model tahminlerinin, karstik alan için elde edilen model tahminlerine göre daha düşük model hatası oluşturduğu görülmüştür. Genel olarak, Altınova bölgesi için YAS akış modeli kalibrasyonu başarılı sonuçlar sağlamıştır. Bununla birlikte, modelden elde edilen YAS seviyesi tahminleri, çalışma alanının güney kesiminde daha az başarılıdır. Hidrolik iletkenlik parametresinin mekânsal dağılımı model kalibrasyonu ile oluşturulmuştur ve literatürde yer alan değerler ile uyumludur.

Simülasyon dönemi için oluşturulan genel su bütçesi, YAS için giren su akışı ile çıkan su akışı arasında iyi bir denge olduğunu göstermektedir. Yağıştan YASın net beslenimi, tüm çalışma alanı için su bütçesindeki en yüksek giriş bileşenidir. Hidrolik yük sınırından (General Head Boundary) çıkan su akışı ise, simülasyon dönemine ait su bütçesinde antropojenik çıkıştan daha yüksek bir çıkış değeri oluşturmuştur. Simülasyon süresince yağıştan net beslenim oranı, YAS çekiminden daha fazladır. Ayrıca model sonuçlarına göre, traverten karstik bölgedeki YAS akışı öncelikle kuzeyden güneybatıya doğru gerçekleşmekte ve daha sonra güneye doğru devam etmektedir. Karstik olmayan alanda ise, YAS akışı güneye doğru hareket etmektedir.

Bu çalışmadan elde edilen model sonuçları, çok katmanlı bir model geliştirilmesi için kullanılabilir ve Altınova bölgesinde YAS içindeki nitrat taşınımını incelemek için kullanılabilir. Farklı senaryolar altında tahmin edilen YAS seviyeleri, önemli değişiklikler (sabit kalma ve düşüşler) göstermektedir. Senaryo (A) koşulunda, çalışma alanının batı kesimindeki YAS seviyelerinde ufak bir düşüş tahmin edilmiştir. Tüm senaryo koşullarında, karstik olmayan alan için tahmin edilen YAS seviyesindeki düşüşler, çalışma alanının karstik bölgesi için tahmin edilen YAS seviyesi düşüşlerinden daha yüksektir. Bu çalışmada tanımlanan yönetim senaryoları için simülasyon süresi bir yıl olarak gerçekleştirilmiştir. Senaryolarda tanımlanan koşullar daha uzun süre devam edecek olursa hem karstik hem de karstik olmayan akiferlerdeki YAS seviyesi azalacak ve birçok kuyu kuru olacaktır. Bu tahminler neticesinde, iklim değişikliğine uyum stratejilerinin geliştirilmesi ve geleceğe yönelik acil yönetim planlarının oluşturulması gerekmektedir.

Model duyarlılık analizinde ortaya konulduğu şekilde, YAS akış modeli hem hidrolik iletkenlik parametresine hem de yağıştan net beslenim miktarına duyarlıdır. Ancak, YAS net beslenim miktarı, hidrolik iletkenlik parametresinden daha yüksek duyarlılığa sahiptir. Karar vericilere yönetim önerilerinin sunulması ve geleceğe dönük tahmin verilerinin oluşturulması, bu araştırmanın amaçları arasındandır. Elde edilecek ek veriler ile model doğrulama çalışmasının yapılması model sonuçlarının güvenilirliğini arttırmak ve belirsizlikleri azaltmak için önerilmektedir. Bu tez çalışmasında Conduit Flow Process model MODFLO-2005 CFP kullanılarak

gerçekleştirilen model uygulaması, çok katmanlı YAS akış modeli geliştirmek için iyi bir başlangıç noktası oluşturmuştur.

5.1. Gelecek Araştırmalar için Öneriler

Bu tez çalışmasının devamı olarak gelecekteki çalışmalarda;

- Ek veriler temin edilerek hidroloji ve iklim değişikliği konularının ele alınması faydalı olacaktır. Bu çalışmalar, iklim değişikliğinin arazi kullanımı ve bölgedeki su ihtiyacı üzerindeki etkilerini değerlendirmek için destekleyici olacaktır. Bu bilgiler, karar vericilerin büyük öneme sahip olan YAS kaynaklarını daha etkin şekilde yönetmesi için planlamalarında fayda sağlayacaktır.

- Karstik bölgelerdeki YAS hareketini daha iyi anlamak için hem kararlı hem de kararlı olmayan durumlar için MODFLOW-2005 için Akış Borusu Süreci (Flow Conduit Process) CFP kullanan dinamik 3 boyutlu ve çok katmanlı modellerin geliştirilmesi faydalı olacaktır.

- Hidrolik iletkenlik parametresinin tanımlanmasındaki veri eksikliği, sahada pompa deneyleri yapılarak giderilebilir. Pompa deneyi verileri, özgül verim (Specific yield) (Sy), depolama katsayısı veya depolayabilme (Storage coefficient) (S), vb. için kararlı olmayan simülasyon çalışmalarına yönelik önemli veri sağlayacaktır,

- Sulama kuyularından gerçekleşen su çekimi miktarları, mahsullerin su ihtiyacına dayanmaktadır. Bu süreçte, tahmin edilen YAS çekim değerleri, alandaki gerçek çekim değerlerinden az veya çok olabilir. Bu nedenle, model sonuçlarının daha güvenilir olması için daha gerçekçi YAS çekim verilerine ihtiyaç vardır ve buna yönelik güvenilir bir yöntem gereklidir, çalışmaya ilişkin ek öneriler Ek-1 (sayfa 92)'de verilmiştir.

6. KAYNAKLAR

Allan R. Cherry, J. A. F. 1979. Groundwater. Prentice Hall, Inc. United States of America, p 624

AMPR. (2016). Antalya Master Plan Raporu", Hidrojeoloji Raporu. Antalya Turkey.

Anderson, M., Woessner, W. W., Hunt, R. 1990. Applied Groundwater Modeling, Second Edition. Simulation of Flow and Advective Transport. https://doi.org/10.1016/B978-0-08-091638-5.00001-8

ArcGIS Online Resources. https://www.esri.com/en-us/arcgis/products/arcgis-online/resources [Accessed Oct 1, 2018]

Bakalowicz, M. 2005. Karst groundwater: A challenge for new resources. Hydrogeology Journal, 13(1): 148–160.

Barackman, M., Brusseau, M. L. 2002. Groundwater sampling. In J. F. Artiola, I. L. Pepper, M. Brusseau (Eds.), Environmental Monitoring and Characterization Elsevier, Amsterdam, (pp. 121–139).

Chen, Z. 2017. Modeling a geologically complex karst aquifer system. Doktors Dissertation, Karlsruher Instituts für Technologie (KIT), Xinjiang, PR China

Çil, A., Amil, A., Yenilmez, F., Ozyurt, N.N., Muhammetoglu, A., Muhammetoğlu, H. 2017. Assessment of Groundwater Vulnerability in a Karstic Aquifer Using Index-Based Methods: Altınova-Turkey Case Study, LuWQ 2017 International Interdisciplinary Conference on Land Use and Water Quality, The Hague, The Netherlands, 29 May – 1 June, 2017.

Dipova, N., Doyuran, V. 2006. Characterization of the Antalya (Turkey) tufa deposits. Carbonates and Evaporites: 21(2), 144–160.

Doherty, J., Hunt, R. (2010). Approaches to highly parameterized inversion: a guide to using PEST for groundwater-model calibration. U. S. Geological Survey Scientific Investigations Report 2010-5169. https://doi.org/2010-5211

Efe, R., Soykan, A. 2008. The Formation of Antalya Travertine Deposit and Karstic Ground, (November 2016).

Elc, A., Karadas, D., & Fıstıkog, O. 2010. The combined use of MODFLOW and precipitation-runoff modeling to simulate groundwater flow in a diffuse-pollution prone watershed, Water Science & Technology, 180–189.

Elhatı, H. 1997. The influence of karst features on environmental studies in Turkey. Environmental Geology, 31(May): 27–33.

Ford, D., Williams, P. 2007. Karst Hydrogeology and Geomorphology - Derek Ford, Paul D. John Wiley and Sons Ltd, The Atrium, Southern Gate, Chichester.

Goldscheider, N. 2015. Overview of Methods Applied in Karst Hydrogeology. In Z. Stevanović (Ed.), Karst Aquifers—Characterization and Engineering. Springer, pp. 127–145.

Goldscheider, N., Drew, D. 2007. Methods in Karst Hydrogeology. Taylor and Francis Group London UK .

Groves, C. 2007. Hydrologic Techniques. In Goldscheider, N., Drew, D. (Eds.), Methods in Karst Hydrogeology Taylor and Francis pp. 45–64.

Günay, G. 2001. Present state and future trends of Karst studies, In Günay G. (Ed.), Proceedings of the 6th International Symposium and Field Seminar Vol. I (49), pp. 1–76. Marmaris, Turkey.

Günay, G. 2010. Geological and hydrogeological properties of Turkish karst and major karstic springs. In N. Kresic, Z. Stevanovic (Eds.), Groundwater Hydrology of Springs. (pp. 479–497).

Güner, N., Törk, K., Günay, G. 2015. Turkish karst aquifers. Environ Earth Sci, (Thematic issue): 1–10. https://doi.org/10.1007/s12665-015-4298-6

Hartmann, A., Gleeson, T., Rosolem, R., Pianosi, F., Wada, Y., Wagener, T. 2015. A large-scale simulation model to assess karstic groundwater recharge over Europe and the Mediterranean. Geoscientific Model Development, 8(6): 1729–1746.

Hartmann, A., Goldscheider, N., Wagener, T., Lange, J., Weiler, M. 2014. Karst water resources in a changing world: Review of hydrological modeling approaches Rev. Geophys., 52 (1): 218–242.

Hill, M. C. 2006. The practical use of simplicity in developing ground water models. Ground Water, 44(6): 775–781.

Kum, G., Çelik, M. A. 2014. Impacts of Global Climate Change on the Mediterranean Region: Adana as a Case Study. Procedia - Social and Behavioral Sciences, 120, 600–608.

Lelieveld, J., Hadjinicolaou, P., Kostopoulou, E., Chenoweth, J., El Maayar, M., Giannakopoulos, C., et al. 2012. Climate change and impacts in the Eastern Mediterranean and the Middle East. Climatic Change, 114(3–4), 667–687.

Maliva, R. G. 2016. Aquifer Characterization Techniques. Springer Hydrogeology. Switzerland. https://doi.org/10.1007/978-3-319-32137-0

Muhammetoğlu, A., Özyurt, N. N., Muhammetoğlu, H., Yenilmez, F. 2017. Yeraltısuyu Risk Değerlendirmesi ve Pestisit Risk İndikatörleri Kullanılarak Tarımsal Karstik Bölgelerdeki Yeraltısuyu Kalitesinin Entegre Yönetimi. Antalya Turkey.

Muhammetoğlu, A., Yalcin, O. B. 2003. An Integrated Water Pollution Control Project to Protect Groundwater of Antalya Plain From Diffused Sources, Diffuse Pollution Conference, Dublin 2003, 39–45.

Murat, H. 2015. Hydrogeology of the Kaklik (Denizli) Aquifer in Turkey. Procedia Earth and Planetary Science, 15(2015): 345–352.

Panagopoulos, G. 2012. Application of MODFLOW for simulating groundwater flow in the Trifilia karst aquifer, Greece. Environ Earth Sci, 67(2012), 1877–1889.

Piccini, L., Mecchia, M. 2009. Solution weathering rate and origin of karst landforms and caves in the quartzite of Auyan-tepui (Gran Sabana, Venezuela). Geomorphology, 106 (1–2), 15–25.

Qadir, A., Ahmad, Z., Khan, T., Zafa, M., Qadir, A., Murata, M. 2016. A spatio-temporal three-dimensional conceptualization and simulation of Dera Ismail Khan alluvial aquifer in visual MODFLOW: a case study from Pakistan. Arab J

Geosci, 9 (2016).

Sargin, A. H., Gorkmen, A., Dogdu, M. S. 2000. A groundwater management plan according to EU Groundwater directive (80/68/EEC) and Water Framework directive (2000/60/EC). A new approch for groundwater management plant in Turkey.

Scanlon, B. R., Mace, R. E., Barrett, M. E., Smith, B. 2003. Can we simulate regional groundwater flow in a karst system using equivalent porous media models ? Case study , Barton Springs. Journal of Hydrology, 276 (2003): 137–158.

Tayanç, M., Im, U., Doğruel, M., Karaca, M. 2009. Climate change in Turkey for the last half century. Climatic Change, 94 (3–4): 483–502.

Unal, Y. S., Deniz, A., Toros, H., Incecik, S. 2012. Temporal and spatial patterns of precipitation variability for annual, wet, and dry seasons in Turkey. International Journal of Climatology, 32 (3): 392–405.

Varouchakis, E. A., Karatzas, G. P., Giannopoulos, G. P. 2015. Impact of irrigation scenarios and precipitation projections.pdf. Environ Earth Sci, 73 (2015): 7359–7374.

Vrba, J., Hirata, R., Girman, J., Haie, N., Lipponen, A., Neupane, B., et al. 2006. Groundwater Resources Sustainability Indicators. International Symposium on Groundwater Sustainability, (July 2016): 33–52.

Wang, S., Shao, J., Song, X., Zhang, Y., Huo, Z., & Zhou, X. 2007. Application of MODFLOW and geographic information system.pdf. Environ Geol, 55 (2008):

Waterloo. (2018). User Manual Visual MODFLOW Flex 5.0. Canada. Waterloo Hydrogeologic. Retrieved from www.waterloohydrogeologic.com

Xu, X., Huang, G., Qu, Z., & Pereira, L. S. 2011. Using MODFLOW and GIS to Assess Changes in Groundwater Dynamics in Response to Water Saving Measures in Irrigation Districts of the Upper Yellow River Basin, Water Resour Manage 25 (2011): 2035–2059.

7. EKLER

7.1. EK-1 Tezin İngilizce versiyonu

T.C.

AKDENİZ UNIVERSITY

MANAGEMENT OF GROUNDWATER RESOURCES IN KARSTIC AQUIFER USING VISUAL MODFLOW: CASE STUDY OF ALTINOVA TURKEY

Alex Modi Lomoro WANI

INSTITUTE OF SCIENCE

ENVIRONMENTAL ENGINEERING

DEPARTMENT

MASTERS'S THESIS

JANUARY 2019

T.C.

AKDENİZ UNIVERSITY

MANAGEMENT OF GROUNDWATER RESOURCES IN KARSTIC AQUIFER USING VISUAL MODFLOW: CASE STUDY OF ALTINOVA TURKEY

Alex Modi Lomoro WANI

INSTITUTE OF SCIENCE

ENVIRONMENTAL ENGINEERING

DEPARTMENT

MASTERS'S THESIS

JANUARY 2019

ANTALYA

T.C.

AKDENİZ UNIVERSITY

MANAGEMENT OF GROUNDWATER RESOURCES IN KARSTIC AQUIFER USING VISUAL MODFLOW: CASE STUDY OF ALTINOVA TURKEY

Alex Modi Lomoro WANI

INSTITUTE OF SCIENCE

ENVIRONMENTAL ENGINEERING

DEPARTMENT

MASTERS'S THESIS

JANUARY 2019

ANTALYA

T.C.

AKDENIZ UNIVERSITY

MANAGEMENT OF GROUNDWATER RESOURCES IN KARSTIC AQUIFER USING VISUAL MODFLOW: CASE STUDY OF ALTINOVA TURKEY

Alex Modi Lomoro WANI

INSTITUTE OF SCIENCE

ENVIRONMENTAL ENGINEERING

DEPARTMENT

MASTERS'S THESIS

JANUARY 2019

ANTALYA

T.C.

AKDENIZ UNIVERSITY

INSTITUTE OF SCIENCE

MANAGEMENT OF GROUNDWATER RESOURCES IN KARSTIC AQUIFER USING VISUAL MODFLOW: CASE STUDY OF ALTINOVA TURKEY

Alex Modi Lomoro WANI

ENVIRONMENTAL ENGINEERING DEPARTMENT

MASTERS'S THESIS

This thesis was accepted by the jury committee on the 30/01/2019

ABSTRACT

MANAGEMENT OF GROUNDWATER RESOURCES IN KARSTIC AQUIFER USING VISUAL MODFLOW: CASE STUDY OF ALTINOVA TURKEY

Alex Modi Lomoro WANI

MSc Thesis in Environmental Engineering

Supervisor: Prof. Dr. Habib MUHAMMETOĞLU

January 2019; 119 pages

The karstic aquifers in Turkey hold significant amount of water that is extensively used to meet irrigation and domestic water demands along the Mediterranean region south of the country. Therefore, understanding and modeling this fragile aquifer is crucial for the management of groundwater resources.

Groundwater resource originating from karts aquifer is under pressure and continuous shrinking in Mediterranean regions of Antalya. The aim of this study is to simulate groundwater in the karst region of Altınova using Visual MODFLOW flex. The study also aims at assessing the current situation of groundwater in Altınova and formulate scenarios to predict the future groundwater level status based on the available data.

The scope of this research is to obtain the required data from the completed TÜBİTAK project No 114Y696 to simulate groundwater using the graphical user interface Visual MOFLOW Flex based a Single Continuum Porous Equivalent approach in Altınova. The groundwater simulation was achieved with the help of the MODFLOW-2005 engine using Finite Difference Method. The model was designed over an area of about 75 km^2. The numbers of rows and columns were equal to 87 and 62; respectively. The model domain was divided into two recharge and hydraulic conductivity zones based on geological formation. The model was run as two dimensional in steady-state.

Model inputs under hydrological framework such as groundwater table elevation were obtained from completed TÜBİTAK database. In the model calibration, the only parameter included was hydraulic conductivity in a lateral direction. The calibration results of groundwater table elevations in the Kurşunlu non- karstic area tend to be more satisfactory with lower residual values than in the travertine karstic area. Overall the correlation coefficient between measured and simulated groundwater table elevation was good with the value of 0.99. However, the model was less successfully in the southern part of the study area which could be due to karstification feature of the area.

The findings presented in this research was the first attempt to apply model in Altınova, to improve understanding of hydrological system in the study area. Considering the use of Single Continuum Porous Equivalent approach through the MODFLO-2005 in the karst area, the model yields a promising correlation coefficient of 0.99. This indicated that the calibration results were reasonable. The study attempted the first estimate of hydraulic conductivity in Altınova using automate calibration tool PEST. The calibrated

values of hydraulic conductivity in both karst and non-karst area were ranging from 0.01 - 266 m/day. Overall, the calibrated values of hydraulic conductivity in both karst and non-karst areas of the Altınova are within the literature. The water budget in the period of the simulation shows a good balance between inflow and outflow. Recharge is the highest component of inflow in the water budget for the entire study area and was sensitive in the model. Following the model calibration, three management scenarios were developed. The groundwater table elevation imperiled to decline under different three hydrological scenarios. The highest decline of groundwater table elevation was in non-karst area with relatively lower hydraulic conductivities comparably the decline was lower in karst area. A Groundwater flow direction map was produced based on modeling outputs. Overall, the groundwater flows from north to southwest then to south in the karstic travertine. In the Kurşunlu non-karst area, the groundwater flows southwards. The findings of this study are very important to examine the groundwater flow under the current conditions. Further investigations using multi layers may be required for further analyses. This could be accomplished using conduit flow conditions capability of the same tool (MODFLOW-2005). Moreover, the model could be used to study the flow path of nitrate in this area.

KEYWORDS: Groundwater table elevation, Modelling, Visual MODFLOW flex, Karstic aquifer, Altınova

PREFACE

Groundwater resource originating from karts aquifer is under pressure and continuous shrinking in Mediterranean regions of Antalya. Therefore, protection of the quantity and quality of this fragile karst resource is essential. To sustain and manage the vital karst groundwater resource, it is necessary to investigate as well as simulate the aquifer conditions under different scenarios. This work aims at enabling the decision makers to take appropriate measures to conserve the groundwater resources. The data set made up this document was obtained from database of completed TÜBİTAK project No 114Y696 directed by Prof. Dr. Ayşe MUHAMMETOĞLU.

I would like to express my special gratitude to Prof. Dr. Habib MUHAMMETOĞLU for accepting me as his student and providing me with the first lesson in groundwater pollution and control and encourage me in this thesis topic. It would have been impossible to carry out this work with confidence without his wholehearted involvement, supervision, valuable criticism, scientific advice, support, and constant encouragement throughout. He has not only help me in my thesis work, but he took me under his wings and taught me many things as well as motivate me to proceed further in my life. Prof. Dr. Habib MUHAMMETOĞLU this study would never have been realized without your help.

I would like to express my sincere thanks to Prof. Dr. Ayşe MUHAMMETOĞLU for providing me with necessary data and research tools, critical thinking, and a practical data analysis in the class. Prof. Dr. Ayşe MUHAMMETOĞLU without your support I don't know what I would have done. I would like to also thanks Dr. Ziyad ABUNADA for his valuable comments during the model application. Thanks Dr. Ziyad ABUNADA for the fabulous amount of help.

Finally, but not the least, I would like to express my appreciation to Turkish scholarship (YTB) for granting me a financial support, without their support this dream would have not been come to reality. I would like to thank Ms. Diana THOMAS for her mentorship and immeasurable help. Finally, I would like to thank my parents for their infinite and constant support, and encouragement throughout my life and academic journey. Their sacrifices towards achieving my goals will never be forgotten.

TABLE OF CONTENTENT

ABSTRACT i
PREFACE iii
ACADEMIC STATEMENT iv
SYMBOLS AND ABBREVIATIONS v
LIST OF FIGURES viii
LIST OF TABLES xii
1. INTRODUCTION 1
1.1. Background of the Study 1
1.2. Aims and Objectives of the Study 2
1.3. Significance of the Study 3
1.4. Scope and Structure of the Study 3
1.5. Layout and Thesis Structure 4
2. LITERATURE REVIEW 5
2.1. Overview of Groundwater 5
2.2. Overview of Karst Aquifers in Mediterranean Countries 5
2.2.1. Potential effect of climate change on karst groundwater 8
2.3. Distribution of Karstic Aquifers in Mediterranean Cities of Turkey 8
2.4. Groundwater Modeling Techniques and Categories 9
2.5. Categories of Groundwater Models 10
2.5.1. Analytical model 11
2.5.2. Numerical model 12
2.5.3. Data requirements for groundwater modeling 15
2.5.4. Model layers and elevation in groundwater modeling 16
2.5.5. Boundary conditions in numerical groundwater modeling 16
2.6. Model Calibration 17
2.6.1. Manual calibration approaches in groundwater modeling 17
2.6.2. Automate groundwater calibration 18
2.7. Approaches for Characterizing Groundwater Flow in Karst Systems 20
2.7.1. Speleological method 20
2.7.2. Geological method 20
2.7.3. Geophysical method 21

2.7.4. Hydraulic and hydrogeologic method 21
2.7.5. Hydrochemical and isotopic method 22
2.7.6. Tracer method 22
2.8. Modeling methods in karst aquifers and synopsis of previous work 22
3. MATERIALS AND METHODS 27
3.1. General Discerption of the Study Area 27
3.1.1. Geological formation. 29
3.1.2. Climate 31
3.2. Material Methods and Model (MMM) 33
3.2.1. Field work 33
3.3. Software Applied in the study 40
3.4. Model Design and Discretization Techniques 41
3.4.1. Model design and discretization 41
3.4.2. Hydrological model surfaces/layer development 42
3.5. Model Parameters and Property Zones 47
3.5.1. Hydraulic conductivity 47
3.6. Model Boundary Condition 50
3.6.1. General head boundary (GHB) condition 50
3.6.2. No flow boundary 50
3.6.3. Recharge 51
3.6.4. Pumping wells 55
3.6.5. Set-up of the solver used in the numerical model run 57
3.7. Model Setting 58
3.8. Model Calibration 58
3.9. Model Prediction Evaluation 60
3.10. Analysis of Different Management Scenarios 61
4. RESULT AND DISCUSSION 63
4.1. Pre-calibration Result of the Groundwater Modeling 63
4.2. Calibrated Hydraulic Conductivity 65
4.3. Calibrated Groundwater Table Elevation Result 69
4.4. Comparison between Karst and Non-Karst Result of Calibrated Groundwater Table Elevation 73

4.5. Water budget for calibrated model 76
4.6. Groundwater Flow Direction in the study area 77
4.7. Impacts of Different Management Scenarios 79
4.7.1. Groundwater table elevation under scenario (A) 80
4.7.2. Groundwater table elevation under scenario (B) 81
4.7.3. Groundwater table elevation scenario (C) 82
4.8. Model Sensitivity Analysis 84
4.9. Comparation of Calibration Groundwater Table Elevation with Seasonal Measured Groundwater Table Elevation 86
4.10. Limitations of the Developed Groundwater Flow Model 89
5. CONCLUSION 91
5.1. Recommendations for Future Work 92
6. REFERENCES 93

ACADEMIC STATEMENT

Thesis name “Management of Groundwater Resources in Karstic Aquifer Using Visual MODFLOW: Case Study of Altınova Turkey” is written in accordance with academic rules and ethical values. I declare that I had references all of the information that does not belong to me.

30/01/2019

Alex Modi Lomoro WANI

SYMBOLS AND ABBREVIATIONS

Symbols

C : Conductance

°C : Degree celsius

M : Meter

Mm : Millimeter

M^3 : Cubic meter

% : Percentage

Km^2 : Square kilometer

K : Hydraulic conductivity

Δh :The difference between the user-specified boundary head and model-calculated head near the boundary

ha : Hectare

h_B : User-specified boundary

R : Recharge

S_y : Specific yield

S_s : Specific storage of the porous media

Mg : Milligram per liter

L : Litre

W^* : Volumetric flux per unit volume

Abbreviations

CAVE : Carbonate Aquifer Void Evaluation

CCPF : Coupled Continuum Pipe Flow

CDC : Combined Discrete-Continuum

CFP : Conduit Flow Process

CSV : Comma-Separated Values

DCN : Discrete Conduit Network

DEM : Digital Elevation Model

DF : Discrete Fracture

DFN : Discrete Fractures Network

DMFN : Discrete Multiple Fracture Network

DPM : Double Porosity Model

DSI : State Hydraulics Works (DSI

EPM : Equivalent Porous Medium

ESRI : Environmental System Research Institute

FD : Finite-Difference

FE : Finite Element

GCM : Global Circulation Models

GDM : General Directorate of Meteorology

GHB : General Head Boundary

GIS : Geographical Information System

GWTE : Groundwater Table Elevation

GUI : Graphical User Interface

HDB : Head Dependent Boundary

HM : Hybrid Model

LSM : Linear Storage Models

KML : Keyhole Markup Language

MAE : Mean Absolute Error

NRMSE : Normalized Root Mean Squared Error

PSA : Pilot study area

PCG : Precondition Conjugated Gradient

PEST : Parameter Estimation Tool

RMSE : Root Mean Square Error

RMS	: Root Mean Square
SD	: Stocks-Darcy
SCM	: Soft Computing Methods
TÜBİTAK	:The Scientific and Technological Research Council of Turkey
USGS	: United States Geological Survey
UTM	: Universal Transverse Mercator
VMF	: Visual MODFLOW Flex
WOKAP	: World Karst Aquifer Mapping

LIST OF FIGURES

Figure 1.1. Map shows location of Antalya 2

Figure 2.1. Karst aquifer shows karst features such as dissolved sinkholes, caves, and frac-tures, Figure is from (Marshak, 2015) 6

Figure 2.2. Distribution map of karst areas in Turkey 9

Figure 2.3. Stepwise workflow for groundwater modelling (Anderson et al, 2015) 10

Figure 2.4. Types of numerical models mesh/grids Finite Difference Grids FDG **a)**; Finite Element Grids FEG **b)** 12

Figure 2.5. Generalized model development by Finite-Difference and Finite-Element method adapted from (Faust and Mercer 1980)..... 13

Figure 2.6. Finite-Difference (FD) grid and notation figure from (McDonald and Harba-ugh 1984). 14

Figure 2.7. General workflow for manual trial and error adopted from (Mary P. Anderson et al., 2015) (ME, MAE, RMSE)..... 18

Figure 2.8. A schematic diagram of a general workflow for parameter estimation adopted from (M. P. Anderson et al. 2015)..... 19

Figure 3.1. Land cover map (a) and basic land use map (b) of the pilot study area. 28

Figure 3.2. Location of the study area..... 29

Figure 3.3. Geological formation of study area 30

Figure 3.4. Hydrogeological map of the study area 31

Figure 3.5. Total yearly precipitation in the year between (1994 -2017)..... 32

Figure 3.6. Monthly average max. temperature in the year (1994 – 2017)..... 32

Figure 3.7. Monthly average minimum temperature in the year (1994 – 2017)..... 33

Figure 3.8. Shows average groundwater table elevation (GWTE) in Karstic and Non-Karstic area of Altınova 34

Figure 3.9. Average measured depth to groundwater in the months of (Nov 2015, Feb 2016 and May 2016) 35

Figure 3.10. Measured groundwater table elevation Nov-2015..... 37

Figure 3.11. Measured groundwater table elevation Feb-2016..... 38

Figure 3.12. Measured groundwater table elevation May-2016 39

Figure 3.13. 2D view of model domain and grid cells....42

Figure 3.14. Spatial distribution of aquifer thickness in the model domain 44

Figure 3.15. Well depths (m) and yields (m^3/s) recorded during the time of drilling....45

Figure 3.16. D-2 Top **a);** and bottom **b)** surface elevations of the model domain in units of meters....46

Figure 3.17. D-3 Top and bottom surfaces of the model domain in units of meters 47

Figure 3.18. Pre-calibration hydraulic conductivity zones and values for the model domain....48

Figure 3.19. Range of hydraulic conductivity values for different geological formations (Allan and Cherry, 1979)....49

Figure 3.20. Boundary conditions applied for steady-state model run 51

Figure 3.21. Map view of average recharge values in a year (2015 – 2016) 53

Figure 3.22. Monthly average precipitation and recharge in karst aquifer in year (2015 – 2016)....54

Figure 3.23. Monthly average precipitation and recharge in non-karst aquifer in year (2015 – 2016) 54

Figure 3.24. Spatial distribution of irrigation wells and the pumping rates in the model do- main....56

Figure 3.25. Spatial distribution of pilot points used in model calibration....60

Figure 4.1. Pre-calibration scatter plot of simulated to measured groundwater table elevat- ions (m) 64

Figure 4.2. Pre-calibration graph of simulated to measured groundwater table elevations (m)....64

Figure 4.3. Pre-calibration map of measured (a) and simulated (b) groundwater table ele-vations 65

Figure 4.4. Hydraulic conductivity pre-Calibration (a) and calibrated hydraulic conducti- vity (b)....67

Figure 4.5. Residual values for simulated vs. measured groundwater table elevations....69

Figure 4.6. Calibration map view of observed (a) and simulated (b) groundwater table elevations....71

Figure 4.7. Calibrated graph view of simulated to measured groundwater table elevations (m)....71

Figure 4.8. Calibrated scatter plot of simulated to measured groundwater table elevations (m)....72

Figure 4.9. Calibrated graphical view of simulated versus measured groundwater table elevations in the non-karst area....73

Figure 4.10. Calibrated graphical view of simulated versus measured groundwater table elevations in the karst area....74

Figure 4.11. Residual values for simulated groundwater table elevations in karst area(Simulated – Measured)....74

Figure 4.12. Residual values for simulated groundwater table elevations in non-karst area (Simulated – Measured)....75

Figure 4.13. Groundwater flow direction and groundwater table elevation....78

Figure 4.14. Map view of base simulation groundwater table elevation (GWTE)....80

Figure 4.15. (a) Computed decline in groundwater table elevation under scenario (A), and its corresponding percentage change (b)....81

Figure 4.16. a) Computed decline in groundwater table elevation under scenario (B), and its corresponding percentage change **b)**....82

Figure 4.17. a) Computed Decline in Groundwater Table Elevation Under Scenario (C) Left, and its Corresponding Percentage Change **b)**....83

Figure 4.18. Changes in groundwater table elevation under scenario (A), (B), and C....84

Figure 4.19. Graphical view of model sensitivity (NRMSE = Normalize Root Mean Square Error)....85

Figure 4.20. Comparison of simulated versus average measured groundwater table elevations for Nov-2015....86

Figure 4.21. Comparison of simulated versus average measured groundwater table elevations for Nov-2015 at monitoring wells level....87

Figure 4.22. Comparison of simulated versus average measured groundwater table elevations for Feb-2016....87

Figure 4.23. Comparison of simulated versus average measured groundwater table elevations for Feb-2016 at monitoring wells level....88

Figure 4.24. Comparison of simulated versus average measured groundwater table elevations for May-2016 88

Figure 4.25. Comparison of simulated versus average measured groundwater table elevations for Feb-2016 at monitoring wells level..... 89

LIST OF TABLES

Table 2.1. summary of physical and hydrological framework data for groundwater modeling....16

Table 2.2. Differently named distributed modeling approaches in the literature....25

Table 3.1. Monitoring Wells Database (Muhammetoğlu et al., 2017)....36

Table 3.2. Software applications utilized for research....41

Table 3.3. Model parameters for pre-calibration and steady-state simulation....49

Table 3.4. Initial recharge rates values in the years between 2015-2015 for the pilot study area....52

Table 3.5. Estimated withdrawal rate....56

Table 3.6. Property settings of solver used in the model application....57

Table 3.7. Model Management Scenarios....62

Table 4.1. Model performance statistics for pre-calibrated groundwater table ele vation....63

Table 4.2. Statistical Values for estimated hydraulic conductivity at monitoring wells level....68

Table 4.3. Model performance statistics for calibrated groundwater table elevation....70

Table 4.4. Compression of calibrated model performance between karst and non-karst area....75

Table 4.5. Calibrated volumetric water budget for entire model....76

Table 4.6. Management Scenarios Values for Recharge and Pumping rate....79

Table 4.7. Comparison of Model Performance Statistics for Different Scenarios Residual (Base Simulation – Scenario) Groundwater Table Elevation....83

Table 4.8. Analysis of statistical sensitivity values of the model for decreased/ increase of hydraulic conductivity by 50%....85

Table 4.9. Statistical comparison of model performance for seasonal groundwater table elevation....89

1. INTRODUCTION

1.1. Background of the Study

The term ‘karst’ is generally used in a geomorphological perspective to describe terrain that developed because of the high dissolution of rock, such as limestone, with well-developed secondary (fracture) porosity. They are extensive in the Mediterranean part south of Turkey. Karst aquifer regions hold significant volumes of water in the country (Güner et al. 2015) and account as the main for both agriculture and drinking water demand along the Mediterranean regions of Turkey (Elhatı 1997; Günay 2010; Sargin et al. 2000).

Antalya province is one of the significant karstic areas in Turkey. Antalya is a metropolitan city located on the Mediterranean coast of Southwestern Turkey (Figure 1.1) and it covers an area of about 20791 square kilometers (World Data Atlas 2014)[1]. A large part of Antalya city is covered by a travertine formation, which is porous, permeable and karstified, the thickness of the travertine reaches to 240 m in upper plateau and ranges between 60 to 120 m in lower plateau (Ekmekci 2003). The groundwaters obtained from travertine formation play an important role in meeting water needs in Antalya city.

Groundwater resources originating from karst aquifers are over stressed and are continuously shrinking in Mediterranean regions of Antalya due to the overuse for agricultural purposes. Therefore, water conservation with regards of quantity and quality in this fragile karst travertine is essential. The main problems in the travertine karst regions include rapid expansion of agricultural areas, industrialization, and urbanization. Currently, a part of Antalya region is lacking a proper wastewater collection system where some areas have not been served with such systems. In some parts of the Antalya province, septic tanks are still common. In non-sewer coverage parts, municipal wastewaters have been directly discharged into the travertine aquifer via septic tanks. Antalya also is a well-known agricultural region in Turkey with a leading greenhouse that cover an area of 53% of the total greenhouse in the country (Yilmaz et al. 2005). The extensive use of fertilizers and pesticides in agricultural land within the travertine region is very common leading to groundwater pollution. The decline of water quality has been reported in some travertine karstic region of Antalya(Gültekin 2001; Ayse Muhammetoğlu and Yalcin, 2003).

Moreover, Antalya is one of the main touristic cities in Turkey and has been experiencing a rapid increase in population especially in summer seasons where population of Antalya increases to more than 2 million people. This increase in population calls for an expansion of industries and agricultural areas to meet basic needs. This was resulted in growing water demand in all sectors, which may lead to water quantity and quality problems.

The study area is located in the Mediterranean region of Turkey in Antalya. Therefore, another potential problem is that Mediterranean regions of Turkey are prone

[1] https://knoema.com/atlas/Turkey/Antalya

to climate change (Tayanç et al. 2009; Lelieveld et al. 2012). The important impact resulting from climate change are increase temperature, and changes in the precipitation regime. Unal, Deniz et al. (2012), noted that reduction in the precipitation is anticipated in the Mediterranean region of Turkey. This may further increase pressure on surface and groundwater in the region. Consequently, groundwater conservation measure is essential. Therefore, it is possible to incorporate groundwater conservation measures into the planning process through research of this kind.

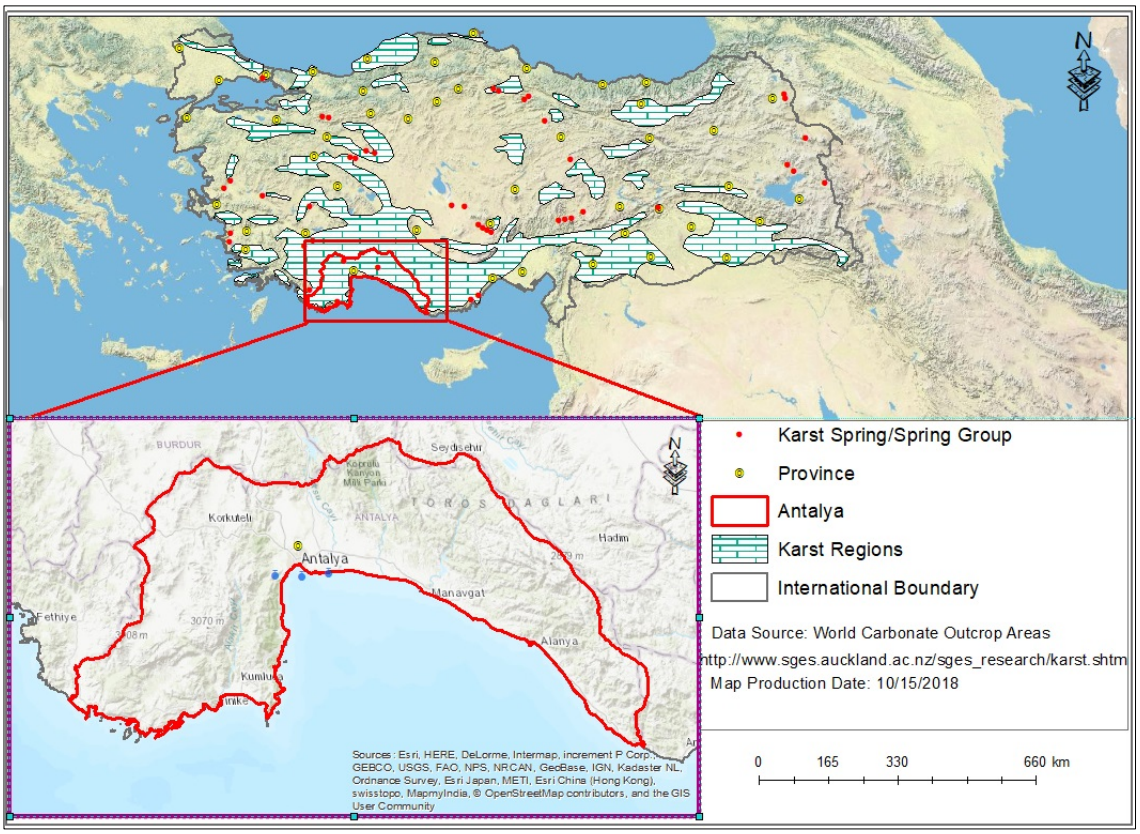

Figure 1.1. Map shows location of Antalya

1.2. Aims and Objectives of the Study

The aim of this study is to investigate and analyze the current situation of the groundwater aquifer in the karst region of Altınova using Visual MODFLOW flex. It also aims at developing scenarios to predict the future groundwater level status based on the current practices. The specific objectives of this study, therefore, are threefold:

1- To use the available data collected under the scope of a previous TÜBİTAK project to simulate groundwater in the karst system using Visual MODFLOW flex for management purposes.
2- To develop scenarios using Visual MODFLOW to predict the forthcoming groundwater level.
3- To recommend management strategies to karstic aquifer systems

1.3. Significance of the Study

Groundwater is the most important source for drinking water and irrigation in Turkey where it represents70% of the total available water resources (Sargin et al. 2000). However, the groundwater aquifer is vulnerable and has high potential of being depleted under the current practices and the future influence of climate change. The current research intends to support the decision makers by providing reliable analyses and investigations of the groundwater conditions using sensitivity analysis accounting for various scenarios. Numerical modelling using MODFLOW was used to conduct such analysis. On the other hand, the traditional numerical model is challenging in karst regions (Scanlon et al. 2003; Worthington 2009; Ghasemizadeh et al. 2012). This study was the first carried out in the travertine of Altınova to evaluate groundwater system using Visual MODFLOW flex. This first trial is believed to positively impacting the knowledge of groundwater flow in the Altınova region and similar regions. Visual MODFLOW was chosen because of its user-friendly environment, and its proven capability for standard professional two-dimensional and three-dimensional groundwater flow and contaminant transport simulation.

1.4. Scope and Structure of the Study

The scope of this study is to obtain the required data from the completed TÜBİTAK project No 114Y696 (Muhammetoğlu et al. 2017), for the following tasks: first to apply a user-friendly computer program Visual MODFLOW flex, in simulating groundwater flow in the karst system of Altınova, second to calibrate the steady-state groundwater flow model using Visual MODFLOW flex, third to analyze the various previously collected groundwater data and develop a scenario to predict the forthcoming groundwater table elevation in the study region, the fourth task is to propose a management strategy for groundwater resources in the fragile karst aquifer of Altınova.

The first step employed in this study involved meeting with the director of TÜBİTAK project No 114Y696. The second step was a collection of data from literature and the existing database. The third task was the work which involved preprocessing and cleaning of the data using Geographical Information System (GIS). Surfer version 13 was used in the preprocessing stage to create model surfaces. The fourth stage was to develop a conceptual groundwater flow model in which the model domain was divided into several discrete finite grid cells. In the fifth phase, the model was converted to a numerical model. In the sixth stage, the model was calibrated using parameter estimation tools (PEST). The groundwater table elevation was calibrated with the average seasonal groundwater measurement. To evaluate the accuracy of the model predictions, post-processing statistical analyses was carried out. A Scatter plot of simulated versus calculated groundwater table elevation was developed with the help of MS. Excel. Contour maps of simulated and calculate groundwater table elevations were created using licensed GIS software version 10.3.1. The velocity vector map and groundwater flow direction were generated. Finally, three different scenarios were formed using different pumping and recharge scenarios, and the model was run to evaluate the impacts of the scenarios.

1.5. Layout and Thesis Structure

The presented thesis work consists of five chapters. Chapter one contains an introduction and describes the background of the study region. Chapter two gives a review of the literature. In this chapter a review of groundwater is described. A subsection of chapter 2 discusses karst aquifers in the Mediterranean countries, their position and distribution in Turkey. Relevant approaches for simulating groundwater flow in a karst system are described, and the application of MODFLOW in karst areas are reviewed. Chapter three presents a modeling approach and data collection techniques. Also, necessary steps and strategies employed in analysis, model discretization and simulation of groundwater in the karstic area of Altınova are described. The process employed in the conceptualization and development of the numerical model and calibration process is discussed. A brief overview of the study area and its climatological condition and geology is presented. The result and discussion are given in chapter four, followed by the conclusion and recommendation in chapter five.

2. LITERATURE REVIEW

This chapter provides a review of groundwater modeling approaches, and a summary of the karst aquifer and its characterization. In the review of the literature, the main sources used were books, journals, conference proceedings, and other study materials. A large part of the literature shows the contribution of various researchers on solving groundwater problems in non-karst aquifers. Perhaps the complexity and heterogeneity of karstic aquifers makes them problematic when attempting to develop groundwater flow models. Despite all these challenges, various approaches are applied in simulating groundwater in karstic aquifers around the globe. In this chapter, first an overview of groundwater is described. Second, a review of karst aquifers in the Mediterranean countries, and their positions and distribution in Turkey, are discussed. Third, relevant approaches for simulating groundwater flow in karst aquifers are described. And finally, application of MODFLOW in karst region are reviewed.

2.1. Overview of Groundwater

Groundwater account for about one-third of freshwater on the earth. It is an important natural resource for energy and food security, human health and ecosystem. Many parts of the world are facing a shortage of fresh water. The water shortage is anticipated to increase in the future due to changes in climatic condition and the increase in water uses associated with economic development and increase in population (Lelieveld et al. 2012). Groundwater is the most extracted natural resource in the world. Groundwater plays a major role in the water supply in European Union countries and contributes significantly to agriculture and industrial sectors in many parts of the world (Vrba et al. 2006). Groundwater has been contaminated and decreased in many aquifers around the world either by over-pumping or other anthropogenic activities (Maliva 2016). The Context of this study focuses on the karst aquifer system of Turkey, specifically in the Mediterranean region south part of the country in Antalya province.

2.2. Overview of Karst Aquifers in Mediterranean Countries

Karst aquifers are resourceful aquifers in terms of groundwater availability. Because of their productive nature, karst regions emerge as a subject of the hydrological and scientific research in recent years. The term ‘karst’ is generally used in a geomorphological perspective to describe terrain that developed because of the high dissolution of rock, such as limestone, with well-developed secondary (fracture) porosity (Figure 2.1). Karst regions exhibit distinctive hydrology and landforms such as sinkholes, caves, sinking stream, and springs (Ford and Williams 2007). Kaçaroğlu (1999) defined the karst aquifer as a landscape environment that basically developed insoluble rock (for instance gypsum, salt rock, quartzite). Karst systems are normally characterized by specific surface and underground landforms and features such as caves, closed depressions, and dry valleys. Gallegos (2011), stated that karst terrain is characterized by springs, caves, sinkholes, and a unique hydrogeology that results in aquifers that are highly productive but extremely vulnerable to contamination. Karst aquifers cover a large region, approximately 20%, of the earth’s surface, which account for about a quarter of the world’s surface area (Ford and Williams 2007). Roughly 20 to 25% of the earth’s population depends partly or entirely on the groundwater extracted from karst aquifers (Ford and Williams 1989; Ford and Williams 2007; Ronald and Scott 2006). Similarly,

Bakalowicz et al (2008) and Stevanović et al (2015), pointed out that countries in Southeastern Europe and the countries in the Middle East depend largely on karstic groundwater resources. Zwahlen (2003), estimated that groundwater originating from karst regions meet 50% of the total water demand in some European countries such as Slovenia, Austria, and Croatia. Similarly in Southwest China karst aquifers contribute 50% or more to regional freshwater supply (Hartmann et al. 2014).

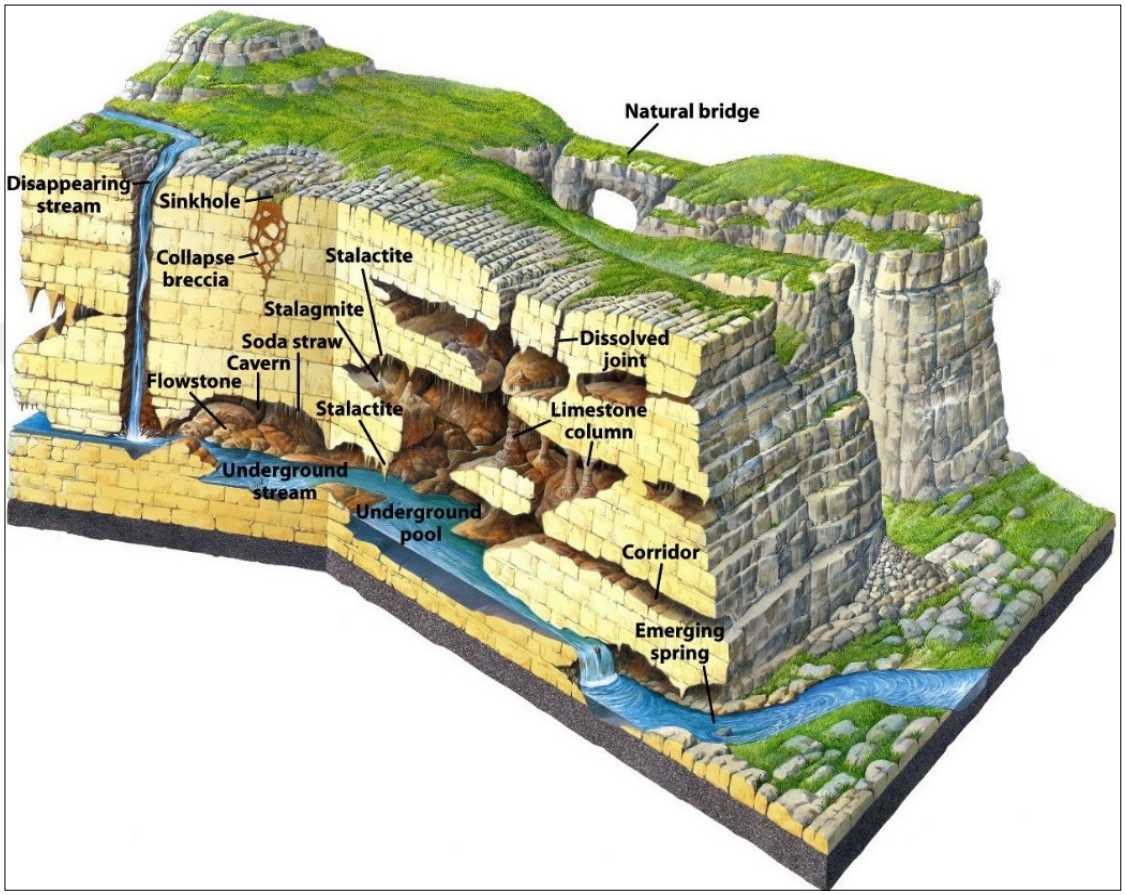

Figure 2.1. Karst aquifer shows karst features such as dissolved sinkholes, caves, and fractures, Figure is from (Marshak, 2015) [1]

Karst aquifers developed in soluble rock by the movement of groundwater and are characterized by enlarged fractures, bending planes and conduits that form a hydraulically connected drainage network (Goldscheider and Drew 2007). A karst system can develop in quartz, sandstone, or quartzite regardless of hydro-climatic condition and its less alterable rocks nature (Piccini and Mecchia 2009). Furthermore, Goeppert et al. (2011) stated that karst can also be found in other rocks types with predominantly carbonatic composition, including carbonatic conglomerates. Evaporitic formation, which includes gypsum and anhydrite, are also highly karstified (Chen et al. 2017). In our case study, the karst system is found in travertine and conglomerates formations of Antalya, Turkey.

[1] Karst features such as dissolved sinkholes, caves, and fractures are well described in (Marshak, 2015) Earth: Portrait of a Planet (5th ed.).

Karst aquifers naturally interconnect over a large region (Chen et al. 2017), and are considered as transboundary aquifers. These examples highlight the need for a fully integrated water resources map. The maps showing regional distribution of carbonate rocks are presented in (Ford and Williams 2007). The updated version of the regional distribution map of the world karst aquifers was produced by the World Karst Aquifer Mapping (WOKAP) team and is available at the WOKAP website[1].This distribution map was produced based on available references and the opinions of the local expert, in addition to detailed high-resolution Global Lithological Maps (GLiM) (Hartmann and Moosdorf 2012).

According to Stevanović (2018), the Mediterranean countries, namely Turkey, Spain, France, and the countries of North Africa covered a karst area of nearly 25 – 35% of its total area. Stevanović (2018) further stated that the largest area of karst is found in Asia and roughly covers more than 7.5×10^6 km^2. Furthermore, the Russian Federation, the largest country in the world, also has a prodigious karst area that covers approximately 15 percent of its total land. Other large areas of karst can also be found in Mexico, Algeria, Egypt, Iran and Saudi Arabia. When considering water supply systems in the karstic aquifers, Montenegro has a higher percentage of water supply followed by Austria. On the other hand, Turkey, Iraq, Slovenia, Herzegovina, and Croatia have a lower proportion of water supply. This is because of the lesser extent of aquifers (Stevanović et al. 2015). There are 29 springs in the karst Mediterranean basin that regularly discharging higher than 2 m^3/s and eight of them are in the Mediterranean region of Turkey (Stevanović 2018).

Groundwater resources in the Mediterranean karst regions are essential for the development of both early cities and kingdoms throughout history. Bakalowicz (2005), Piccini and Mecchia (2009), stated that karst springs are one of the cleanest water resources extracted directly for consumption. with high alteration in term of discharges and quality. Qualitatively groundwater abstracted from karst aquifers requires less treatment if they are not anthropogenically polluted. Unfortunately, due to unique hydrogeological characteristics and the feature of karst system render them susceptible to contamination by the wide ranges of anthropogenic activities. The natural reduction of pollutants effects in karst aquifers is substantially limited (Bottrell et al. 1989) for many reasons:

1- significant insufficiency of the convenient surface zone for adsorption, particles exchange

2- a high infiltration rate of water which lessens the chance of evaporation of highly volatile chemical compounds

3- large secondary voids and naturally thin soil cover which makes the process of infiltration relatively infective, thus allowing rapid transport of contaminants into karst aquifers

[1] http://www.sges.auckland.ac.nz/sges_research/karst.shtm

4- turbulent flow regimes generally related to conduit aquifers which catalyze transportation of pollutants to the karst system

5- inadequate time for the elimination of contaminants due to high flow rates

Therefore, karst aquifers are vulnerable to pollution. The fragile karst aquifers are under pressure, because of expansion in the agricultural areas, industrialization, and urbanization to meet the demand of growing development and population increase.

2.2.1. Potential effect of climate change on karst groundwater

Climate change is one of the critical factors that cause a series of karst hydrogeologic and water environmental problems. The climate change projection drawn from Global Circulation Models (GCMs) suggest a significant alteration to precipitation and temperature regimes in many karst regions (Chen 2017). Hartmann et al. (2014), stated that due to a climate change, a dramatic increase of stress on karst water in both quality and quantity is expected. Similarly, the significant impact of potential climate change on groundwater recharge was reported in European karst region (Hartmann et al. 2015). Mediterranean regions of Turkey are prone to climate change (Tayanç et al. 2009; Lelieveld et al. 2012). These will further increase the pressure on groundwater resources in the Mediterranean karst region.

2.3. Distribution of Karstic Aquifers in Mediterranean Cities of Turkey

The karstic aquifers in Turkey cover approximately one-third of the country's total area. These karst regions hold a significant amount of water and satisfy a significant portion of water demand around the country, especially in the Mediterranean basin. Approximately 20% of irrigable land surface is feed with karst groundwater. Intensive karstification is present in almost all regions of the country (Elhatı 1997; Günay 2010; Güner et al. 2015). Groundwater originating from karst aquifers play an important role in meeting irrigation, industry and drinking water demand along the Mediterranean region of Turkey (Elhatı 1997; Günay 2010; Güner et al. 2015).

The karst terrain of Turkey is categorized into four regions, namely; Southeast Anatolia karst region, Central Anatolia karst region, Northwest Anatolia and Thrace karst region as well as the Taurus karst region (Güner et al. 2015). The four different karst region is depicted in Figure 2.2. The Taurus karst region is one of the most interesting and largest karst regions in the world (Güner et al. 2015). Furthermore, Güner et al. (2015) estimated that the Mediterranean carbonate rock of Turkey covers an area about 200 km along the Taurus Mountains.

Geographically, the Thrace karst region is a transboundary region that occupies territories of three South-eastern countries of Europe, namely Greece, Turkey and Bulgaria. Many springs exist in and around Antalya province. These include the Finike-Tekke Elmalı-Akçaçay-Demre plains, Salur, the Boğaçay plain, Kırkgöz, Düdenbaşı (underground river) and Köprüçayı River valley Springs (Dumanlı). (Güner et al. 2015) noted that the discharge rate of these springs ranges from 3 – 60 m^3/s. Furthermore, (Günay 1985) highlights that the Düdenbaşı underground river in the Mediterranean

region of Turkey is the largest spring in the world. Dumanlı discharges a maximum of about 60 m^3/s from a single crack and it sometimes discharges a minimum of 38 m^3/s.

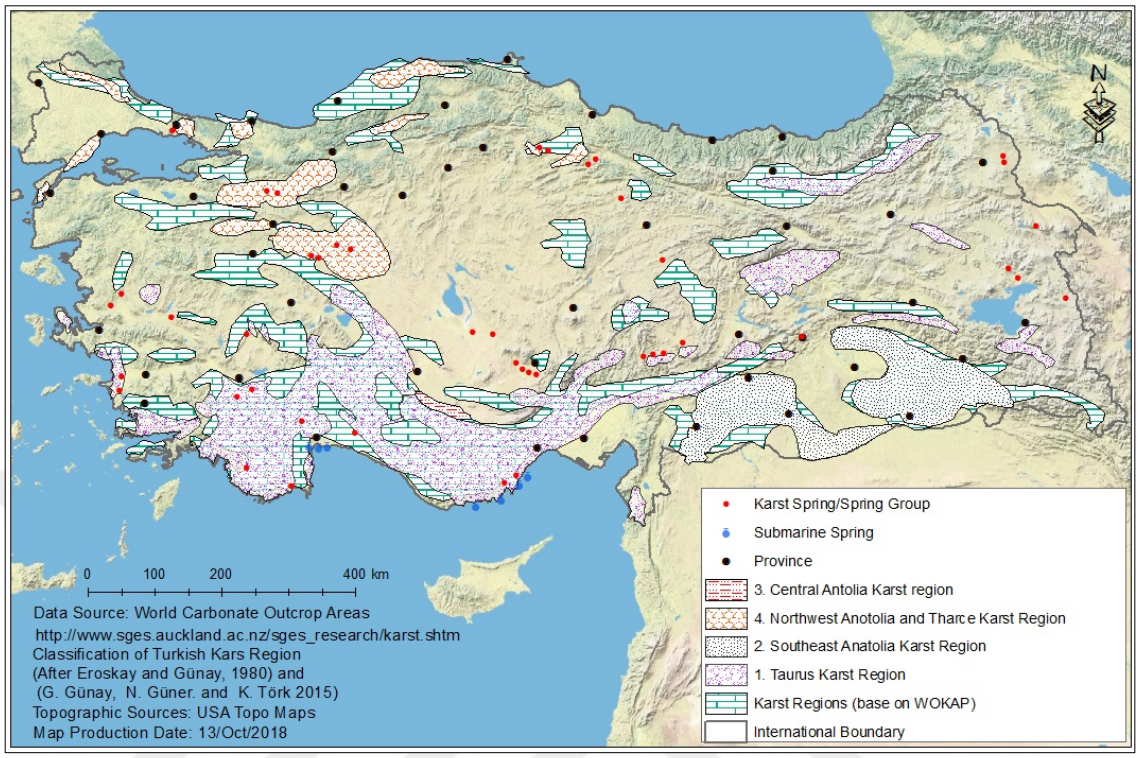

Figure 2.2. Distribution map of karst areas in Turkey.

2.4. Groundwater Modeling Techniques and Categories

Groundwater modeling is a simplified picture of the intricate, natural, real world and is therefore, not exact description of physical system (Anderson et al. 1990). The most important and fundamental step in modeling, however, is model conceptualization. Groundwater modeling plays an important role in understanding the past and present and predicts the future state of the aquifer. Groundwater modeling can be simple such as one or two dimension or sophisticated three-dimensional models. Hill (2006) argues that starting with the simple model in groundwater modeling is valuable as long as the model concept satisfies the modeling objectives. The stepwise general methodology of groundwater modeling is depicted in Figure 2.3.

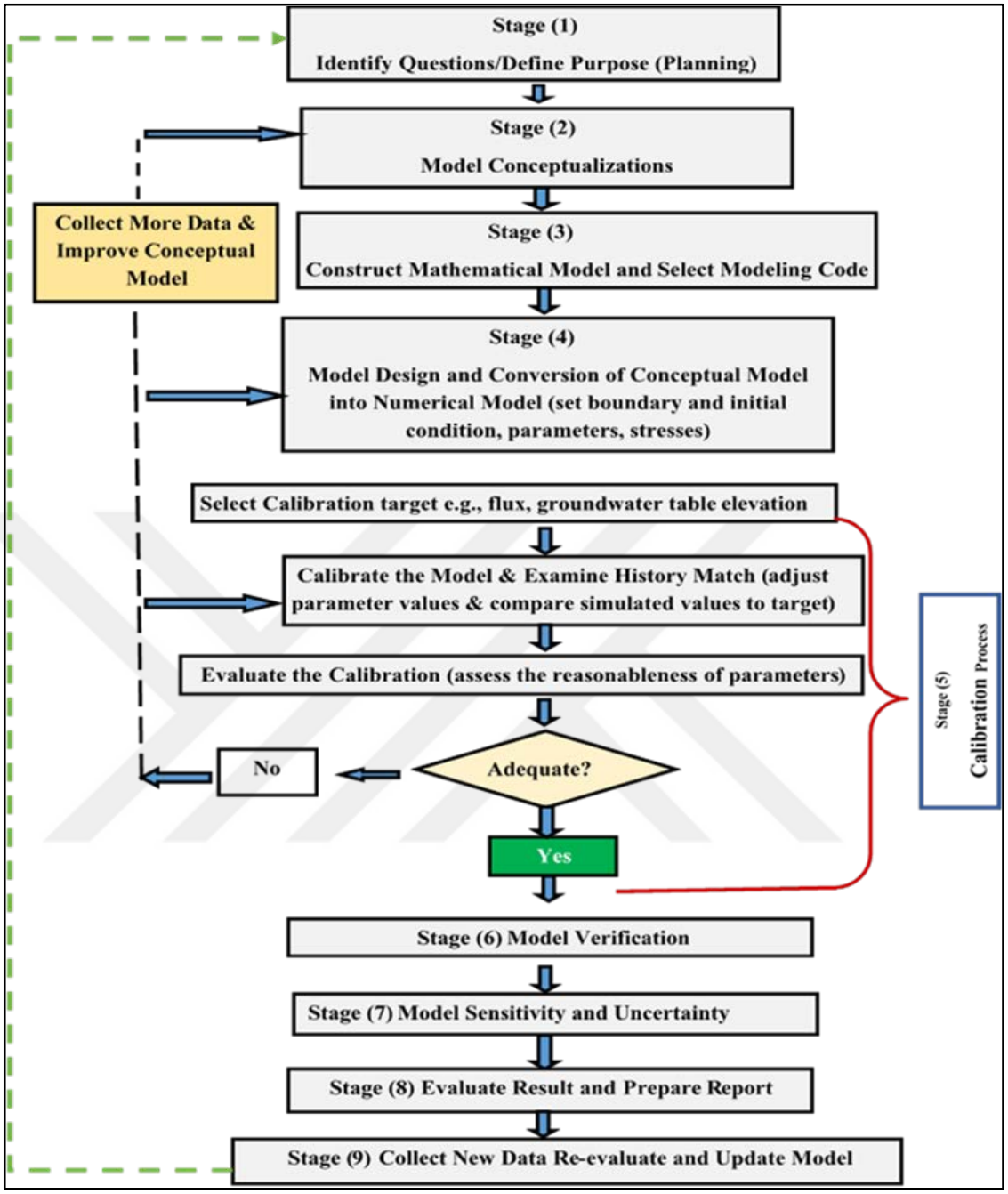

Figure 2.3. Stepwise workflow for groundwater modelling (Anderson et al, 2015)

2.5. Categories of Groundwater Models

In general, there are many ways to classify groundwater modeling: (1) a physical model (e.g. a sand tank) replicates physical features, usually on a smaller scale than encountered in the field. (2) an analog model and (3) a mathematical model. For this present work, a mathematical model is employed to achieve the objective of the research. The mathematical model in hydrogeology modeling needs simplifying assumptions. These hydrological assumptions are embodied in the governing equation because, in general, it is nearly impossible to simulate the exact field situation especially in a complex

aquifer such as karst aquifer. The general governing equation for three-dimensional and two-dimension transient groundwater flow is given in equation (2.1) and equation (2.2) respectively.

$$\frac{\partial}{\partial x}\left(k_{xx}\frac{\partial}{\partial x}\right)+\frac{\partial}{\partial y}\left(Kyy\frac{\partial h}{\partial y}\right)+\frac{\partial}{\partial z}\left(K_{ZZ}\frac{\partial h}{\partial z}\right)=S_s\frac{\partial}{\partial t}\pm W^* \quad (2.1)$$

$$\frac{\partial}{\partial x}\left(k_x h\frac{\partial h}{\partial x}\right)+\frac{\partial}{\partial y}\left(k_y h\frac{\partial h}{\partial y}\right)+\frac{\partial}{\partial z}\left(K_Z\frac{\partial h}{\partial z}\right)=s_y\frac{\partial}{\partial t}\text{-}R \quad (2.2)$$

where,
K_{xx}, K_{yy}, and K_{zz}: are the values of hydraulic conductivity along the x, y and z direction.
h : is the potentiometric aquifer head.
W^* : is the volumetric flux per unit volume representing sources and/or sinks of water (negative for in-flow, positive for outflow).
T : is time
S_y : is specific yield
R : is recharge rate
Ss : specific storage of the porous media.

(Harbaugh, Arlen, 2005), used a finite difference version of equation (2.1) and equation (2.2) in MODFLOW, where the groundwater flow system is divided into a grid of cells. Mathematical descriptions of groundwater flow modeling are based on two principles: Darcy's law and conservation of mass (H. M. Haitjema, 1995). The mathematical model can be further categorized into: the analytical model, and numerical model.

2.5.1. Analytical model

An analytical model needs simple geometry and boundary conditions. Therefore, it is best compared to the numerical solution. H. Haitjema (2006), asserted that an analytical solution can be employed as a guide for the numerical model. Kelson, Hunt, and Haitjema (2002) claimed that an analytical solution is useful in assessing model conceptualization. On the other hand, the analytical model is incapable of simulating complex problems because of its partial limitation in area of extensive local heterogeneity. Chamberlin (1899) emphasizes that an analytical element uses a superposition of multiple analytic solutions to solve relatively complex groundwater flow problems. Analytical models are computationally effective and provide more accurate solutions than numerical models, they are suitable for limited data, and are used for quick initial estimation of systems behavior (Anderson et al. 1990). On the other hand, analytical models are problematic to apply in complex model geometry, and they are restricted to one-dimension and two-dimension model.

2.5.2. Numerical model

A numerical groundwater model uses an estimate form of the governing equation to simulate groundwater. Therefore, it is one of the important tools in hydrogeological studies. A numerical model breaks up regions and time into discrete divisions. Features of the governing equation and boundary conditions such as aquifer geometry, hydrogeological properties, and pumping rate are designated in the numerical model with temporal and spatial variation. This enables a more complex, and potentially more accurate approximation of groundwater than could be accomplished with an analytical model (Kumar 2015). In other words, a numerical model can handle more complicated problems than analytical model.

The recognized main numerical models for solving groundwater equations are the "Finite Difference" Method (FD) and the "Finite Element" Method (FE). These two methods are documented in (Anderson et al. 2015). These two methods differ in concept although they produce comparable results, even for more complex versions of the governing equation than the Laplace equation. Figure 2.4 shows the Finite Difference (FD) mesh/grids and Finite Element (FE) mesh/grids. The general stepwise development approaches for both Finite-difference and Finite-element is depicted in Figure 2.5. The decision of which technique to utilize relies basically on the factors and the nature of the complexity of the problem and the modelers familiarity with each method. The advantages and disadvantages of both the Finite Difference (FD) and the Finite Element FE methods are discussed by (Faust and Mercer 1980).

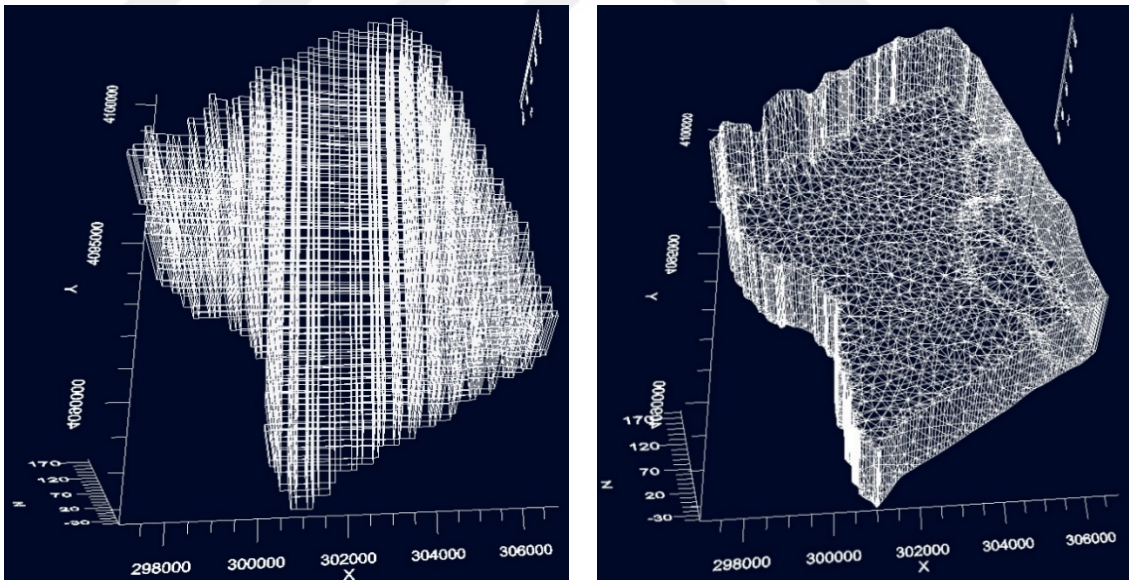

(a) (b)

Figure 2.4. Types of numerical models mesh/grids Finite Difference Grids FDG **a)**; Finite Element Grids FEG **b)**

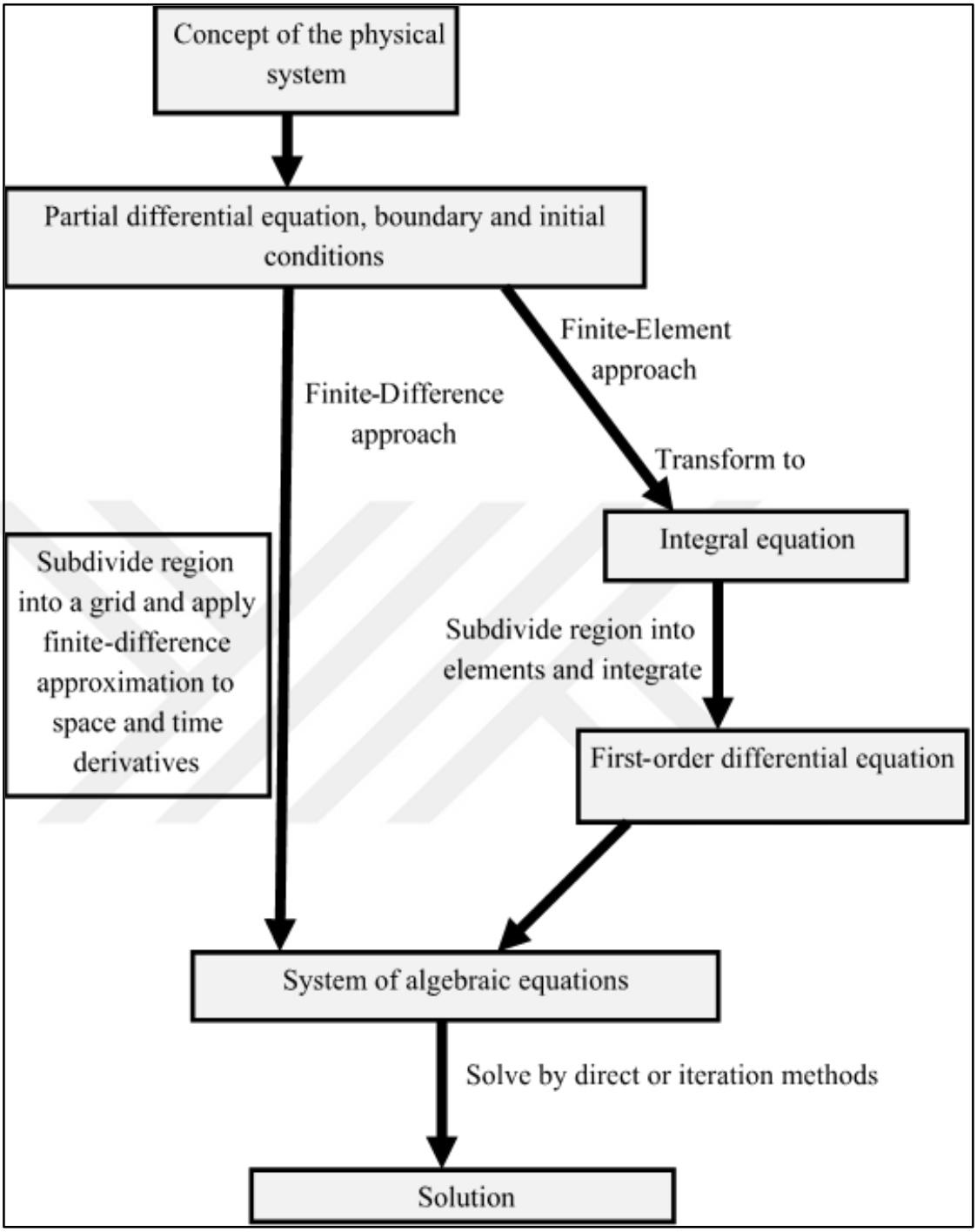

Figure 2.5. Generalized model development by Finite-Difference and Finite-Element method adapted from (Faust and Mercer 1980)

2.5.2.1. Finite differences method FD

The Finite-Difference (FD) method is one of the oldest methods for solving partial differential equations. The Finite Difference method is extensively described by (Trescott et al. 1980). Many codes exist such as MODFLOW-88, MODFLOW-96, MODFLOW-2000 and MODFLOW-2005, that can be used in groundwater flow modeling using the

Finite Difference method (FD), in our study MODFLOW-2005 was used. In the Finite Difference approximation, the computational domain is discretized by rectangular or quadrilateral cells where the spacing of nodes along rows, columns, and the spacing between layers is designated by *i,j,k* respectively (Figure 2.6). Anderson et al (1990), stated that a standard FD grid is rectangular and structured, although an unstructured FD grid is more flexible in terms of grid design and provides much of the flexibility of an FE mesh or grids, in our study standard rectangular FD grids with the resolution of 25600 m^2 were used. According to Franklın and Zhang (2003), the accuracy of the Finite-Difference (FD) method depend on the homogeneity and the extent of the grids. Franklın and Zhang (2003) stated that when the FD grids spacing is close to zero, the approximation of the derivative improves. On the other hand, the level of numerical dispersion and truncation error increases. Finder and Gray (1977) grouped the Finite Difference method based on its application into forward, backward, and central differences. Finder and Gray (1977) claimed that the central difference method in Finite Difference yield more accurate results than the other three methods.

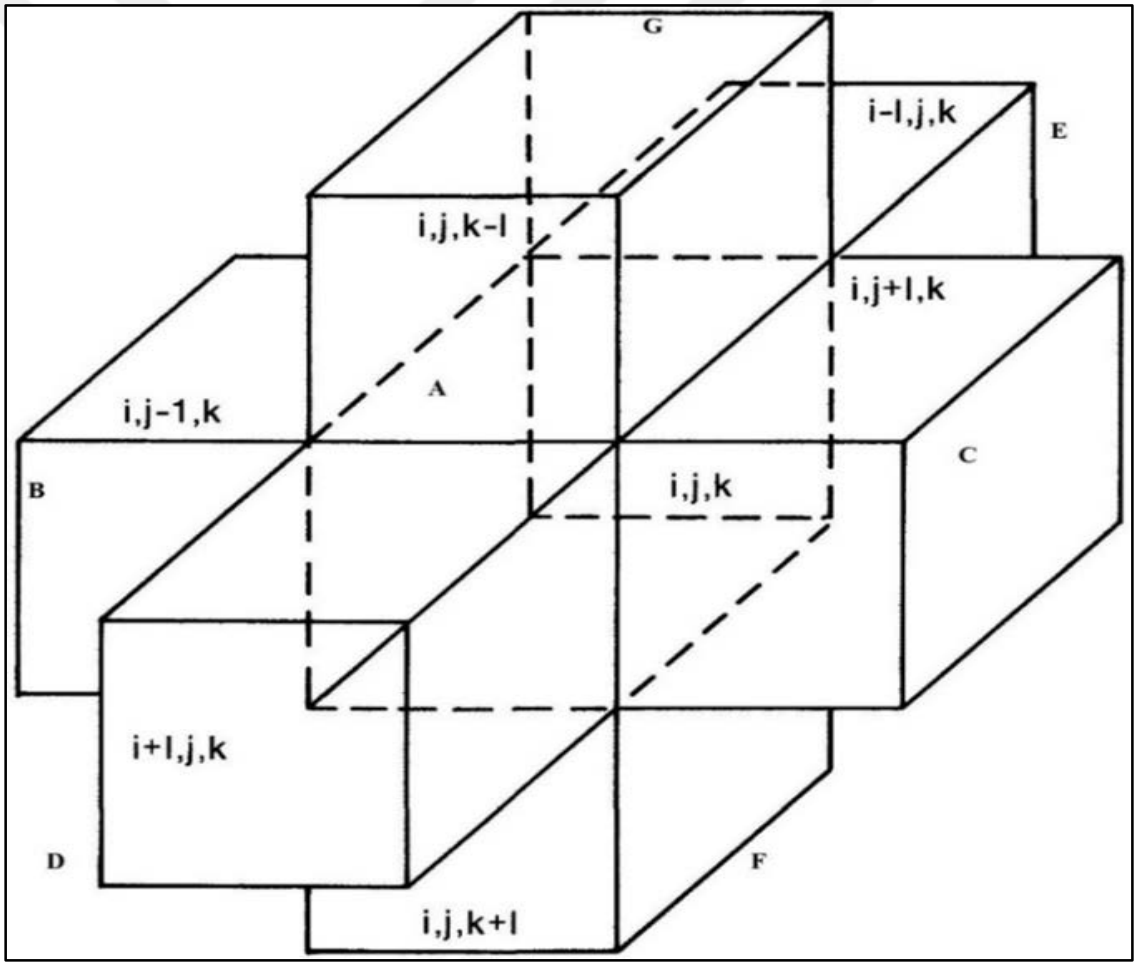

Figure 2.6. Finite-Difference (FD)[1] grid and notation figure from (McDonald and Harbaugh 1984).

[1] In the FD method, nodes are located in 3D space using indices (i,j,k) to assign relative locations within a rectangular grid.

2.5.2.2. Finite-element method

In the literature, the Finite Element (FE) method was introduced into groundwater modeling in the mid-1960's. Since then, the Finite Element method has developed into a very powerful numerical tool for solving a variety of groundwater flow problems (Holz et al. 1982). As mentioned by (Anderson et al. 1990) an application of the Finite Element (FE) method to groundwater problems is a relatively new in contrast to the Finite Difference method.

The FE model approximates the flow equation by integration compared to the Finite Difference method which estimate by differentiation (M. Anderson et al., 1990). Therefore, the calculation of the Finite-Element FE method is more complicated than the Finite-Difference (FD) method. Wang and Anderson (1982), stated that the Finite Element method solves the transient flow equation by incorporating both finite element and finite difference concepts. According to Mikszewski and Kresic (2015) the Finite-Element (FE) Method is the best method in handling point sources and sink and large variations in water table elevation, such as those found in karst. On the other hand, Faust and Mercer (1980) state that the Finite-Element method is characterized by a high standard mathematical basis that makes its programming and data input difficult.

2.5.3. Data requirements for groundwater modeling

Data collection is one of the vital components in the model development process. The quantitative hydrological data needed for developing and testing a numerical model can be grouped into two sections: (A) physical, and (B) hydrological frameworks.

The physical framework data includes: (1) topography showing surface water body, surface elevation contour, and other man-made water courses (2) geology data showing geological information of the system, and structural areas impacting the movement of groundwater, (3) type of aquifer, such as confined aquifer, unconfined aquifer and semi-confined aquifer, (4) aquifer thickness and lateral extent, (5) aquifer boundaries, (6) lithological variation within the aquifer and aquifer characteristic.

Data within the hydrological framework includes: (1) groundwater table elevation which is needed to formulate the conceptual model and check model calibration, (2) hydrological data which also includes the rate of the recharge, (3) type and extent of discharges such as pumping wells, evapotranspiration. (4) data on the hydrological framework including precipitation. Generally, data in physical framework define the geometry of the system including thickness and real extent of each hydrostratigraphic unit. Data within hydrological frameworks define hydrological properties and hydrological stress. The data required under physical and hydrological framework are summarize in the Table 2.1 below

Table 2.1. summary of physical and hydrological framework data for groundwater modeling

Physical framework	**Type of data used in this study**	**Hydrological framework**	**Type of data used in this study**
Topography	✓	Groundwater table elevation	✓
Geology	✓	Rate of recharge	✓
Types of aquifers	✓	Rate of discharge (pumping)	✓
Aquifer thickness	✓	Type and extent of recharge areas	✓
Aquifer boundaries	✓	Type and extent of discharge areas	
Lithological data		Evapotranspiration	
Aquifer characteristics		Hydraulic conductivity values	✓
		Transmissivity	

2.5.4. Model layers and elevation in groundwater modeling

Most numerical groundwater models simulate flow in two or three spatial dimensions; one-dimensional numerical models are rarely used. The two-dimensional represents the groundwater system as a one layer. Two-dimensional (2D) model, replicated flow in two horizontal dimensions to represent flow in either a confined or unconfined layer. Hamlet (1990), pointed out that it is preferable to designate all of the layers as a convertible layer. The conceptual model layer within the context of our study was designated as a convertible layer. Anderson et al. (1990) stated that:

"*top elevation of the top layer can be set arbitrarily higher than the expected maximum elevation of the water table to avoid unintended conversion to confined conditions"*

However, in practice, the top elevation is usually set equal to the elevation of the land surface by using a GUI or GIS M. Anderson et al (1990). This is in line with the top elevation in our research.

2.5.5. Boundary conditions in numerical groundwater modeling

Boundary conditions are significant, and their use is standard practice in groundwater modeling. Boundary conditions normally describe inflow and outflow from the model domain and are considered as the first step in model conceptualization. There are three different types of boundary conditions:

- type 1–boundary with specified head (Dirichlet conditions)
- type 2–boundary with specified flow
- type 3–boundary with head dependent flow

The General Head Boundary (GHB) condition (type 3) represents the most general boundary condition available on MODFLOW. All three types of model boundary conditions can be assigned either constant or variable with time. In our study type (3) General Head Boundary was applied in simulating groundwater. These different boundaries are documented by (Franke et al. 1987).

2.6. Model Calibration

Model calibration involves finding a set of parameters such as hydraulic conductivity, recharge, and boundary conditions, that fit historical field-measured values within a pre-established range of error. Calibration is a compulsory part of the modeling process that enables predictive simulation. Model calibration in groundwater can be categorized into manual calibration which is through trial-and-error, and automated calibration (parameter estimation) with the help of a computer algorithm. Anderson et al. (1990) recommended manual calibration in the first step of groundwater modeling, and then automate calibration (parameter estimation) can follow. In this study both approaches were attempt with more emphasis on automate calibration using parameter estimation tool (PEST).

2.6.1. Manual calibration approaches in groundwater modeling

Manual calibration (trial-and-error) remains a fundamental first step in groundwater modeling because it helps to develop a modeler's "hydrosense". Manual groundwater calibration is the process whereby the modeler changes the parameter values initially assigned to the model and compares the model result with the targets for example groundwater table elevation. Subsequent trial runs insensitive parameters are set as invariant, or fixed, values that are based on field data, literature values, professional judgment, and/or other expert knowledge. According to Anderson et al (1990), manual calibration is not practicable in a complex groundwater system because it is tough to track the effect of all variations in calibration parameters. The general workflow for manual trial and error calibration is depicted in Figure 2.7.

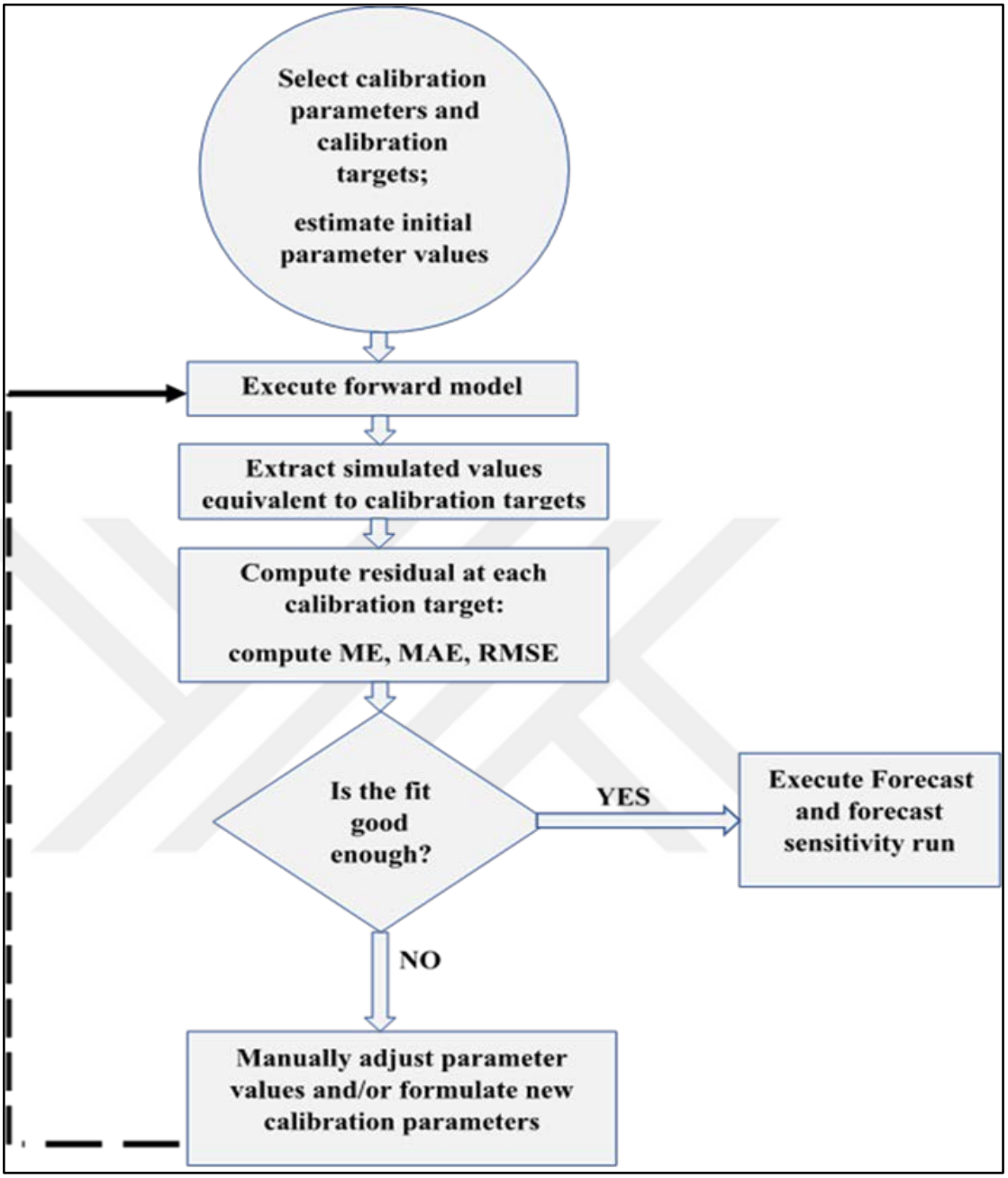

Figure 2.7. General workflow for manual trial and error adopted from (Mary P. Anderson et al., 2015) (ME, MAE, RMSE)[1]

2.6.2. Automate groundwater calibration

Automated calibration is the simple type of calibration process, which lessen modeler bias, and increases the fit between measured and computed hydrographs. The automated calibration method is performed using especially developed computer codes. The automate calibration solves inverse problem in two ways, direct or indirect. When

[1] ME, mean error; MAE, mean absolute error; RMSE, root mean squared error

solving inverse problems using a direct solution in automated calibration, the value of the head must be specified for all model. The head in the whole model mesh/grids is estimated from the head at the observation well by means of an interpolation method such as kriging (Anderson et al. 1990). A well know automated trial-and-error groundwater calibration is Parameter Estimation Tool (PEST) (Doherty and Hunt 2010). This tool is supported by several current commercial Graphical-User Interfaces (GUI) groundwater modeling software. Borchers, and Thurber (2013) express that advanced statistical theories such as singular value decomposition, Tikhonov and regularization play a significant role in addressing highly parameterized problems in the field of geophysics. Many of these advanced methods are now available to groundwater modelers through the Parameter Estimation Tool (PEST) software. The details of Parameter Estimation Tool (PEST) are documented by (Doherty and Hunt 2010). A stepwise schematic diagram of a general workflow for parameter estimation is depicted in Figure 2.8.

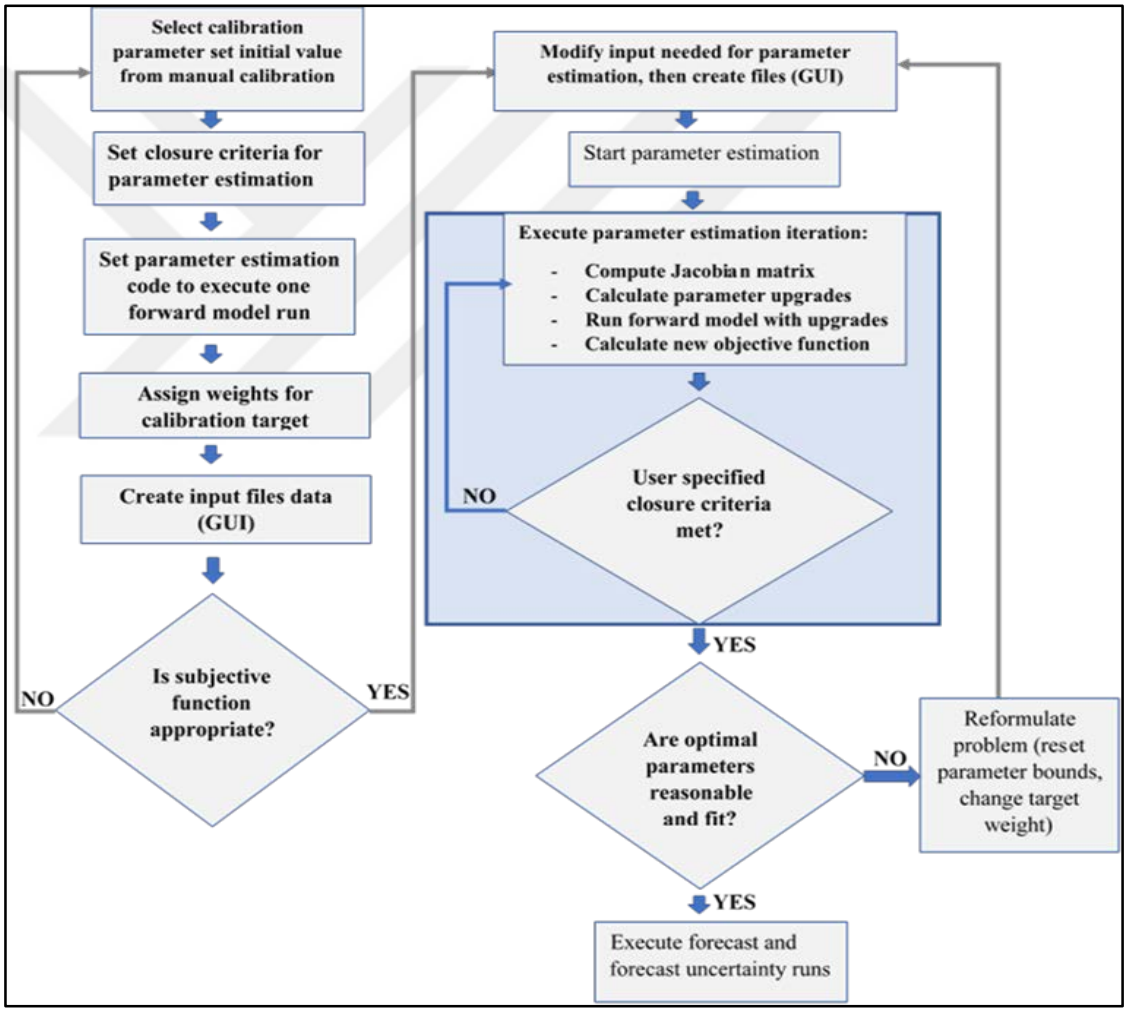

Figure 2.8. A schematic diagram of a general workflow for parameter estimation adopted from (M. P. Anderson et al. 2015)[1]

[1] Shaded box is the parameter estimation code, steps in the unshaded areas require modeler intervention

2.7. Approaches for Characterizing Groundwater Flow in Karst Systems

Karst aquifers are characterized by high complexity, heterogeneity and discontinuity, prompt in duality of recharge, infiltration porosity, storage and flow (Ford and Williams, 2007; Goldscheider and Drew 2007). Consequently, karst systems need special investigation techniques of modeling. As the nature of karst aquifers differs significantly from porous media, their characterization methods are also different (Groves 2007). Goldscheider (2015b) argue that most of the karst methods used in karst aquifers are similar to those methods used in non-karstic aquifer. Goldscheider (2015a) further noted that, specific adjustments are required when using these methods in a karst area.

Different approaches for modeling groundwater flow in karst aquifer are described in this section. Many investigation techniques use for karst modeling were mentioned in the literature for example (Bechtel et al. 2007; Benischke et al. 2007; Criss et al. 2007; Geyer 2008; Goldscheider and Andreo 2007; Groves 2007; Hunkeler and Mudry 2007; Kresic 2007; Chalikakis et al. 2011; Kuniansky 2014). These karst methods include: (1) geophysical and speleological , (2) geological, (3) hydrological, (4) hydraulic, (5) tracing , (6) isotopic , and (7) hydrochemeical. The application and selection of the karst method mostly depend on the kind of hydrological problem and resources availability (Goldscheider, 2015a). These approaches possess their own set of advantages and disadvantages.

2.7.1. Speleological method

A speleological approach is a special and distinctive method for caves characterization in a karst system. White (2007), mentions that the principal source of data in the speleological investigation are the compass, tape measure, and notebook sketches, and slogging through the cave, station by station. A speleological method in combination with other methods such as hydrology and tracer techniques are more effective to obtain a more precise understanding of the position of underground drainage systems(Jeannin et al. 2007). According to Bakalowicz (2005), the speleological techniques generally require direct inspection of caves, principally described as abandoned conduits. This method is advantageous in the karst because it aids in pinpointing and mapping the past and functional/flow conduit network. On the other hand, this method is imperfect because on various occasions a restricted number of conduit system are accessible and perhaps are not representative part of the aquifers that are likely to be accessible. Additionally, Maliva (2016), stated that the speleological method needs more effort and to some extent is dangerous and is not practically possible for conduits that may be too small for human exploration.

2.7.2. Geological method

Understanding the geological and external and internal (geomorphological) structure of the karst system is an essential part in the management and characterizing of karst hydrology. The geological method helps in guiding regional drainage patterns. A geological investigation is an initial facet in developing a conceptual and numerical model. Therefore, the geological method is important for management of groundwater in karst aquifers. Geological information can be collected from the field or compiled from literature in the form of geological maps and cross-sections. The problem that hinders the

application of this method is lack of data in deep and confined aquifers, and lack of link between geological data and groundwater flow. The detail of this method are described in (Goldscheider and Andreo 2007).

2.7.3. Geophysical method

Geophysical methods are used to identify hydraulic karst features, such as caverns and sinkholes, fractured zones or large conduits. The geophysical technique has been applied in solving geotechnical problems related to void are sinkhole detection in epikarst structures since the early 1960s (Chalikakis et al. 2011). Kindinger, Davis, and Flocks (2001), stated that geophysical methods played an important role in the geotechnical investigation of karst aquifers. Kindinger et al (2001) further mention that the geophysical method helps in assessing the presence of sinkholes, detecting large-scale karstification or dissolution of the underlying limestone and collapse of paleokarst. Kindinger (2001) noted that, geophysical techniques are convenient tools for exploring, and verifying geological structure, and determining overburden thickness, and for identifying fractured zones.

The advantages of the geophysical method are (1) it is practically feasible and low cost compared to drilling, and (2) data can be collected in large areas coverage (Goldscheider and Drew 2007). On the other hand, a geophysical method is limited because of (1) lack of direct and clear information on groundwater, and (2) poor data resolution in the areas of high depth. There are many methods that can be found in karst geophysics such as seismic methods, gravity methods, and electrical and electromagnetic methods, borehole geophysics (Logging). For more detail about those sub-methods the readers are referred to (Bechtel et al. 2007; Chalikakis et al. 2011).

2.7.4. Hydraulic and hydrogeologic method

Hydrologic techniques essentially focus on investigating and quantifying inflow and outflow from karst systems (establishment of water budget). Groves (2007), noted that the hydrogeologic method is limited due to lack of knowledge on the catchment boundaries.

The hydraulic method includes the creation of groundwater table elevation maps and hydraulic test in wells. Due to the spatial characteristics of karst, such methods require special adaptations when applied to karst Groves (2007). However, in confined aquifers or costal aquifers without accessible springs, such methods may be a preferred choice. The hydraulic technique is also used for determining groundwater flow direction, piezometric variation and boundary condition. The quantitative hydrogeologic and hydraulic parameters used for investigating karst systems include groundwater table elevation, hydraulic conductivity and transmissivity, groundwater velocity and flow rate, porosity, effective porosity, and storage capacity (Andreas Hartmann et al. 2014). Details of the hydraulic and hydrogeologic method and their parameters are described in (Groves 2007; Kresic 2007).

2.7.5. Hydrochemical and isotopic method

Hydrochemical techniques are mainly used to assess the water quality and investigate pollution problems in karst systems. Hydrochemical parameters can also be considered as natural tracers to provide information about travel time, biogeochemical or hydrologic behavior in the aquifers system, and much other information. (Hunkeler and Mudry 2007) classify the hydrochemical parameters according to their factors and origin into five groups: (a) rainfall-related parameters (b) soil-related parameters (c) carbonate-rock-related parameters, (d) parameters related to other rock types, and (e) anthropogenic compounds. The reader is referred to (Hunkeler and Mudry 2007) for a detailed description of hydrochemical parameters. Hydrochemical techniques require continuous monitoring, and they need to be adapted in the karst systems because of the high variability of karst water.

Karst systems can be characterized by isotopic parameters that act as natural tracers. This technique is important because it helps provide knowledge about recharge areas, the origin of water, as well as information about groundwater age and residence time. The isotopic technique is more effective when integrated with the other methods such as hydrochemeical and tracing methods. A detailed description of isotopic techniques can be found in (Criss et al. 2007).

2.7.6. Tracer method

Tracers are one of the useful tools for providing accurate and precise information about underground connections in karst aquifers systems. (Andreas Hartmann et al. 2014) grouped tracer into two classes namely (1) natural tracers (2) artificial tracers. An artificial tracer is a substance introduced into flow water to determine the actual groundwater trajectory, travel path, and flow times. An artificial tracer is one of the promising tools for investigation of conduit systems (Goldscheider et al 2008). A natural tracer is a natural substance introduced into the flowing water in a continuous manor. A Tracer test is a necessary tool for delineating spring catchment areas and for helping in investigating all forms of flow and transport processes. Further reading about trace methods can be found in (Benischke et al. 2007).

2.8. Modeling methods in karst aquifers and synopsis of previous work

Karst systems are characterized by a high degree of heterogeneity and anisotropy, which make them behave very differently from other non-karstic aquifers. Therefore, the application of traditional numerical models in karst is limited (Ghasemizadeh et al. 2012; Scanlon et al. 2003; Worthington 2009). Despite that, mathematical models of groundwater flow that take into consideration hydraulic characteristics of karst systems have been developed in the past twenty years (Kiraly 2003). Today there are a variety of techniques applicable for characterizing groundwater flow in karst aquifers, each with its own set of advantages and disadvantages. There are two general modeling approaches in karst aquifers, (a) spatially lumped models and (b) spatially distributed models.

Spatially lumped models (or global models) deal with mathematical analyses that give fundamental understanding to overall water balance, groundwater quality, and hydraulic behavior of the whole karst system. The lumped parameter requires a low data

set, and accommodates only a few adjustable global parameters, and ignores heterogeneity. Therefore, its calibration is easier than that of complex distributed models. Lumped-parameter models are grouped into two different approaches (1) hydrograph-chemo graph analyses and (2) rainfall-discharge models. Lumped karst models are used to simulate karst processes from infiltration into the soil to discharges at the karst spring. Lumped parameter models are used by many researchers to simulate the hydraulic, and chemical response of a karst spring recharging in the spring catchment (Fleury et al. 2007; Butscher and Huggenberger 2008; Hartmann et al, 2012; Željković and Kadić, 2015). Details about lumped-parameter models are described by (Ghasemizadeh et al. 2012). The advantage of this model is its ability to model water balance and the hydrological dynamic of the karst aquifer. The disadvantage is that the model cannot take into consideration the spatial variation of flow patterns. In the spatially distributed models the model domain is divided into homogeneous sub-unit grids. Specific hydraulic properties (parameters), and specific boundary conditions are allocated to each sub-unit mesh/grids. The task of distributed modeling approaches is to deal with the high spatial heterogeneity (matrix, fractured and conduits) of karst aquifers. Shoemaker, Kuniansky, Birk, Bauer, and Swain (2008), classified spatially distributed groundwater model approaches into various types of deterministic models that are applicable to karst aquifers. The simplest model is the Equivalent Porous Medium (EPM) model, sometimes named smeared conduit approach, single continuum approach, single porosity model, distributed parameter approach, or heterogeneous continuum approach. The other spatially distributed models are the Discrete Fracture (DF) model, Dual or double porosity model (DPM) models, Discrete Multiple Fracture network (DMFN) model, Discrete Conduit Couple to Single Continuum. A brief overview of different modeling approaches in karst system are provided in this section. Table 2.2 gives summary of the different types of distributed modeling approaches.

A single continuum approach is easy to use; however, it has some limitations. EPM models are capable of simulating karst flow at the regional scale although their use is limited for solving flow problems at the local level because EPM models cannot delineate conduit pathways. Furthermore, they are not integrating the turbulent flow equation. EPM models have been successfully used to simulate flow in karst aquifers at a regional scale and are useful when the model is intending to simulate discharges, groundwater flow and hydraulic heads. On the other hand, the application of EPM model for solving steady-state karstic hydrological problem is limited by constrains of discretization, and the transient state is unsuccessful for characterizing karstic area (Kovács. and Sauter, 2007).

Teutsch (1993) used the EPM model to simulate flow within an aquifer of moderate karstification near Heidenheim, in the Swabian. They found a good agreement between predicted and measured groundwater table elevation. This signifies the ability of standard porous media models in moderate karstified terrain. On the other hand, Scanlon, et al. (2003) evaluated the adequacy of two different approaches the lumped and distributed parameter models in the highly karstified aquifer. In their study MODFLOW code was used in developing the distributed parameter model. Scanlon et al. (2003) noted that both models were found fairly accurate and capable of simulating groundwater in the karstic region. Scanlon et al. (2003) recommended that the lumped parameter model is good in evaluating the impact of pumping on spring discharges. However, more detailed

data on evaluating the effect of pumping on groundwater level and spring discharges require a distributed parameter model these findings are in agreement with (Rani et al. 2010). However, (Kunianski 2016) argued that all of the methods and approaches require an understanding of each karst system and its distinct hydrogeological setting. Furthermore, Panagopoulos (2012) claimed that an equivalent porous media model is a valuable tool for planning water resources management strategies in a karst aquifer. In their study, water budget was accurately established.The result of hydraulic conductivity is estimated by an automated inverse method and is in line with values produced in our research. Larocque et al. (1999) examined inverse modeling and an equivalent porous media in the slightly karstified aquifer, the La Rochefoucauld karst (Charente, France). They concluded that inverse modeling and an equivalent porous media is a valuable tool for calibrating groundwater flow. Furthermore, they are useful for determining transmissivities in a karst aquifer. Conversely, Worthington (2009), stated that the EPM approach does not consider the rapid flow in a karst conduit, and it loses realism in a system with a high degree of karstification. Putnam and Long (2009), developed a regional EPM flow model for the Madison and Minnelusa aquifers using USG cod MODFLOW-2000 to synthesize available hydrogeological data and quantify the regional water budget. Saller et al. (2013) further upgraded the above model by including high conductivity values in zones, representing karst conduits in the EMP model. Here, the model results are in better match with the observed transient well data; however, the simulated spring discharges remain the same to the original EMP model.

The dual porosity model is sometimes named double porosity model. In this model, there are two flow regimes for each aquifer, matrix porosity (diffuse flow regime) with low hydraulic conductivity, and conduit flow regime with higher hydraulic conductivity. DPM models assume that flow occurs within both regimes with the flow being an exchange between the two-porosity domain. A flow exchange between the two continuums describes the rate of mass transfer that allows flow exchange from one continuum into another. The DPM approach is capable of simulating contaminant transport, in moderately and highly karstified systems. Teutsch (1993) successfully used a DPM model to simulate flow within a highly karstified aquifer near Reutlingen in the Swabian Alb. Sauter (1993) also used a DPM model to simulate flow in the Gallusquelle karst aquifer. Sauter (1993), and Cherubini (2008) claimed that the difficulties of obtaining data for developing DCN or CDC models, and the inability of the EPM approach of involving strong heterogeneity of karst aquifers, have both motivated the development of a DPM. which can simulate specific karst aquifer without obligatory detailed knowledge about the geometry of conduit. In other words, the DCN or CDC and EPM approaches require a good knowledge of either the fracture systems or the location of the karst conduits, hydrodynamic properties, and geometry. In most cases, information about karst geometry, and karst conduits is not available and only the DPM approach can be used because no details are required about conduit geometry. However, a large amount of hydrogeological field data is required to calibrate DPM (Sauter 1993). Shoemaker et al. (2008), point out that, despite the application of DPM, even when the geometry of a conduit is unknown, DPM tend to have a problem in simulating transport process at small scales karst aquifer.

The Discrete Fracture Network DFN model assumes that the flow basically occurs within the fractures or conduits with the matrix assumed to be impermeable. The DFN

model is useful although information about fractured network geometry is required. In this approach, a simplified karst aquifer is considered as permeable, and the matrix medium is impermeable (Cherubini 2008). Dreybrodt (1990) applied the DFN model to approximate evaluation time of a large karst aquifer. Dreybrodt (1990) further asserted that the DFN model is useful to suggest consequences of land use projects in a theoretical karst conduit. DFN is applied by (Jeannin et al. 2001) to simulate discharges and velocities in the Holloch cave system in Switzerland. Jeannin et al. (2001), further claims that flow model which are capable of simulating a turbulent flow conduit network can adequately model a conduit flow dominated karst system.

Table 2.2. Differently named distributed modeling approaches in the literature

Modeling approach[1]	**Other names in the literature**	**Type**
EPM	Single continuum porous equivalent approach (SCPE) Heterogeneous continuum approach Distributed parameter approach Smeared conduit approach Single continuum approach	Distributed
DPM	Double continuum approach (DC) Double Continuum porous equivalent approach (DCPE)	Distributed
DFN	Parallel plate model Two types: 1- Discrete singular fracture set approach (DSFS) 2- Discrete multiple fracture set approach (DMFS)	Distributed

[1] (EPM) = Equivalent porous medium approach, (DPM) = Double porosity model, (DFN) = Discrete fracture network approach, (DCN) = Discrete channel network approach, (HM) = Hybrid model, (HCA) = Hydrograph-chemograph analyses, (LSM) = Linear storage models, (SCM) = Soft computing methods.

Table 2.2. continue

Modeling approach	Other names in the literature	Type
	2- Discrete multiple fracture set approach (DMFS)	
DCN	Discrete conduit network approach (DCN)	Distributed
HM	Combined discrete-continuum approach (CDC) Combined single continuum–discrete fracture set approach (SCPE–DSFS)	Distributed
HCA	Single event methods	Lumped
LSM	Rainfall-discharge models	Lumped
SCM	Computationally intelligence methods	Lumped

(EPM) = Equivalent porous medium approach, (DPM) = Double porosity model, (DFN) = Discrete fracture network approach, (DCN) = Discrete channel network approach, (HM) = Hybrid model, (HCA) = Hydrograph-chemograph analyses, (LSM) = Linear storage models, (SCM) = Soft computing methods.

Numerical model such as Visual MODFLOW was used by many researchers in modelling and management of groundwater resources (Wang, S et al. 2007;Elc et al. 2010; Xu, et al. 2011; Varouchakis et al. 2015; Qadir et al. 2016; Wang, S. 2017). however, no study has been conducted in the Antalya region specially in Altinova. Panagopoulos (2012) noted that Visual MODFLOW is useful to enhance the conceptual model to estimate aquifer parameters and predict the impact of climate change or pumping change in the aquifer system. This study was the first carried out in the travertine of Altınova using Visual MODFLOW flex. This first trial is believed to positively impacting the knowledge of groundwater flow in the Altınova region and the same approached could be used in a similar karstic region.

3. MATERIALS AND METHODS

This chapter presents a brief overview of the study region and its climatological condition and geology. The fieldwork techniques used by the TÜBİTAK project team are explained in this section. An overview of the software and hardware applied in the study are also explained in this chapter. Necessary steps and strategies employed in the analysis, model discretization and simulation of groundwater in the karstic area of Altınova are described. Finally, the techniques used for model calibration and development of scenarios are explained.

3.1. General Discerption of the Study Area

The pilot study area PSA of Altınova is situated in an area approximately 10km northwest of Antalya province. Antalya is a metropolitan city located on the Mediterranean coast of southwestern Turkey, and it covers an area of about 20.7 square kilometers. The area of Altınova covered by the Taurus Mountain of the southeastern Anatolia region runs from the east to the western part of the Mediterranean Sea. The small natural bays of Antalya formed by coastal features and mountains plunge sharply into the Sea at the south border of the city.

The case study region of Altınova covered an area of approximately 75 km^2 and is situated on a plain where the mountains recede southward forming flat areas of a travertine plateau. The area is in the northwest border of Antalya international airport between the coordinates of 36 ° 54 '0 "and 37 ° 2' 0" northern latitudes, 30 ° 43 '0 "and 30 ° 50' 0" east longitudes. The Düden river runs along the western border, and across the eastern border is the Isparta road. The plateau is in the northern border. The topography of the region ranges between less than 50 m on the southern border and greater than 300 m on the northern border. The location and the topography of the study area is shown in Figure 3.2. The thickness of the travertine varies between 160-240 meters in the upper plateau and 60-120 meters in the lower plateau of Antalya (Efe and Soykan 2008). In the Northeastern section of Antalya, the total thickness decreases to 20-30 meters. The thickness of both the Kurşunlu and the travertine formations in the Altınova area ranges between 30-180 meters, as depicted in Figure 3.14.

The study region is a home for farmers, in which intensive agriculture in form of greenhouses is practiced almost across the entire PSA. The total area of the greenhouses in the study area is 13.7 km^2. The types of vegetables commonly grown in the greenhouses are tomatoes, peppers, eggplants, cucumbers, beans and melons watermelons and flowers. Also, some fruit trees and cultivation fields in the open exist in the pilot study region. Besides the vegetable growth, livestock keeping are also practices in the area. Groundwater which recharges only during the three to four months in the rainy period of the year is the main source of irrigation. Most of the farmers have private wells for irrigation. Industrial and residential areas also exist in the region and they are dependent on the groundwater for running their daily business and life. Illegal wells also exist in the pilot study. The main pervasive pollutants in the pilot study area are from anthropogenic origins such as domestic waste, industrial waste and fertilizers and chemicals used in agriculture pesticides. Additionally, the region of Altınova lacks a wastewater collection system; only a small network exists in the western part (Çil et al. 2016). Due to this situation, the inhabitants in the region dispose their wastewater directly underground via

the septic tanks which are built into the fragile aquifer of the region. Therefore, due to these various land uses in the flimsy aquifer of Altınova, the quality and quantity of groundwater is deteriorated. The basic land cover and land use map of the area is shown in Figure 3.1. Nitrate concentrations (NO_3) in the aquifer of Altınova showed high spatial variations of between less than 2 mg/l to more than 100 mg/l. However, the temporal variation was insignificant. Based on the land use of the study area, the pollutant sources that threaten the flimsy aquifer of Altınova are from anthropogenic sources, mainly agriculture and domestic.

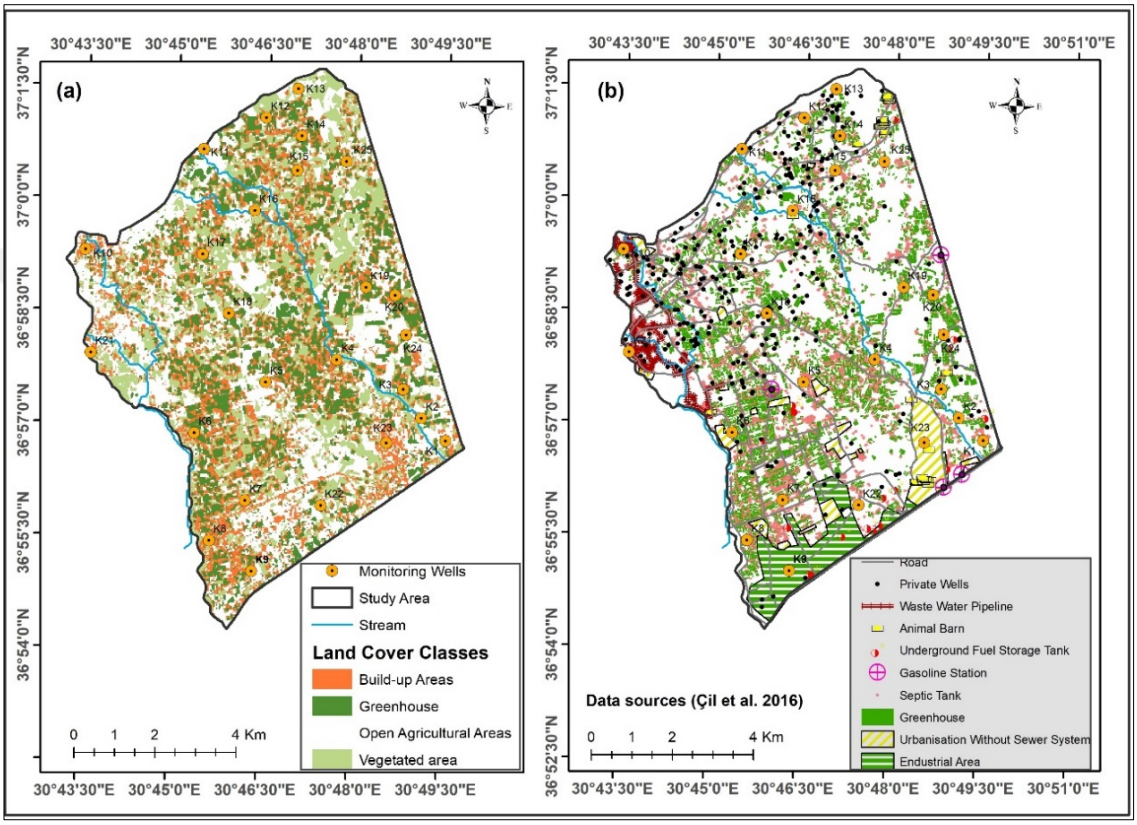

Figure 3.1. Land cover map (a) and basic land use map (b) of the pilot study area.

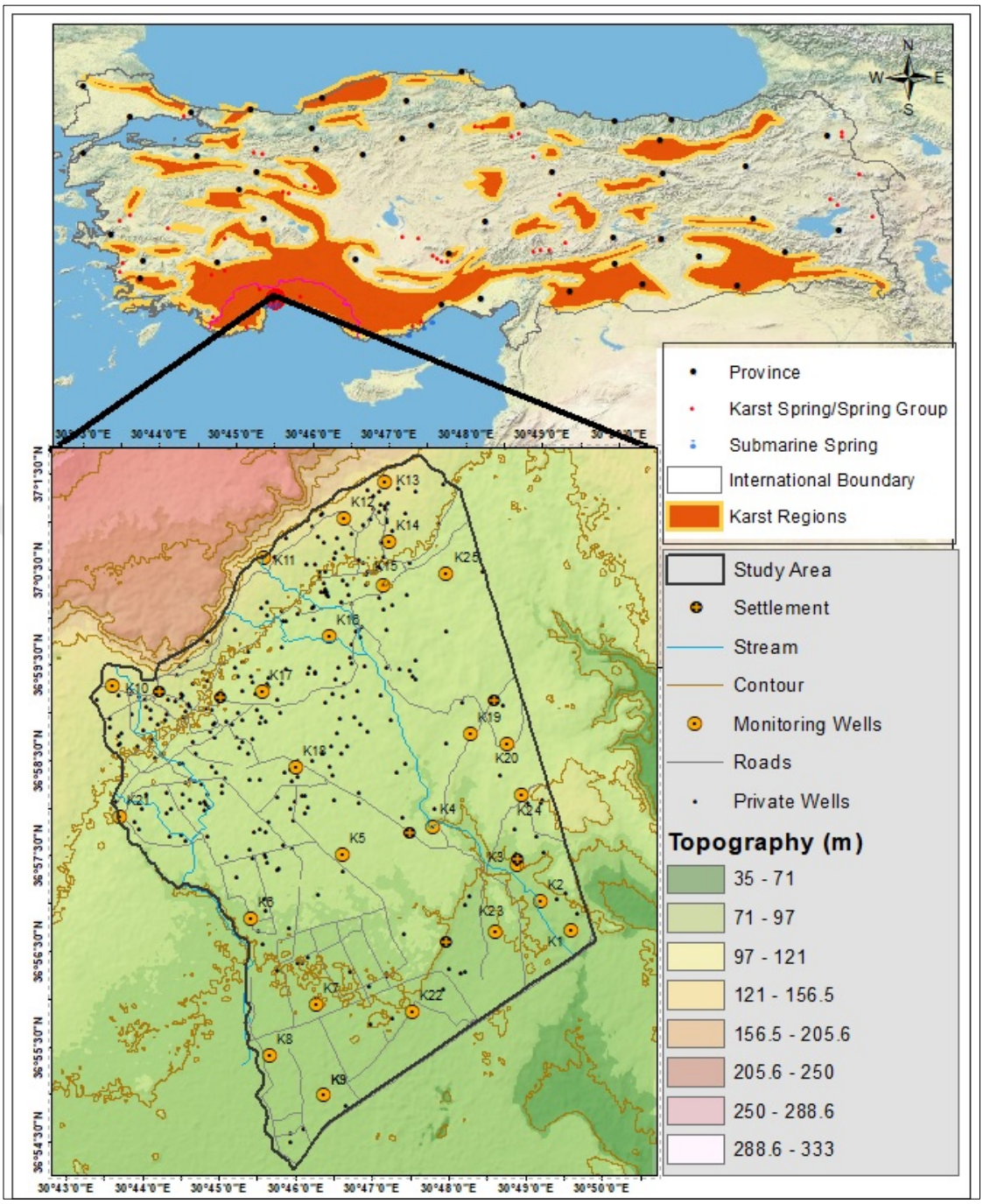

Figure 3.2. Location of the study area

3.1.1. Geological formation.

The geological formations of the Antalya region are sandstone, limestone, conglomerate, clayey limestone, brecciated limestone, claystone and shale (Dipova and Doyuran 2006). The pilot study area is located in the Taurus karst region in an area 10km northwest of Antalya, which is one of the important and largest karst areas in the country. The geological formation of the study area is mainly travertine, conglomerates, and alluvium of the Kurşunlu formation. Approximately 63 km^2 of the study area is covered

by the karst travertine formation. The karst travertine accounts for about 85% of the total study area. The karst travertine is one of the dominant geological formations in the southwest of the Mediterranean region of Turkey. The Kurşunlu formation consists of the conglomerate. Sandstone mostly covers the eastern part of the study area and accounts for approximately 14%. The third geological formation is the alluvium which covers only one percent. The geology of the study area is shown in Figure 3.3. The hydrogeology map constructed by considering the hydrogeological characteristics of the units in the study area is presented in Figure 3.4.

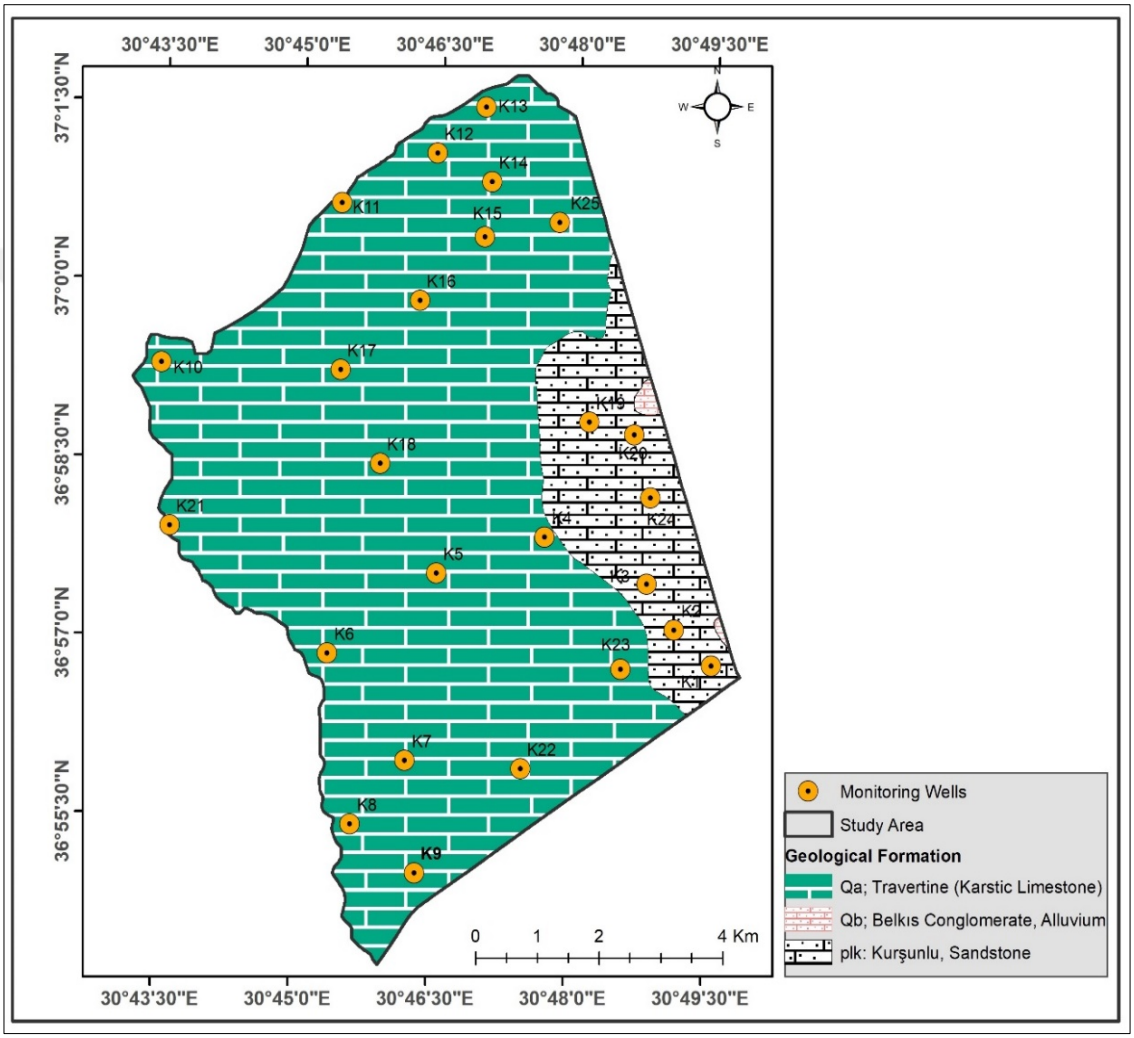

Figure 3.3. Geological formation of study area

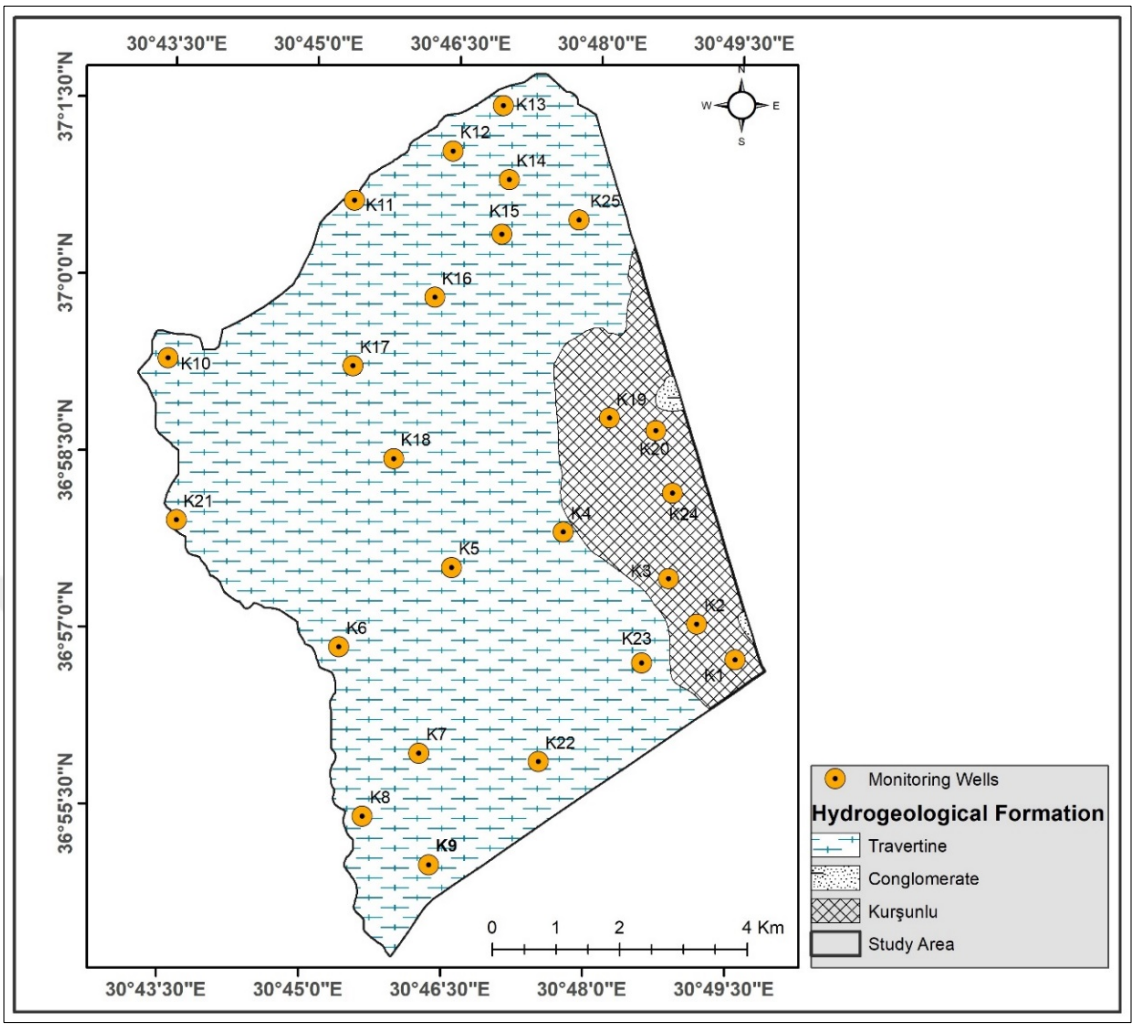

Figure 3.4. Hydrogeological map of the study area

3.1.2. Climate

From the climatological point of view, the study area has a Mediterranean type of climate with mild, rainy winters and hot, dry summers. Based on the meteorological data collected from the nearest station to the study area (Antalya Airport) in the year between 1994 – 2017, the average yearly precipitation of Altınova area reaches 1191.5 mm/year. The highest total precipitation was observed in 2001, with the lowest being in the years 2015, 2016, and 2017 as depicted in Figure 3.5. On a monthly basis, the months of June, July, and August, in the year between 2015 and 2016 the area experience the low precipitation with an average of 4.5 mm/year. These months are the hottest months of the year in the study area. In summer, the mean maximum air temperature in the years between 1994 – 2017 ranges from 25 to 35 °C. The mean maximum air temperature in winter ranges from 14 – 17 °C. The monthly average maximum and minimum temperature are shown in Figure 3.6 and Figure 3.7.

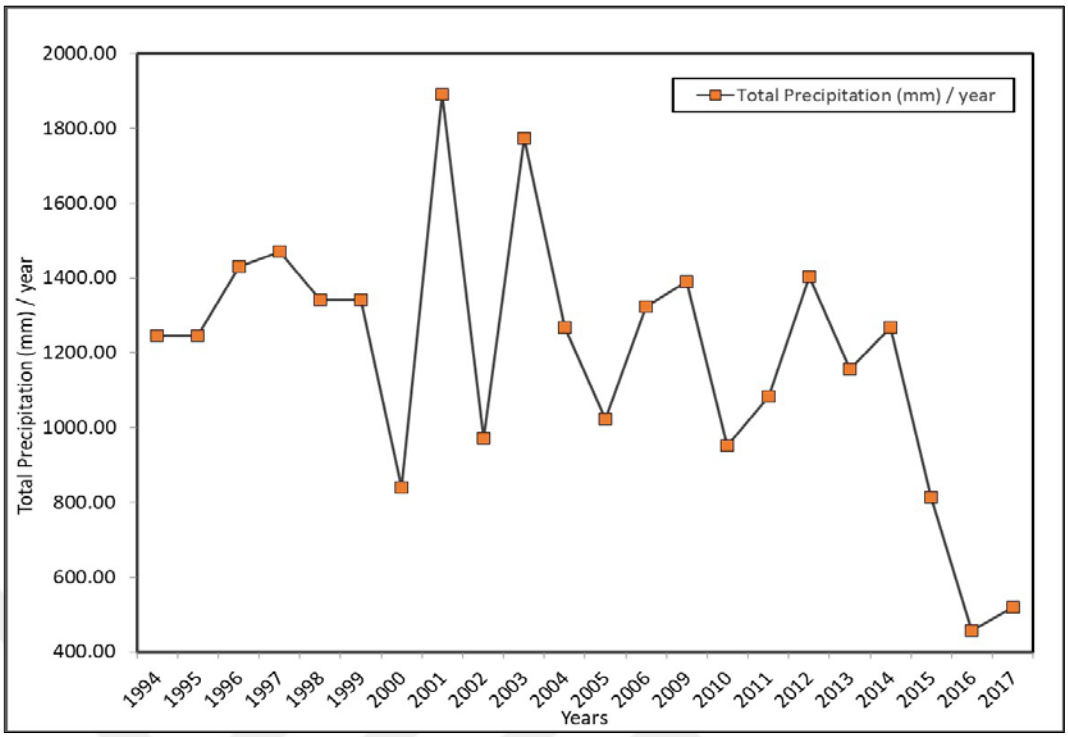

Figure 3.5. Total yearly precipitation in the year between (1994 -2017)

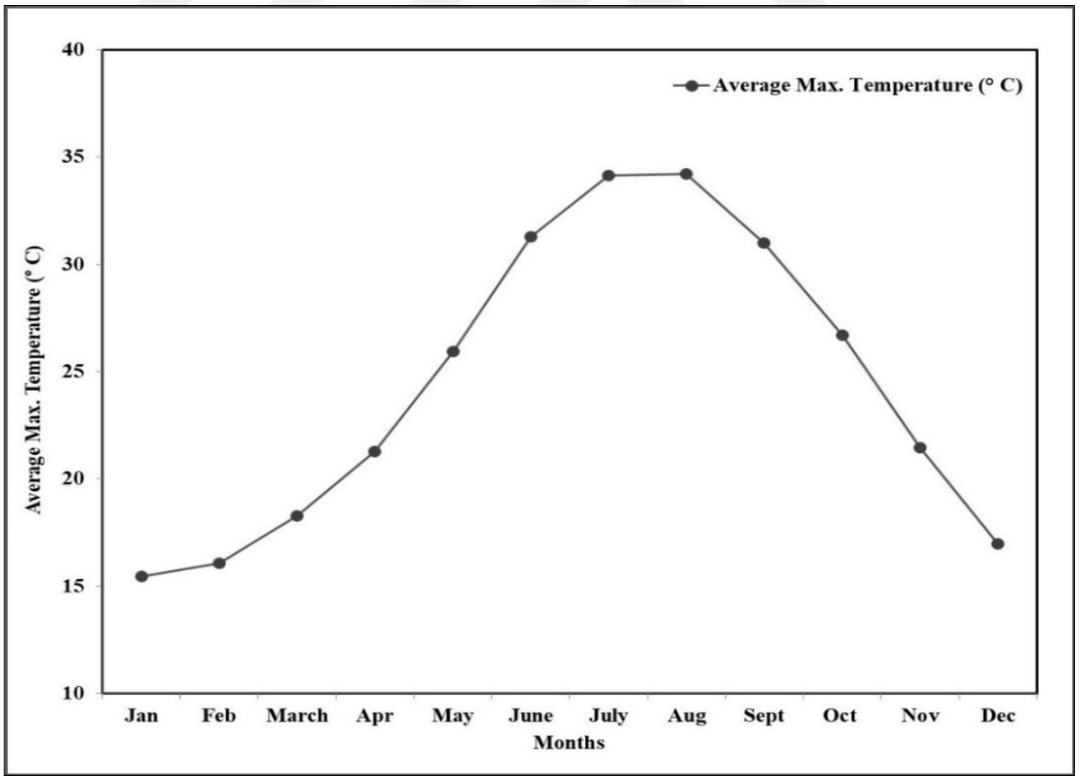

Figure 3.6. Monthly average max. temperature in the year (1994 – 2017)

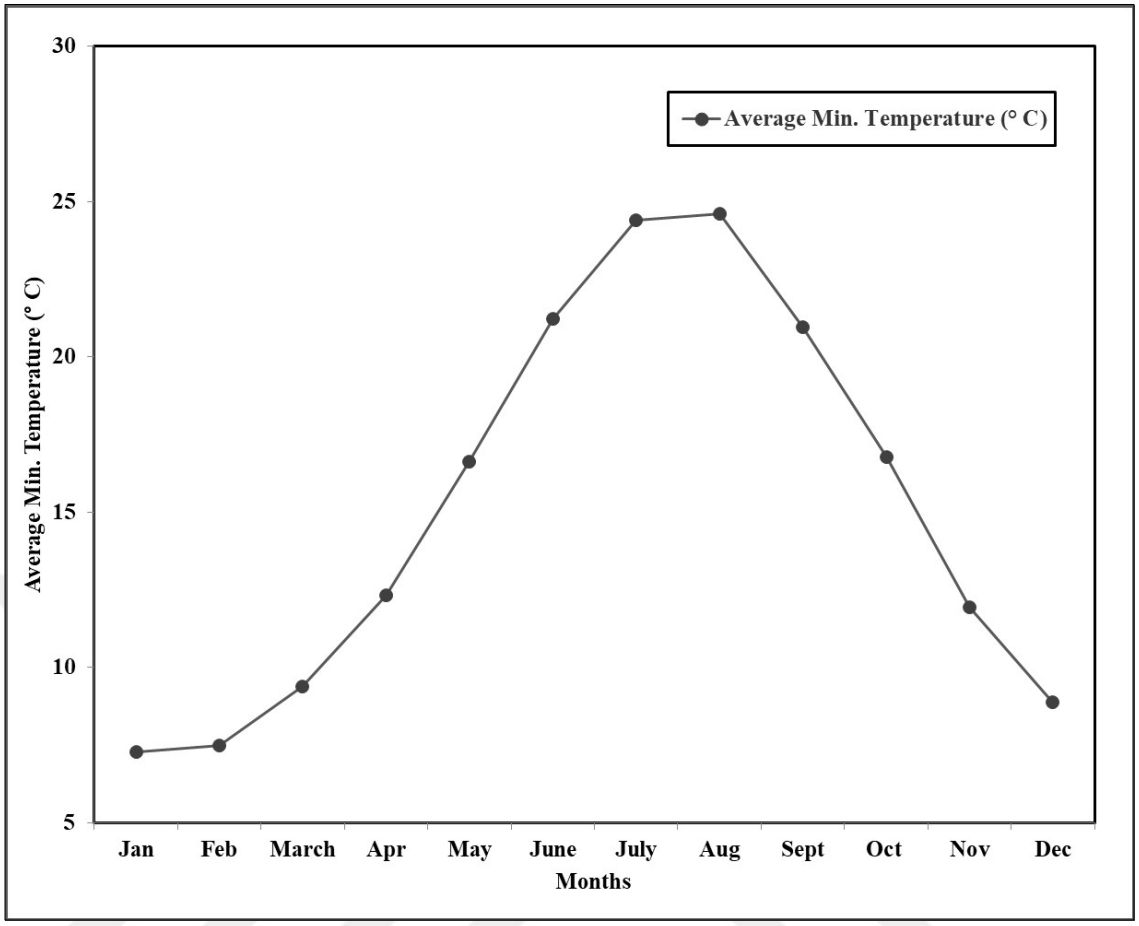

Figure 3.7. Monthly average minimum temperature in the year (1994 – 2017)

3.2. Material Methods and Model (MMM)

3.2.1. Field work

Gathering and organizing data is an important part of implementing a successful groundwater model. The climatological data sets such as precipitation, temperature, wind speed, were collected from the General Directorate of Meteorology (GDM) 4th Regional Directorate in Antalya. The groundwater table elevation dataset was acquired from a database of previously completed TÜBİTAK project number 114Y696 Table 3.1. The procedure and field techniques employed by the TÜBİTAK project team for collecting the groundwater table elevation is explained in this section. The first field visit was carried out on 04.12.2015 by the project team and the technical personnel from State Hydraulics Works (DSI), Directorate of 13th division in Antalya. The aim of the field work was to carry out the first measurement of depth to groundwater for 25 selected monitoring wells in the Altınova area. The depth to the groundwater table for all 25 wells designated for monitoring purposes was measured. To measure the depth to groundwater, a long cable connected to the ends of an ammeter was lowered down into the bottom of the well. As soon as the cable touched the water surface, the current was read on the ammeter and the cable was withdrawn out of the well. Then the length of the cable was measured to determine the depth to groundwater from the surface. The project team conducted the measurement of depth to groundwater in three different periods namely; November 2015,

Feb 2016 and May 2016. The groundwater table elevations were computed by subtracting the measured depth to groundwater from the ground elevation. Average depth to groundwater and calculated average groundwater table elevation is presented in Figure 3.8, Figure 3.9 and Table 3.1 respectively. The hydrological data was analyzed and synthesize with the help of database tool Geographical Information System (GIS). The seasonal groundwater table elevation in the months of November 2015, Feb 2016 and May 2016 are presented in Figure 3.10, Figure 3.11, and Figure 3.12 respectively.

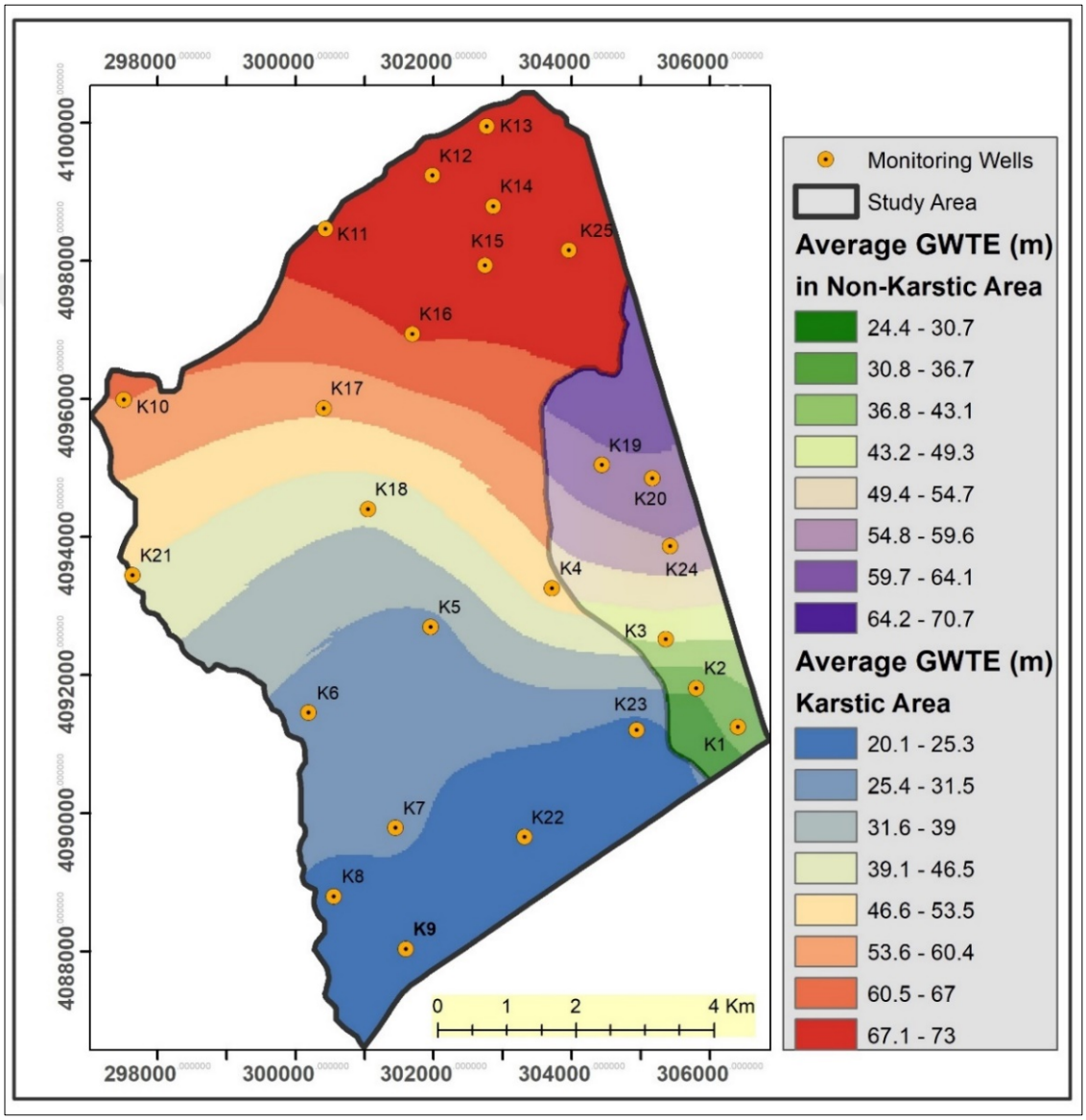

Figure 3.8. Shows average groundwater table elevation (GWTE) in Karstic and Non-Karstic area of Altınova

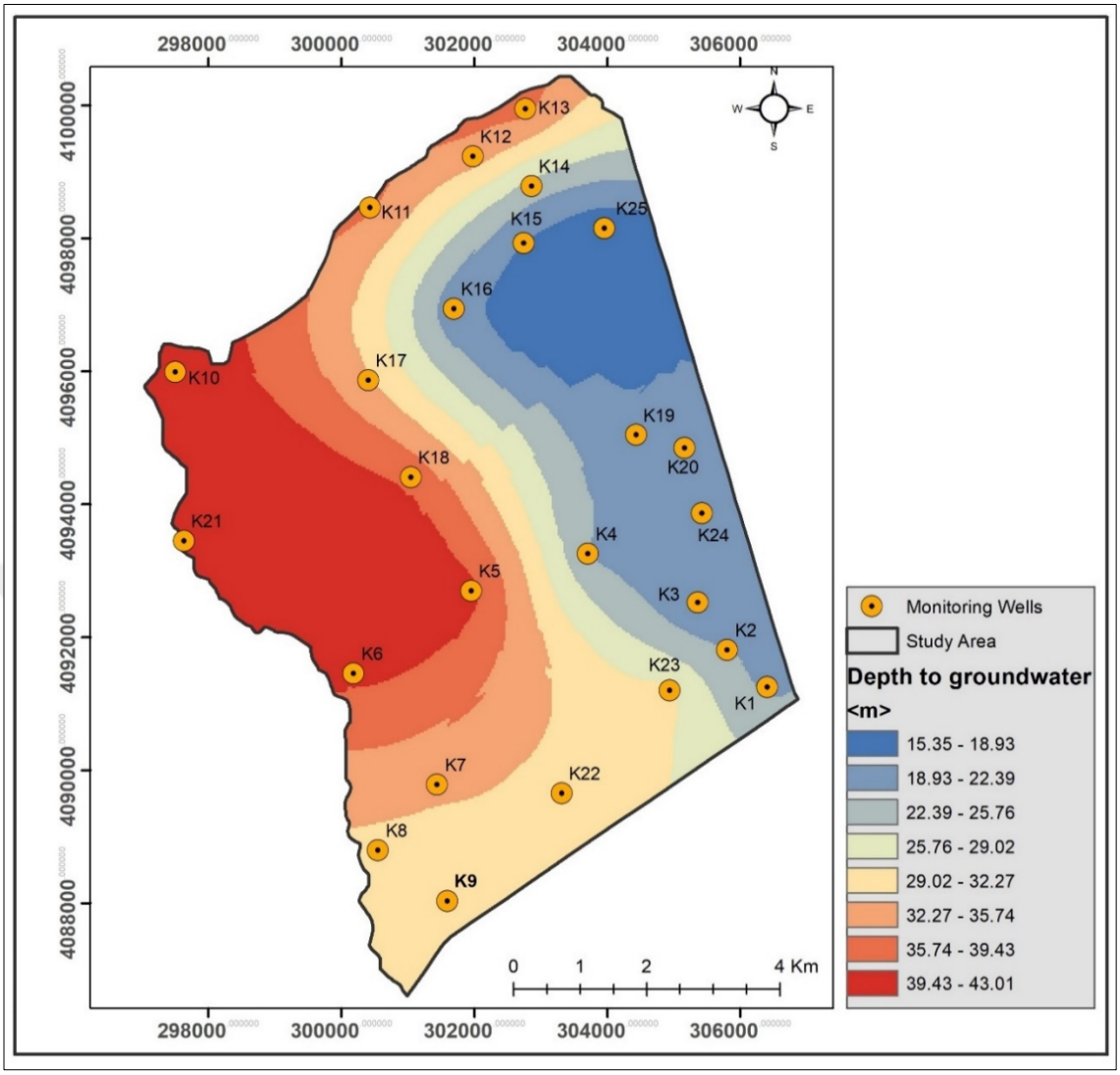

Figure 3.9. Average measured depth to groundwater in the months of (Nov 2015, Feb 2016 and May 2016)

Table 3.1. Monitoring Wells Database (Muhammetoğlu et al., 2017)

Monitoring Well ID	Well Name	X (m)	Y (m)	Elevation Z (m)	Groundwater Depth (m) (Nov 2015)	Groundwater level (m) (Nov 2015)	Groundwater Depth (m) (Feb 2016)	Groundwater level (m) (Feb 2016)	Groundwater Depth (m) (May 2016)	Groundwater level (m) (May 2016)
1	K1	306405.73	4091246.24	**53.21**	19.52	**33.69**	20	**33.21**	20.65	**32.56**
2	K2	305804.52	4091806.02	**53.92**	23.4	**30.52**	22.09	**31.83**	22.48	**31.44**
3	K3	305361.43	4092518.89	**60.51**	18	**42.51**	12.24	**48.27**	18.4	**42.11**
4	K4	303714.38	4093255.25	**70.03**	18.09	**51.94**	19.41	**50.62**	20.49	**49.54**
5	K5	301956.29	4092696.06	**72.56**	42.6	**29.96**	43.12	**29.44**	44.91	**27.65**
6	K6	300191.61	4091450.83	**69.5**	39.02	**30.48**	40.74	**28.76**	42.23	**27.27**
7	K7	301446.53	4089783.02	**58.87**	30.9	**27.97**	32.46	**26.41**	33.04	**25.83**
8	K8	300557.05	4088793.5	**55.15**	30.13	**25.02**	31.61	**23.54**	33.04	**22.11**
9	K9	301600.55	4088028.73	**52.9**	27.87	**25.03**	30.08	**22.82**	31.27	**21.63**
10	K10	297512.78	4095987.76	**103.25**	41.36	**61.89**	42.52	**60.73**	44.2	**59.05**
11	K11	300436.68	4098461.03	**108.9**	36.88	**72.02**	38.21	**70.69**	39.46	**69.44**
12	K12	301981.87	4099230.68	**106.06**	33.99	**72.07**	35.26	**70.8**	36.47	**69.59**
13	K13	302771.65	4099943.35	**112.49**	38.19	**74.3**	39.42	**73.07**	40.76	**71.73**
14	K14	302864.97	4098785.63	**94.79**	21.97	**72.82**	24.08	**70.71**	24.37	**70.42**
15	K15	302746.42	4097927.49	**87.82**	16.09	**71.73**	17.12	**70.7**	18.43	**69.39**
16	K16	301696.23	4096938.21	**84.85**	15.31	**69.54**	16.42	**68.43**	19.33	**65.52**
17	K17	300410.93	4095862.12	**86.55**	31.35	**55.2**	32.73	**53.82**	**Unmeasured**	**Unmeasured**
18	K18	301053.53	4094400.72	**81.24**	38.7	**42.54**	40.00	**41.24**	43	**38.24**
19	K19	304439.61	4095039.45	**81.08**	17.05	**64.03**	17.66	**63.42**	19.37	**61.71**
20	K20	305166.43	4094844.94	**84.87**	21.56	**63.31**	21.49	**63.38**	23.17	**61.7**
21	K21	297643.46	4093443.47	**87.73**	40.34	**47.39**	41.78	**45.95**	43.22	**44.51**
22	K22	303319.04	4089651.78	**50.27**	34.45	**15.82**	27.15	**23.12**	28.52	**21.75**
23	K23	304944.5	4091199.22	**55.6**	31.41	**24.19**	33.15	**22.45**	34.35	**21.25**
24	K24	305429.21	4093862.74	**82.92**	22.9	**60.02**	20.91	**62.01**	27.63	**55.29**
25	K25	303961.59	4098147.74	**86.41**	13.76	**72.65**	14.80	**71.61**	**Unmeasured**	**Unmeasured**

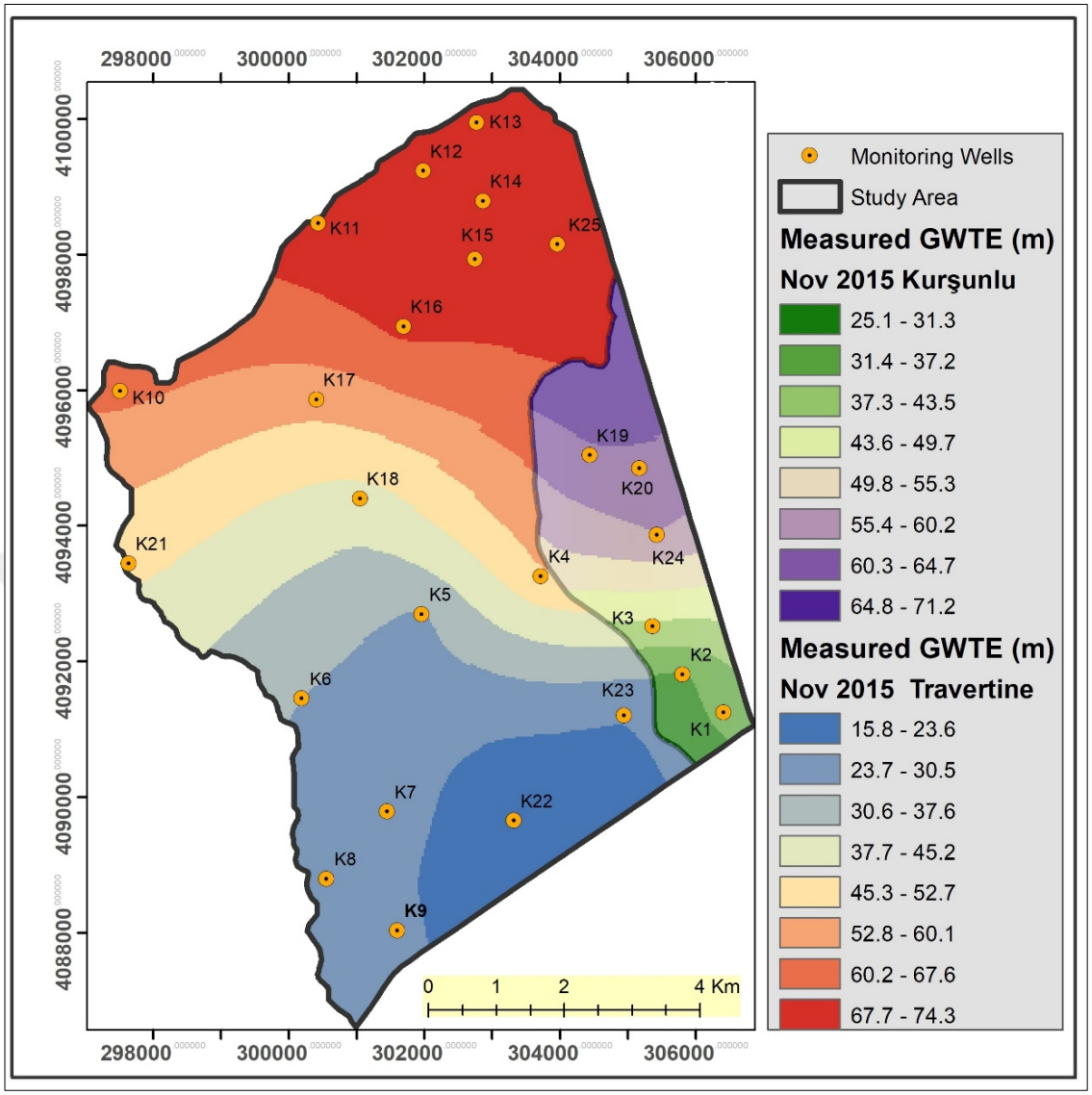

Figure 3.10. Measured groundwater table elevation Nov-2015

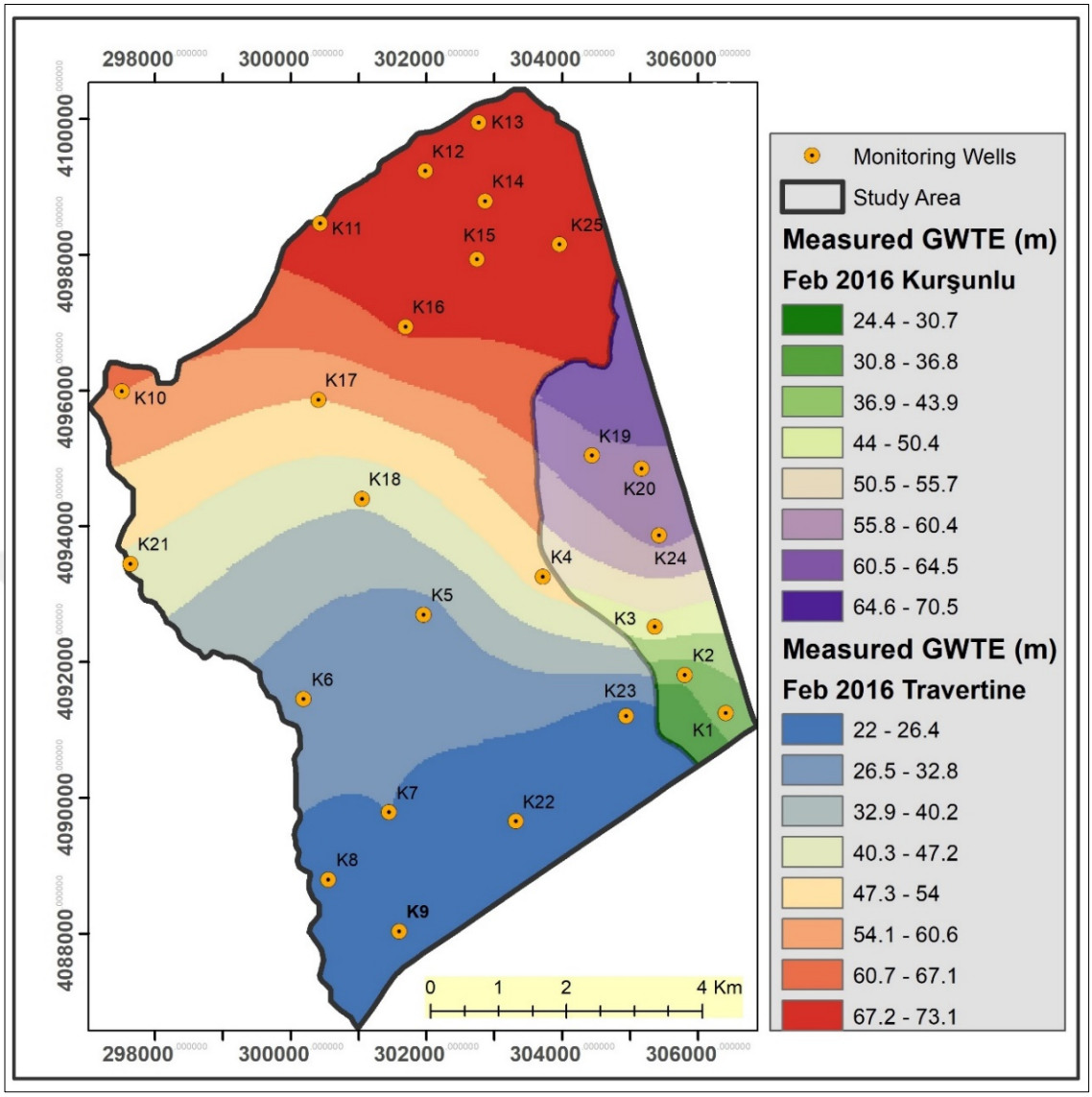

Figure 3.11. Measured groundwater table elevation Feb-2016

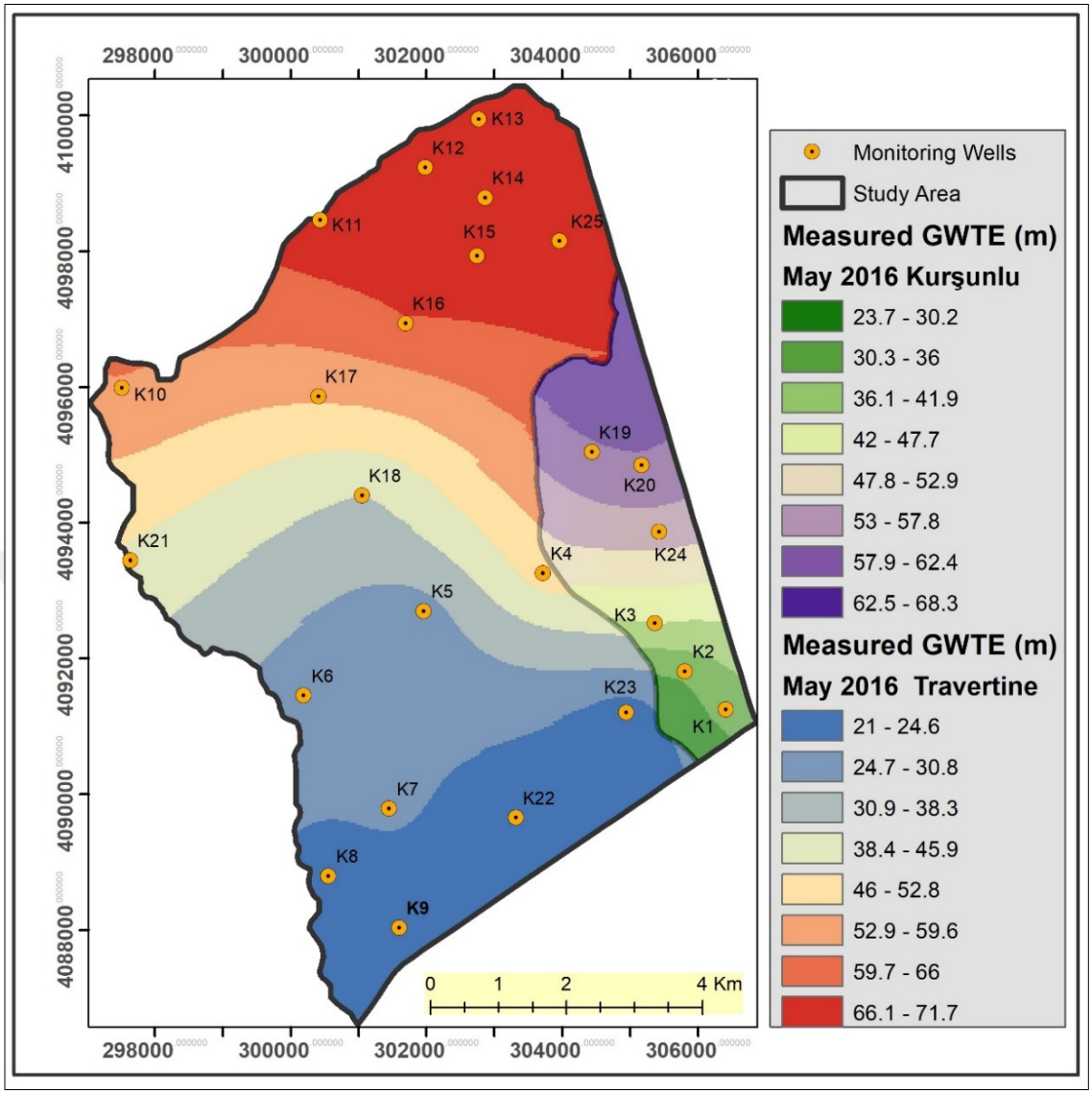

Figure 3.12. Measured groundwater table elevation May-2016

3.3. Software Applied in the study

The hardware tool used in this research study was a laptop computer designated under the scope of previous TÜBİTAK project number 114Y696.The software, such as Visual MODFLOW flex for Windows, GIS, and other statistical packages, was obtained under the scope of the previous project directed by Prof. Dr. Ayşe Muhammetoğlu. The main aim of this study was to test the capabilities of Visual MODFLOW flex in simulating groundwater in the karst area of Altınova. Therefore, MODFLOW-2005 code that built on the finite-deference grids model within the sophisticated Graphical User Interface (GUI) in Visual MODFLOW flex Version 5.0 developed by Waterloo was applied to accomplish the task. For the pre- and post-processing tasks, software such as ArcGIS version 10.3.1, Sufer software version 13 and Excel were used.

Visual MODFLOW flex is a three-dimensional groundwater flow and contaminant transport modeling application that integrates MODFLOW-2000, MODFLOW 2005, MODFLOW-LGR, MODFLOWNWT, MODFLOW-SURFACT SEWAT, MT3DMS, Win PEST, River Package, Zone Budget and other packages. The software is used primarily by hydrologists to simulate groundwater flow and contaminant transport. Visual MODFLOW flex developed by Waterloo Hydrogeologic contains computer code capable of importing and exporting data in various formats, including tabulated data and ESRI shapefiles. This model was chosen because it is a user-friendly graphical tool that allows visualization of the results in two-dimensional 2D or three-dimensional 3D graphics. In addition, Visual MODFLOW flex is a well-known Graphical User Interface (GUI) available for computing three-dimensional groundwater flow and contaminant transport modeling.

A Geographical Information System (GIS) is a computer program or set of programs that stores, manipulates, analyzes, retrieves, and displays data referenced in space and time. As such, a GIS is a convenient tool for storing, organizing and displaying data that form the conceptual model of a groundwater flow system. Geographical Information System GIS is one of the useful tools for assessing water quality and managing water resources and producing vulnerability maps on the local or regional scale. The ArcGIS spatial analysis tool includes a variety of tools for manipulation of data and visualization of the result. ArcGIS version 10.3.1 was used extensively in this study for pre- and post-processing tasks such as re-projection of data, digitizing a hardcopies map, interpolation, and creating maps in the post-processing stage for better visualization. The reader is referred to the ESRI ArcGIS online manual for some technical terminology available at ESRI web site[1]

Surfer version 13 is a three-dimension visualization, contouring software that converts raw data into contours using different mathematical interpolation techniques. Surfer is capable of landscape visualization, bathymetric modelling, surface analysis, watershed and three-dimension surface mapping, gridding, and much more. In this study Surfer version 13 was used to accomplish the task of interpolation and preparation of the model surfaces.

[1] (https://www.esri.com/en-us/arcgis/products/arcgis-online/resources).

Table 3.2. Software applications utilized for research

Software	Description	Version
Visual MODFLOW flex	Graphical User Interface (GUI) that integrate MODFLOW-2000, MODFLOW 2005, MODFLOW-LGR, MODFLOW-SURFACT SEWAT and PEST	V.5.0
MODFLOW 2005	USGS three-dimensional finite-difference ground-water model	V.1.12.00
PEST	Parameter Estimation Tool (Calibration Program) – author John Doherty	V.12.3
GIS	Geographical information system	V. 10.3.1
Surfer	Three-dimension visualization, contouring software	V.13
Google Earth Pro	cloud computing platform for processing satellite imagery and other geospatial and observation data.	V. 7.3

3.4. Model Design and Discretization Techniques

This section describes the modeling approaches. The conceptual and numerical modeling methods are also elucidated in this section, besides the process used in discretizing hydrological model surfaces.

3.4.1. Model design and discretization

The step employed in the model discretization and design are explained in this section. The groundwater simulation was performed using a numerical solution that incorporates Graphical User Interface GUI Visual MODFLOW flex V.5 with MODFLOW-2005 code under the numerical solution option, Finite Difference method. Graphical User Interface GUI Visual MODFLOW flex Software Version 5.0 was developed by Waterloo Hydro (Guiger et al. 2010), and MODFLOW-2005 code was developed by the U.S. Geological Survey. Since the aim of the research is to test the capability of Visual MODFLOW flex in simulating groundwater flow, we set the model objective to simulation flow. The flow model was set to saturated constant density. The simulation start time was set as 18/Nov/2015 which is exactly the starting date corresponding with the first field measurement of depth to groundwater in the study area. The dimension of the modeling area was set the same as the extent of the study area borderline shown in Figure 3.2. The steps employed in model discretization are the following: First, the conceptual model domain was discretized and designed using uniform extent finite-difference grids, in such a way that the spatial resolution has a dimension of 160 by 160 meters. The numbers of rows and columns were equal to 87 and 62 respectively. In the simulation the finite-difference method was chosen this is because

of its intuitive basis, easer of programming, less data input requirement, and its efficiency in matrix techniques (Anderson et al. 2015). Furthermore, the Finite Difference FD method exhibits better mass conservation. The inactive cell was defined automatically during the conversion of the conceptual model to the numerical model. The cells outside the model domain were marked as inactive and inside model domain as active. The model domain consists of 10792 grids cells, of which 5800 are active and 4992 are inactive. The second step employed in model discretization was the conversion of the conceptual model to the numerical model. The two-dimensional views of the model grids cells are shown in Figure 3.13.

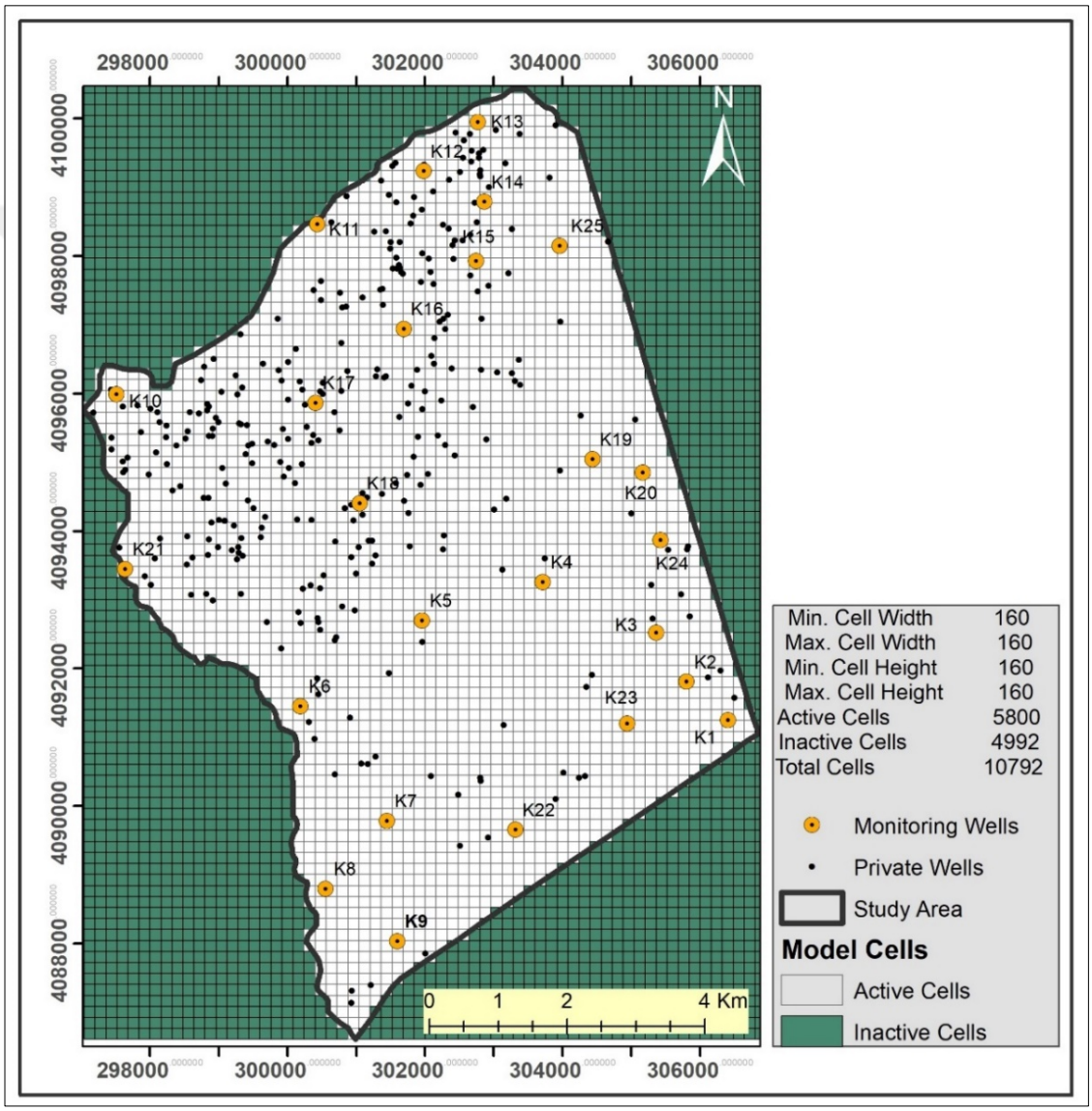

Figure 3.13. 2D view of model domain and grid cells

3.4.2. Hydrological model surfaces/layer development

The groundwater flow model was set as one layer in steady-state. The top surface of the model was derived directly from Digital Elevation Model (DEM) 30 m resolution,

downloaded from the United States Geological Survey (USGS) website[1]. To import the top surface, the DEM raster was converted to vector point data using the conversion tool in ArcGIS 10.3.1. The vector points were then converted to Universal Transverse Mercator coordinate system (UTM) zone 36N. Using a geometrical calculation tool, the associate XY coordinate was calculated and converted to Comma-Separated Values (CSV) format. The CSV points files were imported to Surfer 13 for interpolation, and raster surfaces were generated using the kriging raster interpolation tool in Surfer 13. The raster surface was clipped to the model domain and exported as ESRI grids which were later imported as a top surface into the Visual MODFLOW flex environment. The Universal Transverse Mercator coordinate system (UTM) zone 36N was maintained to ensure that the dimensions in the raster files and Visual MODFLOW were in meters. This coordinate system i.e. (UTM) was maintained to properly match the depth data in the model domain.

The topography of the surface ranges from 40 to 187 m from south to north. The thickness of the travertine which represents the karstic formation, was obtained from a researcher at Hacettepe University (Naciye Nur ÖZYURT, personal communication, Apr 10, 2018), and the thickness of the non-karstic area was obtained from the final report of TÜBİTAK project (Muhammetoğlu et al. 2017). These thickness values were preprocessed in ArcGIS. The thickness of the model domain varies between 180 m in the far north to 37 m in an area around the southeast boundary of the study region. From Figure 3.14 it can be seen clearly that the thickness of the travertine is higher in the northwest, and lower in the area southeast of the study area. This variation is consistent with the travertine thickness map in the Antalya Kırkgözler Project Preliminary Investigation Report″ prepared by State Hydraulics Works DSI 2005.

The bottom surface of the model was computed with help of the raster calculator tool in ArcGIS, by subtracting the aquifer thickness from the Digital Elevation Model (DEM). The bottom surface layer was then converted to ESRI grids and imported to the Visual MODFLOW environment. Using the top and bottom surfaces of the model layer, the horizon was created in Visual MODFLOW flex. The structural zone between the defined horizons in the horizontal extent of the conceptual model boundary was automatically generated by Visual MODFLOW flex. The two-dimensional and three-dimensional views of the top and the bottom surfaces of the model are shown in Figure 3.16 and Figure 3.17, respectively.

Many wells were identified in the pilot study area. Only 25 of them spread over the up and down stream were used as monitoring wells in this study because they have necessary data about depth to groundwater top and the bottom level of the screen. The wells depth in the study area varies from 30 to more than 100 m. Figure 3.15 shows the wells depths and their corresponding yields recorded during the drilling.

[11] https://earthexplorer.usgs.gov/

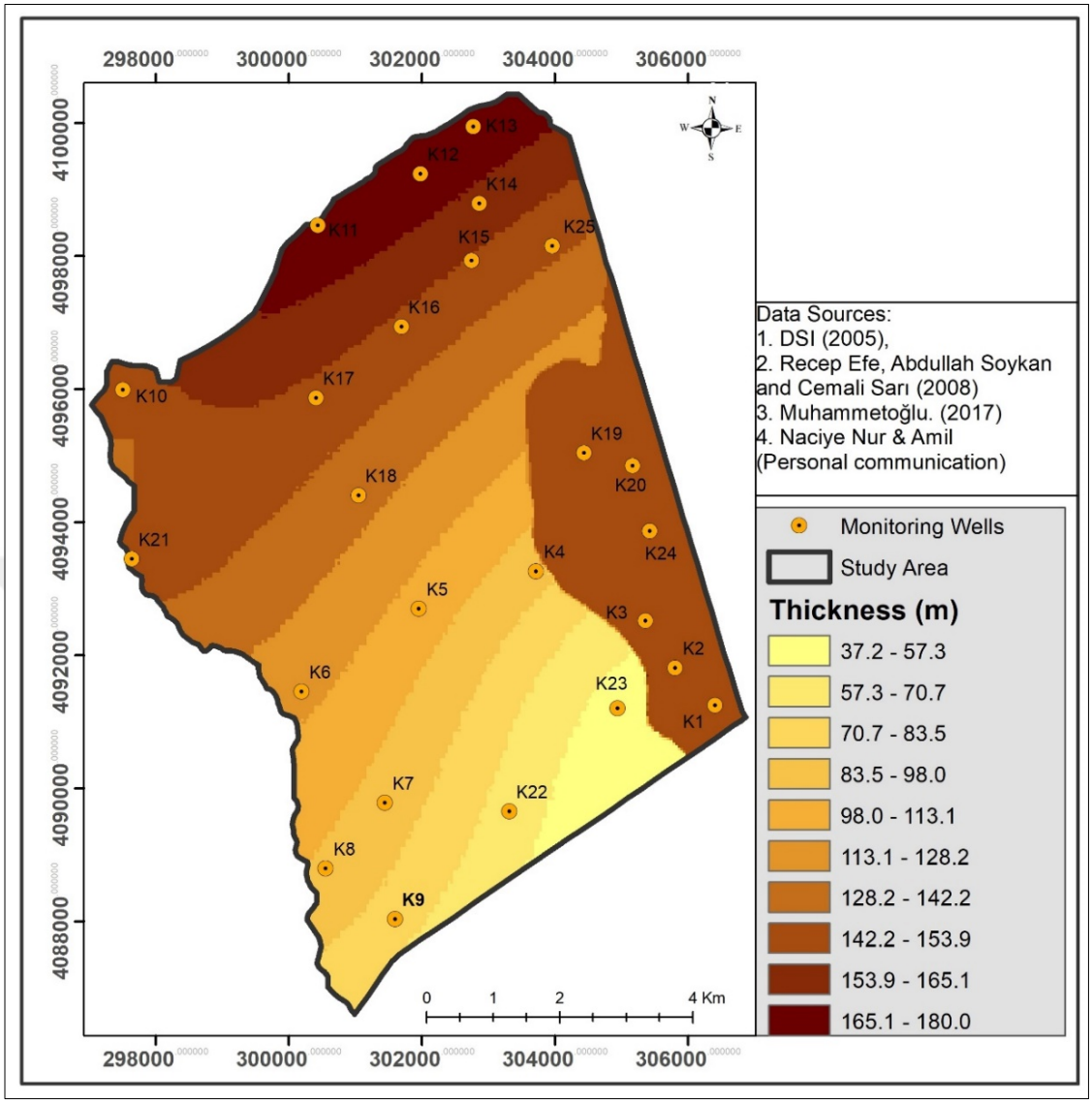

Figure 3.14. Spatial distribution of aquifer thickness in the model domain

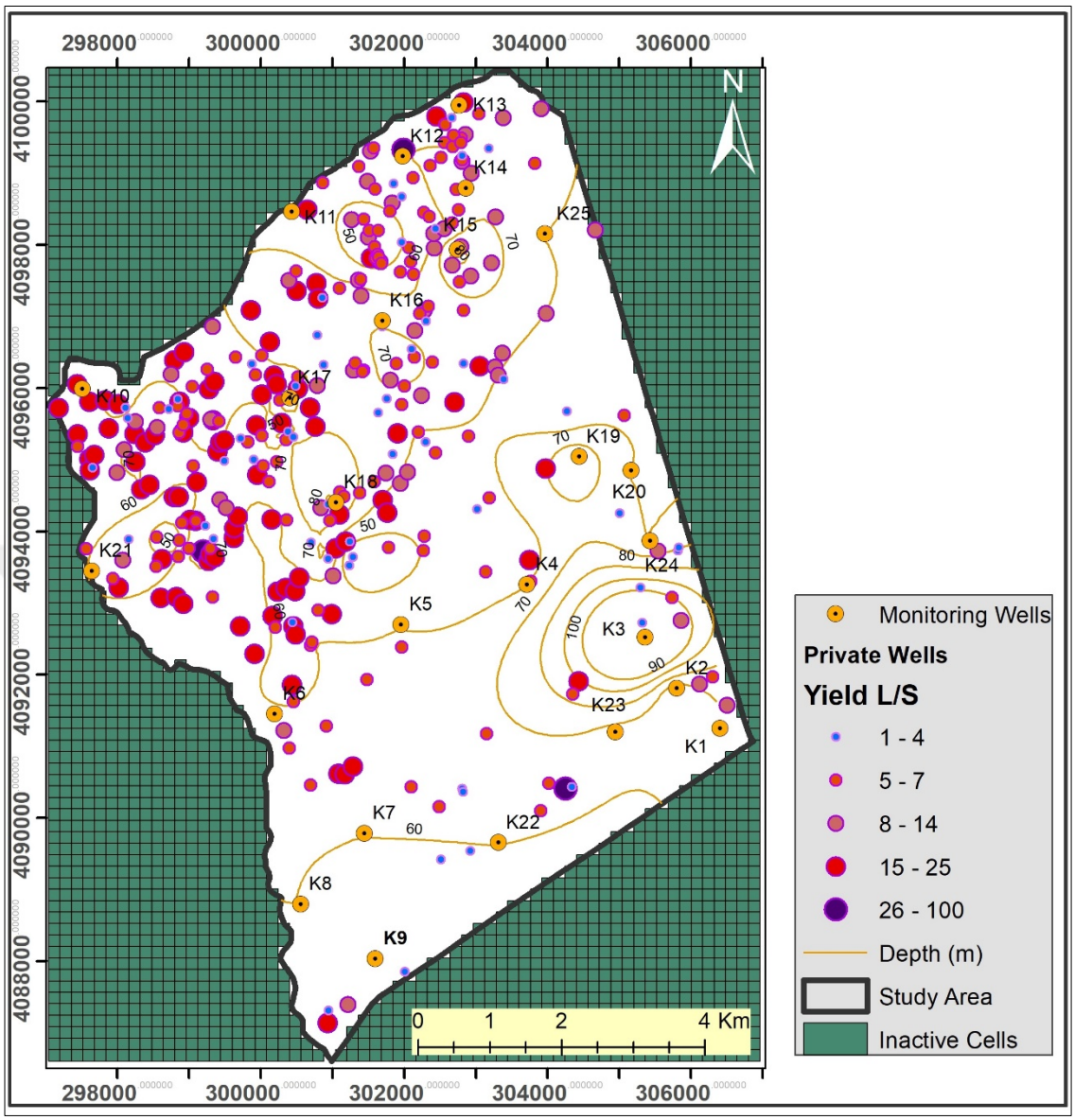

Figure 3.15. Well depths (m) and yields (L/S) recorded during the time of drilling

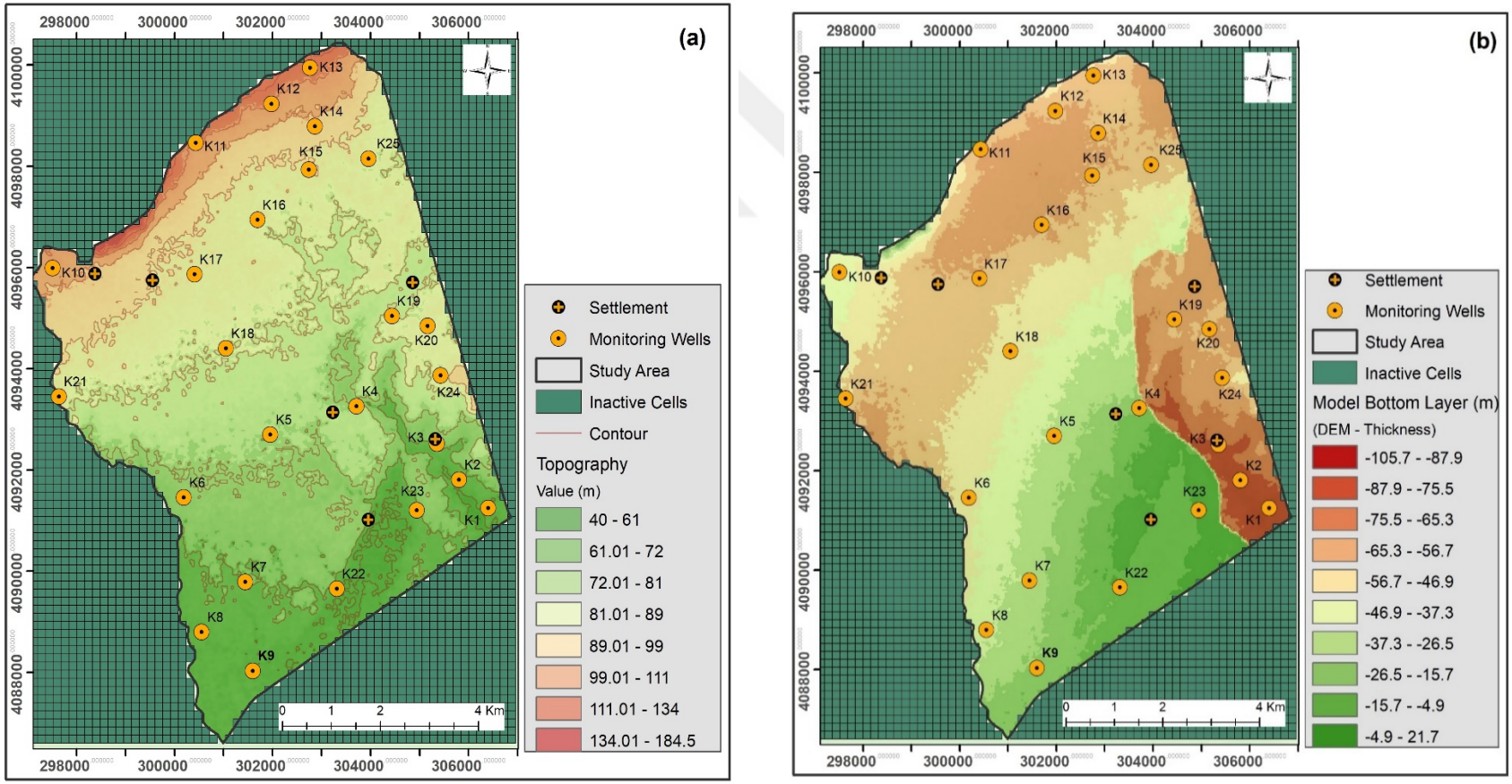

Figure 3.16. D-2 Top **a);** and bottom **b)** surface elevations of the model domain in units of meters

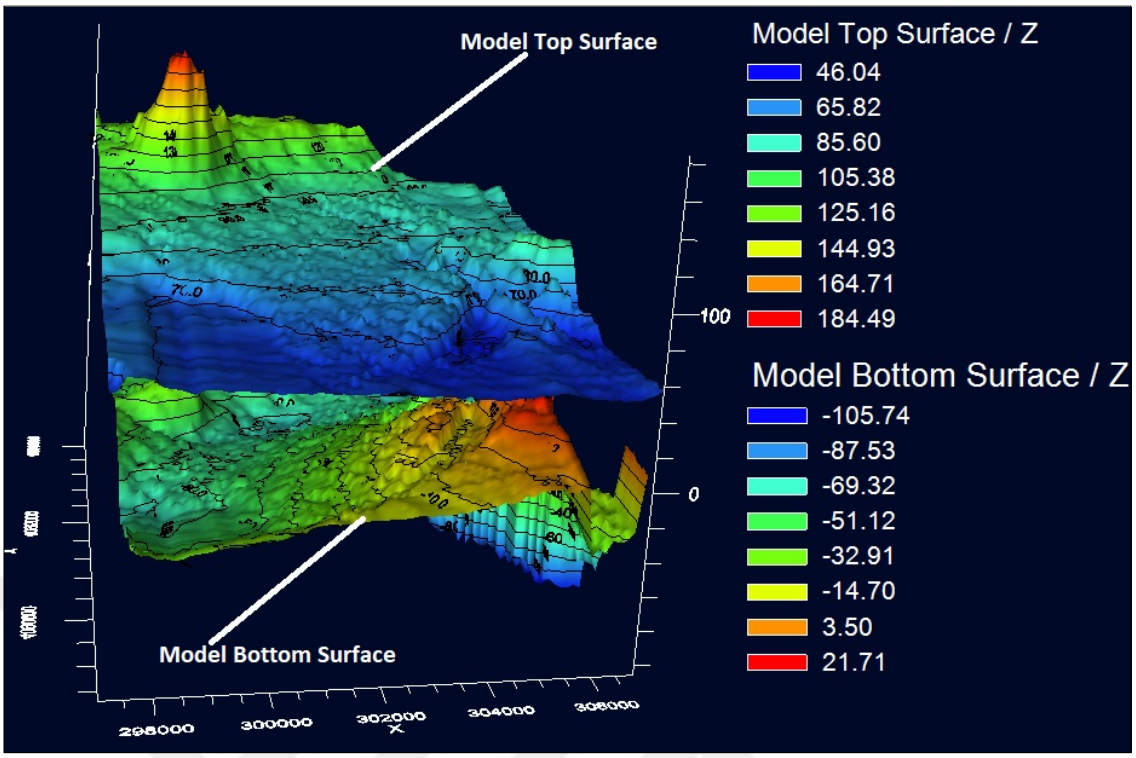

Figure 3.17. D-3 Top and bottom surfaces of the model domain in units of meters

3.5. Model Parameters and Property Zones

The approach employed in defining property zones, and model parameters such as hydraulic conductivity, initial heads, boundaries condition (recharge, pumping wells), specific storage, and specific yield are described in this section. Due to the lack of vertical hydraulic conductivity the model was set as a one-layer steady-state model. Consequently, specific storage (Ss), specific yield (Sy), and effective porosity values were maintained as default in the model with the same values as 0.2 $1.00E^{-05}$ 1/m and 0.14 respectively. the values of model parameters are shown in Table 3.3.

3.5.1. Hydraulic conductivity

Hydraulic conductivity is the crucial parameter needed to be defined prior to the conversion of a steady-state or transient conceptual model to numerical modeling. Hydraulic conductivity can be measured by different techniques such as a pumping test; however, a measurement of hydraulic conductivity using pumping test is expensive and was not available in the study area. The initial lateral/horizontal hydraulic conductivity (kyx) values were adopted from the final report of TÜBİTAK project (Muhammetoğlu et al. 2017). Uniform values of horizontal conductivity in the horizontal/x-direction (Kx), and in the horizontal/y-direction (Ky) were assigned to different zones based on the geological formation. In the travertine formation the initial value of hydraulic conductivity was set to 86.4 m/day, and in the Kurşunlu formation the value was set to 0.864 m/day. Initially the assigned values of hydraulic conductivity were in agreement with the values given in the literature (Allan and Cherry 1979) (Figure 3.19). Hydraulic conductivity in the vertical/z-direction (kz) was not available in the study area. Therefore,

the model was set as one-layer in which conductivity in the vertical/z-direction (Kz) is not considered. To assign the hydraulic conductivity, the model domain was divided into two zones based on the geological formation of the study area as shown in Figure 3.18. Different values of hydraulic conductivity in the horizontal/Kxy-direction were assigned to each zone based on the geological formation. Initial values of conductivity and other model parameters used in the model application are shown in Table 3.3.

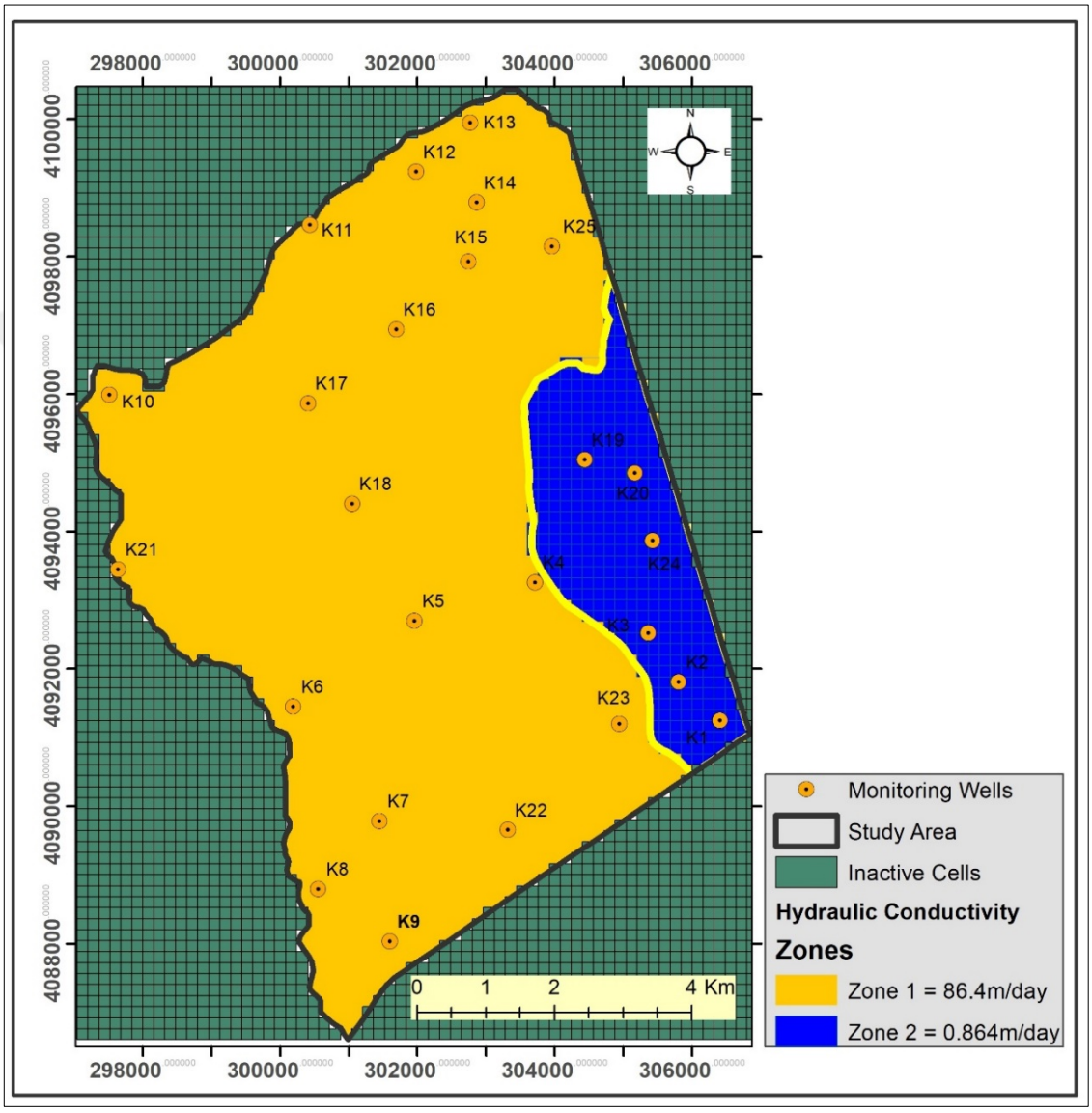

Figure 3.18. Pre-calibration hydraulic conductivity zones and values for the model domain

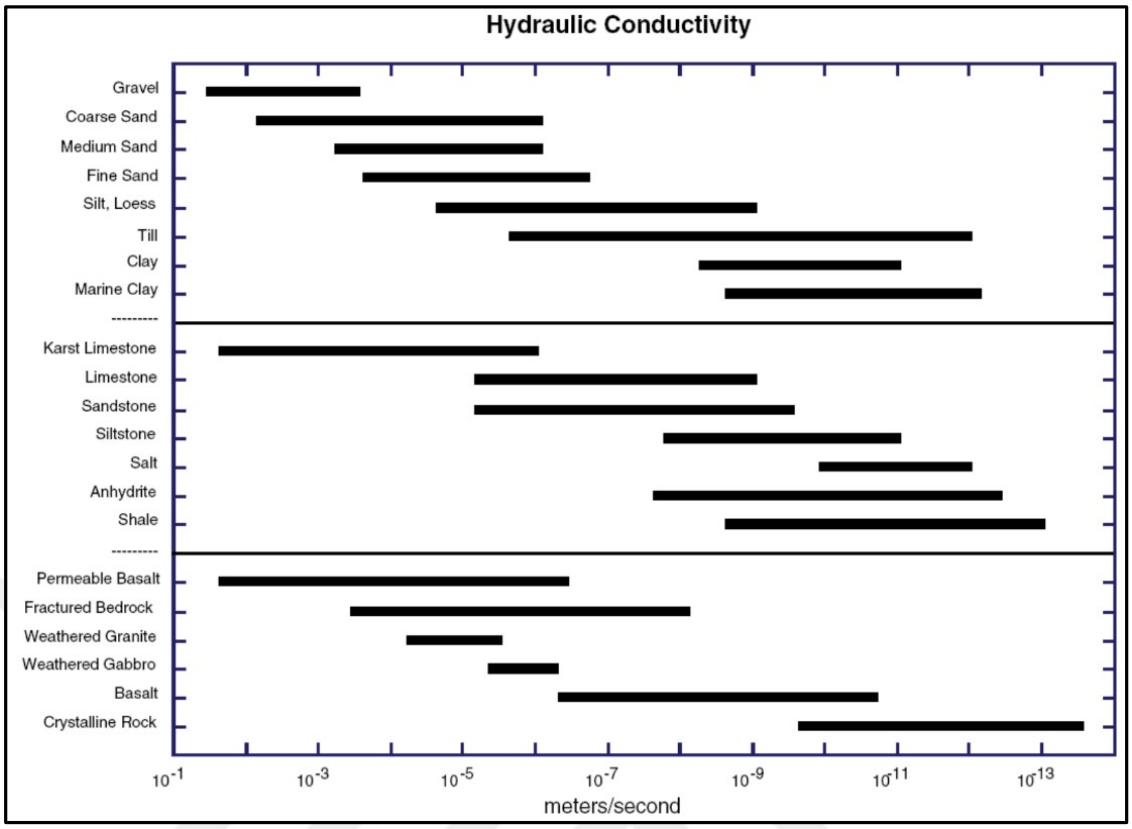

Figure 3.19. Range of hydraulic conductivity values for different geological formations (Allan and Cherry, 1979)

Table 3.3. Model parameters for pre-calibration and steady-state simulation

S/No	Model Parameters	Zone	Initial Value	Unit
1	Hydraulic conductivity (Kxy)	1	86.4	m/day
2	Hydraulic conductivity (Kxy)	2	0.864	m/day
3	Specific storage (Ss)	Uniformed	0.2	
4	Specific yield (Sy)	Uniformed	$1.00E^{-05}$	1/m
5	Effective porosity (Ep)	Uniformed	0.14	
6	Total porosity (Tp)	Uniformed	0.3	
7	Initial Heads	Uniformed	60	m

3.6. Model Boundary Condition

The boundary condition is essential in the process of developing a conceptual model. For this reason, four types of boundary conditions were set in the model domain, namely, general head boundary, recharge, pumping wells and No flow boundary conditions. The types of boundary conditions used in this study are described in this section. Various types of model boundaries are shown in Figure 3.20.

3.6.1. General head boundary (GHB) condition

Visual MODFLOW flex support General-Head Boundary GHB (type 3) package, is also called specific -head boundary, and its application tend to be general as specified by its name. A GHB was selected because there is not enough data available for a proper selection of boundary conditions that could represent the characteristics of the function.

A type 3 boundary package GHB is mathematically similar to that of the River package, Drain and ET packages. Here, the inflow or outflow of a cell from an external source is provided in proportion to the difference between the head in the cell and the reference head allocated to an external source.

To assign the General Head Boundary GHB, basically three types of data were required, namely, conductance values, head values and boundary distances. The head values were assigned from reference groundwater level measurements at the neighboring monitoring wells as suggested by (Franke et al. 1987). For this study average, groundwater level measurement at the neighboring monitoring wells was used as a reference head in GHB.

The seasonal measurements of depth to groundwater and calculated groundwater elevations are presented in Table 3.1. The average conductance value was initially assigned as 10 m then Visual MODFLOW Flex automatically generated conductance values in the magnitude of 25600 m^2/day based on the assigned reference water level heads.

The purpose of selecting GHB was basically to avoid unnecessary outward extensions in the model domain in order to meet the element influencing the head in the model. As a result, the General Boundary Condition (GHB) was set along the outside edges of the model domain.

3.6.2. No flow boundary

This type of boundary condition consists of inactive cells where no inflow or outflow occurs. No flow boundary condition was aligned with the extent of the study area. The No flow boundary was aligned automatically by Visual MODFLOW to match the edge of the model domain.

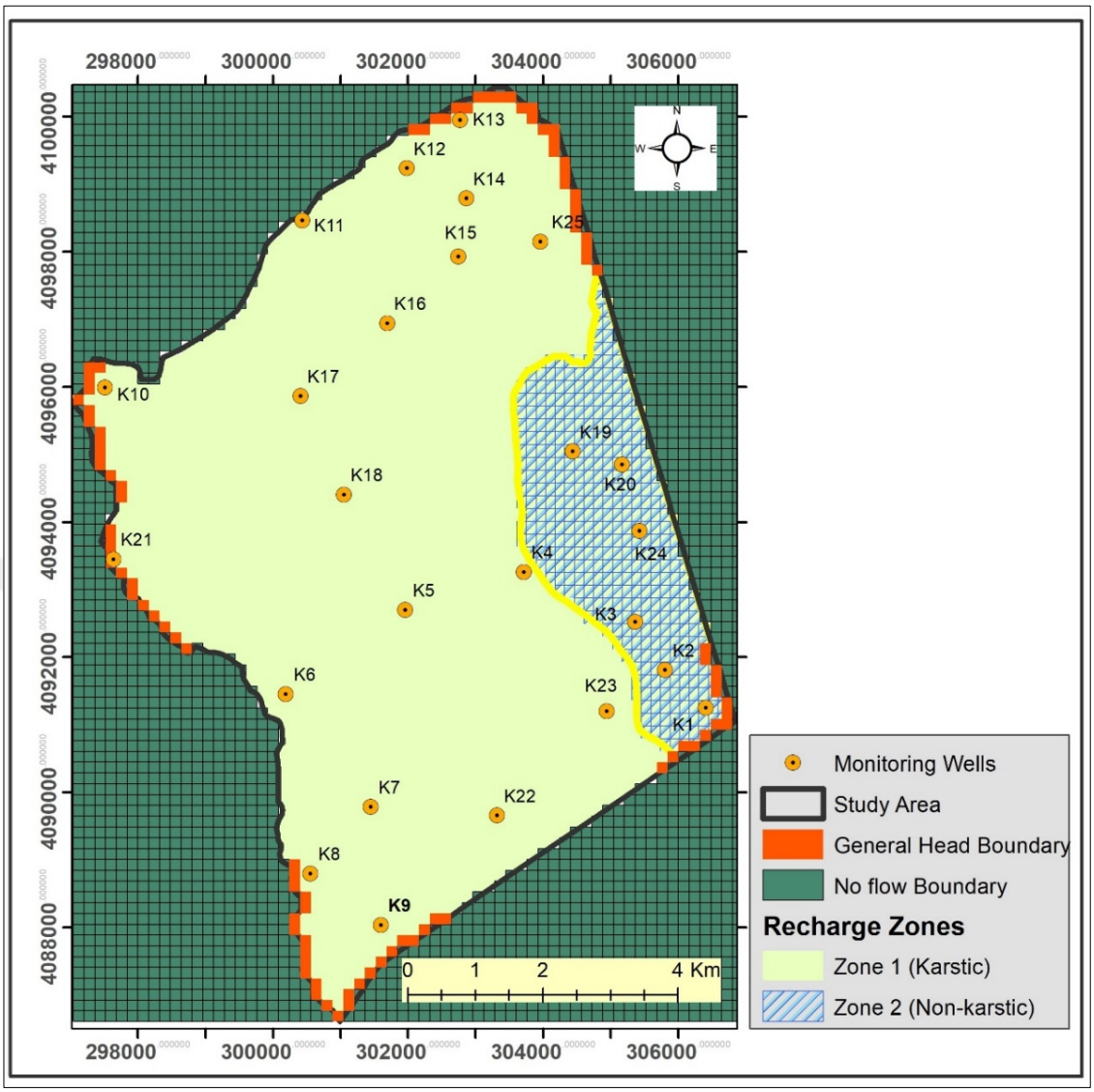

Figure 3.20. Boundary conditions applied for steady-state model run

3.6.3. Recharge

Recharge is water that infiltrates at the land surface, flows through the unsaturated zone, and crosses the water table to enter the groundwater system. Visual MODFLOW Flex supports the recharge package. Recharge is not a parameter that is always measurable but rather occurs as a result of rainfall infiltrating into the groundwater system. Therefore, the precise calculation of the aquifer recharges by precipitation and the adjacent groundwater inflows are perhaps the most problematic and nearly impossible task. However, it is possible to estimate. For this study, the recharge rate is assumed to be a percentage of the precipitation. The initial value of the steady-state recharge was estimated as the percentage of the local annual precipitation recorded in the year between 2015 -2016. This year was chosen because it coincided with the simulation period and actual year of the field activity. According to the meteorological data obtained from the nearest meteorological station for the years between 2015 and 2016, the total amount of yearly precipitation was 812.6 mm/year, and 456.3 mm/year respectively with the yearly

average rate of approximately 634.45 mm/year. The Regional Directorate of State Hydraulic Works in Antalya has conducted a recent and intensive hydrogeological research in Antalya. Based on the findings of the research, approximately 44% of the precipitation contributes to groundwater recharge in the karstic zone, whereas approximately 15% of the precipitation infiltrates to the aquifer in the non-karstic zone of the study area (AMPR, 2016). Therefore, to assign recharge values, the same zoning used for assigning hydraulic conductivity values was adopted. The assigned recharge values were the product of the mean annual rainfall and the corresponding infiltration coefficient of each geological formation. Therefore, as an estimate from the meteorological data, the net recharge in the karstic zone was determined to be 279.2 mm/year, and for the non-karstic zone, it was approximately 95.2 mm/year. Figure 3.21 shows the spatial distribution of average recharge values at different zones. The assigned recharge rate is shown in Table 3.4.

The study area lacks a sewage collection system and only small wastewater collection network exists in the northwest part of the study area. Due to lack of information, recharge from water and wastewater leakages, as well as irrigation return were neglected in this study. It is recommended that the leakage values from water and wastewater networks could be considered in the future for comprehensive groundwater modeling. The monthly average precipitations and recharge in karst and non-karst aquifer are shown in Figure 3.22. and Figure 3.23.

Table 3.4. Initial recharge rates values in the years between 2015-2015 for the pilot study area

Year/Months	**Total Precipitation (mm)/year**	**Recharge in Karst Area**	**Recharge in Non-Karst Area**
		44% of Total Precipitation	15% of Total Precipitation
2015	812.6	357.6	121.9
2016	456.3	200.8	68.5
Average Precipitation	**634.5**	**279.2**	**95.2**

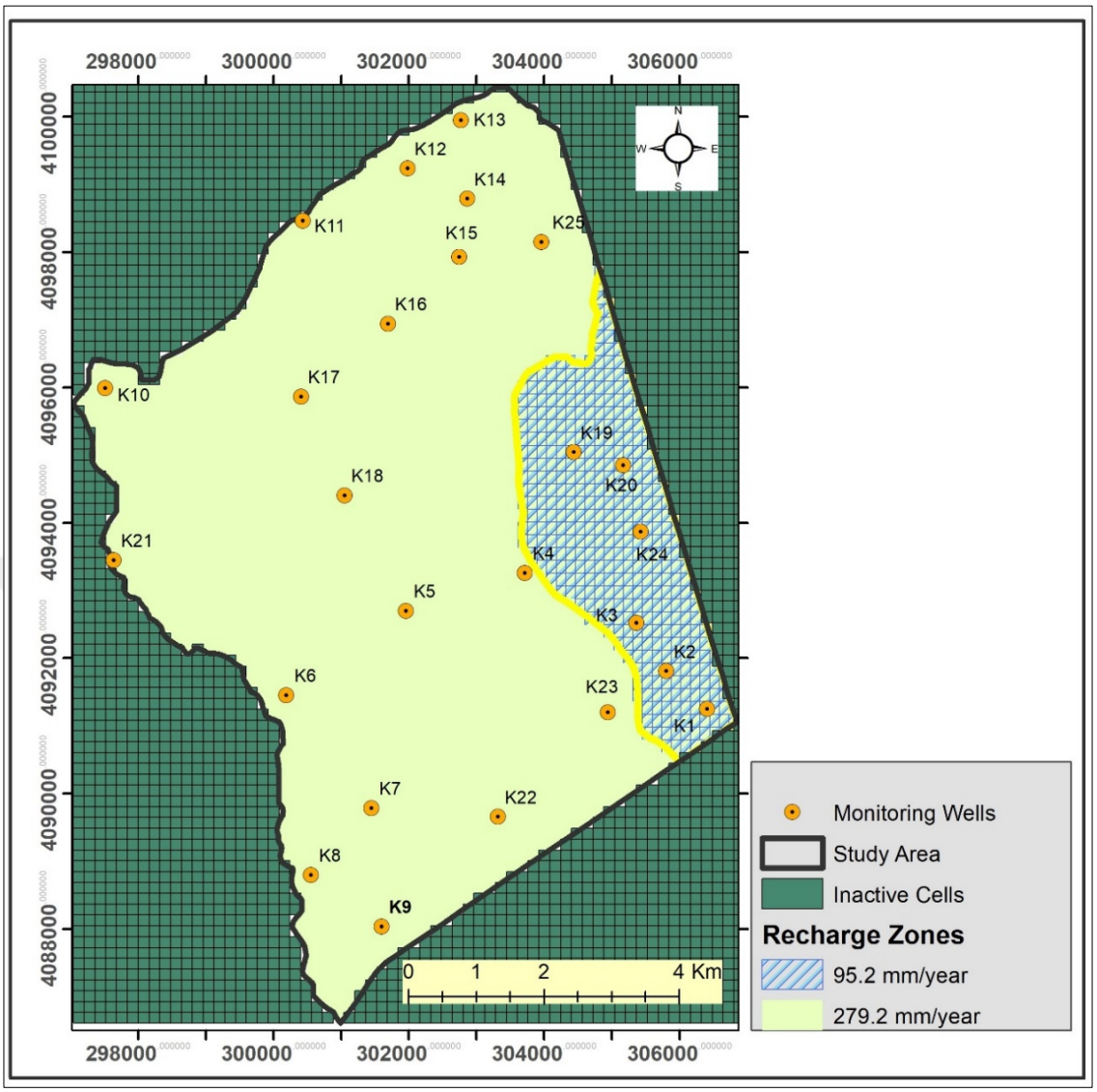

Figure 3.21. Map view of average recharge values in a year (2015 – 2016)

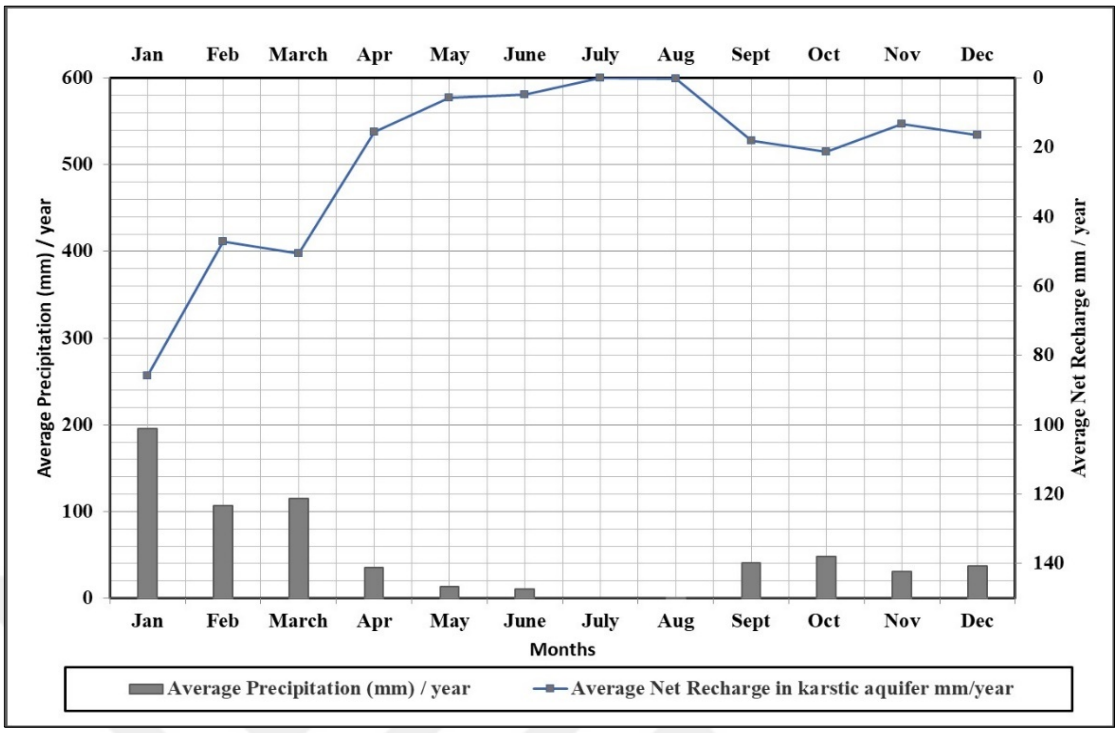

Figure 3.22. Monthly average precipitation and recharge in karst aquifer in year (2015 – 2016)

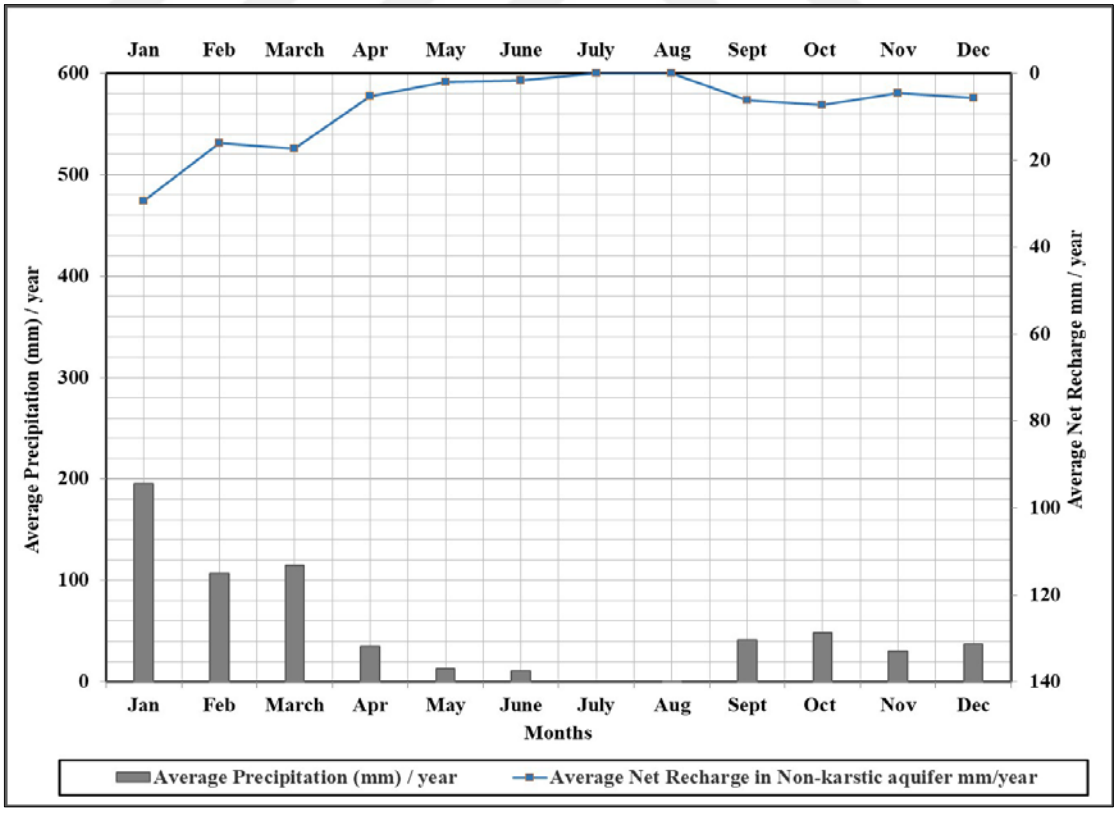

Figure 3.23. Monthly average precipitation and recharge in non-karst aquifer in year (2015 – 2016)

3.6.4. Pumping wells

As a part of the data collection efforts, the data regarding wells location was obtained from a database of the State Hydraulics Works, Directorate of 13th division in Antalya under the scope of the previous TÜBİTAK project, number 114Y696. These wells are distributed all over the Antalya region. Therefore, the preprocessing employed in the identification of production wells within the study area was first the reprojection of the wells coordinate to the UTM coordinate system zone 36N. Then the vector wells points were converted to Keyhole Markup Language (KML) and uploaded to Google Earth Pro V 7.3. A total of 315 wells were identified within the study area, in addition to 25 monitoring wells for a total of 340 wells. To estimate the groundwater withdrawal rates from the identified wells in the study area the following step were used :

- A remote sensing-based GIS approach was used. All the agricultural areas in the form of greenhouses in the study area were digitized from the satellite imagery by using combination of ArcGIS and Google earth software.
- The surface area of the digitized agricultural areas was calculated with the help of a field calculator in the ArcGIS environment.
- All the greenhouses in the study area were assumed to grow the same crops which include: tomato, cucumber, pumpkin, pepper, eggplant, watermelon, lettuce, parsley, strawberry and gerbera flower. The average water needs of the crops were estimated in a previous study by (Muhammetoğlu et al., 2017), as 6250 m^3/ha/year. The estimated water needs were used to determine the pumping rate.
- The pumping rate was estimated by multiplying the average water need by the surface area of the greenhouses (average water needs of crops X surface area of the greenhouse).

The withdrawal rate for all 340 pumping wells was assumed to be uniformed. Consequently, the estimated pumping rate values were divided by the total number of wells. The estimated withdrawal rate is presented in Table 3.5. For the model application, these 340 wells were used as pumping wells**.**

The groundwater withdrawal rate for all wells was estimated because data on the withdrawal rates were not available in the study area. To import the pumping wells data into Visual MODFLOW flex, we converted the vector points data to Excel with the help of the conversion tool in ArcGIS. Then the excel files was imported.

The starting pumping time was set as 18/Nov/2015 which is exactly the starting simulation date, and the date coincident with the first field measurement of depth to groundwater in the study area. Figure 3.24 shows the density map of the greenhouses in the study area and the spatial distribution of the 340 pumping wells.

Table 3.5. Estimated withdrawal rate

Estimated Ratio	Value	Units
Average water needs by crops	6250	m^3/ha/year
Total greenhouse area	1371.9	ha
Total wells	340	
Total yearly withdrawal rate	8574464	m^3/year
Yearly withdrawal rate per well	25219.0	m^3/year
Total daily withdrawal rate	23491.7	m^3/day
Daily withdrawal rate per well	69.09	m^3/day

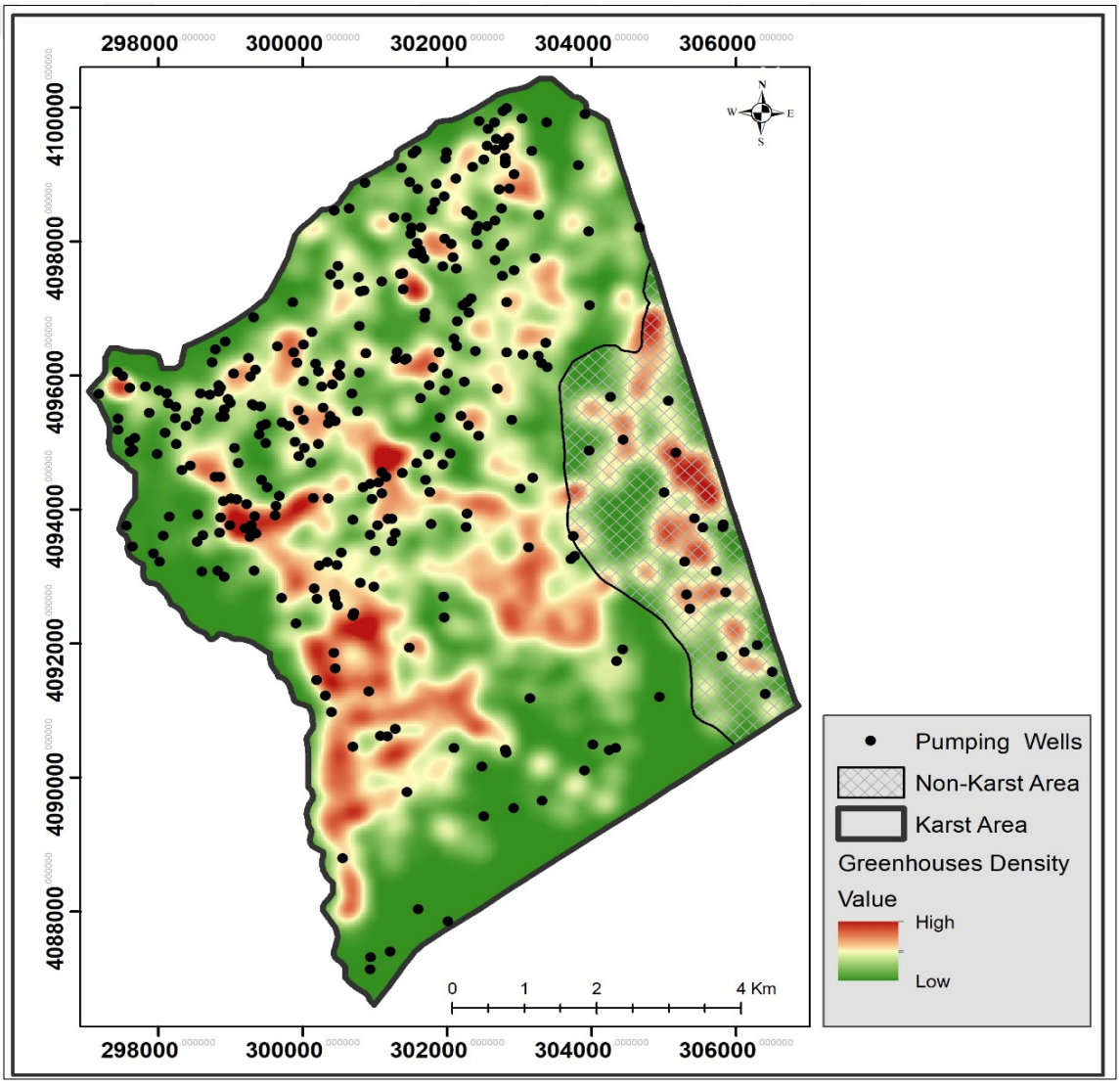

Figure 3.24. Spatial distribution of irrigation wells and the pumping rates in the model domain

3.6.5. Set-up of the solver used in the numerical model run

The groundwater flow equation is solved in MODFLOW-2005 using the finite difference method (Harbaugh, Arlen 2005).Within the steady-state model, the layer property package was used, and the simulation time was set to one year, 365 days. In this analysis Precondition Conjugated Gradient Solver (PCG) package supported in MODFLOW-2005 to solve the finite difference equation was used. The PCG solver provided within MODFLOW-2005 includes an extra variable that can influence convergence. For the full documentation of the PCG solver, the reader is referred to (Hill 1990). The property settings of the solver used in this model application is shown in Table 3.6. The model layer was set to one-layer LYCON = 3. In other words, the layer was set to a convertible layer. The model was set to convertible layer in order to maintain consistency of the input structure across the model domain and to allow the flexibility of the model to treats layer as confined or unconfined, accordingly.

Table 3.6. Property settings of solver used in the model application

(PCG) Properties	**Value/Set up**
Max. outer iteration (MXITER)	100
Max. inner iteration (ITER)	50
Pre-conditioning Methods (NPCOND)	Modified Incomplete Cholesky (NPCOND = 1)
Head change criterion (HCLOSE)	0.01
Residual criterion (RCLOSE)	0.01
Relaxation parameter (RELAX)	1
The printout interval (IPRPCG)	20
Convergence output control (MUTPCG)	Only the number of iterations (MUTPCG =1)
Damping factor (DAMP/DUMPPCG)	1

From Table 3.6 the properties of the (PCG) are explained as follows:

Maximum Number of Outer Iterations is the parameter that provides an upper limit on the number of outer iterations. For most groundwater modeling problems, default values of 50 are adequate to meet convergence criteria. For our study, the maximum number of outer iterations was adjusted to 100 to meet the convergence criteria of General Boundary Condition (GHB) used in the model.

Maximum Number of Inner Iterations is the variable that define the maximum quantity of inner iterations for each outer iteration. The default value in Visual MODFLOW flex is 25. For this study the value was adjusted to 50. this was done to match the maximum number of outer iterations.

The PCG solver provided in MODFLOW–2005 includes an additional variable, DAMP/DUMPPCG, that can influence convergence.

Damping Factor is a flag that controls adaptive damping. The damping parameter is adaptively varied on the basis of the head change, using Cooley's method for subsequent iterations (Hill 1990). This variable functions as a multiplier of the head change computed by the PCG algorithm. As a general rule, DAMP initially should be given a value of one (Hill 1990). Therefore, in this analysis, the default value of 1 was maintained.

Head change criterion is the property of the solver that checks for the maximum change in the solution at every cell. For this study a default solution of 0.01 was maintained because it is sufficient for most problems.

Residual criterion is the residual convergence criterion for the inner iteration. This PCG property is, by default set as the same value as Head Change Criterion (HCLOSE). This is done to help the solver to solve with sufficient accuracy.

Relaxation parameter in the PCG solver was used to help improve the spectral number of the ILU preconditioned system. The default value was used in this analysis.

The printout interval for the PCG solver is used to print the residual (positive or negative) for each iteration. It occurs at the end of each stress period regardless of the value of . The default value in the model is 10. For this study the default value of was adopted.

The Preconditioned Conjugate-Gradient Solver (PCG) Package is documented in (Hill 1990).

3.7. Model Setting

- The spatial distribution of groundwater recharge assigned to each zone was assumed to be constant, the model was set as one layer. Therefore, the only parameter included in calibration was conductivity in the horizontal/x-direction (Kx).

-The layer type was set to the confined/unconfined variable whereby Visual MODFLOW Flex automatically chooses the appropriate layer. The model layer was set to one-layer LYCON = 3, the interlock transmissivity was set to harmonic mean.

- Since the model is run in the steady-state mode, specific storage **(Ss)**, specific yield **(**Sy), effective porosity, and total porosity values were maintained as default in the model. The initial head was set as uniform throughout the model domain with the value equal to 60 m.

3.8. Model Calibration

Calibration of the groundwater model is the most challenging task in the entire modeling process due to the existence of a large number of parameters in groundwater modeling (Doherty and Hunt 2010). Therefore, calibration of the model in this study was performed automatically using the parameter estimation tool (PEST), linked as an extension in Visual MODFLOW Flex (Waterloo 2018). The purpose of the calibration process was to adjust the model parameters in a systematic manner such that the model simulated groundwater table elevation properly matches the field condition. Initially the

model parameters were adjusted manually, then followed by automatic calibration using the Parameter Estimation Tool (PEST). PEST uses gradient-based methods to search for an optimal solution. The purpose is to minimize the sum of squared differences between observed and simulated groundwater table elevation (Residual).

The model domain was divided into two zones based on the geological formation. Each zone has a unique hydraulic conductivity. For this analysis, the model parameter included in the PEST run is hydraulic conductivity (Kx). The reason for choosing Kx in the calibration is that PEST in Visual MODFLOW Flex only supports Kx and Kz. Since the model was set as one layer, conductivity in the vertical direction Kz was neglected and only conductivity in the lateral (horizontal) direction Kx was included in the calibration.

The first step employed in the PEST run was the identification of observation wells and its corresponding field measurements (Groundwater table elevation). The next step is to assign the pilot points. Pilot points are the user defined points where the PEST algorithm optimizes the parameters. A total of 47 pilot points was created in the karstic zone with an initial hydraulic conductivity of 86.4 m/day. And in the non-karstic zone, 18 pilot points, were created and each point was assigned a conductivity value of 0.864 m/day. There is no fixed rule set for placement of the pilot point, although suggestion given by (Doherty and Hunt 2010) was employed. The spatial distribution of pilot points is depicted in Figure 3.25.

Once the pilot points were assigned, the next step was to define the range of optimized parameters. An ordinary kriging method was used in Visual MODFLOW flex to interpolate between pilot points. This method was selected because it is numerically efficient. Additionally, it helps the model to recognize the values assigned to the points. Furthermore, this method performs the regularization and interpolation based on the variograms analysis (Waterloo 2018). This step is an important part of the calibration process because variograms are used by PEST in the calculation of regularization weights. The variogram used in this analysis was set to exponential. Before running PEST, a sensitivity analysis was run to identify the parameters to be included in a PEST run.

The other parameters such as Specific storage (Ss), Specific yield (Sy) were kept constant with the value of 0.2 and $1.00E^{-05}$ 1/m respectively as shown in Table 3.3. For this application, only hydraulic conductivity was included in the PEST run. After the PEST tool was run, the calibrated groundwater table elevation results were exported to an Excel program for visualization and further post-analysis. Then the model was re-run with updated PEST calibrated parameters.

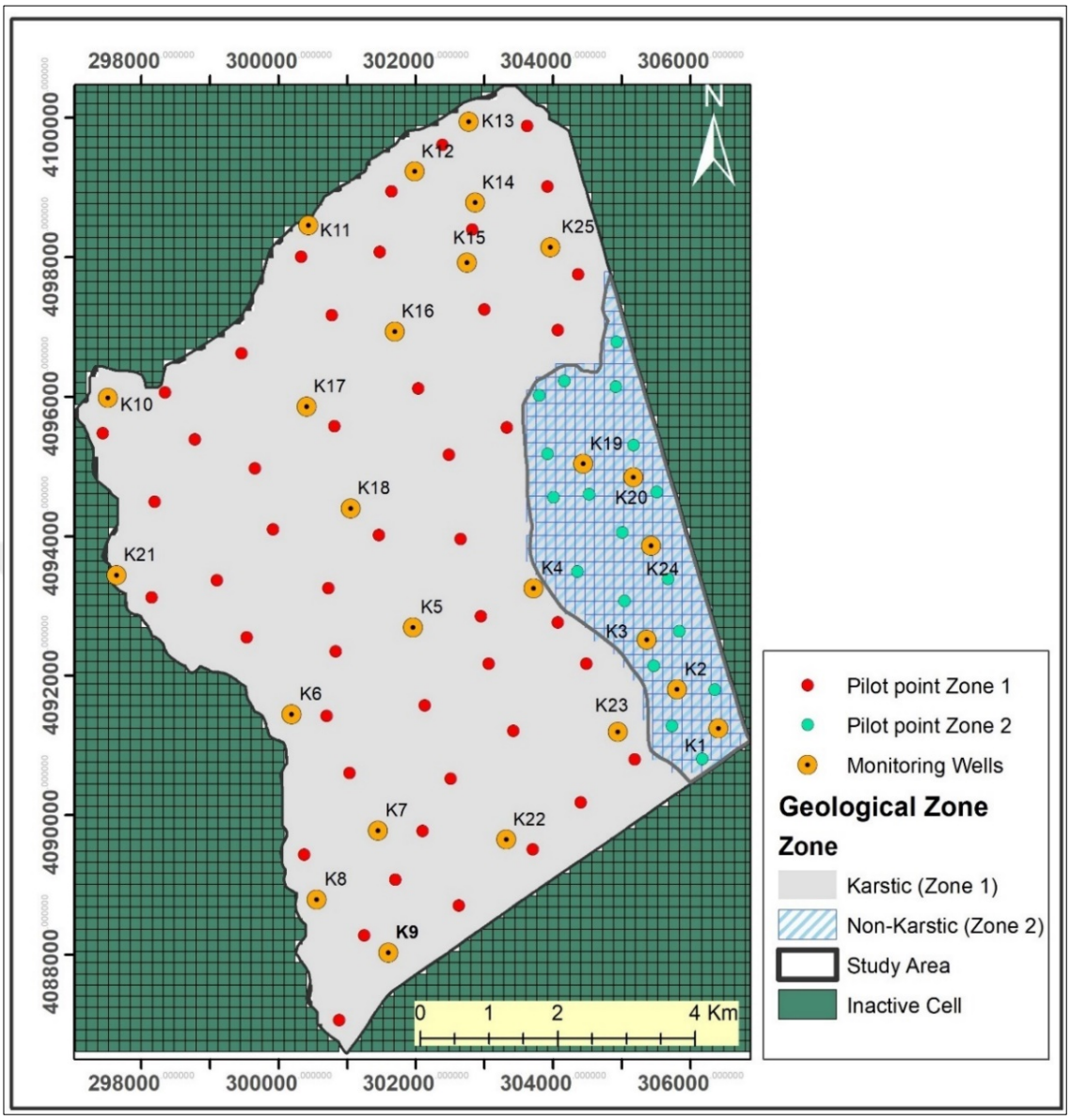

Figure 3.25. Spatial distribution of pilot points used in model calibration

3.9. Model Prediction Evaluation

To prove the accuracy of the model, the post-analysis statistics was performed, and summary results was produced. The difference between the measured and calculated groundwater table elevation (Residual) was computed. The residual mean, standard deviation, and root mean square RMS were determined. Measured and simulated groundwater table elevation was plotted in a scatter plot and the correlation coefficient were determined to assess the possible presence of systematic errors in the model.

To evaluate the model prediction result, four error metrics are adapted to analyze the differences between the computed and measured groundwater table elevation (Residual). First, the Mean Absolute Error (MAE), which gives the average of the absolute, non-squared value of the differences between the measured and simulated groundwater table elevation. This metric was used because it is a more intuitive metric to

assess the model performance. MAE was calculated from the equation (3.1)

$$MAE = \frac{1}{n}\sum_{i=1}^{n}|h_m - h_s|_{ii} \quad (3.1)$$

The second metric adopted for assessing the model performance was Root Mean Square Error (RMSE). This statistical criterion gives the average of the squared difference of measured and observed groundwater table elevation. RMSE was computed using equation (3.2).

$$RMSE = \sqrt{\frac{\sum_{i=1}^{n}(\mathrm{h_m} - h_s)^2}{n}} \quad (3.2)$$

Where: n, total number of monitoring wells, h_m , measured groundwater table elevation h_s simulated groundwater table elevation

the third criterion used for assessment of the steady-state model calibration adequacy was by defining the ratio of the root mean square error. In other words, standard deviation to the total change in groundwater table elevation over the model domain (M. Anderson et al., 1990).This is defined by the following equation:

$$E = \frac{\left[\frac{1}{n}\sum_{i=1}(h_m - h_s)_i^2\right]^{0.5}}{\Delta H} \quad (3.3)$$

Where: E, error, h_m , measured groundwater table elevation, h_s , simulated groundwater table elevation, ΔH, total change in groundwater table elevation in the model domain. The fourth metric used as a measure of the accuracy in this study was Normalize Root Mean Square Error (NRMSE). This statistic criteria were computed by dividing RMSE by the mean actual measured as shown in equation (3.4).

$$NRMSE = \frac{RMSE}{\bar{h}m} \times 100 \quad (3.4)$$

Where: n, total number of monitoring wells, hm, measured groundwater table elevation, hs, simulated groundwater table elevation, $\bar{h}m$, mean actual measured groundwater table elevation

3.10. Analysis of Different Management Scenarios

The Mediterranean regions of Turkey are susceptible to climate change. The consequences of climate change in the Mediterranean region are known to include a rise in temperature and a decrease in recharge and water exiguity (Tayanç et al. 2009; Lelieveld et al. 2012; Unal et al., 2012; Kum and Çelik, 2014;). Similarly, pumping is in

an increasing trend due to an increase in agricultural activities in the Antalya consequently, this will stress the groundwater resources. Both decreases in recharge and increase in groundwater abstraction for irrigation is also anticipated as a decrease in precipitation will lead to an increase in pumping. Therefore, the main aim of this study is to develop a management scenario using a numerical model to understand the repercussion of the decrease in recharge and increase in groundwater abstractions in the aquifer of Altınova.To achieve the research aims, three scenarios were developed. Scenario (A) anticipated decrease in groundwater, Scenario (B) increase in the abstraction rate, and Scenario (C) combination of both scenario (A) and (B). The primary objective of developing model scenarios is to assess the groundwater table fluctuation in the karst and non-karst area of Altınova.

Scenario (A): assume decrease in precipitation by 50% with the current rate of groundwater withdrawal, Scenario (B): assume increase in the groundwater withdrawal by 50% at the current state of precipitation. Scenario (C): assume decrease in precipitation by 50% and increase in the current withdrawal rate by 50%, as described in Table 3.7.The impacts of changes in the groundwater table elevation under different scenarios on the karst and non-karst aquifer of Altınova was evaluated by obtaining the difference between base simulation and the different scenarios of groundwater table elevation.

In addition to management scenarios, a sensitivity analysis was conducted by decreasing and increasing the calibrated values of hydraulic conductivity component by 50%. During simulation, when the effect of parameter was being tested, the other model parameters were kept to the steady-state . In the sensitivity analysis a parameter was changed uniformly over the whole model domain. A total of two model runs were made by changing the hydraulic conductivity by 50% percent.

Table 3.7. Model Management Scenarios

Rate of Increase/Decrease	**Scenarios**
50% reduction in (Recharge)	Scenario (A)
50% increase in (Pumping Rate)	Scenario (B)
Combination of (A &B)	Scenario (C)

4. RESULT AND DISCUSSION

The distributed parameter approach through the MODFLOW-2005 engine was used to simulate groundwater in the karst area of Altınova. For this study, MODFLOW-2005 in Graphical User Interface GUI Visual MODFLOW flex was used. The good of fitness was evaluated based on the approach recommended by M.Hill, 1998. The simulation results of Visual MODFLOW flex in the travertine karst and the Kurşunlu non-karst region of Altınova were compared with target data (groundwater table elevation). Following the evaluation of model predictions of Visual MODFLOW flex, the second objective was to develop a management scenario and predict forthcoming groundwater level under different conditions.

4.1. Pre-calibration Result of the Groundwater Modeling

The initial values of hydraulic conductivity used in the model pre-calibration stage were 86.4 m/day in karst area and 0.864 m/day in non-karst. These values were obtained from expert knowledge and are in line with the literature (Allan R. Cherry, 1979). The trials model runs were performed using the initial values. At the pre-calibration stage the position of boundary condition was adjusted in the model domain. This was done in order to match between simulated and measured groundwater table elevation. However, these changes did not provide a reasonable match between the measured and simulated groundwater table elevation. The obtained correlation coefficient in the pre-calibration stage was 0.81 as depicted in Figure 4.1. Based on the statistical analysis of the pre-calibration model, the Root Mean Squared error (RMSE) is 9.33 m, and the Normalized Root Mean Square error NMRSE is 17.7% as shown in Table 4.1. This statistical analysis suggests that further automated calibration is needed. Furthermore, from Figure 4.2 it can be seen clearly that the pre-calibration model yielded less comparable results for groundwater table elevation for all the measurement points. The pre-calibration contour map of groundwater table elevation is illustrated in Figure 4.3. From the map it can clearly be seen that the simulated groundwater table elevation line did not match well with the measured groundwater table elevation. The poor fit obtained from the pre-calibration model run shows how important it is to calibrate and assign calibrated values of hydraulic conductivity to each model grid cell.

Table 4.1. Model performance statistics for pre-calibrated groundwater table elevation

Statistical Criteria	Pre-Calibration
Minimum Residual (m)	-21.20
Maximum Residual (m)	8.00
Median	0.68
Residual Mean (m)	-2.46
RMSE (m)	9.33
NRMSE (%)	17.67
Regression Coefficient (R^2)	0.81
Standard Error of the Estimate (m)	1.84
Abs. Residual Mean (m)	7.03

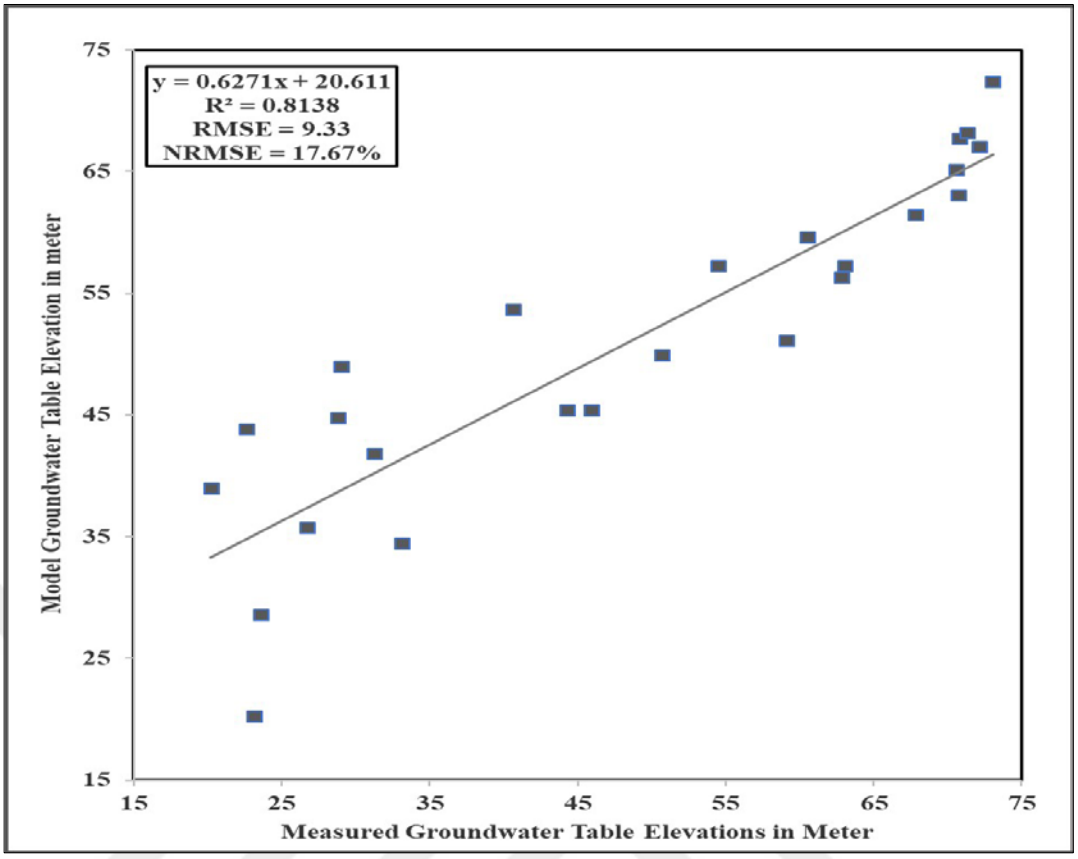

Figure 4.1. Pre-calibration scatter plot of simulated to measured groundwater table elevations (m)

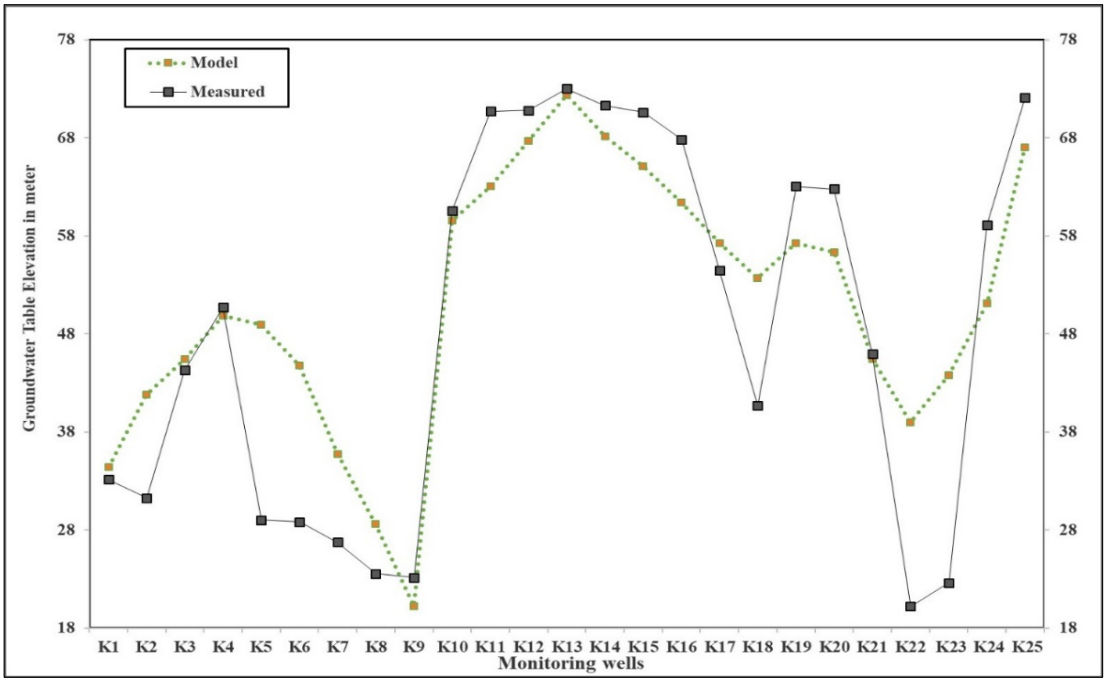

Figure 4.2. Pre-calibration graph of simulated to measured groundwater table elevations (m)

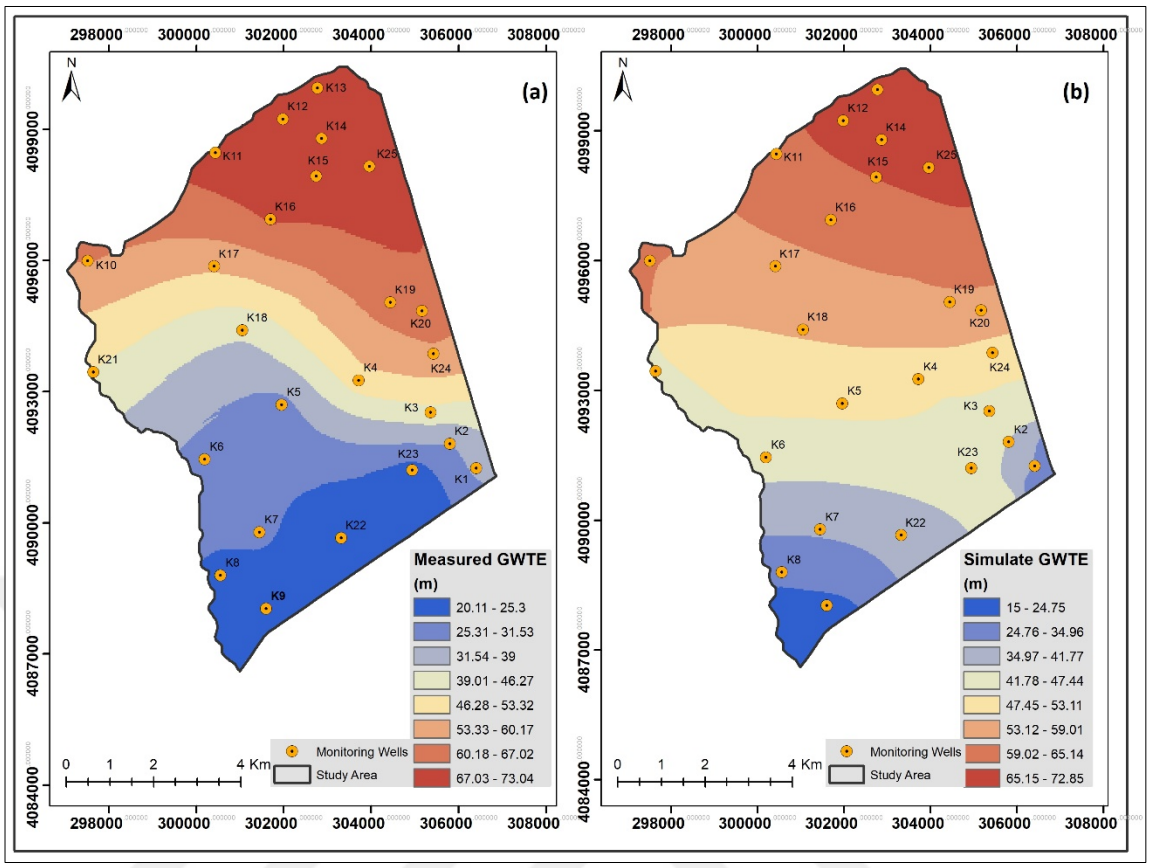

Figure 4.3. Pre-calibration map of measured (a) and simulated (b) groundwater table elevations

4.2. Calibrated Hydraulic Conductivity

In the steady-state, the only parameter included in the calibration was hydraulic conductivity in lateral direction. The reason for choosing Kx in the calibration is that PEST in Visual MODFLOW Flex only supports Kx and Kz. Since the model was set as one layer due to lack of conductivity in vertical direction Kz, only conductivity in lateral (horizontal) direction Kx was included in the calibration. This was done in order to reduce the difference between simulated and measured groundwater table elevation. The calibration was done automatically by using PEST. The initial values of hydraulic conductivity in karst area was 86.4 m/day and non-karst area was 0.864 m/day. The aim of the calibration here is to estimate the values of hydraulic conductivity based on the literature ranges while obtaining the best fit relation between measured and computed groundwater table elevation. The results of the calibrated hydraulic conductivity are presented spatially in Figure 4.4. Table 4.2, shows calibrated values of conductivity at monitoring wells while the statistical analyses for conductivity are presented in Table 4.3. In general, the higher values of hydraulic conductivity are in the karst travertine of the study area. However, in the non-karst region, the hydraulic conductivity is low. This is consistent with what one would expect in a karst environment. Furthermore, the higher values of conductivity in the southern parts of the karst travertine occur in the lower groundwater table elevation, and vice versa in the northern part of the karst travertine. The higher values of calibrated hydraulic conductivity up to 266 m/day was observed in

the south part of the karst travertine (Figure 4.4). We further interpreted that the variation of hydraulic conductivity within the karst travertine might be associated with the variation in the degree of karstification and lithological heterogeneity in the area.

Table 4.2. Estimated values of hydraulic conductivity and transmissivity at the monitoring wells in both Travertine and Kurşunlu formation

Kurşunlu Non-karstic formation		
Monitoring wells	**K_{xx} m/day**	**Transmissivity m^2/day**
K1	0.11	16.50
K2	0.01	1.50
K3	0.01	1.50
K4	0.17	28.73
K19	0.16	23.68
K20	1.13	169.50
K24	0.90	135.00
Travertine Karstic formation		
Monitoring wells	**Kx m/day**	**Transmissivity m^2/day**
K5	54.40	9628.80
K6	146.00	25112.00
K7	239.00	42303.00
K8	162.00	28026.00
K9	122.00	21716.00
K10	8.30	1253.30
K11	12.30	2140.20
K12	32.60	5802.80
K13	12.30	2177.10
K14	14.90	2607.50
K15	12.40	2194.80
K16	2.10	375.90
K17	0.60	104.40
K18	6.60	1168.20
K21	16.90	2551.90
K22	178.00	30972.00
K23	209.50	31425.00
K25	12.80	2150.40

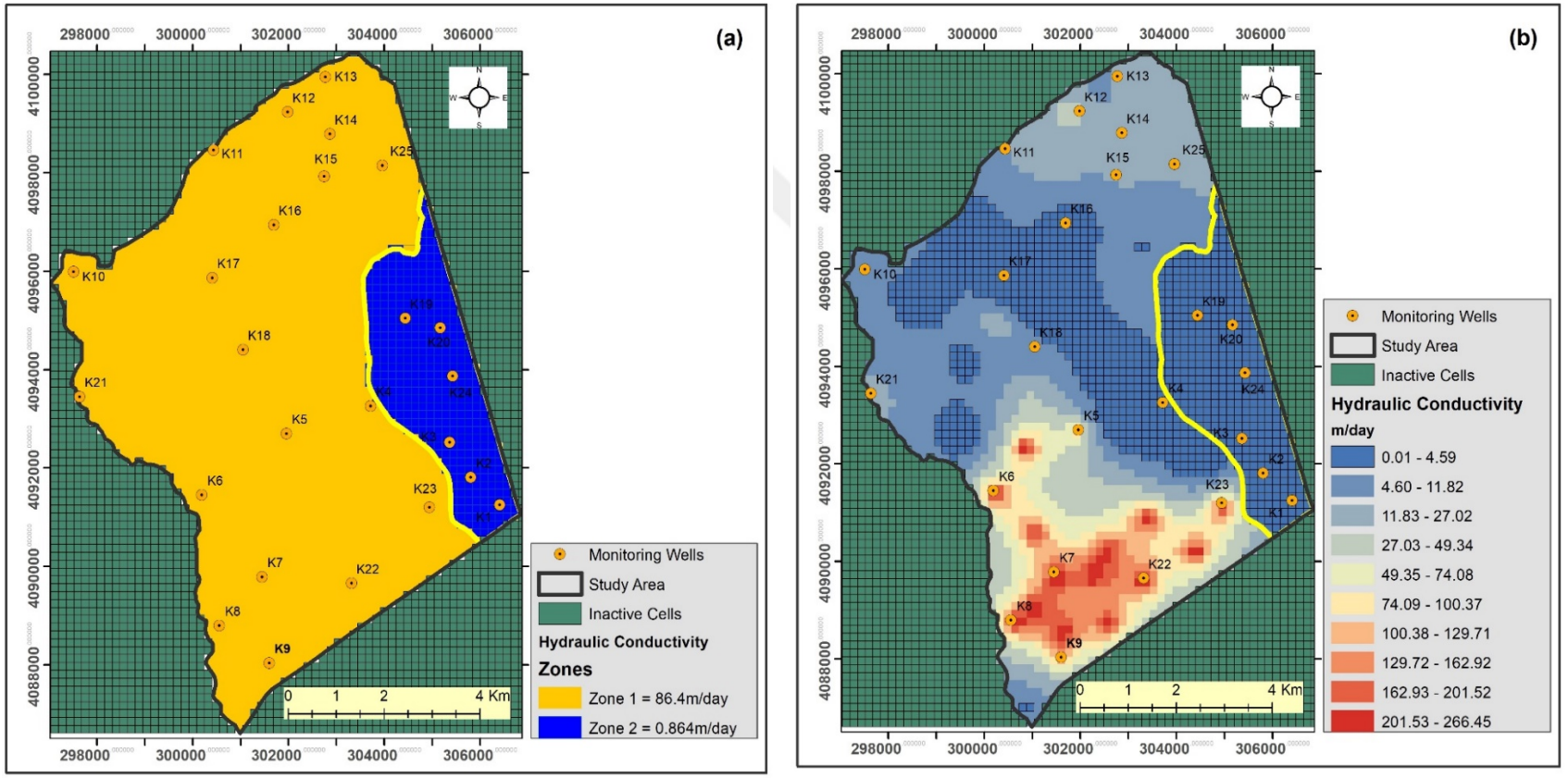

Figure 4.4. Hydraulic conductivity pre-Calibration (a) and calibrated hydraulic conductivity (b)

This modeling work is the first attempt carried out to estimate hydraulic conductivity at the travertine karst region of Altınova. Generally, the spatial distribution of hydraulic conductivity in the study is within the range of literature values (Allan and Cherry 1979). The distribution of horizontal conductivity produced by our study is the critical start point in the study of the karst travertine of Altınova. However, our model does not account for the heterogeneity of karst aquifers. Furthermore, due to the lack of the proper geological data in the karst system of the study area, the accurate locations of the caves and sinkholes were not determined. This might cause an inaccurate estimate of hydraulic conductivity in some parts of the study area.

At the monitoring wells level, the hydraulic conductivity ranges from 0.6 to 239 m/day in the travertine karst aquifer, while in Kurşunlu non-karst area the calibrated hydraulic conductivity ranges from 0.01 to 1.2 m/day. The minimum values of 0.01, and 0.6, m/day in karst and non-karst area respectively are consistent with the study conducted in a similar aquifer in Kalik-Denizli (Murat 2015). Conversely, the maximum values of hydraulic conductivity in our study are twice higher than the values estimated by (Murat 2015). The variation in maximum values might be linked with the pumping test estimation approach use by (Murat, 2015), because the hydraulic conductivity of karst aquifers computed from wells (pumping test) tend to underestimate, oftentimes dramatically than the actual values (Scanlon et al. 2003). Likewise, the estimated transmissivity is not in agreement with (Murat 2015). The transmissivity ranges between 1.5 and 42303 m^2/day which is twice the value estimated in Kaklik Aquifer (Murat 2015). This is due to variation in the aquifer thickness. Overall, the calibrated values of hydraulic conductivity in both karst and non-karst area of the Altınova are within the literature.

Table 4.2. Statistical Values for estimated hydraulic conductivity at monitoring wells level.

Statistical Criteria	**Kxy m/day**	**Transmissivity m^2/day**
Mean	49.8	8483.4
Median	12.3	2150.4
Minimum	0.01	1.5
Maximum	239.0	42303.0
Range	239.0	42301.5
Standard Deviation	75.9	12887.9

4.3. Calibrated Groundwater Table Elevation Result

Calibration of the model in this study was performed automatically using the parameter estimation tool (PEST). The result of the steady-state groundwater simulation was evaluated by comparing the measured with the simulated groundwater table elevation. Overall the calibration result of the steady-state in the study area show good-fit between simulated groundwater table elevation and measured groundwater table elevation. It can be understood clearly from Figure 4.5 that the residual values were dispersed arbitrarily around zero. The residual mean, Absolute Mean residual (AM), Root Mean Square Error of residual (RMSE), and the Normalized Root Mean Squared Error (NRMSE) were 0.6 m, 1.5 m, 1.7 m and 4.0% ; respectively as shown in Table 4.3

To date, there is no standard protocol for evaluating the calibration results (Anderson et al. 1990), although the common rule of thumb is that the RMSE should be less than 10% of the difference of groundwater table elevation across the model domain. The error was defined as the ratio of root mean squared error to the total groundwater table elevation change over the model domain (Anderson et al. 1990). The result of this study indicated that the RMSE was less than 4% of the range of measured values. These values were consistent with the rule of thumb suggested by (Anderson et al. 1990). Taking into consideration the use of Equivalent Porous Media EPM approach through MODFLOW-2005 in both karts travertine and non-karst kurşunlu formation of Altınova, the statistical values suggest that the calibration result is satisfactory. The model is less successful in the monitoring wells located at the lower elevation of the study area (Figure 4.6). Furthermore, the higher values of groundwater table elevation in the northern part of the study area yield a better prediction than the lower values of groundwater table elevation in the southern part.

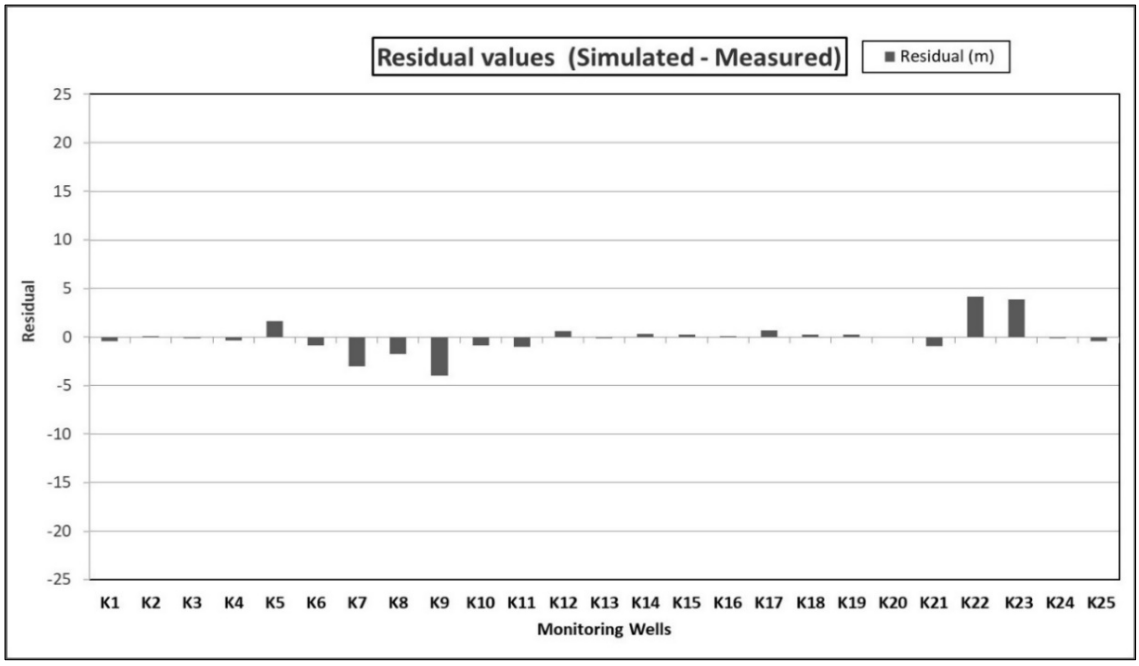

Figure 4.5. Residual values for simulated vs. measured groundwater table elevations

Table 4.3. Model performance statistics for calibrated groundwater table elevation

Statistical Criteria	**Calibrated Model Values**
Minimum Residual (m)	-3.98
Maximum Residual (m)	4.14
Median	-0.12
Residual Mean (m)	0.09
RMSE (m)	1.67
NRMSE (%)	4.00
Regression Coefficient (R^2)	0.99
Standard Error of the Estimate (m)	0.5
Abs. Residual Mean (m)	1.04

From Figure 4.6 it can clearly be seen that groundwater-table elevations are high in the topographic features with high elevations, especially in the north part of the study area. However, groundwater-table elevations are low in the areas of low elevations in the south portion of the study area. These observations tie well with the concept that the groundwater table often follows the terrain of the land surface. Furthermore, it is evident from Figure 4.6 that the simulated groundwater table elevation follows a similar trend as the measured groundwater table elevation. However, the model is less predictable in the south part of the study area, that can be clearly seen in Figure 4.7.

From Figure 4.7 it can be noticed that the calibration result in both karst and non-karst area shows a good fit between measured and simulated groundwater table elevation with an exception of 7 wells namely K5, K6, K7, K8, K9, K22, and K23. These 7 monitoring wells are located in the travertine karstic formation in southern part of the study area. Therefore, the less predictable result in these well might be mainly due to the karst feature of the area. Overall taking into consideration the use of Visual MODFLOW Flex approach that does not consider pipe flow or ambulance flow in karts travertine, these 7 wells shown acceptable residual value between measured and simulated groundwater table elevation. The underestimate of the groundwater table elevation in the south portion of the study area is clearly associated with karst features of the study area.

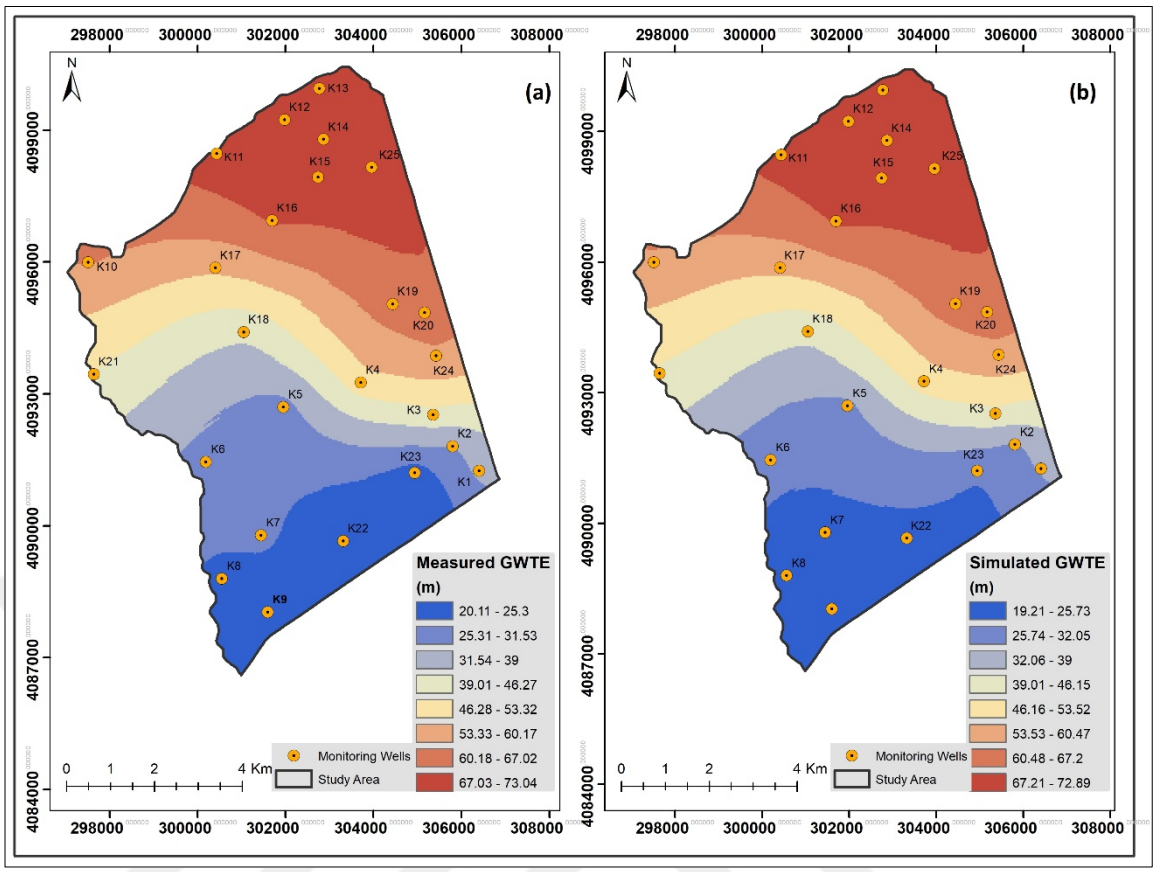

Figure 4.6. Calibration map view of observed (a) and simulated (b) groundwater table elevations

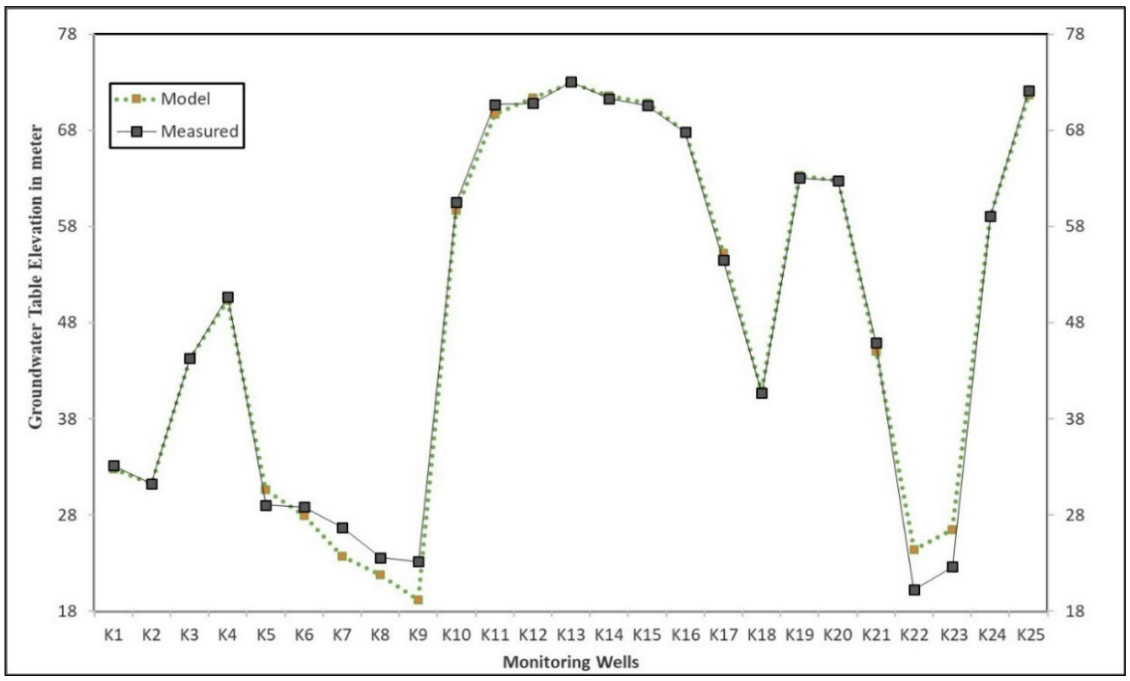

Figure 4.7. Calibrated graph view of simulated to measured groundwater table elevations (m)

The calibrated groundwater table elevation in the study area ranges from 19 m to 72 m above mean sea level. The groundwater table elevation provides important information on groundwater flow direction. The information regarding groundwater flow direction will be discussed in the next subsection.

A Scatter calibration diagram of simulated versus measured groundwater table elevation is shown in Figure 4.8. Overall the calibration results in the study area show good fit between simulated and measured groundwater table elevation. The correlation coefficient is reasonable with a value of 0.99. The best calibration model tends to have a correlation coefficient close to one. Furthermore, the correlation coefficient obtained from our study is within the acceptable limit mention by (Hill 1998). Therefore, it is safe to say that our model is satisfactory in the area of Altınova.

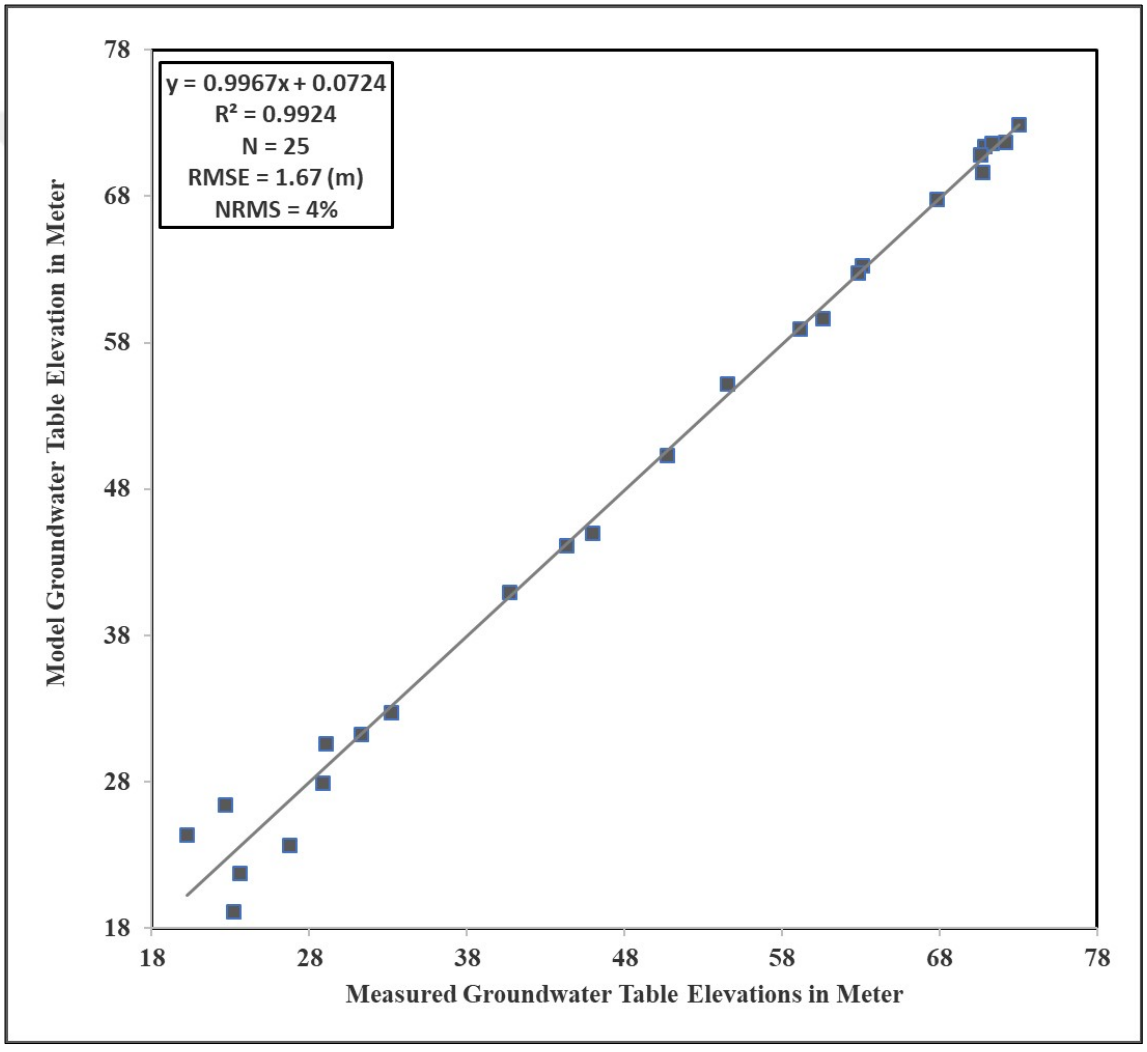

Figure 4.8. Calibrated scatter plot of simulated to measured groundwater table elevations (m)

4.4. Comparison between Karst and Non-Karst Result of Calibrated Groundwater Table Elevation

Figure 4.9 and Figure 4.10 show a comparison of groundwater table elevation in the karst and non-karst regions. The calibrated groundwater table elevation ranges from 29-69 m In Kurşunlu no-karst aquifer of Altınova (Figure 4.9). From Figure 4.10 it can clearly be seen that the calibrated groundwater table elevation in travertine karts area has an interesting variation that ranges from 19 to 72 m.

From the Figure 4.9 and Figure 4.10, it is clear that the model is less successful in the karst region than in the non-karst region. From the Figure 4.11, it is visible that the difference between measured and simulated groundwater table elevations (Residuals) for individual wells in the karst area are larger. In contrast to Figure 4.12, the residual values are distributed around zero in the non-karst region. Furthermore, at the monitoring wells level, the predicted groundwater table elevations in the non-karst region accurately follow the trend of measured groundwater table elevation.

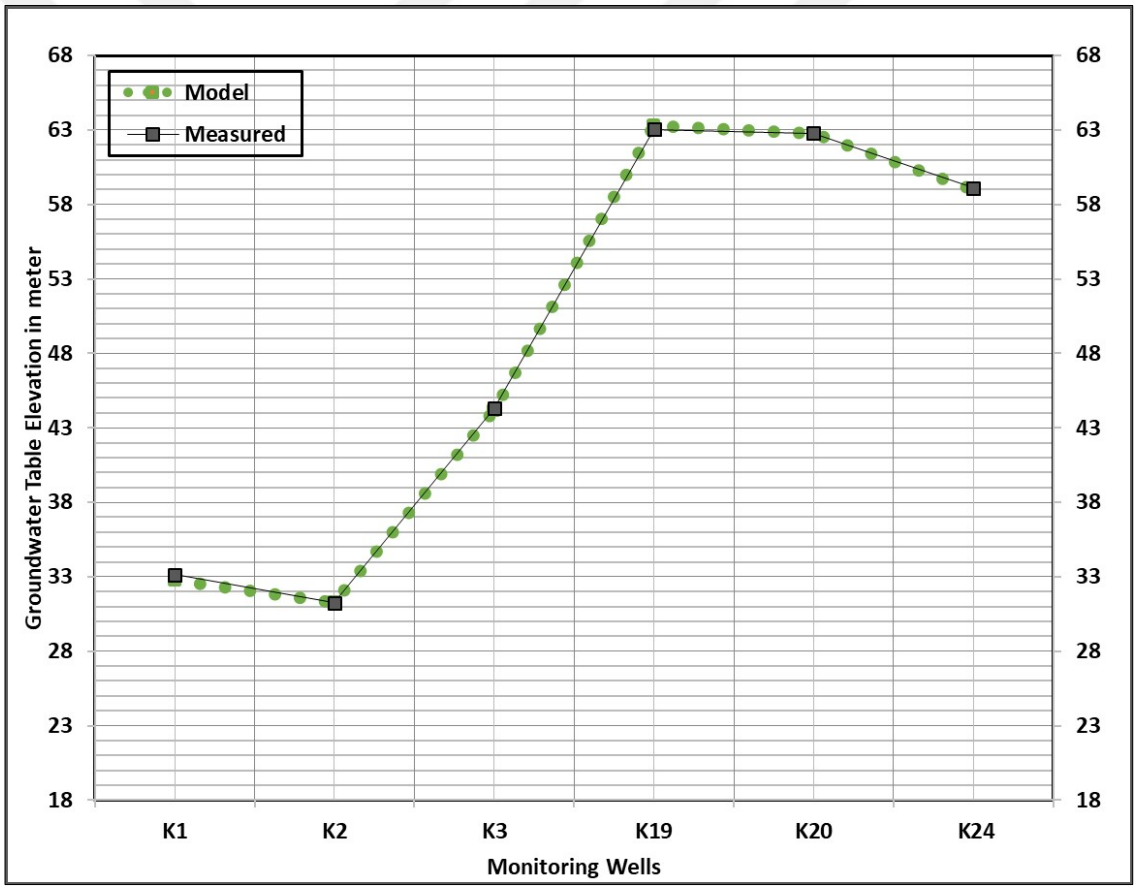

Figure 4.9. Calibrated graphical view of simulated versus measured groundwater table elevations in the non-karst area

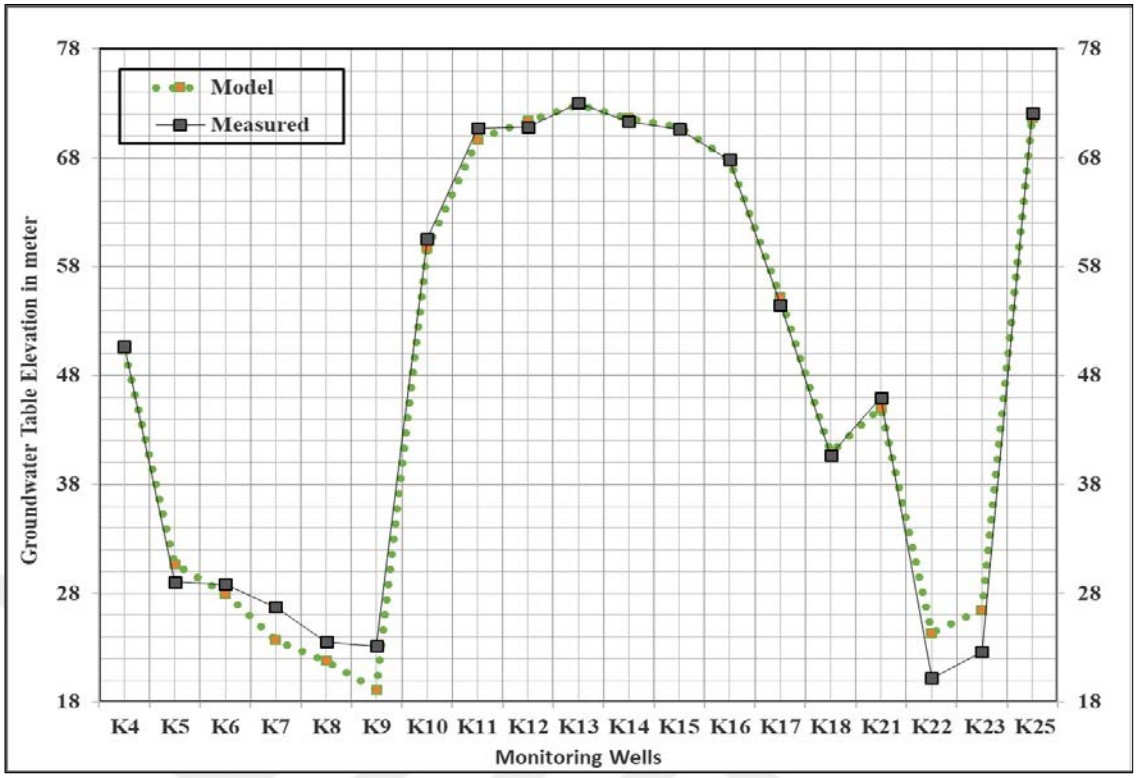

Figure 4.10. Calibrated graphical view of simulated versus measured groundwater table elevations in the karst area

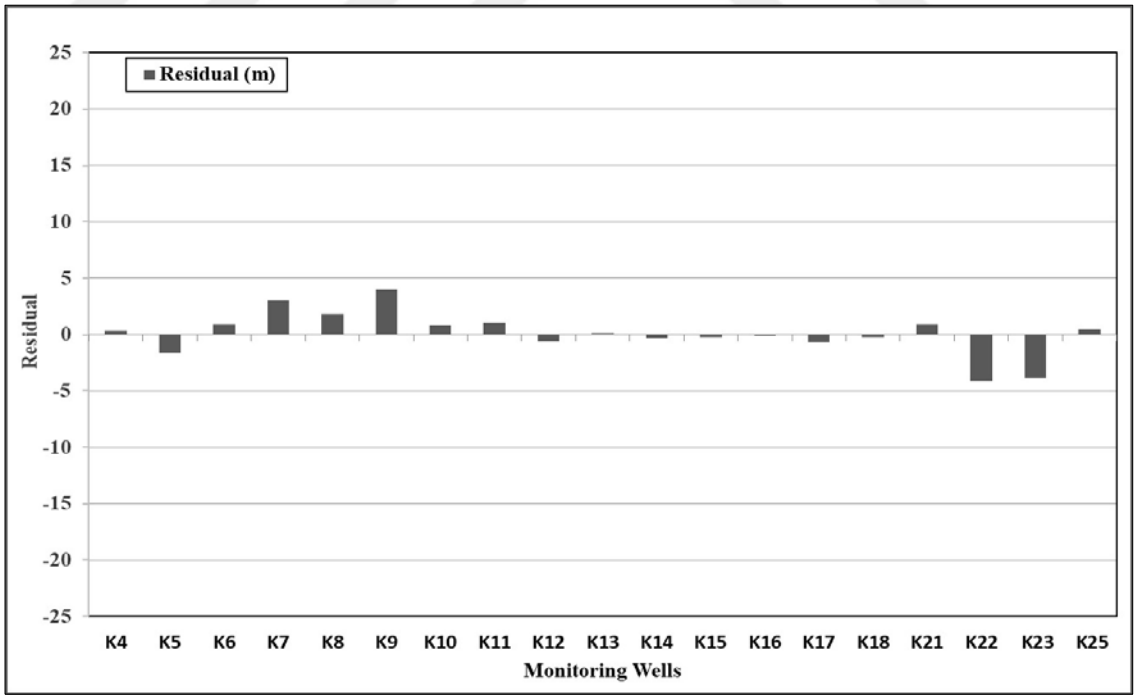

Figure 4.11. Residual values for simulated groundwater table elevations in karst area(Simulated – Measured)

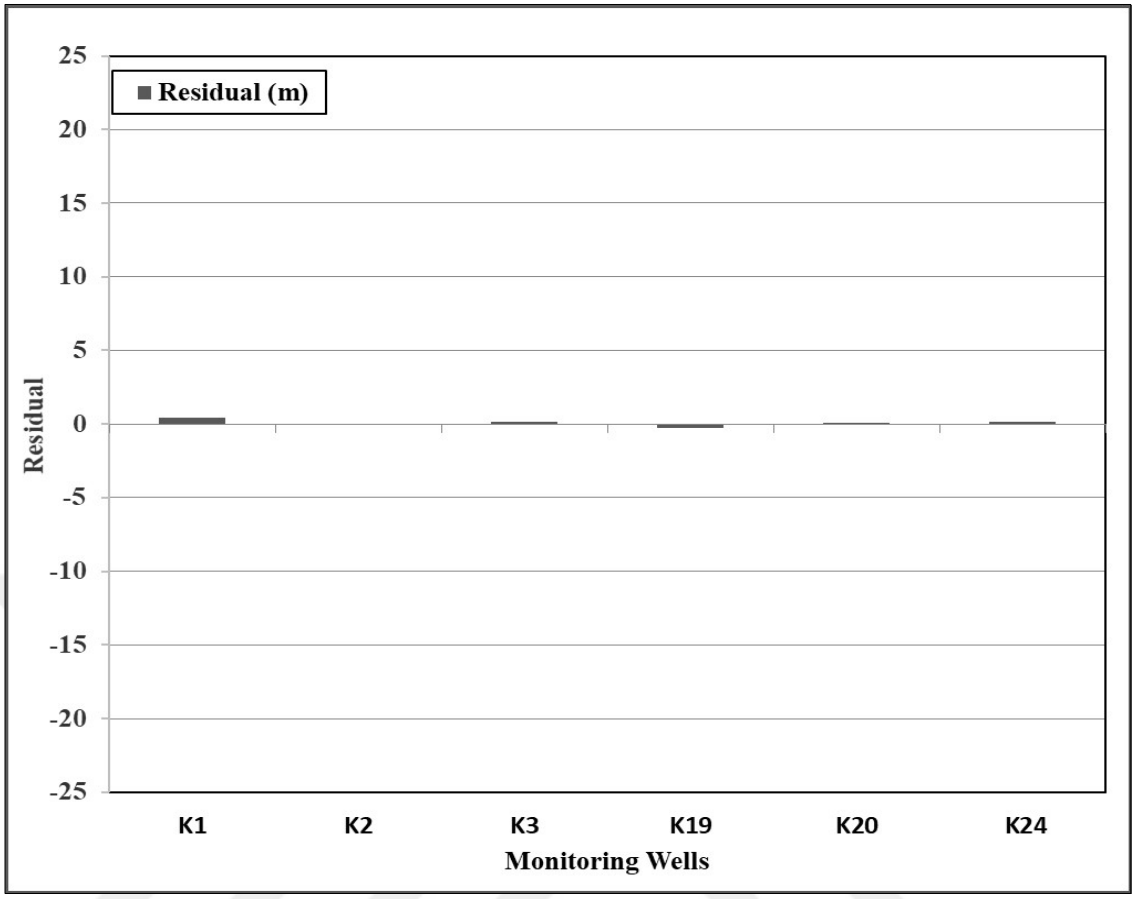

Figure 4.12. Residual values for simulated groundwater table elevations in non-karst area (Simulated – Measured)

Table 4.4. Compression of calibrated model performance between karst and non-karst area

Statistical Criteria	**Residuals in Karst Area**	**Residuals in Non-Karst Area**
Minimum Residual (m)	-3.98	-0.41
Maximum Residual (m)	4.14	0.24
Median	0.14	0.06
Residual Mean (m)	0.09	0.07
RMSE (m)	1.60	0.21
Regression Coefficient (R^2)	0.991	0.999
Standard Error of the Estimate (m)	0.44	0.09

Although the model result is acceptable in the karst area, the model tends to be less accurate in the southern part of the study area. This variation in residuals groundwater table elevation in the non-karst and karst region are shown in Table 4.4. The result in Table 4.4 indicated that Visual MODFLOW is more predictable in the Kurşunlu non-karst region than in the travertine karst area. It should be born in mind that the approach of this study did not consider the strong heterogeneity of the karst system. Furthermore, there are not accurate detailed data sets regarding aquifer parameters. Most of the aquifer parameters are based on literature and professional judgment. These factors may result in some degree of error in the simulation result.

4.5. Water budget for calibrated model

Given the uncertainties in the estimation of recharges and discharges (withdrawal rate), the overall water balance can be taken as a fair approximation of groundwater system analysis in the karst and non-karst area of Altınova. The inflow in the groundwater budget in this study includes recharge from precipitation and head dependent boundaries. Outflow includes the groundwater discharges to surface water, pumping wells and head dependent boundaries. Water budget output of the model, shown in Table 4.5 revealed that groundwater recharge accounts for 73.4% of the total inflow for the whole study area, making it the major sources of aquifer inputs, on the other hand, the head dependent boundaries account for 26.6%. It is also observed that the outflow cause by human activates (Pumping wells) accounts for 33% of the total outflow in the water budget, while head dependent boundaries account for 67%. It is evident from the water budget given in Table 4.5 the ratio of pumping over recharge, pumping/recharge, in the simulation period reach up to 46%. From the result above it can be expected that both climatic variability such as precipitation which alter the recharge, and pumping which alter the groundwater table elevation will have impact on the aquifer of Altınova. The water budget in the simulation period shows a good balance between inflow and outflow.

Table 4.5. Calibrated volumetric water budget for entire model

Cumulative volumes m^3/year		**Cumulative volumes m^3/year**	
In		**Out**	
Storage	0.00	Storage	0.00
Constant head	0.00	Constant head	0.00
Wells	0.00	Wells	8574464.00
Head dependent boundaries	6778737.00	Head dependent boundaries	16942572.00
Recharge	18738299.00	Recharge	0.00
Total in	25517036.00	Total Out	25517036.00
IN - Out	**0.00**		

4.6. Groundwater Flow Direction in the study area

The groundwater flow direction in the travertine karst region and the Kurşunlu non-karst region of Altınova is depicted in Figure 4.13. It can be seen clearly from the map that the general ground-water flow direction is perpendicular to the groundwater-table elevation. Water is moving from areas of high groundwater table in the north to lower groundwater-table elevations in the south. This movement of groundwater in the study area is what one would expect. Additionally, this flow behavior is consistent with concept presented by (Barackman and Brusseau 2002) that groundwater flows from regions of higher hydraulic head to the region of lower hydraulic head and also confirmed by the study conducted by DSI (2005).

According to the groundwater flow map given in Figure 4.13. the groundwater flow direction of the non-karst Kurşunlu aquifer is from north to the south. Likewise, in the travertine karst aquifer, the groundwater flows from north to southwest and then the direction changes to the south part of the study area. Primarily, the changes of groundwater flow to the southwest in the karst travertine region of Altınova are likely influenced by the high density of pumping wells. These findings further suggest that there is extensive groundwater withdrawal in the western part of the study area that can be easily conformed from the higher density of wells, greenhouse, and other land use in the western part of the study area.

Generally, the groundwater flows mimicking the topography of both the travertine karst region and the Kurşunlu non-karst region. From the distribution map of the calibrated hydraulic conductivity, the hydraulic gradient/hydraulic conductivity in the southern part of the study area is relatively high. Therefore, elevated flow velocities in the groundwater are likely to occur in the southern part of the study region. This is in line with Darcy's law that the velocity of the groundwater flow is relative to the magnitude of the hydraulic gradient and the hydraulic conductivity of the aquifer. Furthermore, this result is consistent with facts in the literature that groundwater flows faster where the hydraulic gradient and/or hydraulic conductivity are higher (Barackman and Brusseau, 2002). Additionally, higher flows of groundwater normally occur in the karst formation, where groundwater flows through caves. Therefore, it can be noted that karst caves exist in the southern part of the study area, although this could be investigated. The groundwater flow direction presented in this study is a representative of the real natural system of the study region.

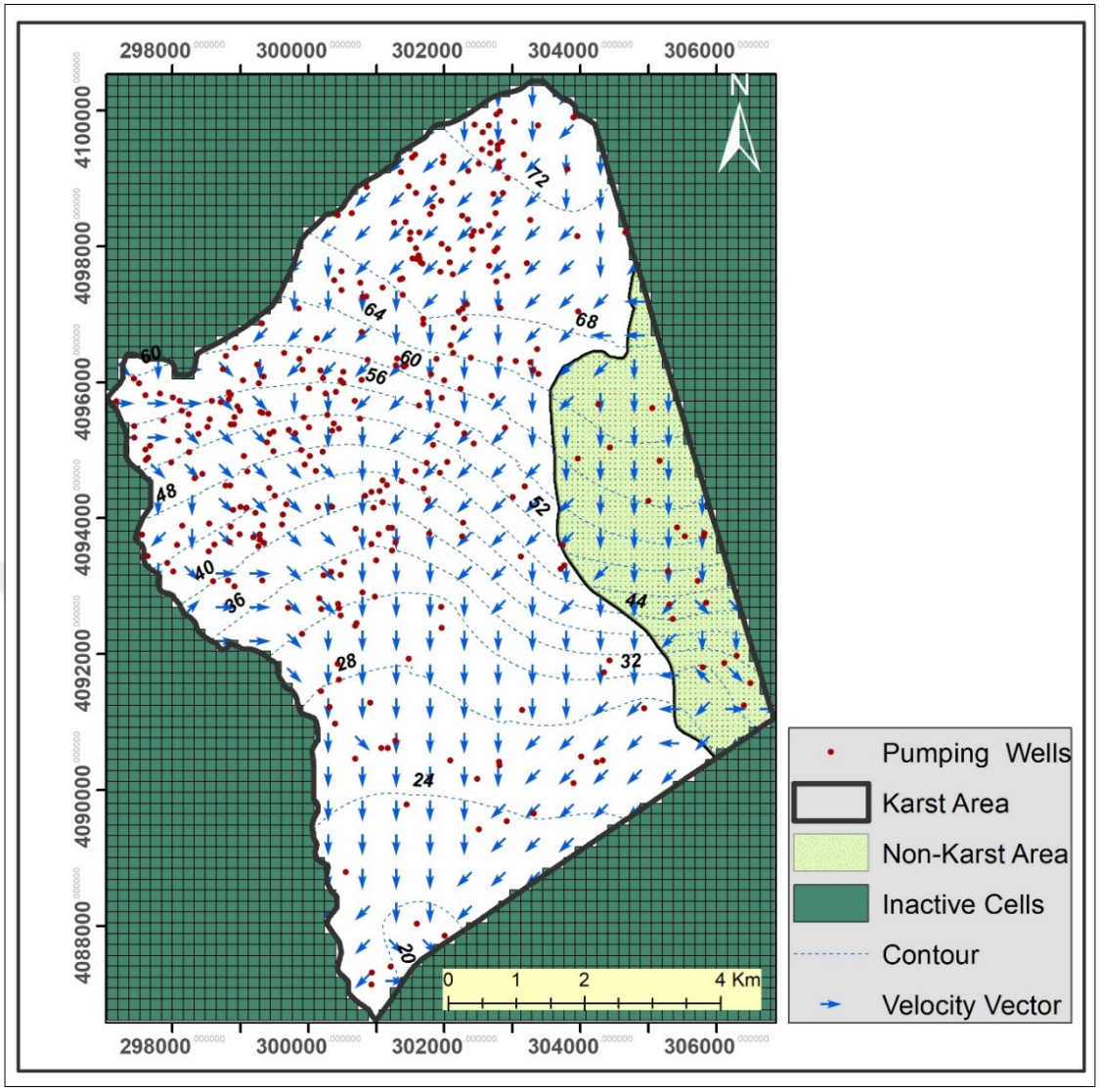

Figure 4.13. Groundwater flow direction and groundwater table elevation

4.7. Impacts of Different Management Scenarios

Impact of different three scenarios in this study were obtained from the analysis that involves changes in various model parameters such as recharge and groundwater abstraction. The simulation of groundwater table fluctuation was assessed based on precipitation input data and estimated withdrawal rate from the year between 2015-2016.

Scenario (A): assume decrease in recharge by 50% with the current rate of groundwater withdrawal and Scenario (B): assume increase in the groundwater withdrawal by 50% at the current state of precipitation. Scenario (C): assume decrease in precipitation by 50% and increase in the current withdrawal rate by 50%, as described in Table 4.6. In all scenarios, the aquifer parameters such as Specific storage (Ss), Specific yield (Sy) were kept constant with the value of 0.2 and 1.00E-05 1/m respectively. The other surrounding factor such as boundary condition was assumed to be the same.

Table 4.6. Management Scenarios Values for Recharge and Pumping rate

Rate of Increase/Decrease	**Zones**		**Total Pumping (m^3/year)**	**Scenarios**
	(Karst Area) Recharge mm/year	**(Non-karst Area) Recharge mm/year**		
Initial Values	279.158	95.1675	-8574464	(Base simulation calibrated)
50% Reduction in rainfall (Recharge)	139.58	47.58	-8574464	Scenario (A)
50% Increase in (Pumping Rate)	279.158	95.1675	-12861696	Scenario (B)
Combination of (A &B)	139.58	47.58	-12861696	Scenario (C)

The calibrated hydraulic conductivity was used to develop a base simulation model. In the base simulation result the groundwater table elevation is 18 m in the southern porting of the study area, while in the northern part of the study area a value of 72 m was observed (Figure 4.14). This variation is consistent with the calibrated values of groundwater table elevation. Therefore, the simulated groundwater table elevation for the scenarios (A), (B) and (C) were compared with the base simulation. The decline of the groundwater table elevation was estimated by obtaining the difference between the base simulation and the groundwater table elevation level of the different scenarios.

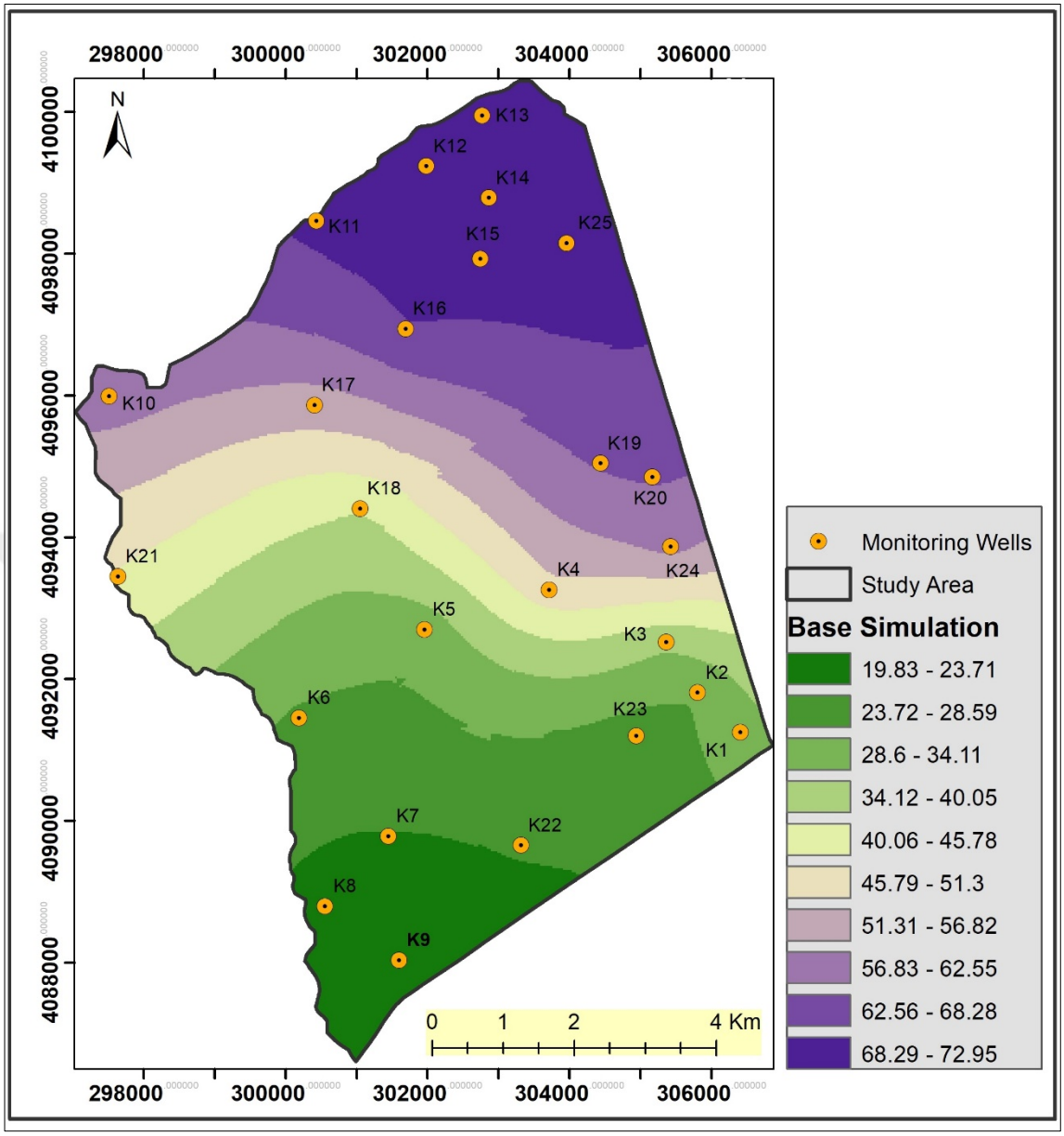

Figure 4.14. Map view of base simulation groundwater table elevation (GWTE)

4.7.1. Groundwater table elevation under scenario (A)

The result of scenario (A) demonstrated that with decrees of recharge by 50% at the current rate of groundwater withdrawals, groundwater table elevation decreases with a minimum and maximum of 0.1 m and 14 m, respectively over the all area (Figure 4.15). A significant decrease in groundwater table elevation up to 15 m was observed in the non-karst area under scenario (A). Under scenario (A) groundwater table elevation over the entire study area declined with an average of 4.6 m. Furthermore, the normal temperature will likely to elevate in the future, this may increase the evaporation rate. With such high evaporation, the capacity of the soil to hold moisture for percolation will decrease, which in turn will reduce recharge and lower the groundwater table elevation. The minimum decline rate of 0.2 m under scenario (A) occurs in the travertine karst area precisely at

well number K10. whereas the maximum drop of 8 m was observed in the same karst area at well number K4. The simulation result under scenario (A) shows that the maximum decrease in groundwater table elevation reaches up to 15 m in the non-karstic area at well number K24, while the minimum decline of 1.1 occurred in well number K1. Generally, there is a higher drop in the groundwater table elevation in non-karstic area than in the karst area. This is partly due to the variation of hydraulic conductivity that basically connects with the geological structure of the study area. In the karst area, the rate of infiltration is higher compared to the non-karst area.

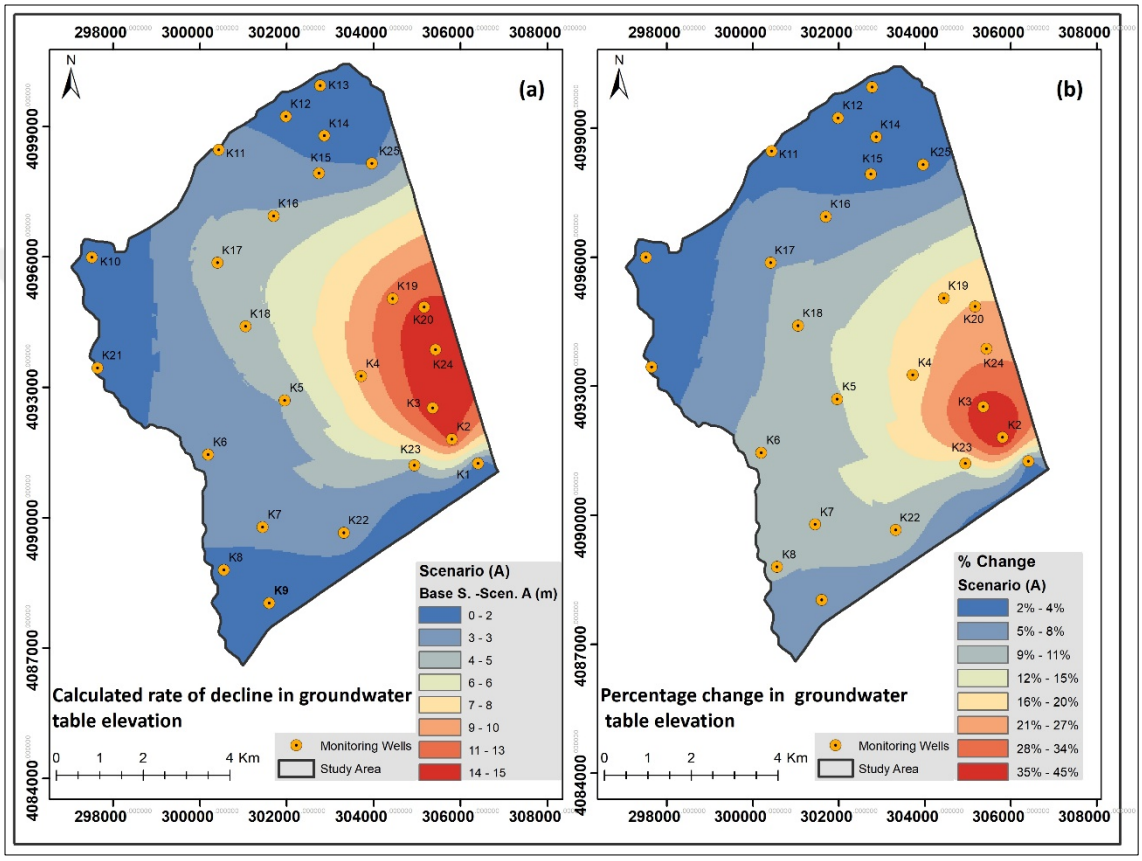

Figure 4.15. a) Computed decline in groundwater table elevation under scenario (A), and its corresponding percentage change **b)**

4.7.2. Groundwater table elevation under scenario (B)

Under scenario (B) which implies %50 percent increase in pumping with the current rate of recharge, groundwater table elevation dropped with a maximum of 14 m the minimum dropped observed was 0.3 m as depicted in Figure 4.16. A drop in the groundwater table elevation up to 15 m was observed in the non-karst area under scenario (B). Under scenario (B) the groundwater table elevation is declining with an average of 2.8 m in both karst and non-karst area. The maximum values of groundwater decline occur in the non-karst area. By keeping constant recharge and increase the current withdrawal rate in scenario (B), the prediction indicated that there is distinct lowering of groundwater table elevation in some wells both in the karstic and non-karstic aquifer of Altınova. For example, in the karstic area, the maximum decline in groundwater table

elevation reached to 14 m and occurred at well number K3, while the minimum rate of drop in groundwater table elevation in the karstic area was 1.3 m and occurred at well number K1. In the non-karstic area, the maximum drop in groundwater table elevation was 4 m and occurred at well number K4, whereas the minimum value of 0.1 was observed in well number K10.

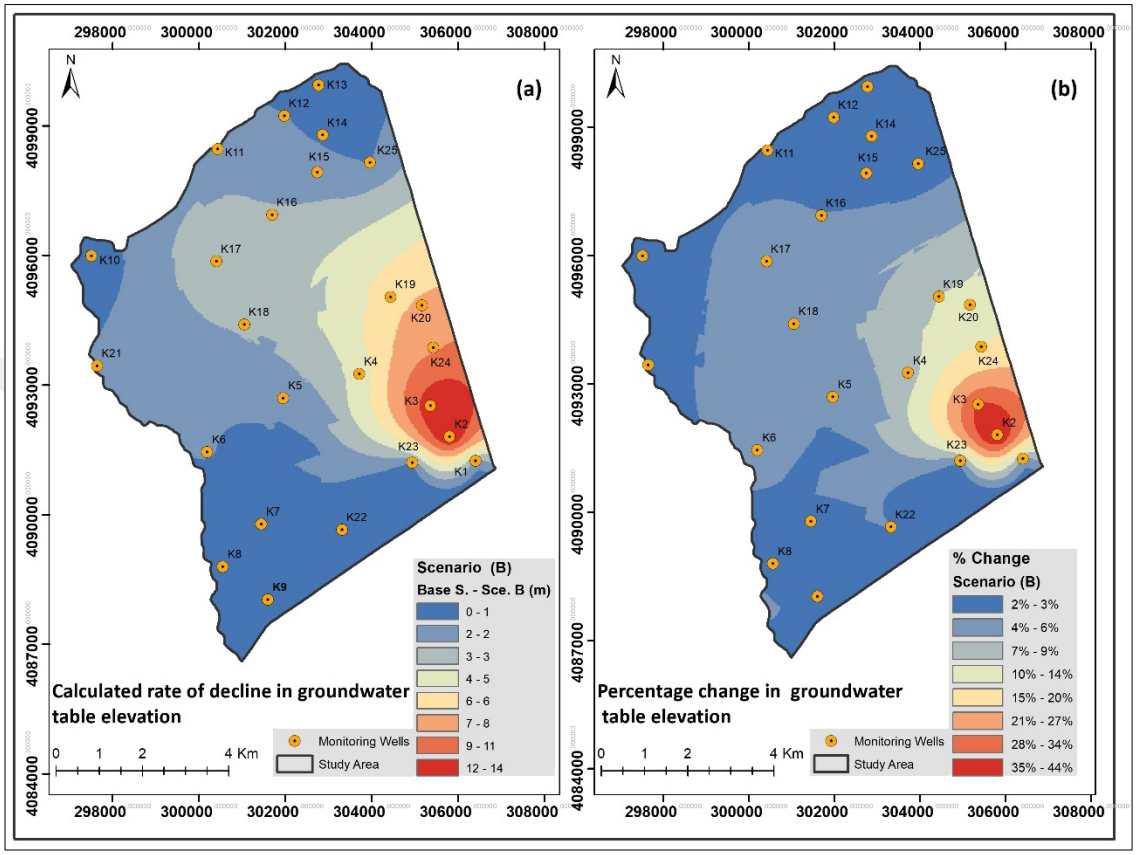

Figure 4.16. a) Computed decline in groundwater table elevation under scenario (B), and its corresponding percentage change **b)**

4.7.3. Groundwater table elevation scenario (C)

Scenario (C) implies the combined effect of both reducing the recharge by %50 and increasing pumping by %50. Significant drops were observed with the minimum and maximum value of 1.4 m and 29 m respectively in scenario (C) (Figure 4.17). The simulation result under scenario (C) shows that groundwater table elevation in karstic aquifer drop with a maximum of 12 m and a minimum of 1.4 m at wells number K4 and K9 respectively. While in a non-karstic area significant decline of 2 m and 29 occurred in well number K1 and K2. The statistical analysis of different scenarios is described in Figure 4.7. The results demonstrate that, if the condition of the third scenario (Scenario C) continues for long periods, many wells in the karst part of the study area are likely to run dry. The decline in the groundwater table elevation was mostly higher in scenario (C) compared to the other scenarios simply because scenario (C) assumes the worst-case scenario. Therefore, control and sustainable water use in the area are necessary to avoid diminution of groundwater in this fragile aquifer of Altınova. Under all three scenarios, groundwater table elevation is declining at a high rate in almost all wells in the non-karst

part of the study region. This situation is contrary to the wells in the karst areas. The variation in groundwater decline between two hydrological regions might be directly related to variation in hydraulic conductivity. In the non-karst region, the hydraulic conductivity is lower compare to karst area. This implies that lesser groundwater recharge translates to lower water table elevation. On the other hand, the decline in groundwater table elevation is low in the karst portion of the study area. Here the hydraulic conductivity is higher compared to the non-karst areas.

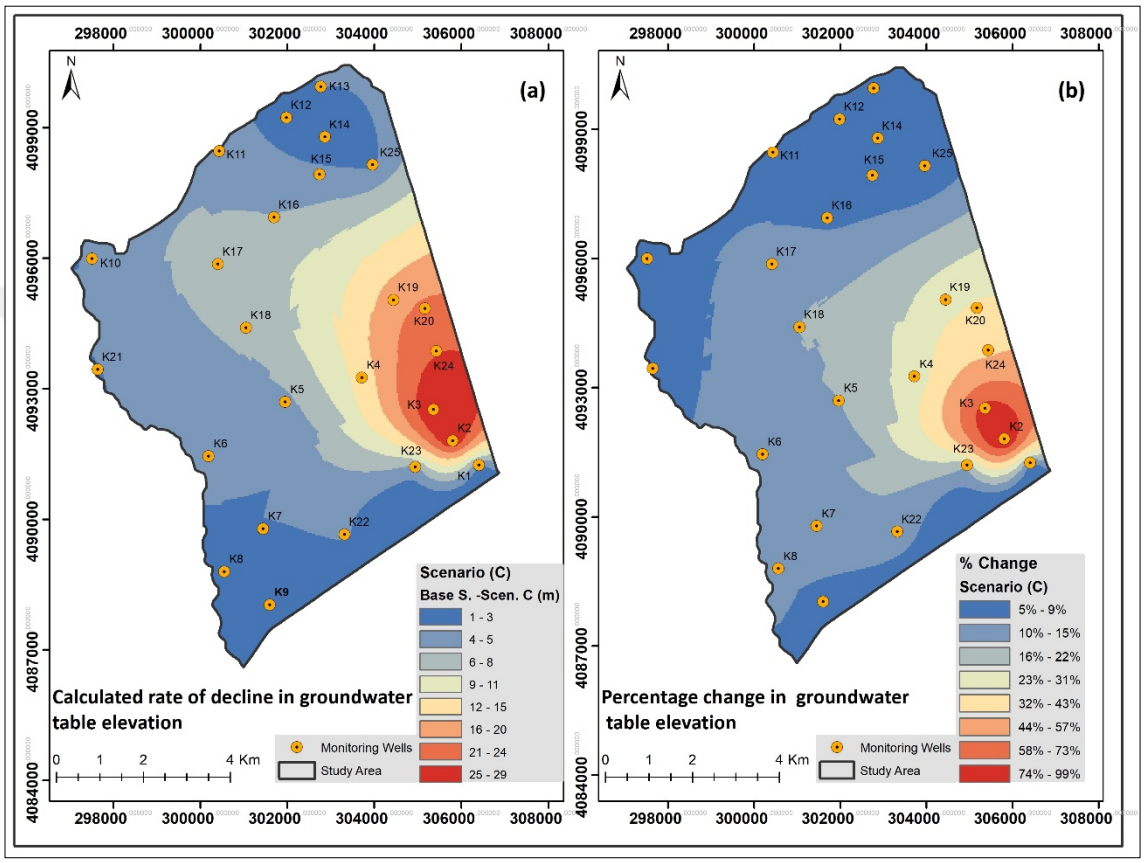

Figure 4.17. a) Computed Decline in Groundwater Table Elevation Under Scenario (C) Left, and its Corresponding Percentage Change **b)**

Table 4.7. Comparison of Model Performance Statistics for Different Scenarios Residual (Base Simulation – Scenario) Groundwater Table Elevation

Statistical Criteria	**Scenario (A)**	**Scenario (B)**	**Scenario (C)**
Minimum Residual (m)	0.1	0.3	1.4
Maximum Residual (m)	14.5	13.8	29.2
Median (m)	2.6	1.2	3.8
Mean (m)	4.6	2.8	8.0
Standard Error (m)	0.9	0.7	1.7
Standard Deviation (m)	4.7	3.7	8.8
Range (m)	14.4	13.6	27.8

Comparation between different three scenarios at monitoring wells level is depicted in Figure 4.18. It can be clearly seen from Figure 4.18 that some wells such as K10, K13, and K21 are unaffected under all scenarios. This insensitivity might be because of varying connections with the main karst conduits, and subsurface karst features. This behavior is consistent with the study conducted in a similar karst aquifer where the groundwater level in piezometers, which were close to one another (less than 10 m), responded differently to recharge (Drogue, 1980). The findings demonstrate clearly that if the current rate of decline continues, the area of Altınova is likely to have insufficient water for irrigation.

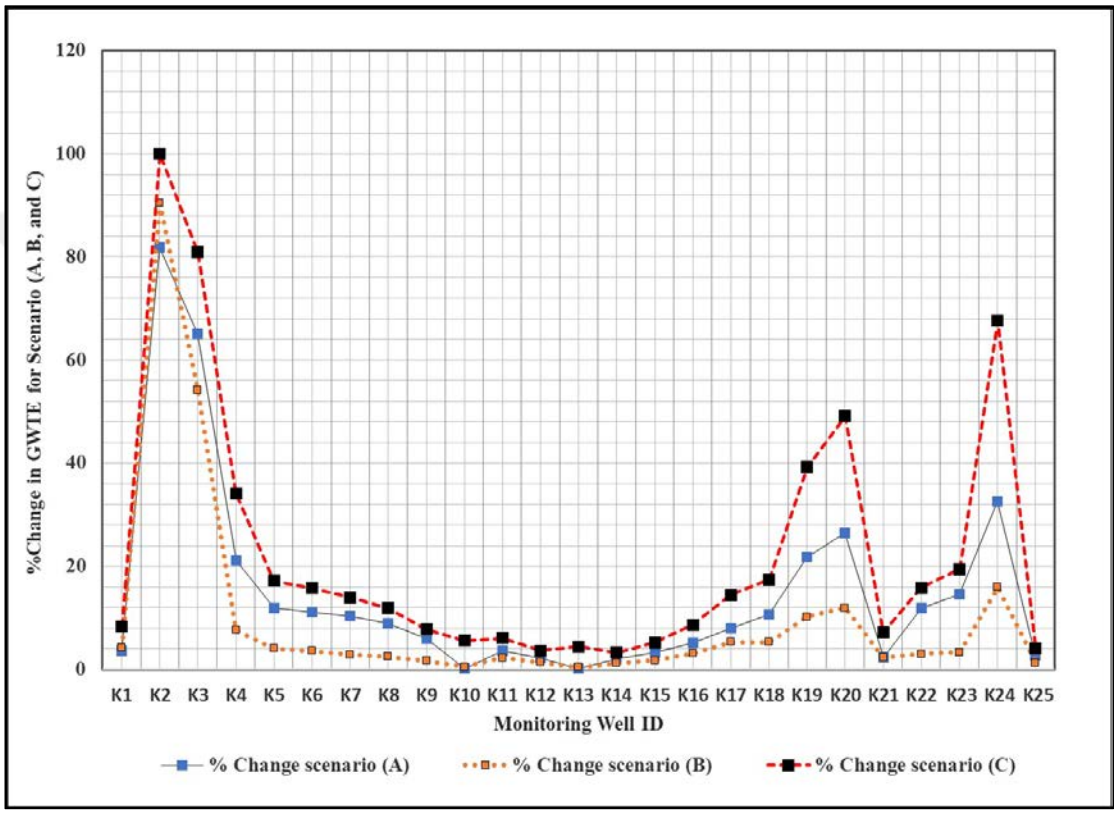

Figure 4.18. Changes in groundwater table elevation under scenario (A), (B), and C

4.8. Model Sensitivity Analysis

In addition to management scenarios, a sensitivity analysis was conducted by decreasing and increasing the calibrated values of hydraulic conductivity component by 50%. This was done to test the model sensitivity. The statistical results of the sensitivity analysis are shown in Table 4.8 and Figure 4.19. In the sensitivity analysis, increase in hydraulic conductivity tends to decrease groundwater table elevation. A percentage decrease of 4% was observed. In contrast percentage increase of 3.9% was observed by decreasing hydraulic conductivity by 50%. It can be seen clearly from the analysis that the model is sensitive to hydraulic conductivity.

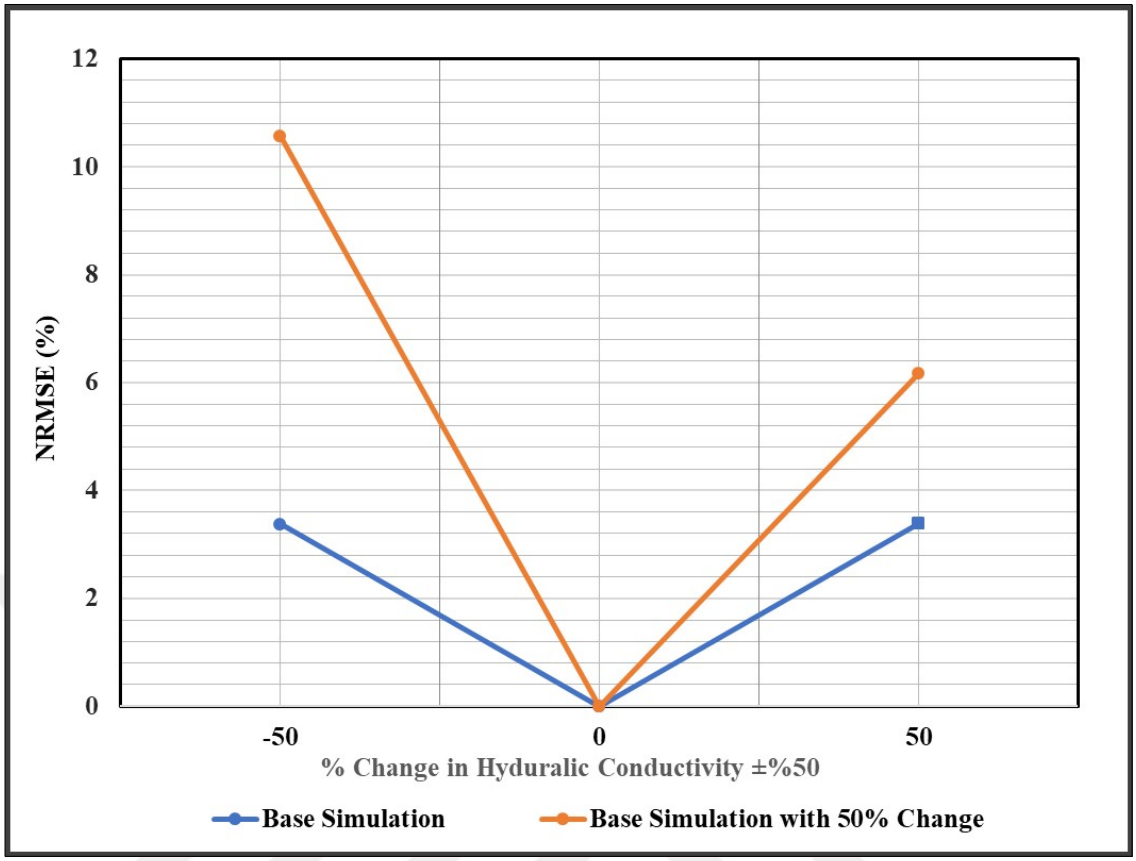

Figure 4.19. Graphical view of model sensitivity (NRMSE = Normalize Root Mean Square Error)

Table 4.8. Analysis of statistical sensitivity values of the model for decreased/increase of hydraulic conductivity by 50%

Statistical Criteria	Base Simulation	Hydraulic Conductivity	
		(+50%)	(-50%)
Average % Change	1.33	- 4.56	3.93
Max. Residual (m)	0.3.	3.14	7.49
Mini. Residual (m)	-4.05	-9.66	-11.03
Regression Coefficient (R^2)	0.99	0.98	0.94
RMSE (m)	1.65	3.00	5.15
NRMSE (%)	3.38	6.17	10.58

4.9. Comparation of Calibration Groundwater Table Elevation with Seasonal Measured Groundwater Table Elevation

Following the calibration study, different seasonal field measurements of groundwater table elevations were separately compared with the calibration groundwater table elevation. Comparison of calibration study steady-state simulation results of groundwater table elevations with the seasonal field measurements in Nov 2015, Feb 2016, and May 2016 are presented at Figure 3.20 through Figure 4.25.

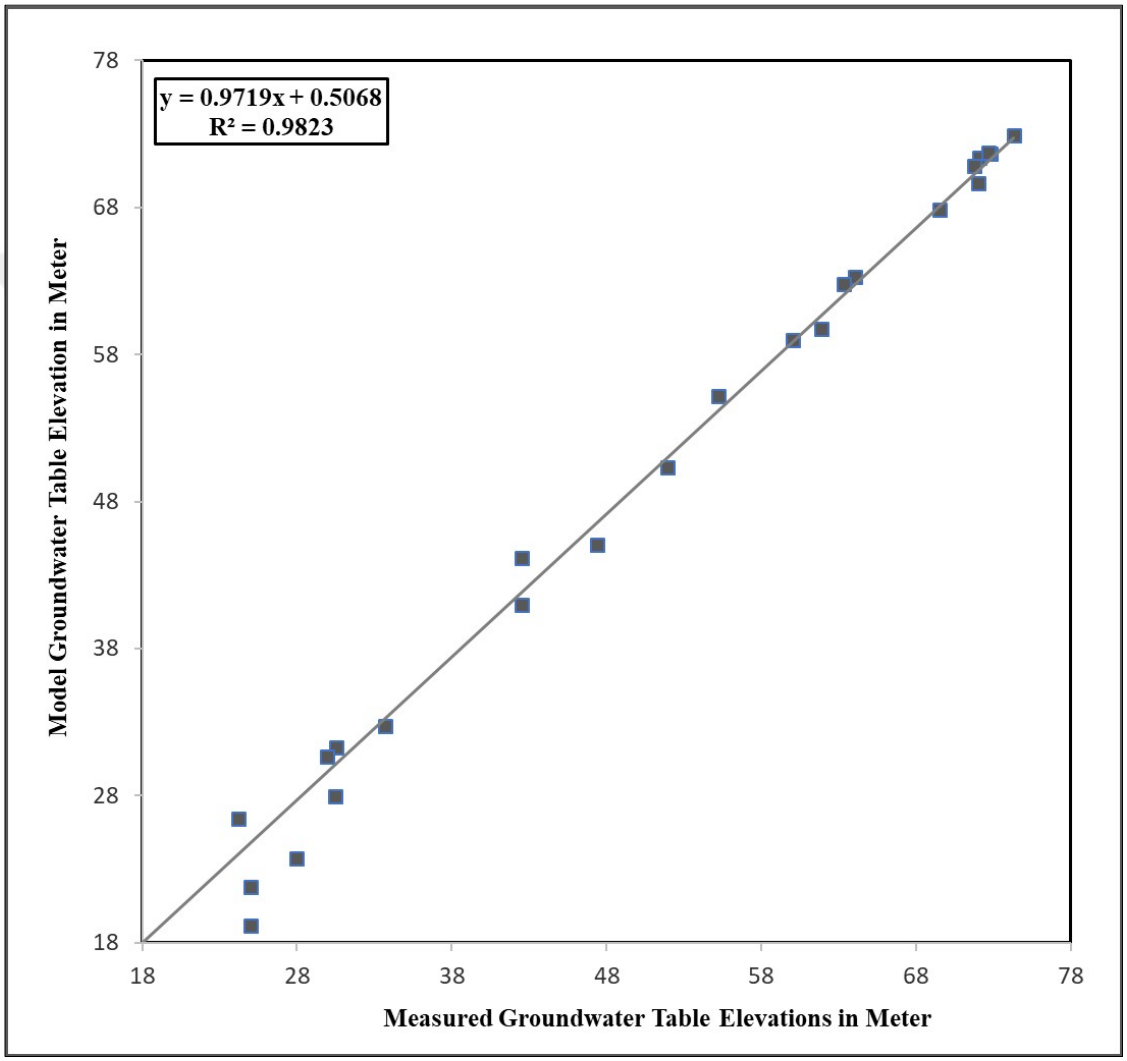

Figure 4.20. Comparison of simulated versus average measured groundwater table elevations for Nov-2015

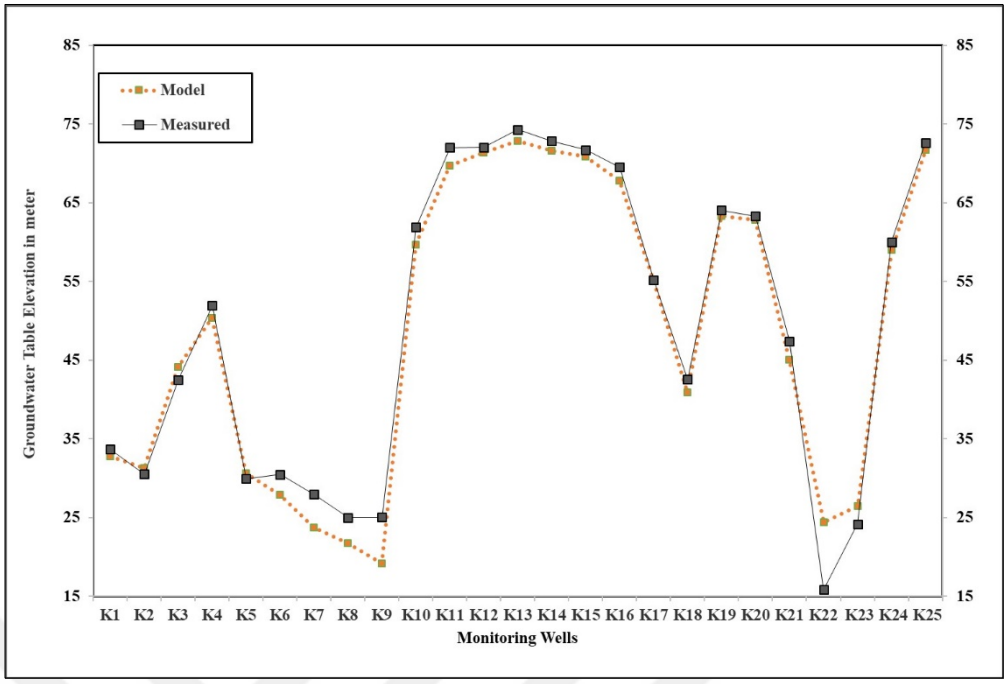

Figure 4.21. Comparison of simulated versus average measured groundwater table elevations for Nov-2015 at monitoring wells level

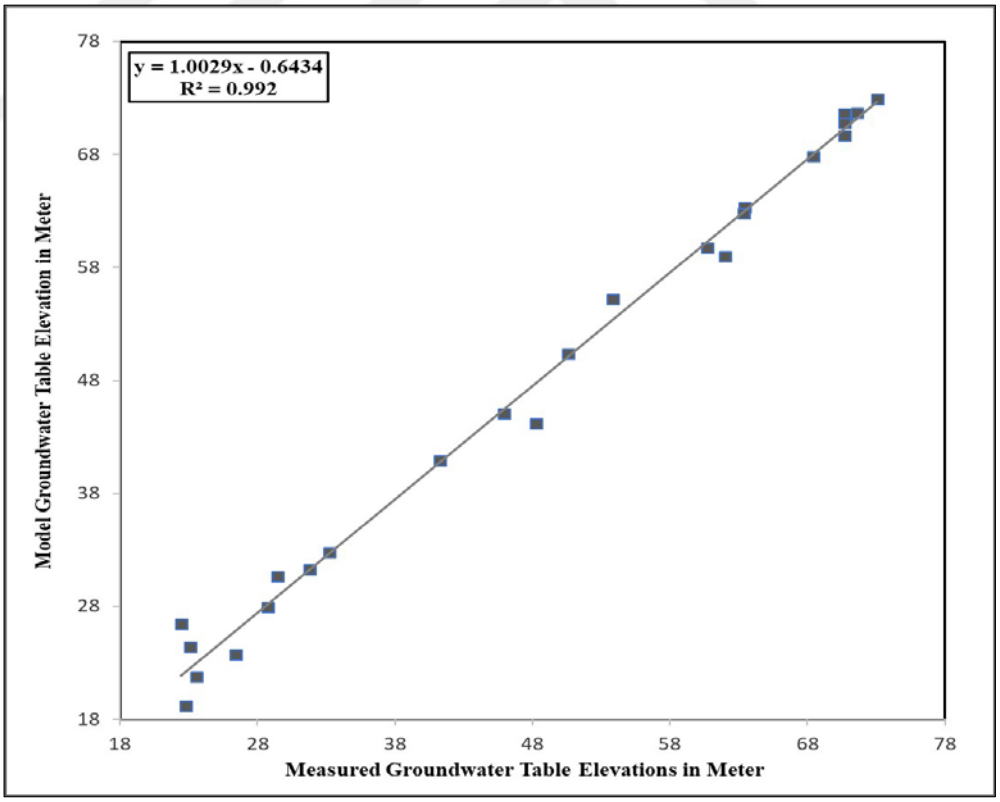

Figure 4.22. Comparison of simulated versus average measured groundwater table elevations for Feb-2016

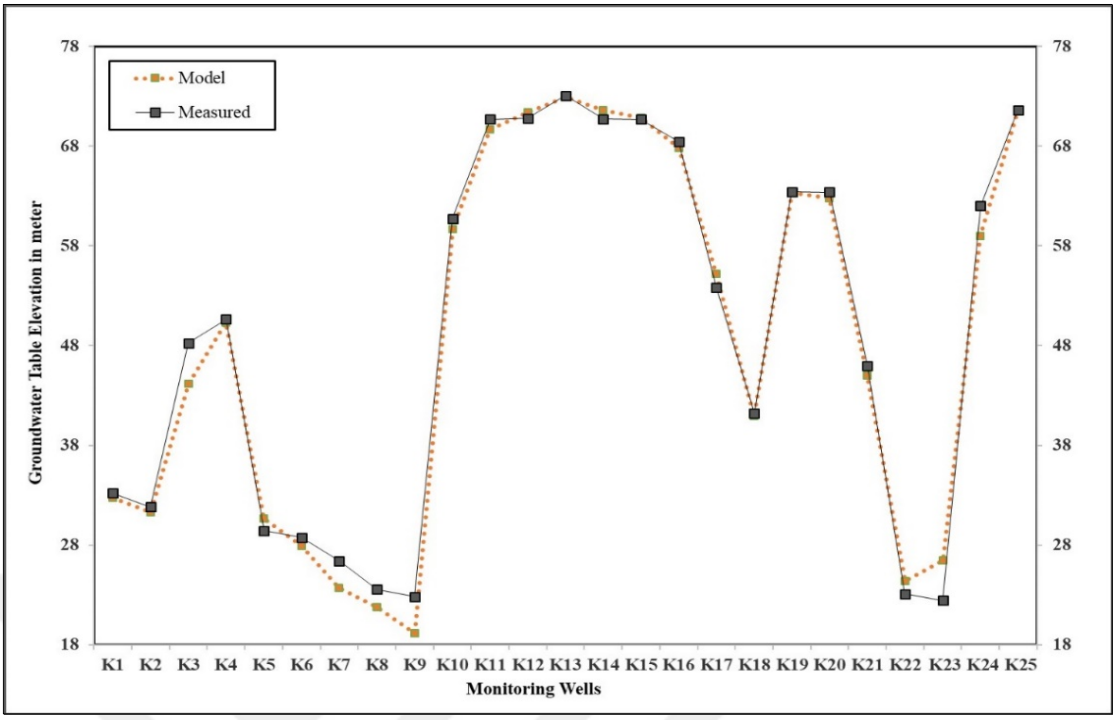

Figure 4.23. Comparison of simulated versus average measured groundwater table elevations for Feb-2016 at monitoring wells level

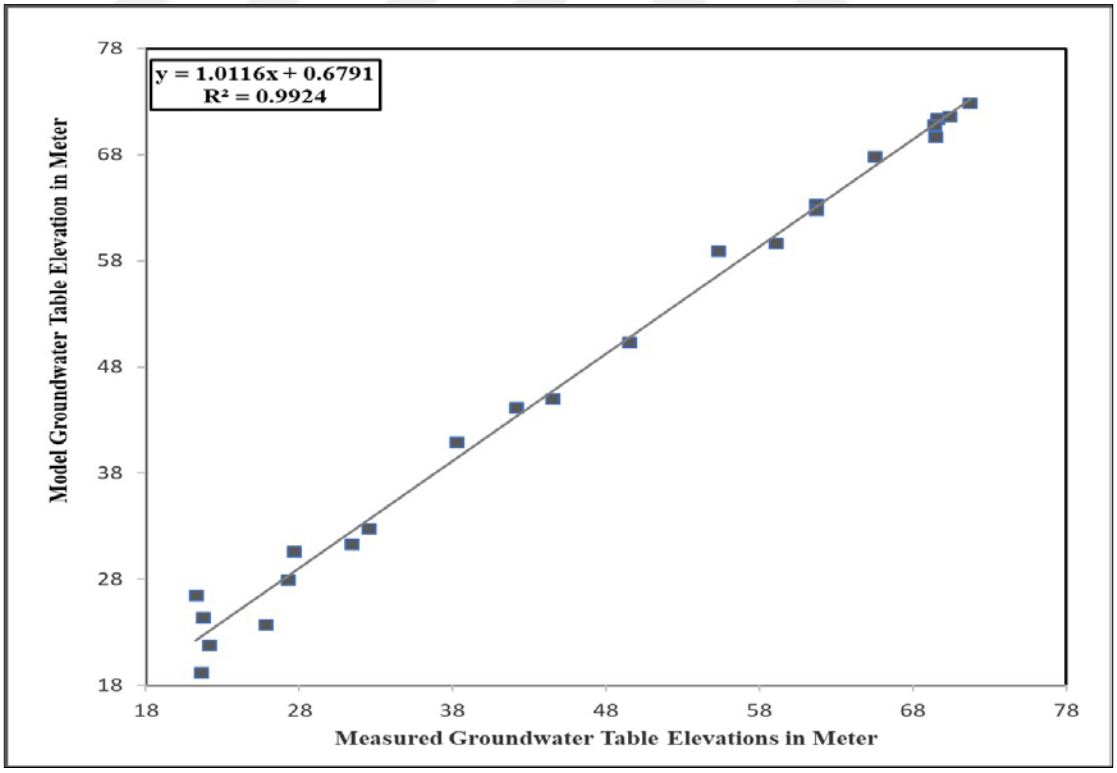

Figure 4.24. Comparison of simulated versus average measured groundwater table elevations for May-2016

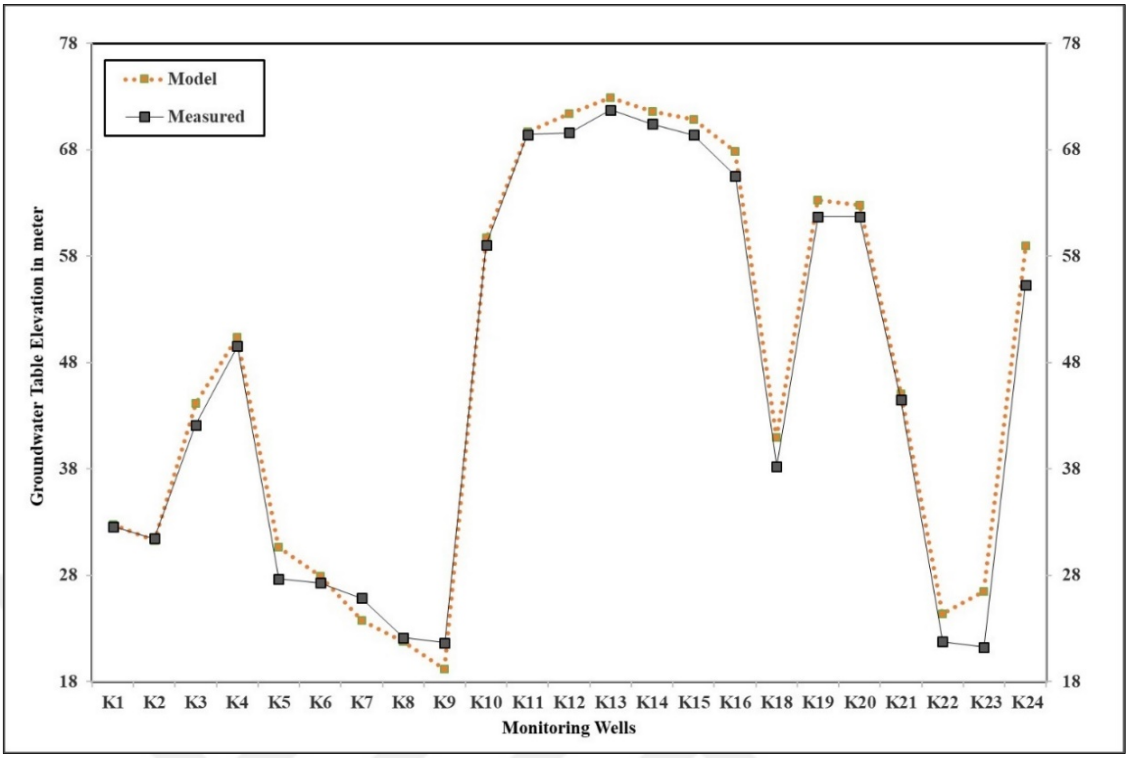

Figure 4.25. Comparison of simulated versus average measured groundwater table elevations for Feb-2016 at monitoring wells level

Table 4.9. Statistical comparison of model performance for seasonal groundwater table elevation

Statistical Criteria	Months		
	Nov-15	Feb-16	May-16
RMSE (m)	2.71	1.75	2.06
Correlation Coefficient (R^2)	0.980	0.992	0.992
Minimum Residual (m)	-8.55	-4.01	-5.21
Maximum Residual (m)	5.85	4.09	2.45
Median (m)	1.06	0.47	-1.16
Residual Mean (m)	0.89	0.50	-1.21
Standard Error (m)	0.52	0.34	0.36

4.10. Limitations of the Developed Groundwater Flow Model

Overall, the simulated groundwater table elevation replicates the field condition. It is safe to say that the model has provided valuable hydrological information for the travertine karst area and Kurşunlu non-karst area. Therefore, this model will serve as basis towards developing a future multi-layer model for better understanding of the complex travertine karst system of Altınova and Antalya in general. On the other hand, the steady-state model is limited in characterizing groundwater for management purposes because of the limitation on data regarding aquifer parameters. In every groundwater model, there is a level of uncertainty. Therefore, there are some limitations and assumptions that need to be born in mind when using this model result.

The result obtained from our study should not be interpreted as a perfect simulation, rather as a system response projection within the fairly realistic model input parameter. The limitation and the model assumption, and how they may affect the model result are described in this subsection.

The application of this model did not account for the strong heterogeneity of karst aquifers. This may likely result in some errors in the model output. Considering all the karst features and heterogeneity would have produced a more reliable result of groundwater flow in the study area.

Limitations in the pumping data may constitute the principal cause of error in this model. The amount of groundwater withdrawal in the study area was an estimation of the water needs by crops. The actual pumping/withdrawal rate in the study area is unknown. It is well known that any pumping mis-estimation may have a significant impact on the model. This will impact predictions made by the model and recommendations based on the model prediction.

The decision to apply the third type of boundary condition, specified head boundary (head dependent boundary), in the model was made to simplify the model implementation and bridge the data gap, because the other boundaries need more data such as conductance, evapotranspiration rate, extinction depth which are unavailable in the time of the study.

By applying the specified heads boundary most of problem regarding evapotranspiration data and seepage rate were alleviated. The downside of this boundary is that the water budget may not be accurately simulated in the model. This is expected to be a minor problem since recharge accounts for 73.4% of the total inflow.

The model has not been properly verified, because of lack of data. Using model predictions to establish water management policy would be premature. This limitation could be solved by collecting more data.

The average recharge in the model domain was taken as a fraction of precipitation for the whole karstic area and another fraction for the whole non-karstic area. Therefore, recharge values and boundary condition are uncertain parameters and subject to change in the future.

5. CONCLUSION

Groundwater modeling in the karstic system remains a challenging task for the hydrologist, because of its high degree of heterogeneity. Although the application of MODFLOW in the karstic region remains controversial, the finite difference steady-state groundwater analysis was developed and calibrated with a satisfactory result over the karstic area of Altınova. The discrepancy between simulated and average measured groundwater elevation table in the periods of November 2015, Feb 2016 and May 2016 shows a reasonable fit with the correlation coefficient of 0.99. In comparison to the geological formation, the model calibration results in the non- karstic area tending to be more satisfactory with lower residual values than in the karst area. In general, the model calibration produces an acceptable result. However, the model is less successful in the south part of the study area. Taking into consideration the use of the equivalent porous media approach through MODFLOW-2005 in the karstic travertine, the statistical values of the model calibration are acceptable. The spatial distribution of automatic hydraulic conductivity generated by the model in the calibration process are within literature ranges. The use of the pilot point in PEST dose much to facilitate groundwater model calibration. The water budget in the period of the simulation shows a good balance between inflow and outflow. Recharge is the highest component of inflow in the water budget for the entire study area. The natural outflow from head dependent boundary contributes about 67% of the total outflow, while the anthropogenic outflow pumping rate in the period of simulation accounts for 33% of the total outflow. The ratio of pumping over recharge, pumping/recharge, in the simulation period reach up to 46%. The model results also demonstrated that the groundwater flow is primarily from north to southwest in travertine karstic region and, then continues towards the south. Conversely in the non-karstic area the groundwater flow southwards. The outputs of the model could further be utilized to develop multi-layer model and could be used to study the flow path of nitrate in Altınova area.

Groundwater table fluctuation under different scenarios was simulated using Graphical Unser Interface (GUI) Visual MODFLOW flex. The result clearly shows that there are significant variations and drops in groundwater table elevation under all scenarios. Although scenario (A) shows a minor decrease in groundwater table elevation in the western part of the study area. Under all scenarios, the decline in groundwater table elevation is low in the karst part of the study area compared to the non-karst area. The simulation of scenarios employed in this study was carried out over a period of one year. However, if the same condition repeatedly occurs for many years, many wells in both the karst and non-karst aquifers of the study area will run dry. Consequently, this has called for formulation of adaptation strategies and planning for the future. In the model sensitivity analysis, the model is sensitive to both hydraulic conductivity and recharge. However, recharge tends to be more sensitive in contrast to hydraulic conductivity. The results generally support the original second hypothesis, that groundwater table elevation will vary by decrease and increase of recharge and withdrawals rates. Formulation of management recommendation to inform the decision makers is the third objective of this research work. Additionally, the model has not been properly verified , because of lack of data. Therefore, additional data collection is recommended to validate and improve the reliability of model results and to reduce uncertainties. Generally, the result of this

model provides a good starting point to develop a multi-layer groundwater flow model using Conduit Flow Process model MODFLO-2005 CFP.

5.1. Recommendations for Future Work

- Future work as a continuation of this research can be focused on covering the data gaps related to hydrology, and future climatological data. This will help evaluate the impact of climate change, land use and water need in the area. This will benefit managers in planning an effective management of this vital resource. Furthermore, future studies need to be focused on developing dynamic 3D multi-layer models using Flow Conduit Process (CFP) for MODFLOW-2005 in both steady and transient-state to better understand this karst region.

- The data gaps in the hydraulic conductivity have to be filled by conducting pumping test. The pumping test data will also provide data for transient simulation such as specific yield, storage coefficient, etc.

- A fair estimate has been done on the groundwater recharge, although more refinements can be made in the future according to the ever-changing land use and expansion of the agricultural field in the study area. It is also essential to determine distributed multi-temporal recharge for transient models by accounting for all influencing hydroclimatic factors.

- Very little is known about the distribution of caves in the study area. It is essential to study this system by the proper method to identify the existent cave in the study.

- Expansion of the model domain to coincide with the natural hydrological boundary and set an appropriate boundary condition in the study area is important to better understand the travertine karst region and Kurşunlu non-karst region of Antalya.

- Investigation of more monitoring wells, and the acquisition of more sets of monitoring data is important for proper calibration and validation of the model

- Precipitation and temperature time series downscaled data from regional climate models are strongly recommended to be used to eventually assess the impact of the climate change in the study area.

- Seasonal variation in agriculture activities occurs in the study area, the estimated pumping rates in the initial calibration run were assumed to be constant throughout the year. Therefore, transient model run that incorporate the seasonal withdrawal rate is recommended.

- The estimation of withdrawal rates is based on the water needs of crops. Consequently, the estimated pumping rate values may be more or less than the actual values in the field. Therefore, a reliable method that accounts for more accurate withdrawal rate is necessary to improve the model result.

6. REFERENCES

Allan R. Cherry, J. A. F. 1979. Groundwater. Prentice Hall, Inc. United States of America, p 624

AMPR. (2016). Antalya Master Plan Raporu", Hidrojeoloji Raporu. Antalya Turkey.

Anderson, M. P., Woessner, W. W., Hunt, R. J. 2015. Applied groundwater modeling: simulation of flow and advective transport *(2nd edition)*. https://doi.org/10.1016/B978-0-08-091638-5.0000

Anderson, M., Woessner, W. W., Hunt, R. (1990). Applied Groundwater Modeling, *Second Edition*: Simulation of Flow and Advective Transport. https://doi.org/10.1016/B978-0-08-091638-5.00001-8

Aster, R. C., Borchers, B., Thurber, C. H. 2013. Parameter Estimation and Inverse Problems. Parameter Estimation and Inverse Problems. https://doi.org/10.1016/C2009-0-61134-X

ArcGIS Online Resources. https://www.esri.com/en-us/arcgis/products/arcgis-online/resources [Accessed Oct 1, 2018

Bakalowicz, M. 2005. Karst groundwater: A challenge for new resources. *Hydrogeology Journal*, 13(1): 148–160.

Bakalowicz, M., El Hakim, M., El-Hajj, A. 2008. Karst groundwater resources in the countries of eastern Mediterranean: The example of Lebanon. *Environmental Geology*, 54(3): 597–604.

Barakman, M., M, B. 2002. Groundwater sampling. In Artiola, J. F, Pepper, I. L., Brusseau M. (Eds.), Environmental Monitoring and Characterization. pp. 121–139.

Bechtel, T. D., Bosch, F. P., Gurk, M. 2007. Geophysical methods. In Goldscheider N., Drew, D. (Eds.), Methods in Karst Hydrogeology. Taylor and Francis/Balkema. London, U. K. pp. 171–199.

Benischke, R., Goldscheider Nico, Smart, C. 2007. Tracer techniques. In Goldscheider, N., Drew, D. (Eds.), Methods in Karst Hydrogeology. Taylor and Francis/Balkema. London, U. K. pp. 147–170.

Bottrell, S. H., Ford, D., Williams, P. 1989. Karst Geomorphology and Hydrology. *The Geographical Journal*, 157 (87).

Butscher, C., Huggenberger, P. 2008. Intrinsic vulnerability assessment in karst areas A numerical modeling approach. *Water Resources Research*, 44: 1–15.

Chalikakis, K., Plagnes, V., Guerin, R., Valois, R., Bosch, F. P. 2011. Contribution of geophysical methods to karst-system exploration: An overview. *Hydrogeology Journal*, 19(6): 1169–1180

Chamberlin, T. C. 1899. Basic Mathematics and the Computer Code. In Anderson, M. P., Woessner, W. W., and Hunt, R. (Eds.), Applied Groundwater Modeling (2nd ed.). Elsevier. pp. 118–176.

Chen, Z. 2017. Modeling a geologically complex karst aquifer system. Doktors dissertation, Karlsruher Instituts für Technologie (KIT). p. 111

Chen, Z., Auler, A. S., Bakalowicz, M., Drew, D., Griger, F., Hartmann, J., … Goldscheider, N. 2017. Le programme de la Carte Mondiale des Aquifères Karstiques: concept, procédure de cartographie et carte de l'Europe. *Hydrogeology Journal*, 25(3): 771–785.

Cherubini, C. 2008. A modeling approach for the study of contamination in a fractured aquifer. *Geotechnical and Geological Engineering*, 26(5): 519–533.

Çil, A., Muhammetoğlu, A., Amil, Yenilmez, & Ozyurt. 2017. Assessment of Groundwater Vulnerability in a Karstic Aquifer. In *International Interdisciplinary Conference on Land Use and Water Quality*. Netherlands.

Criss, R., Davisson, L., Surbeck, H., and Winston, W. 2007. Isotopic methods. In Goldscheider, N., Drew, D. (Eds.), Methods in Karst Hydrogeology. *Taylor & Francis/Balkema Netherlands*. pp. 123–145

Derek Ford, and Paul Williams Derek, F. 1989. *Karst* Hydrogeology and Geomorphology, Hyman, London, 601 pp.

Dipova, N., and Doyuran, V. 2006. Characterization of the Antalya (Turkey) tufa deposits. *Carbonates and Evaporites*, 21(2): 144–160.

Doherty, J., and Hunt, R. 2010. Approaches to highly parameterized inversion: a guide to using PEST for groundwater-model calibration. U. S. Geological Survey Scientific Investigations Repor*t* 2010-5169.

Dreybrodt, W. (1990). The Role of Dissolution Kinetics in the Development of Karst Aquifers in Limestone: A Model Simulation of Karst Evolution. *The Journal of Geology*, 98(5): 639–655.

DSI (2005). Antalya Kırkgozler Project Preliminary Investigation Report, State Hydraulics Works, 21 pages (in Turkish).

Efe, R., and Soykan, A. 2008. The Formation of Antalya Travertine Deposit and Karst Ground, (November 2016).

Ekmekci, M. 2003. Review of Turkish karst with emphasis on tectonic and paleogeographic controls. *Acta Carsologica*. 32(2): 205-218

Elc, A., Karadas, D., and Fıstıkog, O. 2010. The combined use of MODFLOW and precipitation-runoff modeling to simulate groundwater flow in a diffuse-pollution prone watershed, *Water Science & Technology*, 62(1): 180–189.

Elhatı, H. (1997). The influence of karst features on environmental studies in Turkey. *Environmental Geology*, 31(May): 27–33.

Faust, C. R., and Mercer, J. E. 1980. Ground-water Modeling: Numerical Models. *Ground Water*, 18(4): 395–409. Retrieved from https://doi.org/10.1111/j.1745-6584.1980.tb03414.x

Finder, G. F., and Gray, W. G. (1977). Finite Element Simulation in Surface and Subsurface Hydrology.

Fleury, P., Plagnes, V., and Bakalowicz, M. 2007. Modelling of the functioning of karst aquifers with a reservoir model: Application to Fontaine de Vaucluse (South of France). *Journal of Hydrology*. 345(2007): 38–49

Ford, D., and Williams, P. 2007. Karst Hydrogeology and Geomorphology - *Derek Ford, Paul D*. John Wiley & Sons Ltd, The Atrium, Southern Gate, Chichester.

Franke, O. L., Reilly, T. E., and Bennett, G. D. 1987. Definition of Boundary and Initial Conditions in the Analysis of Saturated Ground-Water Flow Systems - An Introduction. *USGS Techniques of Water-Resources Investigations of the United States Geological Survey* (Vol. Book 3, Ap). Denve U.S.A.

Franklın, W., and Zhang, H. 2003. Fundamentals of groundwater, (July), 583.

Gallegos, J. J. 2011. Modeling Groundwater Flow in Karst Aquifers. An Evaluation of MODFLOW-CFP at the Laboratory and Sub-Regional Scales. Master's Thesis. *Earth, Ocean and Atomospheric Science.* Florida State University. 89p.

Geyer, T. 2008. Process-based characterisation of flow and transport in karst aquifers at catchment scale. PhD Thesis. Universität zu Göttingen. 118p.

Ghasemizadeh, R., Hellweger, F., Butscher, C., Padilla, I., Vesper, D., Field, M., and Alshawabkeh, A. 2012. Review: Groundwater flow and transport modeling of karst aquifers, with particular reference to the North Coast Limestone aquifer system of Puerto Rico. *Hydrogeology Journal*, 20(8): 1441–1461.

Goeppert, N., Goldscheider, N., and Scholz, H. 2011. Karst geomorphology of carbonatic conglomerates in the Folded Molasse zone of the Northern Alps (Austria/Germany). *Geomorphology*, 130(3–4): 289–298.

Goldscheider, N. 2015. Overview of Methods Applied in Karst Hydrogeology. In Z. Stevanović (Ed.), Karst Aquifers—Characterization and Engineering. S*pringer International*. Switzerland. pp. 127–145.

Goldscheider, N., and Andreo, B. 2007. The geological and geomorphological framework. In Goldscheider, N. and Drew, D. (Eds.), Methods in Karst Hydrogeology. Taylor & Francis/Balkema Netherlands. pp. 9–23.

Goldscheider, N., and Drew, D. 2007. Methods in Karst Hydrogeology. *Taylor and Francis Group*. London UK

Goldscheider, N., Meiman, J., Pronk, M., and Smart, C. 2008. Tracer tests in karst hydrogeology and speleology. *International Journal of Speleology*. 37(1): 27- 40.

Groves, C. 2007. Hydrologic Techniques. In Goldscheider, N. and Drew, D. (Eds.), Methods in Karst Hydrogeology Taylor & Francis/Balkema Netherlands. pp. 45–64.

Guiger, Nilson, Franz, and Thomas. 2010. Waterloo Hydrogeologic, *INC (WHI)*, Schlumberger Water Services, Visual MODFLOW Ver. *4.1 –User's* Manual Canada.

Günay, G. 1985. Karst groundwater studies in Manavgat river basin, Turkey. *Karst Water Resources (Proceedings of the Ankara - Antalya Symposium)*, 161(161): 333–342.

Günay, G. 2001. Present state and future trends of Karst studies. In G. Günay (Ed.), *Proceedings of the 6th International Symposium and Field Seminar* (Marmaris, Turkey. Vol. I: pp. 1–76.

Günay, G. 2010. Geological and hydrogeological properties of Turkish karst and major karstic springs. In Kresic, N., and Stevanovic, Z. (Eds.), Groundwater Hydrology of

Springs. Elsevier. pp. 479–497.

Güner, N., Törk, K., and Günay, G. 2015. Turkish karst aquifers. *Environ Earth Sci*, (Thematic issue): 1–10.

Haitjema, H. 2006. The role of hand calculations in ground water flow modeling. *Ground Water*, 44(6): 786–791.

Haitjema, H. M. 1995. Analytical element modeling of groundwater flow. *Academic Press Limited*. San Diego, California. 407p.

Hamlet. 1990. Spatial Discretization and Parameter Assignment. In Anderson, M. P. W. Woessner, W. and Hunt, R. J. (Eds.), Applied groundwater modeling: simulation of flow and advective transport (2nd edition) pp. 182–232.

Harbaugh, Arlen, W. 2005. *MODFLOW-2005* , The U . S . Geological Survey Modular Ground-Water Model — the Ground-Water Flow Process. U.S. Geological Survey Techniques and Methods. https://doi.org/U.S. Geological Survey Techniques and Methods 6-A16

Hartmann, A., Gleeson, T., Rosolem, R., Pianosi, F., Wada, Y., and Wagener, T. 2015. A large-scale simulation model to assess karstic groundwater recharge over Europe and the Mediterranean. *Geoscientific Model Development*, 8(6): 1729–1746.

Hartmann, A., Goldscheider, N., Wagener, T., Lange, J., and Weiler, M. 2014. Karst water resources in a changing world: Review of hydrological modeling approaches Rev. Geophys, 52(1): 218–242.

Hartmann, J., and Moosdorf, N. 2012. The new global lithological map database GLiM: A representation of rock properties at the Earth surface. *Geochemistry, Geophysics, Geosystems*, 13(12): 1–37.

Hill, M. 1998. Methods and guidelines for effective model calibration: US Geological Survey Water-Resources Investigations Report 98-4005. US Geological Survey,Water Resources Investigations Report 98-4005, 1–98. 90 p

Hill, M. C. 1990. Preconditioned conjugate-gradient 2 (PCG2), a computer program for solving ground-water flow equations. U.S. Geological Survey Water-Resources Investigations Report (Vol. 2).

Hill, M. C. 2006. The practical use of simplicity in developing ground water models. *Ground Water*, 44(6): 775–781.

Holz, K. P., Meissner, U., Zielke, W., Brebbia, C. A., Pinder, G., & Gray, W. 1982. *Finite Elements in Water Resources Proceedings of the 4th International Conference* (4th ed.).

Hunkeler, D., and Mudry, J. 2007. Hydrochemical methods. In Goldscheider, N. and Drew, D. (Eds.), Methods in Karst Hydrogeology. *Taylor & Francis/Balkema Netherlands* pp. 93–121.

Jeannin, P.-Y., Groves, C., and Philipp, H. 2007. Speleological investigations. In Goldscheider, N. Drew, D. (Ed.), Methods in karst hydrogeology. Taylor & Francis/Balkema Netherlands pp. 25–44.

Jeannin, P. Y. 2001. Modeling flow in phreatic and epiphreatic karst conduits in the Hölloch cave (Muotatal, Switzerland). *Water Resources Research*, 37(2):191–200.

Kaçaroğlu, F. 1999. Review of groundwater pollution and protection in karst areas. *Water, Air, and Soil Pollution*, 113(1–4): 337–356.

Kelson, V. A., Hunt, R. J., & Haitjema, H. M. 2002. Improving a Regional Model Using Reduced Complexity and Parameter Estimation. *Groundwater*, *40*, 132–143. Retrieved from https://doi.org/10.1111/j.1745-6584.2006.00189.x

Kindinger, B. J. L., Davis, J. B., & Flocks, J. G. 2001. Subsurface Characterization of Selected Water Bodies in the St . Johns River Water Management District , Northeast Florida, 124–127.

Kiraly, L. 2003. Karstification and Groundwater Flow. *Speleogenesis. Evolution of Karst Aquifers*, 1(3), 155–190. .

Kresic, N. 2007. Hydraulic methods. In Goldscheider, N., and Drew, D. (Eds.), Methods in Karst Hydrogeology. Taylor and Francis/Balkema. Netherlands pp. 65–92.

Kum, G., and Çelik, M. A. 2014. Impacts of Global Climate Change on the Mediterranean Region: Adana as a Case Study. *Procedia - Social and Behavioral Sciences*, 120: 600–608.

Kumar, C. P. 2015. Modelling of Groundwater Flow and Data Requirements. *International Journal of Modern Sciences and Engineering Technology*, 2(2): 18–27.

Kuniansky, E. L. 2016. Simulating Groundwater Flow in Karst Aquifers with Distributed Parameter Models—Comparison of Porous-Equivalent Media and Hybrid Flow Approaches. *U.S. Geological Survey*, Scientific Investigations Report 2016-5116, 14.p. https://doi.org/0.3133/sir20165116

Kuniansky, E. L. 2014. Taking the Mystery Out of Mathematical Model Applications to Karst Aquifers—A Primer. In Kuniansky, E. L., and Spangler, L. E. (Eds.), *A* Product of the Groundwater Resources Program Prepared in coperation with the National Cave and Karst Research Insititude pp. 69–81. Retrieved from http://dx.doi.org/10.3133/sir20145035

Larocque, M., Banton, O., Ackerer, P., and Razack, M. 1999. Determining Karst Transmissivities with Inverse Modeling and an Equivalent Porous Media. *Ground Water*. 37(6): 897–903.

Lelieveld, J., Hadjinicolaou, P., Kostopoulou, E., Chenoweth, J., El Maayar, M., Giannakopoulos, C., Xoplaki, E. 2012. Climate change and impacts in the Eastern Mediterranean and the Middle East. *Climatic Change*, 114(3–4): 667–687.

Maliva, R. G. 2016. Aquifer Characterization Techniques. *Springer Hydrogeology*. Switzerland. https://doi.org/10.1007/978-3-319-32137-0

Marshak, S. 2015. Earth Portrait of a Planet (5th ed.). Norton & Company Inc. New York, N.Y.981p.

McDonald, M. G., and Harbaugh, A. W. 1984. A modular three-dimensional finite-difference ground-water flow model. *U.S. Geological Survey*. https://doi.org/10.1016/0022-1694(86)90106-X

Mikszewski, A., and Kresic, N. 2015. Mathematical Modeling of Karst Aquifer. In. Stevanović, Z. (Ed.), Karst Aquifers –Characterization and Engineering

Switzerland. pp. 283–298. https://doi.org/10.1007/978-3-19-12850-4_10

Muhammetoğlu, A., Özyurt, N. N., Muhammetoğlu, H., Yenilmez, F. 2017. Yeraltısuyu Risk Değerlendirmesi ve Pestisit Risk İndikatörleri Kullanılarak Tarımsal Karstik Bölgelerdeki Yeraltısuyu Kalitesinin Entegre Yönetimi. Antalya Turkey.

Muhammetoğlu, A., and Yalcin, O. B. 2003. An Integrated Water Pollution Control Project to Protect Groundwater of Antalya Plain From Diffused Sources, Diffuse Pollution Conference, Dublin 2003, 39–45.

Murat, H. 2015. Hydrogeology of the Kaklik (Denizli) Aquifer in Turkey. *Procedia Earth and Planetary Science*, 15(2015): 345–352.

Panagopoulos, G. 2012. Application of MODFLOW for simulating groundwater flow in the Trifilia karst aquifer, Greece. *Environ Earth Sci*, 67(2012): 1877–1889.

Piccini, L., and Mecchia, M. 2009. Solution weathering rate and origin of karst landforms and caves in the quartzite of Auyan-tepui (Gran Sabana, Venezuela). *Geomorphology*, 106(1–2): 15–25.

Putnam, L. D., and Long, A. J. 2009. Numerical Groundwater-Flow Model of the Minnelusa and Madison Hydrogeologic Units in the Rapid City Area,. *U.S. Geological Survey*. South Dakota

Qadir, A., Ahmad, Z., Khan, T., Zafa, M., Qadir, A., and Murata, M. 2016. A spatio-temporal three-dimensional conceptualization and simulation of Dera Ismail Khan alluvial aquifer in visual MODFLOW: a case study from Pakistan. *Arab J Geosci*, 9 (2016): 149.

Rani, F. M., Chen, Z. H., and Studies, E. 2010. Numerical Modeling of Groundwater Flow in Karst Aquifer , Makeng Mining Area Faculty of Engineering , Al-Azhar University , Cairo , 11341 , Egypt. *American Journal of Environmental Sciences*, 6(1): 78–82.

Ronald T. Green, Scott L. Painter, A. S. and S. R. H. W. 2006. Groundwater contamination in karst terranes. *Water, Air, and Soil Pollution*, (6): 157–170.

Saller, S. P., Ronayne, M. J., and Long, A. J. 2013. Comparison of a karst groundwater model with and without discrete conduit flow. *Hydrogeology Journal*, 21: 1555–1566.

Sargin, A. H., Gorkmen, A., and Dogdu, M. S. (2000). A groundwater management plan according to EU Groundwater directive (80/68/EEC) and Water Framework directive (2000/60/EC). A new approch for groundwater management plant in Turkey.

Sauter, A. K. and M. 2007. Modelling karst hydrodynamics. In Goldscheider, N. and Drew, D. (Eds.), *Methods in Karst Hydrogeology Hydrogeology*. Taylor and Francis/Balkema. Netherlands (pp. 201–222).

Sauter, M. 1993. Double porosity models in karstified limestone aquifers: field validation and data provision. *Iahs Publication*, (207): 261–261. Retrieved from http://www.cig.ensmp.fr/~iahs/redbooks/a207/iahs_207_0261.pdf

Scanlon, B. R., Mace, R. E., Barrett, M. E., and Smith, B. 2003. Can we simulate regional groundwater flow in a karst system using equivalent porous media models ? Case

study , Barton Springs. *Journal of Hydrology*, 276(2003): 137–158.

Shoemaker, W. B., Kuniansky, E. L., Birk, S., Bauer, S., & Swain, E. D. 2008. Documentation of a Conduit Flow Process (CFP) for MODFLOW-2005. *U.S. Geological Survey Techniques and Methods, Book 6, Chapter A24*, 50.

Stevanović, Z. 2018. Global distribution and use of water from karst aquifers. *Geological Society, London, Special Publications*, 466.

Stevanović, Z., Ristić-Vakanjac, V., Milanović, S., Vasić, L., Petrović, B., & Čokorilo-Ilić, M. 2015. Karstification depth and storativity as main factors of karst aquifer regimes: some examples from southern Alpine branches (SE Europe and Middle East). *Environmental Earth Sciences*, 74(1): 227–240.

Tayanç, M., Im, U., Doğruel, M., and Karaca, M. 2009. Climate change in Turkey for the last half century. *Climatic Change*, 94(3–4): 483–502.

Teutsch, G. 1993. An extended double-porosity concept as a practical modelling approach for a karstified terrain georg teutsch. *Hydrogeological Processes in Karst Terranes (Proceedings of the Antalya Symposium and Field Seminar, October 1990). IAHS Publ. No. 207, 1993.*, (207): 281–292.

Trescott, P. ., Pinder, G. ., and Larson, S. 1980. Finite difference model for aquifer simulation in two dimensions with results of numerical experiments. *Techniques of Water Resources Investigations of the United States Geological Survey*. Retrieved from https://pubs.usgs.gov/twri/twri7-c1/html/pdf/TWRI_7-C1.pdf

Unal, Y. S., Deniz, A., Toros, H., & Incecik, S. 2012. Temporal and spatial patterns of precipitation variability for annual, wet, and dry seasons in Turkey. *International Journal of Climatology*, 32(3): 392–405.

Varouchakis, E. A., Karatzas, G. P., & Giannopoulos, G. P. 2015. Impact of irrigation scenarios and precipitation projections.pdf. *Environ Earth Sci*. 73(2015): 7359–7374.

Vrba, J., Hirata, R., Girman, J., Haie, N., Lipponen, A., Neupane, B.,Wallin, B. 2006. Groundwater Resources Sustainability Indicators. *International Symposium on Groundwater Sustainability*, (July 2016): 33–52.

Wang, H. F., & Anderson, M. P. 1982. Introduction to Groundwater Modeling: Finite Difference and Finite Element Methods.249p.

Wang, S., Shao, J., Song, X., Zhang, Y., Huo, Z., & Zhou, X. 2008. Application of MODFLOW and geographic information system.pdf. *Environ Geol*, 55: 1450–1462.

Waterloo. 2018. User Manual Visual MODFLOW Flex 5.0. Canada. Waterloo Hydrogeologic. Retrieved from www.waterloohydrogeologic.com. 600p.

White, W. B. 2007. A brief history of karst hydrogeology: contributions of the NSS. *Journal Of Cave And Karst Studies*, 69(1): 13–26.

Williams P, Fong YT World map of carbonate rock outcrops http://web.env.auckland.ac.nz/our_research/karst. [Accessed on April 5, 2018]

Worthington, S. R. H. 2009. Diagnostic hydrogeologic characteristics of a karst aquifer (Kentucky, USA). *Hydrogeology Journal*. 17: 1665-1678.

Xu, X., Huang, G., Qu, Z., and Pereira, L. S. 2011. Using MODFLOW and GIS to Assess Changes in Groundwater Dynamics in Response to Water Saving Measures in Irrigation Districts of the Upper Yellow River Basin, *Water Resour Manage* 25 (2011): 2035–2059.

Yilmaz, I., Sayin, C., and Ozkan, B. 2005. Turkish greenhouse industry: Past, present, and future. *New Zealand Journal of Crop and Horticultural Science*, 33(3): 233–240.

Željković, I., & Kadić, A. 2015. Groundwater balance estimation in karst by using simple conceptual rainfall–runoff model. *Environmental Earth Sciences*. https://doi.org/10.1007/s12665-015-4624-z

Zwahlen, F. 2003. Vulnerability and Risk Mapping for the Protection of Carbonate (Karst) Aquifers. *European Commission for Science*, 42p. https://doi.org/PNR61,

ÖZGEÇMİŞ

ALEX MODI LOMORO WANI

junioralex.modi@gmail.com

amodi@wcs.org

20155107010@ogr.akdeniz.edu.tr

ÖĞRENİM BİLGİLERİ

Yüksek Lisans 2016-2019	Akdeniz Üniversitesi Fen Bilimleri Enstitüsü, Çevre Mühendisliği Bölümü, Antalya
Lisans 2006-2012	Juba Üniversitesi Doğal Kaynaklar ve Çevre Bilimleri Fakültesi, Çevre Çalışmaları Bölümü, Juba

MESLEKİ VE İDARİ GÖREVLER

Ekolojik Araştırmacı / CBS uzmanı 2013-2015	WCS Güney Sudan, Juba

ESERLER

Ulusal bilimsel toplantılarda sunulan ve bildiri kitaplarında basılan bildiriler

1- Wani, A. M., Muhammetoğlu, A. and Muhammetoğlu, H. (2018). Management of Groundwater Resources in Karstic Aquifer using Visual MODFLOW flex, Case Study of Altınova Antalya Turkey, Second International Students Science Congress. (Abstract/Oral Presentation)